A METHODOLOGY FOR PROBABILISTIC AIRCRAFT TECHNOLOGY ASSESSMENT AND SELECTION UNDER UNCERTAINTY

A Dissertation
Presented to
The Academic Faculty

by

Turab Zaidi

In Partial Fulfillment
of the Requirements for the Degree
Doctor of Philosophy in the
School of Aerospace Engineering

Georgia Institute of Technology
August 2016

A METHODOLOGY FOR PROBABILISTIC AIRCRAFT TECHNOLOGY ASSESSMENT AND SELECTION UNDER UNCERTAINTY

Approved by:

Professor Dimitri Mavris, Advisor
School of Aerospace Engineering
Georgia Institute of Technology

Professor Graeme Kennedy
School of Aerospace Engineering
Georgia Institute of Technology

Dr. Hernando Jimenez
School of Aerospace Engineering
Georgia Institute of Technology

Professor Roger Cooke
Department of Mathematics
Delft University of Technology, Netherlands

Professor Daniel Schrage
School of Aerospace Engineering
Georgia Institute of Technology

Date Approved: July 8, 2016

To my parents,

who taught me "that nothing belongs to man,

except what he strives for" [52:39]

ACKNOWLEDGEMENTS

I am most grateful to God Almighty in whose infinite grace, protection, mercy, and strength my goal is accomplished.

I could not have overcome the challenges of a graduate student's Ph.D. journey on my own. I gladly and gratefully express my appreciation to all those who guided, helped, and encouraged me in this endeavor. First I would like to acknowledge my advisor Professor Dimitri Mavris for giving me the opportunity to join the Aerospace Systems Design Lab and allowing me to perform this research under his supervision. I whole-heartedly thank him for his patience, counsel, and support during my time here. I would like to recognize all my committee members for their guidance throughout this work. I extend sincere thanks to Dr. Hernando Jimenez for his constant support and guidance through the many technical challenges encountered in this research. I cannot express in words how much his technical insights, professional mentorship, and personal advice have meant to me over the years. I would like to acknowledge Professor Roger Cooke for his guidance in the latter stages of this work that were instrumental to its success. I want to thank all my colleagues and members of the Aerospace Systems Design Lab for their assistance and for creating a congenial environment to learn and work in.

I want to thank my family and my parents for their unwavering love and dedication throughout my life and my time in graduate school. The sacrifices of my parents, Mohammad Wasi and Shahida Zaidi, are the underpinnings of my accomplishments today and for that I am forever indebted to them. I hope that with the fruits of this achievement, I can try to repay them in some small way. I am grateful for the bonds of family between my siblings Samana, Yasin, and Farhin, that made it possible to

be physically distant in Atlanta but in mind and heart, never far from home. I would like to express my gratitude to my relatives and friends in Atlanta who supported and encouraged me during my time here including Azhar Zaidi and his family, Dr. Kazim Raza and his family, Habib Shirazi and his family, Abbas Mumen and his family, Taqi Qazalbash, and Etizaz Shah. Special thanks to my dearest friends Mehdi Shirazi, Abbas Hasnain, Dr. Asker Razvi, Dr. Ali Hasan, Imran Hussain, Hamid Shirazi, Hasan Jaffar, and countless others in the Atlanta community who have made my time here an unforgettable chapter of my life. I would also like to acknowledge all of my extended family and friends in NY/NJ, Toronto, and around the world who have assisted me with their kind words, thoughtful prayers, and much more which has made this accomplishment possible.

During my time in graduate school I was blessed to marry into the best family a son-in-law could hope for. I want to thank my in-laws Mohammed Zaki and Shehnaz Baqri for their love and prayers, for having faith in me, and accepting me into their family. I am most grateful to my sister-in-law Aeliya Baqri, my brother-in-laws Asad Jafri, Sameer Ali, Muhammad Sibtain, Mohammed Abbas and their families for their unwavering support and constant encouragement. Finally and most importantly, I express my deepest gratitude to my dear wife Sumiya Baqri for all that she is and everything that she has helped me to become. I thank her for believing in me, for supporting me, and inspiring me to become a better human being. These meager words cannot do justice to her dedication towards me but I am whole-heartedly grateful to her for bearing with me through the happy and difficult times of a humble graduate student's life. I also want to thank our son Muhammad-Abid for the joy he brings to me every day which lights up even the most difficult days of my life.

Turab Zaidi

Atlanta, GA

July 2016

TABLE OF CONTENTS

LIST OF TABLES

LIST OF FIGURES

LIST OF SYMBOLS AND ABBREVIATIONS

$\bar{d}$	Average distance
$\bar{d}_{Low}$	Average lower distance
$\bar{d}_{Mid}$	Average middle distance
$\bar{d}_{Upp}$	Average upper distance
$\bar{d}^{-1}$	Average inverse distance
$\bar{d}^{-1}_{Low}$	Average inverse lower distance
$\bar{d}^{-1}_{Mid}$	Average inverse middle distance
$\bar{d}^{-1}_{Upp}$	Average inverse upper distance
ε	Evenness Distribution
ϕ	Pareto frontier point density
ρ_p	Pearson's rho
ρ_s	Spearman's rho
σ_ϕ	Pareto corner density
σ_{Low}	Lower density
σ_{Mid}	Middle density
σ_o	Origin corner density
σ_{Upp}	Upper density
τ_k	Kendall's tau
θ	Copula correlation parameter
Θ	Quantile exceedance probability
υ	Upper to Lower Ratio
AR	Wing aspect ratio
C	Copula function
C_D	Drag Coefficient
C_L	Lift Coefficient

CE	Certainty equivalent
CAST	CopulA Selection Tree
cov	Covariance
D	Drag (lbs_f)
e	Span efficiency factor
EDS	Environmental Design Space
$E(U)$	Expected utility
ERA	Environmentally Responsible Aviation
FB	Fuel burn
F, G	Cumulative Distribution Function, CDF
F^{-1}, G^{-1}	Inverse CDF
FAAST	Future Aircraft Assessment and Selection of Technologies
H	Joint distribution
$HLFC$	Hybrid laminar flow control
L	Lift (lbs_f)
MAUT	Multiattribute Utility Theory
MENU	Multiattribute ENcoding of Utility
NM	Noise Margin
NOx	Nitrogen oxides
PC	Engine power code
R	Aircraft range (nmi)
SME	Subject matter expert
$t_{C_{D,0}}$	Technology impact factor for lift-independent drag
$t_{C_{D,i}}$	Technology impact factor for lift-dependent drag
t_{TSFC}	Technology impact factor for thrust specific fuel consumption
$t_{W_{Empty}}$	Technology impact factor for aircraft empty weight
$TSFC$	Thrust specific fuel consumption ($\text{lbs}/(\text{lbs}_\text{f} \cdot \text{hour})$)

u, v	Random variables
vN-M	von Neumann-Morgenstern
V	Velocity
W_f	Weight final (lbs)
W_i	Weight initial (lbs)

SUMMARY

The high degree of complexity and uncertainty associated with aerospace engineering applications has driven designers and engineers towards the use of probabilistic and statistical analysis tools in order to understand and design for that uncertainty. As a result, probabilistic methods have permeated the aerospace field to the extent that single point deterministic designs are no longer credible, particularly in systems analysis, performance assessment, technology impact quantification, etc. However, as statistics theory is not the primary focus of most aerospace practitioners, incorrect assumptions and flawed methods are often unknowingly used in design.

A common assumption of probabilistic assessments in the field of aerospace is the independence of random variables. These random variables represent design variables, noise variables, technology impacts, etc., which can be difficult to correlate but do have underlying relationships. The justification for the assumed independence is usually not discussed in the literature even though this can have a substantial effect on probabilistic assessment and uncertainty quantification results. In other cases the dependence between random variables is acknowledged but intentionally ignored on the basis of difficulty in characterizing underlying random variable relationships, a strong bias towards methodological simplicity and low computational expense, and the expectation of modest strength in random variable dependence. Probabilistic assessments also yield large amounts of data which is not effectively used due to the sheer volume of data and poor traceability to the drivers of uncertainty. The literature shows optimization techniques are resorted to in order to select from competing alternatives in multiobjective spaces, however, these techniques generally do not handle uncertainty well. The motivating question is, *how can improvements be made to*

the probabilistic assessment process for aircraft technology assessments that capture technology impact tradeoffs and dependencies, and ultimately enable decision makers to make an axiomatic and rational selection under uncertainty?

This question leads to the research objective of this work which is to develop a methodology "to quantify and characterize aviation's environmental impact, uncertainties, and the trade-offs and interdependencies among various impacts" [44], in order to assess and select future aircraft technologies. Copula theory is suggested to address the problem of assumed independence on the input side of probabilistic assessments in aerospace applications. Copulas are functions that can be used to define probabilistic relationships between random variables. They are well documented in the literature and have been used in many fields such as the statistics, finance, and insurance industries. They can be used to quantify complex relationships, even if that is only qualitatively or notionally understood. In this way a designer's knowledge regarding uncertainty can be better represented and propagated to system level metrics through the probabilistic assessment. Utility theory is proposed as a solution to the challenge of effectively using output data from probabilistic assessments. Utility theory is a powerful tool used in economics, marketing, psychiatry, etc., to express preferences among competing alternatives. Utility theory can provide combined valuation to each alternative in a multiobjective design space while incorporating the uncertainty associated with each alternative. This can enable designers to rationally and axiomatically make selections consistent with their preferences, between complex solutions with varying degrees of uncertainty.

This work provides an introduction to copula and utility theories for the aerospace audience. It also demonstrates how these theories can be applied in canonical problems to bridge gaps currently found in the literature with regards to probabilistic assessments of aircraft technologies. The key contributions of this research are (1) an Archimedean copula selection tree enabling practitioners to rapidly translate their

qualitative understanding of dependence into copula families that can represent it quantitatively (2) estimation of the quantified effect of using copulas to capture probabilistic dependence in three representative aerospace applications (3) an expected utility formulation for axiomatically ranking and selecting aircraft technology packages under uncertainty and (4) a strategic elicitation procedure for multiattribute utility functions that does not need assumptions of independence conditions on preferences between the attributes. The proposed FAAST methodology is shown as an encompassing framework for the aircraft technology assessment and selection problem that fills capability gaps from the literature and supports the decision maker in a rational and axiomatic manner.

CHAPTER I

INTRODUCTION

The aviation industry has experienced rapid growth in recent decades with most stakeholders agreeing that these trends will continue well into the future. Aviation has a significant impact on the environment in many different ways including emissions and noise pollution. As the industry continues to expand in response to rising demand, so will its environmental footprint. There are many different efforts underway to help address the challenges presented by this growth. The most potential for enabling solutions is seen in technological development. However future technologies are inherently uncertain and thus present their own challenges.

Whether applied to existing aircraft or completely novel concepts, future technologies carry an inherent risk due to the uncertainty associated with them. The uncertainty is driven by a myriad of factors including the advanced nature of the technologies themselves, but additionally the challenges of incorporation into the aircraft and integration with other required technologies. While there are many obvious difficulties with representing and propagating uncertain information about technologies, designers also encounter challenges in representing the information they do know about technologies. Sometimes this is due to the qualitative nature of their understanding or is based upon engineering judgment which does not easily translate into conventional methods of quantifying and propagating uncertainty.

In light of these numerous challenges various entities have undertaken long term efforts intended to facilitate the growth of the aviation industry. Critical to informing technology development and investment decisions undertaken by these entities is a better understanding of the risks associated with different technologies. While the

majority of the focus thus far has been on quantifying the uncertainty regarding the unknowns of future technologies, a wealth of information is being left behind in regards to the things we do know from the experience of designers and engineers which can help improve uncertainty quantification. The focus of this research is to leverage existing knowledge and engineering judgment to better represent the uncertainty associated with future technologies and use that capability to demonstrate a number of case studies which can better inform technology development decisions.

1.1 Rising Demand for Aviation

Various entities from aircraft manufacturers to regulatory bodies have forecasted strong growth in demand for aviation in the future. While the estimates vary between different groups one thing is clear, the demand for air travel is significantly growing across the globe. These forecasts are based in part on trends from previous decades and on recent developments of commercial aviation becoming more accessible in many parts of the world. In this sense the demand for air travel is expected to increase both domestically and abroad.

In their Long Range Forecasts report, the FAA has predicted approximately 60% increase in commercial aircraft operations at all US airports by the year 2030 [59]. While the FAA acknowledges the dampening of demand for air travel caused by the recent economic downturn it predicts a favorable long-term outlook. It believes that economic activity drives demand for aviation and therefore predicts aviation activity to recover on pace with the economy. They discuss the various strategic changes made by operators to shed less traveled routes and charge for services that have historically been included in ticket prices. These strategies have resulted in record high load factors which have helped operators cope with rising fuel costs and the latest recession. With improving economic conditions the FAA predicts a steady annual increase in passengers for US commercial carriers from approximately 650

million in the current year to nearly 1.1 billion in 2033 [60].

Airframers are also anticipating this demand and are planning to bring many more vehicles to the market. These new vehicles will not just replace existing or aging vehicles but will actually increase the size of the fleet by nearly 58%. In its Current Market Outlook [24] Boeing claims the worldwide fleet will double from nearly 21,000 aircraft to over 42,000 by 2033. Expectations that jet fuel prices would remain high but stable have not proven accurate recently. Brent crude oil prices have traded in the range of $110, plus or minus $5 per barrel since 2012. However, at the start of this year oil prices tumbled down to below $50 per barrel; levels not seen since the early 2000s when crude oil was trading near $40 per barrel. Analysts have attributed this change to high inventories of oil in the United States and rapidly escalating production of oil in the US [72]. The US Energy Information Agency forecasts high uncertainty in the price of oil due to a myriad of global factors including sustained high levels of OPEC production, the emergence of major middle east suppliers reentering the market, the strength of oil consumption growth, and the responsiveness of non-OPEC production to low oil prices [56]. The volatility in the price of oil underscores the need from an economic perspective for newer vehicles to be even more fuel efficient.

Airbus predicts that as the global economy recovers so will the demand for air travel. They state that overall the aviation industry has been very resilient to many historical crises and has actually grown 61% since 2000. In their Global Market Forecast [3] Airbus claims that increasing urbanization worldwide, and in particular the growth of the middle class from 32% of global population today to 62% by 2032, will increase the propensity to fly. They also predict a doubling of fleet size by 2032 indicating that emerging markets across the globe will play a big part in demand for air travel. Other organizations are also predicting increasing passenger traffic in the short term. The International Air Transport Association (IATA) reports an expected rise of 31% in passenger demand by 2017 in their Airline Industry Forecast [87]. The

IATA system wide outlook estimates passenger growth of 930 million by 2017.

While the exact numbers differ among these forecasts they all predict similar trends for the future growth of aviation, both in the short and long term. The aviation industry and the demand for air travel is expected to see significant growth in the coming decades and this present a great number of opportunities and challenges for all stakeholders. Each stakeholder is concerned with addressing the challenges most relevant to them, e.g. aircraft manufacturers are planning to meet the rising demand for aircraft, airliners are addressing the needs of passengers, regulatory agencies are anticipating how to safely accommodate increased system traffic, etc. However all stakeholders are in some way concerned with the environmental impact of a burgeoning aviation industry. The environment is naturally a concern for all stakeholders because we all share it and are all responsible for it. In this sense it is a common and imperative goal to reduce the environmental footprint of the aviation industry.

1.2 Environmental Impact of Aviation

The aviation industry has a complex and far-reaching relationship with our environment which requires in-depth study and analysis. Environmental effects exist both locally near airports and flight paths and on a global scale affecting the climate and all forms of life on the planet.

As a by product of combustion, aircraft engines emit a variety of dangerous gases and solids into the atmosphere including Carbon Monoxide (CO), Carbon Dioxide (CO_2), Ozone, Particulate Matter (PM), Sulfur Dioxide (SO_2), Volatile Organic Compounds (VOCs), and Nitrogen Oxides (NOx) [249]. Each of these pollutants is associated with their own negative health effects and some are considered lethal in high concentrations. NOx emissions in particular have been directly linked to smog formation and adverse human health conditions. US airports are among the top four emitters of these pollutants in the country. Researchers have pointed to NOx and

CO_2 as the most important gases to be reduced. While varying scenarios have been predicted for the amount of these gases in the atmosphere by the year 2050 [160] and the resulting adverse effects, it is clear that they are the most responsible for atmospheric deterioration and climate change. While reducing emissions of these gases from aircraft directly is vital, it is also important to note that these emissions are produced by the combustion of fuel and air inside the engine. Hence if fuel burn in general is reduced, so will the production of these emissions.

Another important environmental impact of aviation is noise pollution. Noise is described as unwanted sound energy emitted from the aircraft. There are many sources of noise on the aircraft and they all contribute to the total noise experienced by observers on the ground. It is particularly harmful for those living around airports where the presence of aircraft noise is most disturbing. Aircraft noise is more than just a nuisance and has been characterized as damaging to human health and significantly reducing quality of life. In a World Health Organization report [164] aviation noise was linked to hearing impairment, pain, sleep disturbance, stress, cardiovascular effects, and mental disorders. Noise is measured in Decibel scale (dB) and it is typically thought that a limit of 55 dB is required for undisturbed sleep. At a noise level of 70 dB normal speech communication is not possible, yet it is not uncommon to find airport operations occurring well above this value [249].

As the amount of airport operations rise to keep pace with increasing demand, especially in developing parts of the world, the environmental impact of aviation will grow increasingly larger. For the sustainability of the environment, both locally and globally, it is imperative that these environmental challenges be addressed and aviation's future footprint be reduced.

1.3 Mitigating Environmental Footprint of Aviation

The aviation community has been working very hard to address the growing environmental challenges faced by the industry. The focus is on reducing the current footprint of aviation on the environment and on developing solutions to sustain the expected growth. There are several different initiatives established for this purpose which are led by various regulatory bodies and industry partners. An important government led effort in the United States is the the Next Generation Air Transportation System (NextGen) [102], which is upgrading the technology infrastructure of the US air transportation network. Included in its mission is the development of systems and procedures which will reduce the negative impact of the aviation sector on the environment.

Similarly in Europe, the Single European Sky and Air Traffic Management Research (SESAR) [212] project is focused on delivering a new level of performance to the European air traffic system. This includes stated objectives of 27% increase in airspace capacity, 6% reduction in cost per flight, and 2.8% reduction in environmental impact per flight.

In order to accomplish their goals both NextGen and SESAR have supporting programs which are investing in a wide range of technologies to improve the performance of aircraft and their operating networks. The goal of these technology development programs is to select and mature potentially valuable technologies to a level where industry can make use of them more easily. The FAA's Continuous Lower Energy, Emissions, and Noise (CLEEN) program is made up of several commercial industry partners with an overarching objective to "accelerate development and commercial deployment of environmentally promising aircraft technologies and sustainable alternative fuels" [93]. CLEEN's technology development program focuses on delivering mature technologies in the 2015-2018 time frame which the industry can use to reduce environmental impact in the near term. This is known as the N+1 aircraft time frame

[207], which represents the next generation of tube-and-wing aircraft.

The National Aeronautics and Space Administration (NASA) leads another technology development program in support of NextGen called the Environmentally Responsible Aviation (ERA) project. This program focuses on maturing "promising technology and advanced aircraft configurations that meet mid-term goals - in the next five to ten years." [36]. ERA focuses on the N+2 aircraft time frame which represents advanced aircraft after the N+1 time frame [207]. In the long term period which is considered 15-20 years from now and beyond (N+3), NASA has multiple research efforts supporting development for NextGen. These include six different research teams led by industry partners focusing on various aviation sectors including the Subsonic Fixed Wing (SFW) program [186], Advanced Concepts Studies for Supersonic Commercial Transport, Small Commercial Efficient and Quiet Air Transportation, etc. [159].

These programs just represent a portion of the current research for designing the next generation of aircraft which will be among many other things, far more environmentally sustainable. While there are multiple technology development efforts proceeding concurrently, each focused on obtaining various benefits, three main areas have been identified for significant reductions in the literature; aircraft fuel burn, noise, and emissions. These areas have been targeted with several aggressive performance goals stated over time for each goal. They are summarized by NASA in Fig. 1 below [71].

These goals are highly visible in the aircraft design community and are stated as improvements over a reference subsonic aircraft baseline. The N+1 and N+3 goals are reductions compared to a Boeing 737-800 aircraft with CFM56-7B engines and the N+2 goals are reductions compared to a Boeing 777-200 with GE-90 engines. Within each time frame these goals represent a significant advancement of the state of the art. Meeting them will be challenging and will require revolutionary breakthroughs.

TECHNOLOGY BENEFITS*	TECHNOLOGY GENERATIONS (Technology Readiness Level = 4-6)		
	N+1 (2015)	N+2 (2020**)	N+3 (2025)
Noise (cum margin rel. to Stage 4)	-32 dB	-42 dB	-52 dB
LTO NOx Emissions (rel. to CAEP 6)	-60%	-75%	-80%
Cruise NOx Emissions (rel. to 2005 best in class)	-55%	-70%	-80%
Aircraft Fuel/Energy Consumption‡ (rel. to 2005 best in class)	-33%	-50%	-60%

Figure 1: NASA subsonic transport system level goals

In order to meet these goals significant improvements will be needed not only from the aircraft itself but from the industry as a whole. The Intergovernmental Panel on Climate Change (IPCC) issued a report addressing the role of aviation and its effect on the atmosphere [169]. In it they outline a number of options to reduce the negative impacts of aviation including aircraft and engine technology options, alternative fuel options, operational, regulatory, economic, and other options. These various alternatives have also been acknowledged by other entities like NASA, the FAA, and the IATA. Among these various areas of improvement, technology infusion within the aircraft has received special attention in the literature and has been identified as a prime area of research focus. The IATA Technology Roadmap report[88] indicates that future technologies will be a large contributor to the reduction of emissions over the next 35 years, as depicted in Fig. 2.

Clearly infusion of future technologies will play a significant role in meeting the goals outlined by NASA in Fig. 1, and as such will be an overarching focus of this work. Examining vehicle level technology impacts and how they impact performance will be used as an intermediate, yet crucial step towards the broader impact at the fleet level, on climate change, and the environment. The development of advanced technologies for aviation has also been given a national mandate from the White House in the National Aeronautics Research and Development Plan (2010) [44]. In

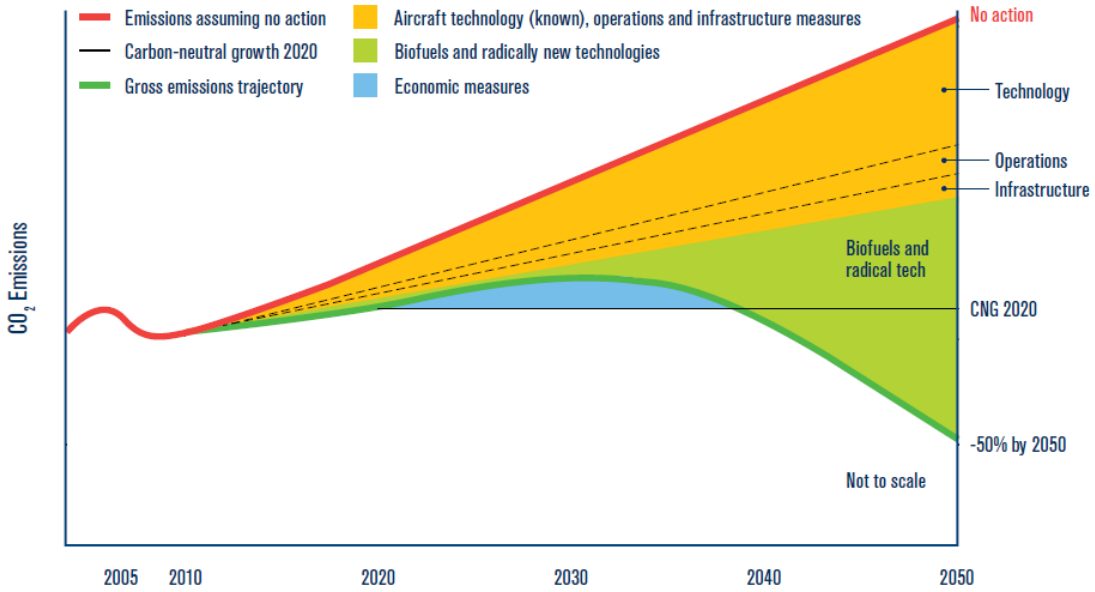

Figure 2: IATA sources of emissions reduction timeline

this report, two goals relating to technology development for aviation have been clearly stated:

1. Advance development of technologies and operations to enable significant increases in the energy efficiency of the aviation system.

2. Advance development of technologies and operational procedures to decrease the significant environmental impacts of the aviation system.

In order to meet these specific goals designers and engineers have been tasked by the federal government with short and long term directives. In the near term they have been asked to develop improved tools, and metrics, "to quantify and characterize aviation's environmental impact, uncertainties, and the trade-offs and interdependencies among various impacts" [44]. This statement is very significant and a key motivator of this work. From it we can understand that adequate characterization and incorporation of uncertainty into the analysis is critical for technology development. How much uncertainty currently exists, how much of it is actually reducible, and what

will it take to reduce it? These are difficult questions to answer but they are very important. Properly understanding how much uncertainty is currently in the system is requisite to being able to reduce it. It is even recognized at the national policy level that understanding the uncertainties, tradeoffs, and interdependencies that currently exist is a fundamental step towards reducing uncertainty in the long term. This will form the first research objective:

Research Objective
Develop a methodology "to quantify and characterize aviation's environmental impact, uncertainties, and the trade-offs and interdependencies among various impacts" [44], in order to assess and select future aircraft technologies.

Many sources of uncertainty exist in this problem, so it is important to discuss the kind of uncertainty we are referring to in this work. Characterizing a technology's impact(s) means establishing a correct mapping between attributes of the system and their resulting effects on the vehicle performance and on the environment. If this mapping is well understood, then it can be quantified to understand how the technology will impact the vehicle. In this context, uncertainties exist when it is difficult to quantify what that impact is going to be for a number of different reasons but mainly because development of future technologies is inherently uncertain as they do not yet exist.

It is also important to understand what is meant by tradeoffs and interdependencies in this context. Given a multivariate function $Z = f(x, y)$, the interdependency is the underlying coupling relationship between x and y in the function f. These interdependencies can exist in a number of ways among technologies. They can be present as underlying relationships between a technology's benefits and degradations, across

multiple technologies, or between technologies and design inputs. A tradeoff exists when there is an underlying relationship that drives x and y in opposite directions that prevents them from reaching optimum levels simultaneously. This necessitates a compromise to balance 2 or more different objectives. Tradeoffs in this problem are not just between competing environmental metrics but also exist with other factors like cost. For example, the number of technologies to apply on a vehicle or pursue and develop (x), versus the cost of doing so (y). The more technologies that are added, the better the system will perform environmentally speaking (Z), but the cost of the system will also increase, so a tradeoff exists for the number of technologies x, and the cost y. It is understood even at the national policy level [44] that recognizing, incorporating, and optimizing for these tradeoffs and interdependencies is critical to achieving the future goals of the aviation community.

1.4 Challenges Posed By This Problem

Government entities and the public sector must lead efforts to push for environmental improvements. Even with public support, it is still extremely challenging to model, predict, and test technologies that will mature 10 to 30 years in the future. Generally speaking, "commercial aerospace systems require 7 to 15 years from concept formulation until the product launch date." [113] The extended timeline makes it very important to make proper technology selection decisions at the outset, or risk significant implications to cost and schedule. Assuming the proper technologies can be matured in the right amount of time, integrating them on the aircraft and within the fleet is extremely complex. On the aircraft level compatibilities with existing and other future technologies must be ensured. Technology impacts that improve performance in one area must be weighed against their potential adverse effects in other areas. On the fleet level benefits must be integrated and proven consistently across many different aircraft. Even if these technologies are successfully developed

and integrated and the long-term goals are met in the future, the cost today of programs like NextGen and SESAR cannot be overstated. NextGen has an estimated cost between 14-22 billion dollars [102] and SESAR will carry an approximate price tag of 30 billion Euros [37]. This is only a brief summary of the many challenges associated with future technology development in the aerospace industry, yet they are still seen as as having significant potential to reach the goals envisioned for the future of the industry.

No single technology exists that will meet all of the different goals which have been stated. As each technology is developed and assessed, its performance relative to the given goals will have to be evaluated. There are multiple objectives in this problem like improvements in fuel burn, reduction of engine emissions, decreasing noise pollution, lowering costs, and others. A technology that brings improvement towards one objective may simultaneously reduce performance in another. Tradeoffs and compromises are necessary to find an optimal solution. Compounding this problem is the fact that these tradeoffs must incorporate the uncertainty associated with the future technology impacts. There are many stakeholders in the industry, each interested in their own specified goals such as emissions reduction or decreasing noise, etc. Each party places differing levels of importance on each goal which must also be captured before making future technology decisions.

Finally, the literature contains extensive amounts of research on potential technologies for future aircraft. There are hundreds of promising ideas to pursue and many future platforms for novel applications. Each technology and future architecture has a set of design variables, noise factors, and evaluation metrics necessary to assess that future system. Additionally all of these aspects have varying levels of uncertainty associated with them. The combinatorial space is excessively large when one tries to capture all of the aspects involved in this problem, particularly when

including the variations in uncertainty in the technologies themselves and their integration into larger systems. This makes the selection of an optimal set of future technologies under uncertainty a very difficult task.

The national mandate [44] mentioned earlier in this section uses specific verbage that directly corresponds with each of the major aspects of this problem. It states that analysts are tasked "to quantify and characterize aviation's environmental impact, uncertainties, and the trade-offs and interdependencies among various impacts." The uncertainty in this problem is directly related to the technology impacts which are not yet fully known. The tradeoffs will take the form of multiple objectives which characterize this problem including reduction of fuel burn, noise pollution, and engine emissions. Related to the uncertainty aspect is the issue of interdependencies between technology impacts, which is also not yet fully known. As a result they are sometimes disregarded altogether, and even in deterministic formulations the interdependencies between technologies are often times ignored. However it is recognized even at the international policy level that interdependencies are important and yet the state of the art fails to capture those trends, at least in the context of uncertain nature of the interdependencies. In light of this national mandate the motivating question for this works is, how can improvements be made to the probabilistic assessment process for aircraft technology assessments that capture technology impact tradeoffs and dependencies, and ultimately enable decision makers to make an axiomatic and rational selection under uncertainty?

1.5 Problem Characterization

The problem described here has several key aspects that can be used to characterize it and approach it axiomatically. First, uncertainty will play a key role and cannot be ignored, so the approach must capture this in some way. It has multiple competing objectives so the approach must be able to account for multiple goals simultaneously.

Each objective also has different target thresholds that can have varying levels of importance for decision makers so the approach must be able to include targets and the preferences of the decision maker. Finally a key aspect of the problem that can't be ignored is the large combinatorial space that exists, so the approach must be efficient and able to handle many different alternatives rapidly. With several different aspects to this problem, it is important to address each of these issues while keeping the scope manageable. This work will examine the quantification of technology impacts at the vehicle level in consideration of uncertainties, tradeoffs, and interdependencies, in order to make a technology selection in light of the relevant aspects of this problem.

CHAPTER II

SURVEY OF PROBABILISTIC ASSESSMENT METHODS

2.1 Introduction

This review will focus on identifying methods and techniques that can address the relevant aspects of the aircraft technology selection problem such as how to capture dependencies between random variables and how to include uncertainty information into the technology selection framework. These can both be addressed by investigating existing probabilistic techniques. Probabilistic methods take on many different meanings in a variety of disciplines from combinatorial mathematics to actuarial sciences. For our purposes in engineering analysis we refer to probabilistic methods as non-deterministic assessment techniques that allow for the inclusion of uncertainty in engineering analysis and design. There is significant literature on probabilistic assessment of future subsystem technologies and concepts for which the impact on system performance is uncertain. Applications such as future aircraft technologies for higher efficiency and lower environmental impact have received significant attention, particularly as they inform policy and direction for research and development. This review identifies and examines the most relevant aspects of this body of work, focusing on probabilistic technology impact assessment for aerospace applications, while giving due consideration to broader applications in engineering.

Probabilistic methods allow the systems analyst or designer to go beyond point solutions and deterministic answers, enabling uncertainty management and the creation of robust designs. Aerospace systems have multiple sources of uncertainty and a main concern is their relative impact on the system response. Probabilistic methods facilitate the observation and assessment of uncertainty so that dominant sources can

eventually be reduced. Zio and Pedroni [257] provide a noteworthy review of the root causes of uncertainty and why probabilistic methods are necessary from a theoretical perspective. They discuss the sources of uncertainty, how it is represented, and how it is propagated with probability theories including imprecise probability, probability bound analysis, evidence theory, and possibility theory. Ryan and Townsend [194] discuss the practical benefits of probabilistic methods in aerospace applications and how they have contributed to the success of key programs such as the space shuttle main engine design. Uncertainty in design requirements and environmental condition necessitates a level of safety in design, formerly mitigated via deterministic safety factors, but more recently with probabilistic methods as a preferred approach.

Probabilistic methods can be broadly categorized as analytical or numerical. A general numerical approach for non-deterministic assessment was reported as early as 1968 [237], summarized in five basic steps:

1. Determine design equations relating properties at lower levels to measures of system level performance
2. Obtain subjective probabilities for subsystem properties
3. Use Monte Carlo to sample from these probabilities
4. Generate statistical measures for resulting systems performance distribution
5. Compare statistical measures across time periods for an indication of progress

This approach has remained largely unchanged since its publication almost 50 years ago, with much of the literature on numerical probabilistic assessment adhering to it. However, there exists a wealth of methodological variations to the above steps, as well as more expansive formulations that build upon it, which over the years have been proposed to resolve distinct challenges and provide greater insight from probabilistic analysis efforts. The aerospace and aeronautics domain has been for

many years one of the most popular and fruitful in terms of relevant applications and methodological improvements. The characterization of uncertain subsystem technology improvements and their impact on system level performance in the aerospace and aeronautics domain are particularly noteworthy. The remainder of this survey article is dedicated to the review of that body of work. In the interest of completeness we briefly review analytical approaches first.

2.2 Analytical Approaches

Analytical approaches are closed-form solutions to uncertainty characterization and propagation. It is generally accepted that analytical methods have more modest system evaluation requirements relative to numerical approaches. The computational power available in past decades, and approximately up to the mid 1990's, made analytical approaches preferable for a vast majority of applications. At the same time, while the fundamental building blocks of analytical solutions offer good generality, important simplifying assumptions are requisite for the development of more useful closed form expressions. Accordingly the value and validity of analytical solutions is predicated on the extent to which said assumptions hold for a problem of interest. Even when some conditions do not fully adhere to methodological assumptions, the analytical approach to assessment may remain preferable over potentially costly numerical solutions.

One of the simplest measures of uncertainty is a sensitivity, or rate of change [150]. In multivariate functions, sensitivities are usually calculated as partial derivatives. Its important to remember that the scale of units will affect the magnitude of sensitivities, so using consistent units is imperative when making comparisons. In uncertainty analysis the practitioner should not only consider the sensitivities, but also the uncertainty of the inputs to those sensitivities. A commonly known first order approximation, the Gaussian approximation [150], includes both sensitivity and

uncertainty by using partial derivatives and standard deviations of the inputs. This method propagates the uncertainty of the inputs by calculating the variance of the output via the input variances and partial derivatives. Sensitivities can also be found by more complex techniques such as the Fourier Amplitude Sensitivity Test (FAST). The FAST method probabilistically determine sensitivities to individual parameter uncertainties of a function. It models multi-dimensional systems as waves and frequencies, then applies a Fourier transform to determine the sensitivities of parameters [46]. Within the aerospace community it has been used in structural analysis [2] and the impact prediction of decaying objects in space [184].

Expansion based methods represent a broad category of expanding analytical techniques for uncertainty characterization. They can be functions of random variables (stochastic expansions) or ordinary dependent variables like the well-known Taylor series expansion which was originally stated by B. Taylor in 1715 [234] and later formalized by J. L. Lagrange in 1772. It uses partial derivatives from a known point to approximate the function value at another point in terms of deviations of the inputs from the known point. It is widely used to model error of approximations provided the error is not large and is measured locally. The expansion can be extended to higher order terms to capture nonlinear behaviors but first order approximations are often used for their simplicity. The first order approximation includes a covariance term between the input variables but this is often ignored based on the assumption of independence between the input variables. In this case the Taylor Series approximation reduces to the first order Gaussian approximation.

Stochastic expansions have been classified under the category of spectral methods [125]. Spectral methods are those that create a functional relationship between the solution and the germ, which is realized through the set of input independent random variables. Different methods exist to create this functional relationship. When this relationship takes the form of a summation of terms, where the arguments of

that expansion are random variables, then they are known as stochastic expansions. Spectral methods like stochastic expansions are advantageous because they converge on the uncertainty moments of the system response faster than traditional Monte Carlo (MC) methods. MC methods are limited in their rate of convergence by the number of realizations and in some systems, MC sampling can be prohibitively expensive motivating the need for faster techniques like spectral methods. Stochastic expansions for uncertainty quantification include many different techniques such as Karhunen-Loeve Expansions, Polynomial Chaos Expansions, Generalized Polynomial Chaos, Galerkin methods, Wavelet Expansion method, etc [125]. While reviewing each is beyond the scope of this work one of the most popular techniques, polynomial chaos theory, is further discussed to provide a sense of how these methods are used.

Polynomial Chaos Expansions (PCE) are a popular stochastic expansion based method because they are functions of random variables. They are a non-sampling based mathematical technique to approximate the uncertainty of a dynamic system. Introduced by Weiner in 1938 [250], the response of the system is approximated using a summation of polynomial functions and a set of unique coefficients for those polynomials. The polynomial functions are known as a chaos basis and are pre-constructed based on the type of random variables used in the system. Since the chaos basis is already known, the challenge lies in solving for the coefficients in the expansion. This can be done intrusively or non-intrusively to obtain the expansion coefficients. Galerkin methods [125] are an intrusive technique which attempts to form a system of governing equations to solve for the PCE coefficients. In contrast, non-intrusive methods use individual realizations of the germ to determine the stochastic model response to random inputs [125]. While both methods have benefits and drawbacks, non-intrusive methods are popular because they leverage information from an existing model familiar to practitioners to determine the expansion coefficients. A key advantage of PCE is that once the coefficients are obtained, they directly provide the

moments of the approximated system response such as mean and variance. In this regard, PCE are more efficient than Monte Carlo based methods. However, for large numbers of random variables PCE become expensive and practically intractable due to the number of terms needed in the expansion [125, Fig 2.7].

Classical PCE require that the germ be a sequence of centered, normalized, mutually orthogonal, Gaussian random variables [125]. Strong dependencies between the random variables or a lack of orthogonality will reduce the accuracy of the expansion. If these conditions are met, Wiener [250] has developed a set of polynomial functions called Hermite polynomials which serve as the set of basis functions in the homogeneous chaos expansion. This work was further extended by Xiu in 2010 [252] to include continuous and discontinuous random variables in the germ. As such, this method is popularly known as generalized polynomial chaos (gPC) framework. Xiu developed the polynomials needed in the chaos basis for a variety of random variables including gamma, beta, uniform, etc [125, Table 2.4]. The gPC framework has been shown to be computationally superior to Monte Carlo methods in a variety of disciplines including stochastic fluid dynamics, stochastic finite elements, solid mechanics, nonlinear estimation, etc. Polynomial Chaos has seen wide use in the aerospace domain for a number of applications including uncertainty quantification of airfoil oscillations [171], analyzing turbulence field for micro air vehicles [183], and for the verification of stochastic solutions [86].

Variance estimating methods are another class of analytical techniques to estimate uncertainty. Among them is weighted sums method which is applied under specific conditions when the approximated function is known to be linear. As the name suggests, a weighted sum of the inputs is used to estimate uncertainty of the response [150]. The expressions for expected value and variance of the response are exact regardless of the distribution over the input vector X. If the distribution over the input is a multivariate normal in the weighted sum model, the resulting distribution

will also be exactly normal. Even if this is not the case, by the central limit theorem, the response will approximate a normal distribution as more and more independent input distributions are included. Another technique in this class is the products of powers of uncertain variables. This technique applies a log transform to a product of the input variables [150]. The transformation turns the function into a weighted sum of the uncertain inputs, similar to the technique described previously. The weights in this case are the powers of the variables. These multiplicative models are widely used in risk assessments of human health, pollution, and the environment [150]. The product of powers model can also be useful for error propagation when applying the Gaussian approximation. In this manner the effort of transforming to and from the log space can be avoided and allows users to make use of arithmetic mean and variances which are better known than geometric means and variances. However the technique only works when the uncertainties are small relative to the means of the variables and leads to a simple formulation for the relative error. This technique is used for error propagation in the physical sciences and engineering fields [30].

Reliability methods are a form of analytical uncertainty analysis popularized in the 1990s by the structural reliability community [57, 111, 128]. These applications used FORM (First-Order Reliability Method) and SORM (Second-Order Reliability Method) techniques that leveraged the most Probable Point (MPP) analysis. The (MPP) method calculates the probability of failure given a constraint in an uncertain multi-dimensional space. This method explores a joint probabilistic space by evaluating limit state functions in an effort to identify the failure region for a particular system. It identifies the failure boundary in the joint probabilistic space while minimizing the number of limit state function evaluations as explained by Du [53]. This approach lost popularity due to the higher dimensionality of recent applications and the proportionally increasing cost of function evaluations with the number of random variables [53]. In the aerospace community the technique did not see extensive use

for technology evaluation and implementation but it did establish how to analyze functions and constraints in a joint probabilistic space defined by multiple random variables. Typical examples of the method exist in the context of aerospace structures and systems analysis [210, 70, 131]. A computer software implementation of this method that was commonly used prior to more efficient surrogate models ([141]) is the FPI technique. Fast Probability Integration is a computerized analytical approach [220] based on MPP analysis that solves the equations representing the limit state function in a joint probabilistic space. FPI has been used to assess individual technologies and their impact on system reliability [26] as well as to examine the effect of uncertain technological impacts from a holistic air traffic system perspective [142]. The process outlined in the latter work describing how to handle uncertainty as a result of technology insertion with probability distributions is particularly relevant and still used in many applications.

In general analytical methods have a couple of key advantages and disadvantages compared to numerical methods [150]. First is the relative ease with which numerical calculations can be executed once the algebraic analysis has been performed. Another advantage is the clarity with which uncertainty contributions can be traced. Generally these methods will separate the variance of each output into the sum of the contributions from each input. There are also several disadvantages including how fast the difficulty of the algebraic analysis increases with the complexity of the model, especially if higher order terms are needed. The tails of the resulting distribution are not well defined because the output is typically given in distribution moments like mean and variance. Analytical methods are generally local approaches and can have large error if the true uncertainties are large, if there are nonlinearities in the model, or if critical dependencies are ignored. These analytical methods can be used to probabilistically handle uncertainty but numerical methods have been far more extensively applied to assess uncertainty for technology modeling in the aerospace community.

2.3 Numerical Approaches

2.3.1 Introduction to Numerical Approaches

Numerical approaches have gained significant popularity in probabilistic assessments over the last two decades, facilitated in part by advanced computing capabilities which make simulations and sampling very efficient and feasible for large-scale applications. In addition modern software packages have simplified the use and implementation of numerical methods, and have made the ensuing analysis much easier through a variety of graphical and visual interfaces. Even with these notable improvements, the basic process used in these numerical probabilistic assessments has not departed significantly from the method outlined by Timson [237], which we also structure our review of the literature pertaining to each of its steps.

2.3.2 System Equations and Response Surfaces as Surrogate Models

The first step in the numerical approach process calls for determining design equations characterizing measures of system level performance as a function of lower-level (e.g. subsystem) properties. This view is particularly relevant for technology impact assessment because technologies are typically applied at the subsystem level, yielding benefits or penalties at that level, but also affecting system-level performance. Models vary vastly in their level of fidelity and sophistication; for most real applications model runtime is not conducive to substantial sampling required by numerical probabilistic approaches. Surrogate models approximate the relationship between model inputs and outputs with reduced runtime cost by virtue of their simpler mathematical form, and thus arise as an enabler to numerical approaches. Common types of surrogate models include but are not limited to, polynomial response surfaces, kriging [192], support vector machines [149], and artificial neural networks [144, 191]. Response surfaces and artificial neural networks are commonly used for aircraft technology impact studies and are discussed further to illustrate how surrogate models are used in

aerospace applications.

Response surfaces can be particularly useful in performing sensitivity analyses, design space exploration, and system optimization. They are generated as an n-variate polynomial regression using a design of experiments as a training data set. Second order response surfaces can sufficiently capture many multinomial systemic behaviors and are a typical starting point in many applications. With greater non-linearity it is possible to include higher order effects or functional transforms. Fundamentals of response surface methodology can be found in various texts [153, 112, 25]. Response surfaces have been used in the probabilistic assessment of large structures [209], space landing systems [213], and many other technology based applications [147, 235, 129]. They have also been used to assess aircraft technology impacts [217] and forecast uncertainty in aircraft technologies [113, 178]. However, response surfaces do not handle non-linear or discrete responses well, which can limit their usefulness in some applications.

Artificial neural networks are a regression technique fundamentally similar to response surfaces but they differ in the form used to capture the relationship between the inputs and the response. They have biological inspiration and are functionally based on the structure of actual neural systems. Their general form incorporates the exponential function and can therefor well capture highly non-linear behaviors and can even be applied to discrete classification problems. Their structure is adaptable using a series of nodes and layers to capture the relationship between the inputs and the response. The set of data to be regressed is used to train the neural network and training algorithm is used to determine the set of coefficients that minimize the training error. Artificial neural networks have recently been used in aircraft technology impact applications for noise modeling [17], propulsion system simulations [126], and comparison of advanced vehicle concepts [91].

2.3.3 Subjective Probability

Modern probabilistic analysis has two main schools of thought concerning probability, the objectivist (frequentist) view and the subjectivist (Bayesian) view. The origins of probability theory help to provide an understanding of which school is the appropriate choice for assessing technology impact uncertainties. This choice will underpin how probability distributions are selected and implemented to represent the uncertain inputs to surrogate models, which is the next step in the numerical probabilistic assessment process. Jacob Bernoulli is credited with formalizing mathematical probability in his seminal book, "The Art of Conjecturing", published in 1713 [19]. In it he provides the definition, "probability is the degree of certainty, which is to the certainty as a part is to a whole" which indicates what probability is but not necessarily how to obtain it. Multiple sources [74, 173, 5] indicate that the frequentist school of thought derives probabilities from the frequency of occurrence over repeated trials. The probability is simply based on the number of observations of an outcome over the total number of trials. In this sense probability is purely empirical and objective. In contrast the subjectivist view is an individual's opinion about how likely an event is to occur. This opinion can be formed in many ways based on experience and can even encompass frequentist observations, but in the end is still a degree of belief. Therefore it is subjective and based upon the knowledge of the analyst who assigns it [74]. This subjective form of probability is particularly useful in situations where it is impractical to hold many repeated trials such as structural reliability analysis or future technology impact assessments.

While subjective probabilities are important tools for practitioners, care must be exercised in the selection of distributions to represent random variables. When distributions are modeled accurately the results of the probabilistic assessment can be credible and meaningful. For instance, it is important to rely on statistical hypothesis testing based on the available data to select the proper distribution type to represent

a random variable, so the choice of distribution can be justified. In some applications [209, 54, 51], the normal distribution is used as a default choice in probabilistic assessments without proper justification because it is easy to understand and familiar to practitioners. This can easily be resolved by using any of a multitude of hypothesis tests available for determining normality of an empirical data set such as the Anderson-Darling test, D'Agostino's K-squared test, the Jarque-Bera test, etc. However, if poor assumptions are made regarding distribution types, parameters, or about relationships between random variables, the results of the probabilistic assessment can be misleading or false. For example, Conrow [40] offers a detailed critique of published literature in which he states that normal distributions should not have been assumed for random variables and provides his own analysis employing the Anderson-Darling and Kolmogorov-Smirnov [120, 216] statistical tests to define distribution type.

Sample size is another important concept when forming subjective opinions about distributions. Jacob Bernoulli [19] stated in a letter to Leibniz that "even the stupidest man knows by some instinct of nature per se and by no previous instruction" that the greater the number of confirming observations, the surer the conjecture [67]. In the absence of these confirming observations, one should not make assumptions about the type of distribution, even through hypothesis testing which requires statistically significant sample sizes [208]. If the proper sample sizes do not exist, one should either generate them following empirical trends using techniques such as copulas [16] or sample from the empirical distribution directly. Significant dependencies among random variables should also be accounted for when determining subjective probabilities. In some applications [177, 143, 255], dependencies are ignored without proper justification for a variety of reasons including a strong bias towards methodological simplicity is preferred, there is high difficulty in characterizing the underlying dependence structure, or there is an expectation of low strength in random variable dependence. Testing for the presence of dependence between random variables is

enabled by the well-known Pearson correlation coefficient [168] or if outliers exist in the data sets, by rank correlations like Kendall's tau parameter [106] or Spearman's correlation parameter [221]. In modern complex systems with many functional relationships, assuming independence may be a simplifying assumption but not necessarily an appropriate one. If dependence does exist between random variables there are techniques to incorporate that dependence into probabilistic assessments, particularly in the context of future aircraft technology impacts. Zaidi, Jimenez, and Mavris [254] suggest a copula based method for better representing the relationships between random variables in probabilistic assessments using subjective input from subject matter experts.

2.3.4 Probability Distribution Encoding

It can be argued that obtaining subjective probabilities and encoding distributions is the most important part of any probabilistic assessment. The validity of the subjectively encoded distributions governs the integrity of the probabilistic assessment results. For this reason, significant attention has been given to examining many different works and processes that demonstrate this critical step. This is to underscore the importance of correctly obtaining these subjective inputs and thereby lending credibility to the outcome of the probabilistic assessment.

Ideally probability distributions would be based on analysis of real world data that form well-defined empirical distributions. This process and the value of sampling from valid empirical distributions is described by Conrow [38]. However in many applications real world data is not available, or difficult to obtain, such as with future technology impacts. Here the literature turns to subject matter experts who provide various forms of information to subjectively inform probability distributions for random variables. Subjective probabilities can also be obtained by other means

such as various forms of interviews and surveys where descriptive phrases are converted into numerical values by respondents. Conrow [39] cautions the use of these types of surveys. He evaluates an earlier subjective probability scales example from 1977 in which qualitative phrases were assigned quantitative probability values from 23 respondents. For example the phrase "probably not" was assigned a probability value of the event occurring ranging from approximately 0% to 45% from the different respondents and the phrase "highly likely" was assigned values for the event occurring from approximately 50% to 95%. The assessment from the original authors has been used in the past in broad applications including defense and industry in order to convert phrases into useful statistics; however Conrow cites several issues with this type of work and specifically with this example including misworded probability statements and incorrect probability bounds. Conrow states that because of these deficiencies, descriptive statistics gathered from this example are not reliable. In light of these results he states from his own text [38] that "estimative probability tables and scales should be viewed as more of a "last resort" than first choice and should not be used in risk analysis unless they are the only available means to evaluate probability".

There is a great deal of established literature on how to properly interview experts and encode probability distributions. Spetzler and von Holstein [222] wrote a seminal paper on probability encoding summarizing the practice of the Decision Analysis Group at Stanford Research Institute. They state that Probability encoding is "the process of extracting and quantifying individual judgment about uncertain quantities" and is a major part of decision analysis. They discuss three main phases of this process, the Deterministic phase, the Probabilistic phase, and the Informal phase. The Deterministic phase establishes variable definitions and the formal model, the Probabilistic phase assigns probability distributions to relevant uncertainties, and

the informal phase is a judgment process where the value of the information is assessed and compared to the cost of obtaining it in order to reduce uncertainty of important variables. The authors provide classifications of variable types such as decision variables which can be controlled by the decision maker and state variables which are outside of their control. They discuss how uncertainty of a variable can be encoded directly or the underlying phenomena can be modeled and the uncertainty of associated variables can be assessed. They provide principles for encoding uncertain quantities and how to best elicit information from subjects in order to enable subject cooperation and obtain meaningful data such as employing a sensitivity analysis to determine important uncertainties and using exact definitions and meaningful scales. They review the importance of Modes of Judgment which is the intuitive process by which people assess uncertainty using cues which are not completely reliable or valid, but still produce reasonable answers while yielding systematic biases. There are three main points to understand from this section of the paper; that people are not aware of the cues they use, it is difficult to control cues used by subjects, and people can be made aware of their biases and trained to control them. The authors continue to discuss sources of bias such as motivational and cognitive biases and other encoding phenomena such as subject adjustment and anchoring. The authors also provide a discussion on encoding methodology and define the basic types including fixed value P-method, fixed probability V-method, or the neither fixed PV method, and how to encode each type such as using a probability wheel. They also provide a description of the interview process with the subject and explain the basic steps which should be taken including motivating, structuring, conditioning, encoding, and verifying. The authors have intentionally given general guidelines for probability encoding and state that each problem will have its own application of these principles. They believe their work is unique because of several distinguishing principles; they believe the pre-encoding steps are critical and more time consuming than the encoding step, they

recommend only ordinal judgments for probability assignments, find the probability wheel as an effective encoding technique for most subjects, and recommend more than one technique be used in order to check for consistency.

Since the early work performed by Spetzler and von Holstein others have also tried to evaluate the most effective encoding techniques. Abbas et al [1] compared two methods for encoding probability distributions of continuous variables; the first gets values of a variable through comparison with a fixed probability wheel and the second through comparisons with fixed values of the variable. Their decision analysis study was conducted using human participants as judges who were asked binary questions based on different decision analysis methods described above. The results of the experiment suggested a slight superiority of fixed value over fixed probability which the authors attribute to the fact that people in general having more experience in their daily lives with making judgments similar to fixed value types of decisions. They mention the difficulty with fixed probability comparisons is that it requires judges to estimate the level at which an event would reach a certain probability which is not as familiar as estimating the likelihood that an event will exceed some predetermined threshold. They conclude that the results were nearly indistinguishable for the two encoding methods but there were systematic differences including the fixed variable method had higher variances which is good because the authors believe subjective probabilities are often too narrow reflecting overconfidence of the judges. In another comparison of encoding techniques, Brooks and O'Leary [27] surveyed professionals whose focus was the evaluation of uncertainty. Their study compared four encoding methods; Bisection, Fractile, Cumulative, and Probability Wheel and surveyed participants who were brokers speculating in the stock market. The authors desired this procedure because they did not want to assume or rely on understanding of statistics from the judges while trying to accurately representing their opinions. In the Bisection method the subject specifies lowest and highest possible values and the analyst

suggests values for comparison beginning with the limits. The Fractile is similar to the bisection but the subject provides the values directly and begins with the median value. In the Cumulative method the subject is asked to provide a probability of falling above or below specified values. The Probability Wheel involves participating in a lottery where the participant wins if the value exceeds a specified threshold, or with a wheel with pointer falling in a wedge. The size of the wedge is varied until the participant is indifferent to the two choices. The authors report that no statistical significance was found in the difference across accuracy rankings but there was among preference ranks. The Probability Wheel was found to be the least desirable, which tends to agree with the results found by Abbas et al [1] in the comparison of fixed probability versus fixed value encoding techniques. This is in contrast to the seminal work done by Spetzler and von Holstein where they found the probability wheel an effective encoding technique for most subjects. Abbas et al, also noted that subjects often asked the analyst to repeat statements multiple times, revealing the importance of the analyst as a resource in eliciting the data.

Some authors have indicated that due to its simplicity the triangular distribution is appropriate for capturing expert knowledge to represent random variables. For example, Williams [251] offers a discussion on how to estimate the proper distribution parameters and which distributions to select when modeling project networks under uncertainty. He acknowledges there are many forms of uncertainty to consider including temporal, financial, technical, and their interactions but focuses on temporal uncertainty and specifically those related to activity-duration which is particularly relevant to technology modeling. He stresses that distribution parameters must be easily understood because difficult estimation can compromise the quality of estimates. He also acknowledges the usefulness of the gamma and beta distribution while noting that they are not as transparent to the project planner. He states that "the parameters and distributions used must be meaningful to the project planner;

thus the problems of selecting a distribution and estimating its parameters are psychological and practical rather than mathematical". This is a key point to understand and account for regarding the encoding of probability distributions in probabilistic assessments. Johnson [97] made a similar case for the triangular distribution. He investigated a method for using a triangular distributions as a substitute for beta distributions in risk analysis. He states that while the beta distribution is suitable for uncertainty studies because it can take a wide array of shapes over a finite interval, its functional form is complex and its parameters are harder to estimate. He proposes the triangular distribution as a suitable proxy for beta because triangular is much simpler in functional form and easier to understand. He states the differences between the two are rarely significant and proposes a method to estimate triangular distribution parameters from two extreme percentiles and a median. The author admits limitations of the triangular distribution in that it cannot reasonably approximate a U-shaped, J-shaped, or uniform distribution, which can be accomplished using a beta distribution.

Still other authors have argued for and demonstrated the use of non-triangular distributions such as the beta or Weibull in uncertainty assessments using technology impacts. Kirby and Mavris [115] examined technology uncertainty in preliminary aircraft design stages due to incomplete knowledge regarding the impact of future technologies. They showed how technology impact uncertainty can be captured using Weibull distributions and justified the choice because it "is a family of distributions that can assume the properties of other distributions such as an exponential, normal, or Rayleigh." They subjectively encoded Weibull distributions for technologies at given TRL (Technology Readiness Level [135]) levels and adjusted the Weibull distribution shape parameters to follow a range of applicable values in the probabilistic assessment. Jimenez et. al. [95] presented a comparison of four different probabilistic assessments performed on the NASA Environmentally Responsible Aviation (ERA)

problem for future aircraft technology section. Each assessment was performed using a different approach to subjectively encode technology impact distributions based on the information available from subject matter experts. The four main types of input distributions evaluated were the uniform distribution, the Weibull distribution, the mode-centered Weibull distribution, and the triangular distribution. Each probabilistic assessment approach reflected varying levels of information availability and encoding effort which ultimately drives the uncertainty in the response metrics in the output of the probabilistic assessments. The authors stated that while general trends can be extracted about the ERA concepts and technologies from all four encoding techniques, they favor the mode-centered Weibull input distribution as having the best balance of data requirements and acceptability of underlying assumptions. In another application of technology impacts Hendricks et. al. [79] discuss a systems engineering approach for strategic planning of the air transportation system in which technology infusion is also considered. The uncertainty they considered stemmed from the risk of the technology in terms the improvement it attempts to make in system performance and from the estimated completion date of a technology based on its maturity. The authors suggested using the beta distribution to model these uncertainties while concurrently employing a weighting scheme based on the TRL of each technology. By varying the beta parameter they were able to model the impact and uncertainty associated with a technology based on information available about the technology program.

2.3.5 Probability Distribution Sampling

The numerical approach for probabilistic assessment relies on sampling the subjective probabilities to quantify system level uncertainties. Timson's method explicitly calls for Monte Carlo sampling but other techniques also exist. Monte Carlo sampling is "the generation of random objects or processes by means of a computer" where "the

idea is to repeat the experiment many times (or use a sufficiently long simulation run) to obtain many quantities of interest using the Law of Large Numbers and other methods of statistical inference [121]." There are different ways to create random numbers but this is a practical consideration that isn't a major concern as they are embedded in most current software packages. Typically these random number generators are actually "pseudo-random" because they rely on large pre-existing data tables and a seed which tells the machine where to start in the table. Theoretically if one could identify and replicate the seed, the same sequence of numbers could be repeated. However, the chances of this are very low because the tables are large enough to avoid this with any randomly chosen seed, so they are really pseudo-random, but treated as truly random in practice. Park and Miller [165] provide further reading on the characteristics of good random number generators, how the are created, and practical considerations when implementing them.

An important technique used in many machines to create a variety of probability distributions is the inversion method. The inversion method is a well known approach in random number generation and vastly documented in the literature [223, 83, 34, 224]. The mathematical formulation and practical considerations are discussed at length by Devroye [52]. The inversion method relates a standard uniform random variable to a cumulative distribution function using the inverse CDF of the function. A pdf distribution can be readily generated by evaluating a randomly sampled standard uniform distribution through the inverse CDF distribution. Closed form analytical solutions for the inverse function do not always exist, so numerical approximations using linear interpolation with small intervals are sometimes necessary.

The random samples are used to evaluate objective functions to generate statistics which provide useful information about the responses of interest. There are different variations of Monte Carlo simulations including Markov chain Monte Carlo [148],

Direct simulation Monte Carlo [21, 228], and others whose evolution has been discussed by Richey [181]. They are found in a plethora of applications in the literature [170, 47, 89, 151] and also specifically for technology modeling purposes [185, 85, 4].

Other techniques to sample from probability distributions include Gibb's sampling [62], Rubin Importance-Sampling [189], Sobol's sequences, and even more methods which are surveyed in detail by [61]. Sobol's sequences for uncertainty modeling are particularly useful in sampling and random number generation due to the distribution of the resulting sequences. The basic theory attempts to create an efficient and quick summation of a function to approximate the integral of the function [218]. It can be used to form quasi-random uniform partitions in a given interval. Quasi-random partitioning results in less randomly scattered points than traditional Monte Carlo methods such that there is more uniform dispersement of the samples. This is because quasi-random sampling generates a set of points that are "maximally self-avoiding" [197]. Sambridge and Mosegaard [197] also provide a helpful graphical depiction of the difference between pseudorandom and quasi-random sequences. The technique has been applied in sampling for design optimization [146] and improving the development of continuous response surfaces [167].

2.3.6 Statistical Measures to Evaluate System Performance

Sampling the subjective probability distributions and evaluating the design equations with these probabilities creates output distributions for system level responses. These distributions reflect the performance of the system responses but also help characterize the uncertainty. The sampling process propagates the uncertainties from the lower level design parameters to the upper level system performance metrics. Statistical measures of the output distributions provide analysts with a method for characterizing uncertainty and managing it. This process represents the last two steps of Timson's numerical probabilistic analysis method and encompasses the ultimate goal

of probabilistic methods.

There are many different ways to statistically evaluate the output distributions. One can examine the pdf of a response to see how frequently a particular value of the response occurs. The CDF of the response can be analyzed to determine the probability that the response is less than or equal to a certain value. The pdf can easily reveal the overall minimum, maximum, and range of values. The pdf can also provide statistical moments that characterize uncertainty like the mean and variance. Higher order moments like skewness and kurtosis can also be obtained for further comparisons. The pdf resulting from a numerical sampling-based simulation also provides well-defined tails relative to some analytical approaches [150]. This can be important when examining remote probabilities or values in the extremes of a distribution where the only feasible solutions exist in many technology applications. Whether statistical comparisons are made over time as Timson's method suggest or between different alternatives, they can help an analyst manage uncertainty in order to reduce it. Comparing means and variances from pdf distributions is relatively straight forward but comparisons between CDFs can be less obvious since they all range from zero to one. While this may sound discouraging, given the right tools, CDFs can actually be better for individual comparisons as they are typically far less noisy than empirical pdf distributions.

Statsical hypothesis tests can provide a useful way to measure how different two CDFs are and quantify that change. Two well documented statistical comparison tests for CDFs in probability and statistics literature are the Kolmogorov−Smirnov test [120, 216] and the Cramer−von Mises test [45, 243, 7]. The null hypotheses for both methods is that the two samples being tested are drawn from the same distribution. The test statistics of both methods can be used to quantify the difference between the two CDFs. The Kolmogorov−Smirnov test statistic is particularly simple to understand and represents the value of the maximum difference between the two

empirical CDFs. It can assume values between 0 and 1 where 0 indicates no difference between the two distributions, and 1 indicates the maximum difference between two distributions. The Cramer−von Mises test statistic is a sum of the squared difference of the two empirical CDF distributions and provides a better representation of the difference between the two curves along the full range of their values rather than just the maximum difference at one point. This statistic assumes values between 0 and infinity where 0 indicates no difference.

Timson's method intended for probabilistic assessments to track uncertainty over time to provide analysts and decision makers with a better understanding of the problem as more knowledge became available. However, with slight modifications this method can be extended to a variety of different applications. Other relevant statistical measures can be used to make trades between uncertain alternatives, determine how far a design is from reaching a goal, or improving the robustness of a design so it can better withstand random noise. Some of these relevant and challenging applications for probabilistic assessment methods are discussed in the next section.

2.4 Applications of Probabilistic Numerical Approaches

2.4.1 Design for Robustness

Originally formulated by Taguchi in 1987 [233], the robust design methodology seeks to find settings of design variables which minimizes the response variation to noise variables that cannot be controlled [172]. When this philosophy is applied to probabilistic assessments, it seeks to answer a specific question of how to reduce the variability in the output subject to uncertain input distributions. This has particular relevance to technology modeling because as technologies mature more information about their impacts becomes available. In some cases this decreasing uncertainty can

inform analysts that distributions of technology impacts may not follow early estimates. Robust design principles can be applied in probabilistic assessments to create designs that are more insensitive to these kinds of uncertainties or other environmental factors.

Design of robustness with respect to technology modeling can also be conducted with a focus on specific responses such as direct operating cost or return on investment. Technologies can be infused in designs to make a particular concepts more insensitive to noise variables in a probabilistic assessment, such as fuel price. DeLaurentis [50] applied a form of stochastic optimization in order to account for uncertainties in conceptual aircraft design and to identify a robust design in the face of those uncertainties. His methodology is formulated to handle uncertainties with mathematical models, operational environments, response measurement, and input requirements. It divides parameters into design variables and uncertain variables. The user must assign pdf distributions to the uncertain variables based on historical data or expert opinion. Through a combined design of experiments a cdf of the response values is created by sampling the pdf distributions in each case repeatedly. The cdf is then discretized into n points, where n is the desired number of probability levels for each objective. The discretized points of the cdf are used to generate the response surfaces which provide a functional relationship between the design variables and the cdf. He suggests not using fewer than 5 points when discretizing a cdf in order to regress it and form an accurate representation of the cdf. This type of approach implies a relatively fast execution time is needed, at least in the preliminary run of the design of experiments which may be computationally expensive depending on the number of variables required. The methodology is applied to the design of a supersonic transport and an optimization procedure is executed where the probability of a specific economic response ($/RPM) is maximized as a function of design variables and uncertain noise variables that are given as less than a particular

threshold value. This shows how the robust design approach can utilize probabilistic assessment techniques to create an aircraft concept less sensitive to environmental factors.

2.4.2 Stochastic Optimization

Stochastic optimization encompasses a general class of optimization techniques characterized by the use of randomness to maximize/minimize an objective function. The objective itself can be a function of random variables, the optimization search technique can include randomness, or a combination of both can exist. Developed around the 1980's and 1990's, many techniques exist for the class of problems where the search of the preferred solution is governed by stochastic processes. Genetic algorithms [82], simulated annealing [117], and random search [256] are some of the most well-known and documented in optimization textbooks [241, 180, 162]. These optimization techniques are well suited for discrete objective topologies or highly nonlinear multi-modal objective functions. In many cases these search algorithms are themselves stochastic, but their objective functions are typically deterministic. In contrast, the other class of stochastic optimization techniques have objective functions that use random variables or constraints, such as stochastic approximations [182] and stochastic gradient descent [119]. The latter class of techniques are more relevant to numerical probabilistic assessment approaches as they rely upon random variables which can follow subjective probabilities. The design equations that relate the inputs and outputs in probabilistic assessments are also functions of random variables, so stochastic optimization can be used to optimize system performance as the objective function. Each iteration could be used to improve upon the settings of input distributions until a global optimum is found while demonstrating an improvement in statistical performance measures with each iteration.

Stochastic optimization techniques can also be used in reliability based design formulations where optimum designs are created for multiple uncertainties such as cost and operating conditions. Sues et al [225] presented a unique stochastic optimization methodology for aeropropulsion components and demonstrated it on the design of an axial compressor. They incorporate 3 types of variables in their methodology; deterministic design variables, random design variables and simple random variables whose mean values do not change during optimization. The optimization technique is nonlinear programming applied to objectives and constraints that are functions of random variables. The main objective is performance based, that being to minimize cost of the compressor blades which is a function of the weight and efficiency of the design. The methodology differentiates between single occurrence random variables (occur once during the component lifecycle) and operational random variables (vary periodically throughout the lifecycle) and uses a two level Monte Carlo simulation to handle each type. The optimization scheme models single occurrence random variables in the upper level ensuring the reliability constraints are met, and models operational random variables in the lower level which maximize the expected value of the objective function during normal operating conditions. The method incorporates a statistical expectation for the efficiency of the design which is a function of two twist parameters in the blade design and a blade thickness variable that are assigned lognormal distributions to account for uncertainties in manufacturing. The authors compared the results of their baseline case, the deterministic optimization, the stochastic optimization, and deterministic optimization with safety factors and concluded that the stochastic optimization yielded the best results because the stress and deflection constraints were reliability based ensuring a moderate overall cost but good performance under extreme rotor speed conditions. Their work demonstrates how probabilistic assessment and stochastic optimization techniques can be combined to find an optimum performance-based design.

2.4.3 Technology Impact Modeling

Predicting the performance of future aircraft is a challenging endeavor for a variety of reasons including many forms of uncertainty and the fact that the development cycle is very long, ranging from 7-15 years for commercial aerospace systems [113]. Future technologies that will be incorporated into the aircraft design may still be under development or may not even exist at the concept formulation stage. Models of technology behavior are needed to make proper technology selection decisions at the outset, or risk significant implications to cost and schedule. Technologies of interest can be modeled by way of performance benefits and degradations at the subsystem level where the effects are approximately known. Intermediate impact factors in the performance model can capture these effects and propagate them to aircraft mission-level measures of performance. By treating impact factors as random variables, the performance model can effectively be made probabilistic with respect to the technology impacts.

The literature contains textual references for how to conduct early forms of technology modeling exercises including Porter et. al. [176] and Twiss [240]. When evaluating multiple technologies simultaneously it can become difficult to accurately represent and predict performance. There are many considerations to make when forecasting the effect of a technology on a future aircraft including its associated benefits and degradations, its holistic vehicle-level impacts, interactions and incompatibilities with other technologies under consideration, maturation timelines, maintainability, cost, etc. Large technology portfolio assessments require a methodology to effectively model and predict performance. Kirby [116] proposes the Technology Identification, Evaluation, and Selection methodology which is one of the most detailed and relevant technology modeling processes in the literature for aerospace applications. This methodology formalizes a normative and explorative approach to design space exploration of the vehicle and technology space. It incorporates two key techniques for

evaluating a portfolio of technologies and making selections between them including the Technology Impact Matrix (TIM) and the Technology Compatibility Matrix (TCM). The TIM contains the predicted impact values of each technology if they were matured to full-scale application (TRL = 9). The TCM allows a designer to quickly remove technology combinations which are "not physically realizable" from consideration. In this methodology Weibull distributions are used to probabilistically represent the uncertainty associated with a technological impact given its current TRL level. The TIM and TCM can be used to create many different future technology concepts with varying levels of technological uncertainty, that can be probabilistically evaluated to determine the best suite of technologies for a particular set of requirements.

Other authors have proposed and demonstrated technology modeling methodologies as well. Weisbin et. al. [248] propose a methodology for technology selection for new initiatives which can support selection and decision making of R&D tasks. Their methodology is demonstrated on Mars exploration rover projects. Technology options are addressed in the methodology by capturing uncertainties in the capabilities using probability distributions on performance attributes. The authors developed a technology costing procedure which includes uncertainty and an interview based peer review of the technology cost estimate. Their selection process is based on evaluations of risk, cost, and performance. Projects are selected in this trade space assuming a given total budget. Their selection process also identifies the main drivers of the result and is flexible enough to adapt many other applications. Suh et. al. [226] propose a methodology for estimating the impact of technology infusion in complex systems including changes to the original system, cost of technology infusion, potential market impact, and an estimation of net present value of the infused technology. Their approach focuses on the creation of Design structure Matrix (DSM) [58] which is a matrix representation of the original product that includes the product components and the connections between them. Their 10 step methodology is applied to

a complex printing system modeled by an 84 element DSM. A delta DSM is created describing the changes between the original and technology infused product. Value and cost of the existing product is calculated by attribute based theories and then the value of the technology infused product is found. Uncertainty in demand and cost is incorporated using probability distributions on annual demand and machine population cost savings to determine the change in net present value of the technology infused system by Monte Carlo simulation. Their work also includes a notable literature survey and gap analysis for technology infusion problems.

Many applications exist for technology impact modeling of future complex systems which employ techniques described earlier in numerical probability assessment methods. For example, Landry and Archer [123] present a high-level state model of the national airspace system (NAS) which can account for uncertainty within the NAS due to incorporation of various technologies and concepts. The authors perform a rigorous mapping of technologies to sources of uncertainty. They utilize multiple probability distributions including Erlang, Gamma, and Bernoulli distributions to model the source of uncertainty with each technology. They indicate the nominal distribution type and parameters for probabilistically modeling the technological uncertainty, noting the sources of uncertainty and the expected effects. They use various settings of the input distributions to reflect different assumptions and run simulations to evaluate the effects of changing these inputs. They hope to identify emergent effects and provide guidance for prioritizing the development and integration of specific technologies into the NAS. Additionally Mavris and Bandte [138] create a holsitic technique for technology impact modeling, to consider all disciplines and lifecycle phases as advocated by advanced product design philosophies. They account for benefits and risks of technologies by replacing point design solutions for ones featuring variability. This is executed using a Robust Design approach that employs RSM (Response Surface Methodology) surrogates as an enabling technique.

RSM is used to conduct analysis of variance in a screening test to pick the most significant contributors to performance and economic metrics, and to conduct Monte Carlo simulations on probabilistic variables. All economic noise variables identified were given triangular distributions based on historical data which was used to determine ranges and mode, with the exception of an engine technology complexity factor that was uniformly varied. Economic target value is compared against statistics of the resulting distribution. They found that the baseline is not good enough to meet targets so technology infusion is used to achieve the required weight reduction. These technology improvements are selected by the designer and have significant impact on the feasibility of the design.

Timson's probabilistic assessment method is meant to compare levels of uncertainty over time. From a technology modeling standpoint, this is useful because technologies mature and assessments should be repeated with the latest information to manage uncertainty. However, a relevant extension of this method leveraging the probabilistic technology impact modeling, is how to make selections between competing technology portfolio options (i.e. specific technology packages) that are uncertain. It is also important to ask what are the proper statistical measures to use when trading off technology packages. This is essentially a decision making problem under uncertainty and the literature has many different techniques to assist decision makers in these situations. Popular techniques include Analytical Hierarchy Process [195], Euclidean Distance to Ideal [163], and the Taguchi Loss Function [232]. These techniques operate on deterministic attributes of the alternatives and do not handle uncertainty well in their frameworks. Additionally they have all received some level of criticism for being inherently flawed or failing to meet certain principles of proper decision making under uncertainty (Ref. [78, 43]. Other approaches for finding optimum designs in the set of technology packages make use of stochastic optimization

techniques. Jimenez et. al. [94] used a genetic algorithm operating on the deterministic values of the technology package's performance to seek out a Pareto frontier of technology solutions in the objective space. However the optimization procedure did not consider or incorporate the uncertainties associated with these future technology packages. The literature also indicates that decision making under uncertainty should adhere to logical, objective, and axiomatic principles that yield a sound and repeatable ranking of the alternatives. It further states that utility theory adheres to these principles and that expected utility is a valid measure for rank ordering alternatives under uncertainty. Therefore expected utility could be applied as a valid measure that incorporates uncertainty in an extension of Timson's framework to make selections between competing technology packages. Questions such as these help to envision future applications of Timson's probabilistic assessment method, underscoring its continuing relevance to uncertainty problems today and in the future.

2.5 Conclusion

This survey performs a broad review of the probabilistic assessment literature and how it handles technology impact uncertainties. It presents key methods and techniques of dealing with uncertainties under two distinct categories, analytical and numerical methods. Timson's numerical method for probabilistic assessment [237] is emphasized as a basic methodology for handling uncertainty, which is knowingly or unknowingly used by many practitioners. Numerous relevant aerospace applications are presented from the literature including technology impact modeling, highlighting Timson's method as a basic, yet extensible framework for dealing with uncertainty problems in the aerospace field and beyond.

2.6 Observations From the Literature

The literature review has shown that the assumed independence of random variables is common among probabilistic assessments in the aerospace field. This is found across a

variety of aerospace disciplines and even in recent applications of probabilistic assessments such as those in Refs. [139, 137, 255, 28, 29, 177]. These random variables can represent design variables, noise variables, technology impacts, etc., which are often difficult to correlate but do have underlying relationships. The justification for the assumed independence is usually not discussed as is the case with Refs. [177, 143, 255] even though this can have a substantial effect on probabilistic assessment and uncertainty quantification results. While it is possible that independence between random variables is the appropriate choice, this should be verified for each case. Generally speaking, many random variables modeled by system analysts do have statistically significant relationships between them and should be tested for correlation to determine the proper input relationships. In other cases, the dependence between random variables is acknowledged but not included on the basis of difficulty in characterizing underlying random variable relationships, a strong bias toward methodological simplicity and low computational expense, and the expectation of modest strength in random variable dependence [28, 29]. Depending on the application, these dependencies can have a significant impact on propagating uncertainty to response metrics and results. This is particularly true for future aircraft technologies which will have to be integrated into a single complex vehicle.

Another recurring observation in aerospace applications of probabilistic theory is the arbitrary or unjustified use of distribution types. Proper statistical tests are not used to accept or reject distributions. When this is ignored, random variables can be represented improperly, and historical trends or physical phenomena can be described poorly by assumed distribution types. Additionally, low sample sizes have been used when choosing distribution types to model a data set. The difficulty with this is that, even if statistical tests are used to accept or reject a particular distribution type, their results will have limited statistical power and accuracy for low sample sizes. Conrow [41] offers a detailed critique of this poor practice within the aerospace domain as is

the case with Refs. [54, 127]. Conrow discusses multiple issues that can be reformed to improve probabilistic assessments including understanding the difference between a statistical test accepting a given probability distribution and not rejecting it, and employing statistical tests at varying significance levels before deciding on a particular distribution type for a given data set. It is also important to note that there is a great variety of distributions that have been suggested by probability and statistics theory and have been used in many applications to model uncertain factors including the Triangular [124, 251], Uniform [11, 140], Beta [97, 104, 12], Weibull [11, 175], and others. The seminal work by Spetzler and Stael von Holstein [222] discusses techniques for encoding probability distributions from experts and even proposes a structured interview method which has become widely accepted. However the normal distribution is often used as a default choice in many fields including aerospace engineering as seen in Refs. [54, 209, 187, 51] due to its familiarity and ease of implementation. Multiple statistical tests exist to check for the appropriateness of the normal distribution including D'Agostino's K-squared test, the Jarque−Bera test, the Anderson−Darling test, etc. Although the normal distribution is certainly useful and versatile, it is not always the best choice, and these methods should be consulted before assuming a normal model. While each case will be different, poor assumptions of distribution types can lead to inaccuracies in uncertainty quantification and probabilistic assessment results.

In early years of modern computing, processors were not as efficient as today. As a result surrogate models were harder to develop and each additional variable in the analysis resulted in significant run time expense. This ensured that analysts only used the most important variables or made simplifying assumptions to reduce the dimensionality of their problems. This also yielded a smaller amount of output data from the probabilistic assessments, relative to today. Today, limitations on computing power have decreased and probabilistic assessments can easily include

hundreds of variables with unique distributions. Correspondingly the amount of data resulting on the output side of the probabilistic assessment is enormous. The problem now is no longer that we are unable to include all the relevant parameters into an analysis, but rather that it is difficult to manage and make sense of the shear volume of output data. There are so many options to choose from on the output side that it is difficult to choose. It was thought that by inputting every relevant variable into the probabilistic assessment, the answer would become clearer on the output side thereby simplifying the selection process. Psychologists have explained why the opposite is in fact true regarding choice. In his book called the "The Paradox of Choice" [206], Schwartz argues that the more options available to a decision maker, the more paralyzed they become in the decision making process and the less satisfied they will be with whatever option is eventually chosen. It is therefor important to enable the decison maker to effectively utilize the output data and logically and axiomatically capture their preferences.

In aircraft technology assessments there are thousands of resulting technology combinations available and the challenge now is how to manage that data in order to make a selection. Even Pareto frontiers have become so populated that alternate coordinate systems are needed to make clearer decisions, as seen in the work by Daskilewicz [48]. Additionally the solutions from optimization schemes that produce the Pareto frontiers are deterministic points, they do not account for the uncertainty associated with each solution. Without including the uncertainty associated with each solution, it is difficult to address how to make a selection between even a few different alternatives, let alone thousands. For example in Fig. 3 there are two notional technology solutions or packages from which a decision maker can choose. Each point represents an identical baseline vehicle with a different set of future technologies applied to it, which result in differing performance along the objectives. In this case the objectives along the axes are noise margin above a certain limit and fuel

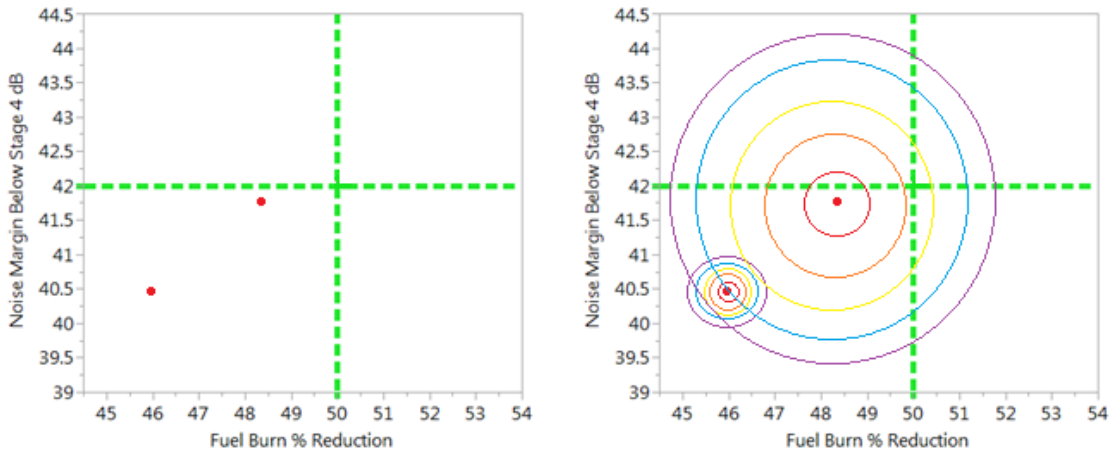

(a) Two deterministic technology solutions (b) Two probabilistic technology solutions

Figure 3: Technology package selection with and without uncertainty

burn reduction over the baseline, so higher values of both are more desirable. The technology impacts associated with each of the technology packages represent how the inclusion of this technology package will change the baseline vehicle's performance. The uncertainty in the technology impacts is captured by a probabilistic assessment.

Examining Fig. 3a the selection may seem obvious in terms of which technology package is preferable. However these points only represent the deterministic value of the solutions, formed by evaluating the technology impacts at their nominal values. Fig. 3b shows the same two notional points but with uncertainty bands surrounding them reflecting the uncertainty associated with that solution's technology package. Including the uncertainty of the technology package makes the decision non-trivial and may even change a decision maker's outcome based on their attitude towards uncertainty. In fact with the uncertainty included it can be difficult to make a selection between just a few points, let alone the hundreds that may be present on a multiobjective Pareto frontier. Current applications will perform probabilistic assessments to track uncertainty but still make decisions based on deterministic results. This indicates the need for a decision making method that incorporates uncertainty into the ranking process in a logical and objective manner in accordance with the

decision maker's preferences.

2.7 Summary of Challenges To Be Addressed

There are many different technologies being developed for future aircraft and lots of other areas of research to help reduce the environmental footprint of aviation. Fayette Collier, the manager of the NASA Environmentally Responsible Aviation project, said that the "real challenge is to integrate ideas and pieces together to make an even larger improvement." The goal of this work will be to enable practitioners with the tools to bridge gaps that exist within probabilistic assessment methods today so that future technology assessment and selection can be conducted in light of the uncertainty that exists. The methodology will aim to provide simple techniques for capturing dependencies between input random variables. The method for specifying dependence structure will need to allow for flexibility of input distributions so analysts can use whichever type is appropriate for their application. On the output side it will have to incorporate the uncertainty associated with the technology impacts into the ranking and selection process. This process will also have to be consistent with the decision maker's preferences so they are satisfied with the selection method and not paralyzed or mislead by it.

CHAPTER III

TECHNICAL APPROACH TO THE AIRCRAFT TECHNOLOGY ASSESSMENT AND SELECTION PROBLEM

3.1 Approach Formulation

The aircraft technology assessment and selection problem must be addressed from both the input and output of the probabilistic assessment process, because aerospace applications employ flawed methods on both sides. The only way to realize full benefit from these analyses is to bridge gaps on both sides and more accurately represent the uncertainty that exists. The approach presented here will therefore be two pronged with analysis of techniques, proposed solutions, hypotheses, and experiments on both the input and output sides of the probabilistic assessment. These two sides will be the core focus of the work in this thesis and will be discussed in detail in the next two chapters. The impetus for this work arises from the need to probabilistically incorporate dependencies between random variables input to probabilistic assessments while including the uncertainty information they output into a ranking and selection process for aircraft technologies, and the opportunities enabled by copulas theory and utility theory for doing so. An overarching framework will also be developed to tie together all the relevant pieces into a generic methodology to enable practitioners in all fields where probabilistic assessments are employed.

The framework is created by starting with a generic decision support process, the Georgia Tech Generic Integrated Product and Process Design (IPPD) Methodology for Trade Studies [200]. The key decision support steps of this process are summarized in Fig. 4. While developed for IPPD processes, this generic framework can

be extended to any application where decisions must be made, such as the aircraft technology assessment and selection problem.

Figure 4: Generic decision support process from Georgia Tech Integrated Product and Process Design

The technical approach will address all of the challenges identified in the observations section of the literature review chapter. These observations can be used to visualize the main problem of this thesis in terms of these generic decision support steps. This is visualized in the right column of Fig. 5.

The evaluation of alternatives and decision making steps are very important to the proposed methodology for the aircraft technology assessment and selection problem. In particular utility theory and Timson's method [237] which were identified in the literature review will be used to create the specific methodology for this problem in a nested fashion. The scientific method will be used to formulate hypotheses and experiments to overcome these challenges. The results of the experiments will help identify the proper techniques for the identified problems. The proposed methodology will include incorporate these techniques to create a generic framework for probabilistic assessments. The main problems identified in the literature review process will help

Figure 5: Aircraft technology assessment and selection problem cast through generic decision support process

form the key requirements of the proposed methodology.

3.2 Methodological Requirements

The methodology must provide practitioners with tools to bridge the gaps that have been observed in the field. There is a need to capture dependencies between random variables that are input to probabilistic assessments. These dependencies can have far reaching effects on uncertainty, particularly in complex systems like aircraft. It is likely that these dependent relationships are not known exactly due to the uncertain nature of future technology impacts. However experts in the field can provide notional or qualitative understandings of these dependence relationships. The methodology must be able to capture this subjective and qualitative knowledge to specify the dependent relationships between random variables.

It was also observed that sometimes normal distributions are used to represent input random variables when they are not appropriate. As a result when dependencies

are specified between random variables, the methodology must allow for flexibility to specify any appropriate distribution type for the input random variables. This specification should not remove or alter the dependence structure desired between the random variables.

The aircraft technology assessment and selection problems has multiple goals and varying targets for each goal. The methodology must be able to handle multiple objectives and the different targets in each objective. It should provide a way to combine the different objectives and their target values into a single metric that can be used to evaluate compare different solutions, rank them, and make a rational selection.

Uncertainty associated with the future technologies is a key aspect of this problem and must be accounted for in the methodology. The level of uncertainty can completely change the choice of a decision maker compared to a strictly deterministic selection. The methodology must be able to incorporate the level of uncertainty associated with the technology packages. This uncertainty presents a level of risk to the decision maker and the methodology must capture their preferences to both risk and the objectives.

3.3 Methodology Outline

The literature review brought to light a fundamental approach for non-deterministic probabilistic assessments. This approach outlined by Timson in 1968 [237], represents the core steps needed in the process and provides a great starting point for the proposed methodology. The basic steps in Timson's method are listed below and it is visualized in Fig. 6.

1. Determine design equations relating properties at lower levels to measures of system level performance

2. Obtain subjective probabilities for subsystem properties

3. Use Monte Carlo to sample from these probabilities

4. Generate statistical measures for resulting systems performance distribution

5. Compare statistical measures across time periods for an indication of progress

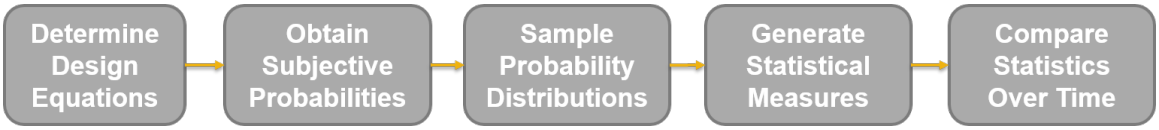

Figure 6: Timson's method (1968) for non-deterministic probabilistic assessments

The aircraft technology assessment and selection problem can be viewed from the perspective of Timson's method. This relies on the foundation provided by Timson but recasts each step as appropriate for this problem. The result is seen in Fig. 7.

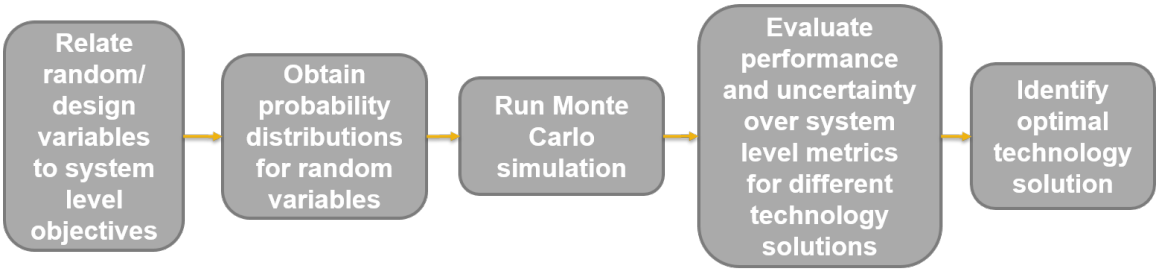

Figure 7: Aircraft technology assessment and selection problem cast through Timson's method

The gaps identified in the literature review phase which have helped to form the methodological requirements can also be placed within this process to create the framework of the proposed methodology. After the design equations in step 1 have been determined, subjective probabilities are obtained in step 2 to help represent random variables in the probabilistic assessment. Step 2a is the first identified gap regarding the dependencies between random variables which will be obtained from subject matter experts (SMEs) when eliciting subjective probabilities. In this step important dependencies between random variables will be captured with simple tools that can probabilistically represent the dependence between the variables. Step 2b

will be to allow for specification of the random variable distribution type independent of the dependence structure. The selection of the distribution type to represent the random variable should be in accordance with empirical evidence, statistical testing, or SME knowledge. This flexibility is important so that poor assumptions regarding inappropriate distribution types can be avoided. These improvements will be input to step 3 of the process where the probability distributions are sampled.

Step 4 entails generating statistical measures from the probabilistic assessment to gauge system performance. Step 4a is to incorporate uncertainty into the system performance measures so that it can be used in the selection process. Step 4b will be to capture the decision maker's preferences and target values into the system performance measures. Step 4c will combine the various performance measure for each of the different objectives into a single multiobjective criterion. Step 5 is to compare statistics over time with the presumption that uncertainty decreases over time and comparison of statistics should yield newer and more accurate information. In the proposed methodology step 5a focuses on using the single multiobjective criterion developed in the previous step to axiomatically and objectively rank order the potential technology package solutions. This logical ranking will allow for a sound comparison of alternatives across the probabilistic design space and enable technology package selection. The outline of the proposed methodology will be as follows:

1. Determine design equations relating properties at lower levels to measures of system level performance

2. Obtain subjective probabilities for subsystem properties

    (a) Capture significant dependencies between random variables by subjectively encoding them as specified by subject matter experts (SMEs)

    (b) For random variables that have dependencies, specify the random variable distribution types independent of the joint dependence structure

3. Use Monte Carlo to sample from improved subjective probabilities

4. Generate statistical measures for resulting systems performance distribution

   (a) Incorporate uncertainty into the system performance measures

   (b) Capture the decision maker's preferences and target values into the system performance measures

   (c) Combine various performance measure for each of the different objectives into a single multiobjective criterion

5. Compare statistical measures across the probabilistic design space to make a selection

   (a) Use single multiobjective criterion to objectively rank order the alternatives in the solution space

   (b) Make selection based on highest rank value

This outline and the gaps identified in the aircraft technology assessment and selection problem can be visualized in Fig. 8.

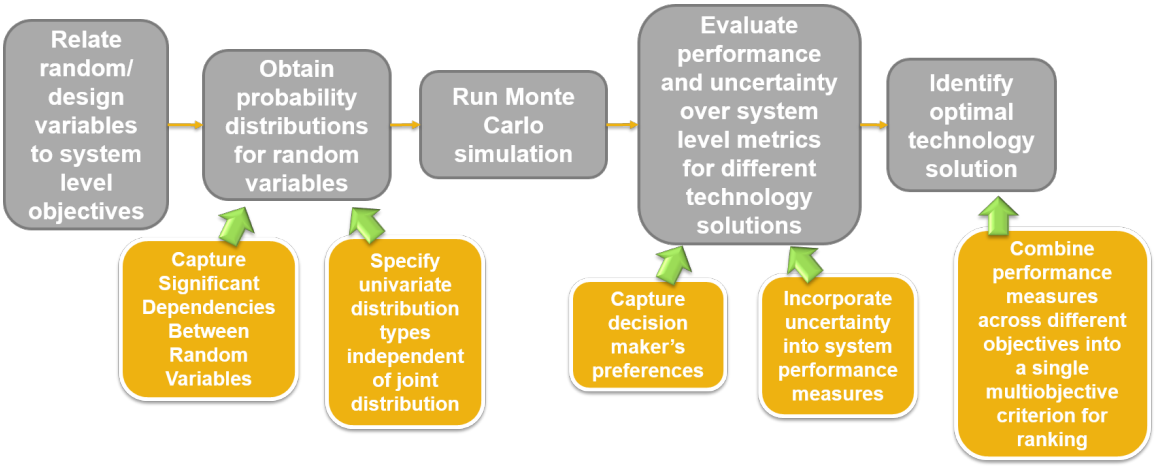

Figure 8: Identified gaps (yellow) in the aircraft technology assessment and selection problem

The different aspects of this problem require that new and existing techniques be identified to find potential solutions. These methods will be incorporated into the generic methodology outlined above on the input and output side of the probabilistic assessment. The next two chapter will detail how this will be accomplished. Combining the different elements of these methods will create a unique formulation that provides a single answer which is intuitive to the decision maker, under a unified framework that does not yet exist.

3.4 Methodology Flowchart

The outlined steps and identified gaps are summarized into a generic methodology for the technology assessment and selection problem. The capability gaps addressed by the method are shown in yellow which extend Timson's method. The green arrows represent new breaks from Timson's method used to fill these capability gaps in the aircraft technology assessment and selection problem. This methodology is called the FAAST Method - Future Aircraft Assessment and Selection of Technologies Method. The FAAST Method is visually depicted in Fig. 9

This proposed approach was formulated using Timson's [237] method for probabilistic assessments. In fact, the top row of blocks represent the basic steps from his method with small variations. It has been extended to fill the gaps identified from the literature survey to form a unique methodology for the aircraft technology selection problem, but generally applicable to probabilistic assessments in other fields. FAAST is an extension of Timson's method for the aircraft technology assessment and selection problem. Timson's method was shown to fit within the generic decision support process in Fig. 5. In this sense FAAST is nested within Timson's method, which is nested within the generic decision support process. The next two chapters will develop and experiment with additional tools nested inside FAAST to demonstrate its capabilities.

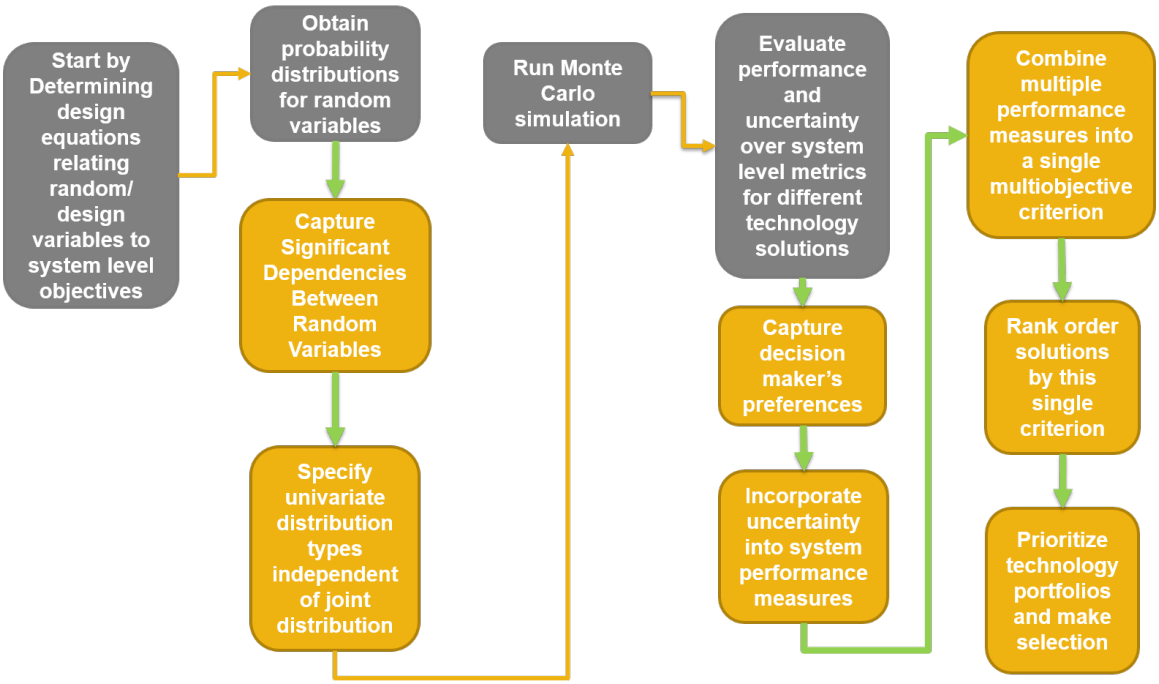

Figure 9: Future Aircraft Assessment and Selection of Technologies (FAAST) Method Flowchart

CHAPTER IV

DEPENDENCE MODELING WITH COPULAS

4.1 Introduction

The literature review has identified that dependencies between random variables are not usually included in probabilistic assessments. The focus of this chapter will be copulas theory which can be used to address this gap from the literature. Probabilistic assessments require input distributions for random variables which are sampled during the analysis. The assessment, whether it is conducted by the popular Monte Carlo procedure or using other techniques, will run regardless of what input distributions are provided. The important issue is that the quality of the output data and the conclusions drawn from it will depend directly on the quality of the inputs. Quality in this sense refers to how accurately the random variables represent physical principles and reality, including the relationships that exist between the random variates. The need to capture these dependencies and the effects of not doing so have been well established in the literature and are outlined in the previous chapters. Several common measures of sample correlation are investigated to determine their usefulness in addressing this part of the problem.

4.2 Measures of Sample Correlations

4.2.1 Pearson's rho

The most commonly used correlation is the Pearson product-moment correlation coefficient. It was created in 1896 by Professor Karl Pearson [168]. The coefficient is a measure of the linear correlation between two variables X and Y, and can range from +1 (highly positively correlated) to 1 (highly negatively correlated) and 0 representing low correlation. It is commonly denoted by the Greek letter ρ and its formula for

a sample of x and y is provided in Eqn. 17.

$$\rho = \frac{\sum_{i=1}^{n}(x_i - \bar{x})(y_i - \bar{y})}{\sqrt{\sum_{i=1}^{n}(x_i - \bar{x})^2}\sqrt{\sum_{i=1}^{n}(y_i - \bar{y})^2}} \tag{1}$$

Pearson's rho is widely used for linear dependencies as an effective measure of correlation. As it can take on negative values, it also provides a measure of correlation in inverse relationships. However, it does not capture nonlinear dependence structures well. So just because a sample has low Pearson correlation does not necessarily mean that some form of nonlinear dependence does not exist. Additionally, Pearson's rho is sensitive to outliers in the sample set. The presence of outliers can drastically change the coefficient value.

4.2.2 Spearman's rho

In 1904 Charles Spearman addressed some of the shortcomings of the Pearson product-moment correlation by publishing his Spearman's rank correlation coefficient [221]. It is called a rank correlation because it is not calculated directly on the values in each set but rather on their ranks within the set. Spearman gives two main advantages of his method. He claims that ranked correlation is less sensitive to outliers or what he calls "accidental error". He also states that by using rank the underlying distribution does not have to be the same to compare sets, "a series presenting the normal frequency curve can be compared on even terms with another series whose curve is entirely different." Spearman's ρ is calculated very similarly to Pearson's ρ as seen in Eqn. 19, except that here X and Y are not the actual values of the sample in the set. They are the rank order number of the values in each set.

$$\rho = \frac{\sum_{i=1}^{n}(X_i - \bar{X})(Y_i - \bar{Y})}{\sqrt{\sum_{i=1}^{n}(X_i - \bar{X})^2}\sqrt{\sum_{i=1}^{n}(Y_i - \bar{Y})^2}} \tag{2}$$

Spearman's ρ also takes on values from -1 to 1, with a 0 value representing no linear rank correlation. When ties exist in rank due to repeating values, the rank given

to the ties is the mean of what the ranks would otherwise be. When determining the ranks in a set, the set can be ordered ascending or descending. Spearman's ρ can capture some nonlinear forms of dependence better than Pearson's, especially if they are completely monotonic, but in general it measures linear correlation better.

4.2.3 Kendall's tau

In 1938 Maurice Kendall developed a rank correlation coefficient known as Kendall's τ [106], that is based on the number of concordant and discordant pairs in a ranked set. A pair of observations (x_i, y_i) and (x_j, y_j) are concordant if the ranks for both elements agree. This is true when both $(x_i > x_j)$ and $(y_i > y_j)$ or if both $(x_i < x_j)$ and $(y_i < y_j)$. A discordant pair is when $(x_i > x_j)$ and $(y_i < y_j)$ or if $(x_i < x_j)$ and $(y_i > y_j)$. Kendall's τ is determined by ranking the samples, determining the number of concordant τ_c and discordant pairs τ_d, and applying Eqn. 18.

$$\tau = \frac{\tau_c - \tau_d}{\frac{1}{2}n(n-1)} \tag{3}$$

Kendall's τ also ranges from -1 to 1, with a 0 value representing no linear rank correlation. Kendall claims an advantage of his coefficient is that it more rapidly approaches normality relative to Spearman's ρ, even for small sample sizes [106]. Kendall's τ is also primarily used to measure linear correlation and can give a low value for nonlinear dependence structures.

4.2.4 Concordance

Lawrence Lin published the concordance correlation coefficient, denoted ρ_c, in 1989 [130]. It is based on a ratio of the covariance between the variates and their individual variances. In mathematical terms it is stated as the difference from unity of the ratio of the expected orthogonal squared distance from the line $x = y$ to the expected orthogonal squared distance from the diagonal $x = y$ assuming independence. For a sample it is calculated as

$$\rho_c = \frac{2s_{xy}}{s_x^2 s_y^2 + (\bar{x} - \bar{y})^2} \tag{4}$$

where s_{xy} is the covariance, s_x is the variance and $\bar{x}$ is the mean. In contrast to Pearson's ρ, by including the covariance term, the concordance correlation coefficient will be sensitive to whether biased or unbiased versions for variance estimation are used.

4.2.5 Brownian covariance

The Browninan covariance is a distance correlation method to determine correlation. It was published by Gabor Szekely in 2007 in order to overcome the inability of other correlation measures to detect non-linear dependence structures. The complex procedure for calculating the covariance is based on the pairwise distances of all pairs in the sample, forming a distance matrix for each set based on the distance variance, distance standard deviation, and distance covariance. The Brownian covariance is then found by calculating the average of the product of the two matrices. The process is detailed further in the literature [231, 230], but the main advantage is its ability to not give a zero value when statistical correlation exists. In fact, a zero value of Brownian covariance implies statistical independence.

4.2.6 Observations from Literature Review

Some correlation measures handle certain dependence structures better than others, but the most popular ones are best for measuring linear correlations. This review brings to light the important distinction between measuring existing correlations and defining correlations. Methods for the latter purpose are not as well known in the literature, yet they are very relevant to modern applications, in particular for this problem. All of the techniques reviewed above can measure the degree of correlation between samples of two random variables but they are unable to dictate that correlation in the generation of new correlated samples. In other words, they cannot specify

the joint distribution between two random variables, they can only measure it. This literature review did reveal methods capable of doing so, the most powerful of which is known as copulas.

4.3 Copulas

4.3.1 Introduction and Usage

Copulas are well known in finance and statistics fields, and are a key enabler for capturing dependencies between random variables. They can specify probabilistic joint distributions between random variables. Copula theory is proposed on the input side of probabilistic assessments to mitigate the problems of ignoring dependence and assuming normal distributions without verification. The objective is to capture significant dependencies between random variables and propagate them through the probabilistic assessment in order to better represent the uncertainty in system level responses. Assuming independence between random variables overestimates the uncertainty of system level metrics and by using copulas to capture dependencies, the variance of these system level responses can be improved.

Copulas are most useful when existing data is not available to define the dependence structure between two random variables, but subject matter experts are able to provide qualitative information about dependencies between random variables. This is particularly relevant to the aircraft technology assessment problem when future technologies make it difficult to quantify technology impacts. In this problem the system analyst is inferring what the dependence structure should look like based on qualitative information from subject matter experts to forecast technology impacts in the future and their dependencies. Ignoring these dependencies can lead to misrepresentation of the uncertainty on system level metrics which will affect the technology selection problem on the output side of the probabilistic assessment. It should be noted that copulas define a specified degree of uncertainty between random variables,

which must be reflected in the the true relationship between these variables. It is important to understand the use of copulas is predicated on some understanding of underlying relationships subject to uncertainty. In this sense copulas enable the system analyst to capture educated qualitative judgments on the relationships between random variables while preserving the uncertain nature of the relationship. The practitioner should be aware that the use of copulas requires engineering judgment and that they should not be applied arbitrarily to relate all random variables, in particular those which are better described by independent or deterministic relationships. However the literature shows that many joint distributions do not meet this criteria, making it prudent to recognize and better characterize relationships between random variates.

4.3.2 Origins and Basic Concepts

The literal meaning of the word *copula* is a link, tie, or a bond. The connection between variables provided by the copula and the manner in which it is created will be the focus of this section. While copulas may have been used and known by other names, the earliest formal reference to copula first appeared in Sklar's 1959 paper [211]. Nelsen, author of one of the most authoritative references on the subject [154], describes how 'The name "copula" was chosen to emphasize the manner in which a copula "couples" a joint distribution function to its univariate margins.' While it is not a formal definition, it helps us to understand that the role of a copula is to join a multivariate distribution function with its one dimensional marginal distribution functions. A marginal probability distribution gives the probability of values that a single random variable may take without reference to the values of any other variables. Alternatively it is the probability distribution of a random variable when considered by itself with no influence from other variables. A multivariate distribution shows how two or more marginal distributions are jointly distributed.

Fundamentally, a copula is a multivariate probability distribution function of which the one-dimensional marginal distributions are each uniformly distributed. The copula function represents a joint distribution which specifies a particular dependence structure between the marginal distributions that it links together. This dependence structure described by the joint probability distribution can be controlled by parameters in the copula function to model varying degrees of dependence between the marginal distributions. A key advantage of copulas is their ability to separately define the joint distribution dependence structure from the univariate marginals. This means that the choice of the marginal distributions is not constrained by the selection of the copula. Statistically speaking, the selected copula links the marginal distributions with a unique joint probability distribution, defined independently of the individual univariate distributions. This is very convenient in many engineering applications because system analysts are able to worry about the dependence or the marginal distributions, one at a time, and specify each as desired. Not having to specify the joint distribution and marginal distributions concurrently enables better representation of the marginal distributions and the underlying relationships between random variables. In fact, the marginal distributions do not even have to prescribe to the same distribution type once the copula is paired with an appropriate transformation procedure.

Copulas are defined on the n-dimensional unit hyper cube for which each of the n random variables is standard uniform distributed $U(0,1)$ (e.g. defined on the unit square for 2 variables). Nelsen further explains that if two random variables X and Y have marginal distribution functions $F(x) = P[X < x]$ and $G(y) = P[Y < y]$, respectively, and a joint distribution function $H(x,y) = P[X < x, Y < y]$, then each pair of real numbers (x,y) will be a point $F(x), G(y)$ in the unit square. Each pair (x,y) will also have a corresponding value in the joint distribution $H(x,y)$. This correspondence, which translates how each pair (x,y) will be appear in the joint

distribution, is a function known as a copula.

Copulas have known functional forms that can be tuned to achieve any degree of dependence between random variable n-tuplets. An interesting and important property of copulas is that while the joint distribution structure it defines can take on a variety of topological features the marginal distributions remain unaffected. Copulas include different parameters which control the degree of dependence between the random variables. The variable θ is commonly used in single parameter families to control the degree of dependence and the shape of the joint distribution between the random variables. One-parameter copulas are the most popular due to their simplicity, although other families of copulas with multiple parameters exist.

4.3.2.1 Sklar's Theorem

Sklar's seminal work outlines the theoretical foundation of copulas predicated on his theorem that expresses the copula as a function of univariate cumulative functions and equates it to a bivariate analogue. The theorem is stated as follows:

Let H be a joint distribution function with margins F and G. Then there exists a copula C such that for all x, y in their domain

$$H(x, y) = C\left(F(x), G(y)\right) \tag{5}$$

Conversely, if C is a copula and F and G are distribution functions, then the function H defined by Eqn. (5) is a joint distribution function with margins F and G. This equation expresses a joint distribution H in terms of a copula C and two univariate distribution functions F and G but in general Sklar's theorem is extensible to n-dimensions. The copula can be expressed in terms of any number of univariate random variables that follow a known distribution. By rearranging Eq. (5) the copula C can be expressed in terms of the joint distribution H and the inverse functions of the univariate marginal distributions as in Eq. (6)

$$C(x, y) = H\left(F^{-1}(x), G^{-1}(y)\right) \tag{6}$$

This basic idea is used to generate many different families of copulas. To uniquely define the copula C, F and G must be continuous. Otherwise C is only uniquely defined on the range of F and G, which is an important detail in the solving for the inverse of F and G to generate the copula C. Similarly the copula and the joint distribution can be used along with the inverse of one univariate distribution to define the remaining univariate distribution. The relationship between the two univariate distributions will correspond to the structure of the specified copula.

As Sklar's Theorem shows in Eqn. (5) the joint distribution function H that represents the copula is defined between two marginal univariate distributions F and G. F and G are the cumulative distribution functions of the random variables x and y. No matter what the value of the continuous random variables x and y, F and G being their CDFs can only take on values between 0 and 1. Therefore, the joint distribution between them H (the copula) can only exist between 0 and 1. This is what limits the domain of the copula. While extensible to multiple dimensions, it will always exist on the unit hypercube because it is constructed by operating on the CDFs of marginal distributions as given by Sklar's Theorem. Additionally, copulas by definition only exist between standard uniform random variables [154, Sec 2.2]. One of the most interesting properties of copula functions that is also reflected in Sklar's Theorem is that they do not alter the marginal distributions because they only affect the joint distribution between the standard uniform random variables. In this way the univariate marginal distributions are never altered and always remain standard uniform. This property greatly facilitates the use of copulas in the many applications because the inversion method can be used to transform the standard uniform marginal distributions to any desired type of distribution.

Copulas have been researched and explored at great lengths in the fields of mathematics and statistics. Numerous papers in these fields that delve into the properties of copulas and how they relate to other mathematical concepts exist. Genest and

MacKay [63] have authored a paper discussing how copulas can be derived from basic calculus and how they relate to Kendall's tau. Kumar [122] describes the appeal of copulas and in particular discusses the Ali-Mikhail-Haq Copula and how it can be used in data analysis. Specific work has also been done in researching copulas themselves and how to develop new families of functions. Hering and Stadtmuller [80] expounded on Archimedean copulas and how they can be simulated in high dimensions even when higher-order derivatives are needed to evaluate the copula functions. Durrleman et al. [55] studied transformations involving copulas and showed how some result in better fits to certain types of dependence structures. Copulas are therefore a well known and established part of the mathematics and statistics literature. Further detailed reading on the fundamentals of copulas can be found in chapter 2 of Nelsen's most recent text [155] and in chapter 8 of Ruppert's text [193] on statistics and data analysis. Additionally, in a thesis written for the field of business and commerce, Chen [33, chapter 2] offers a good review of copulas and their basic formulations.

4.3.2.2 Archimedean Copulas

The Archimedean class of copulas is particularly relevant and useful because of the great variety of important copula families it contains, each with their own unique properties and dependence structures. This work will focus on the Archimedean class of copulas due to the large variety of dependence structures it represents and the wide use of its copula families in the literature and common practice. One of the most important and attractive features of Archimedean copulas is the simplicity of their mathematical formulation, and thus the ease with which they can be created. They are generated using a unique $generator function, \phi_\theta(t)$ that defines a family of copulas, as follows in Eq. (62)

$$C(u, v) = \phi_\theta^{(-1)}(\phi_\theta(u) + \phi_\theta(v)) \tag{7}$$

Table 1: Copula families and corresponding theta values

Family	Copula $C(u,v)$	Generator Function $\phi_\theta(t)$	$\theta \in$
Clayton	$\left[\max\left(u^{-\theta}+v^{-\theta}-1,0\right)\right]^{-1/\theta}$	$\frac{1}{\theta}(t^{-\theta}-1)$	[-1,∞), excluding 0
AMH	$\frac{uv}{1-\theta(1-u)(1-v)}$	$\ln\left(\frac{1-\theta(1-t)}{t}\right)$	[-1,1)
Gumbel	$\exp\left(-\left[(-\ln u)^\theta+(-\ln v)^\theta\right]^{1/\theta}\right)$	$(-\ln(t))^\theta$	[1,∞)
Frank	$-\frac{1}{\theta}\ln\left(1+\frac{\left(\mathrm{e}^{-\theta u}-1\right)\left(\mathrm{e}^{-\theta v}-1\right)}{\mathrm{e}^{-\theta}-1}\right)$	$-\ln\frac{e^{-t\theta}-1}{e^{-\theta}-1}$	(−∞,∞), excluding 0
Joe	$1-\left[(1-u)^\theta+(1-v)^\theta-(1-u)^\theta(1-v)^\theta\right]^{1/\theta}$	$-\ln\left[1-(1-t)^\theta\right]$	[1,∞)

where C is the copula, u and v are standard uniform random variables, and θ is the correlation parameter of the generator function $\phi_{(\theta)}$. The generator function defines a *family* of copulas for which θ can assume values from a prescribed domain. The generator function must satisfy certain conditions. The generator function and its inverse must be convex. They must be monotonically decreasing on the ordinate and their domain on the abscissa must be from 0 to 1. If their domain on the ordinate is finite they are classified as non-strict generators, otherwise they are called strict generators as described by Nelsen [154], section 4.1. Table 1 summarizes some of the most commonly used Archimedean families of copulas, noting their name, generator function, and domain for θ.

A convenient way to visualize copulas is through scatter plots depicting simulations of each random variable and their joint distribution. These scatterplots make it easy to see the unique properties of each copula family and the effect of varying their correlation parameter. Iso-probability contours and three-dimensional figures can also be used to visualize copulas, although they can disguise the differences between copulas in some cases [8]. Procedures for the simulation of random variable

copulas are detailed in subsequent sections. Algorithms typically involve the cumulative distribution function, its inverse, its derivative, and the inverse of the derivative. Numerical approaches are often needed as the analytical solution for said functions is not trivial or does not exist. Simulations for selected copula families are illustrated in Fig. 10 (Clayton), Fig. 11 (Gumbel), Fig. 12 (Frank), and Fig. 13 (Joe), with n=10,000 data points and varying values of the correlation parameter θ as per the allowable domain in each copula family. Some copula families have been named after their original proponent as shown in Table 1, otherwise the copulas are unnamed by Nelsen and are referred to by their enumeration in his text [154, chap. 4]. These figures also illustrate the marginal distributions of random variables u and v to show that they remain standard uniform regardless of the choice of copula family, their corresponding generator function ϕ_θ, and the correlation parameter θ. The most interesting cases include when θ significantly varies from negative to positive as seen with the Clayton (Fig. 10) and Frank (Fig. 12) families.

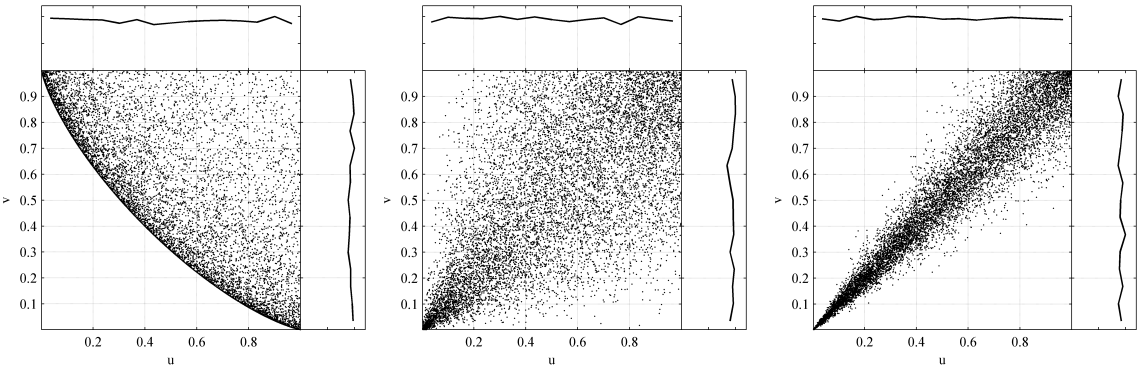

(a) θ = -0.75 (b) θ = 2.0 (c) θ = 10.0

Figure 10: Simulations of Clayton copula with 10,000 points at various values of θ

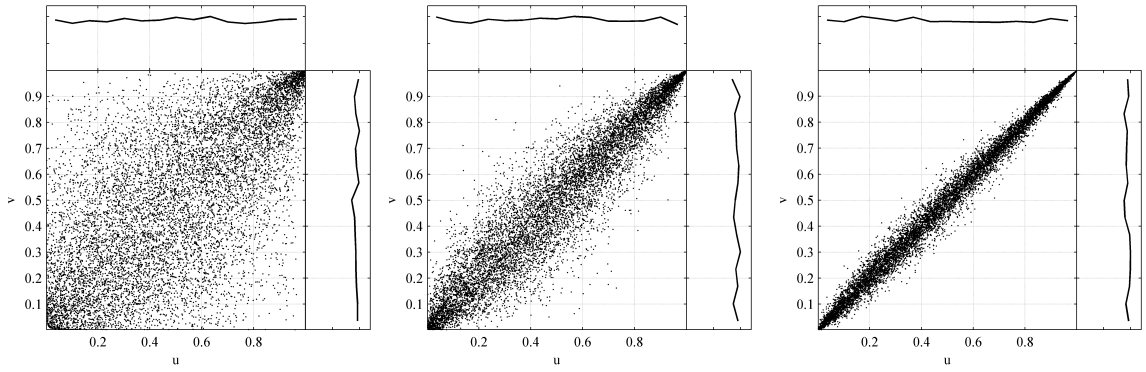

(a) $\theta = 2.0$ (b) $\theta = 5.0$ (c) $\theta = 15.0$

Figure 11: Simulations of Gumbel copula with 10,000 points at various values of θ

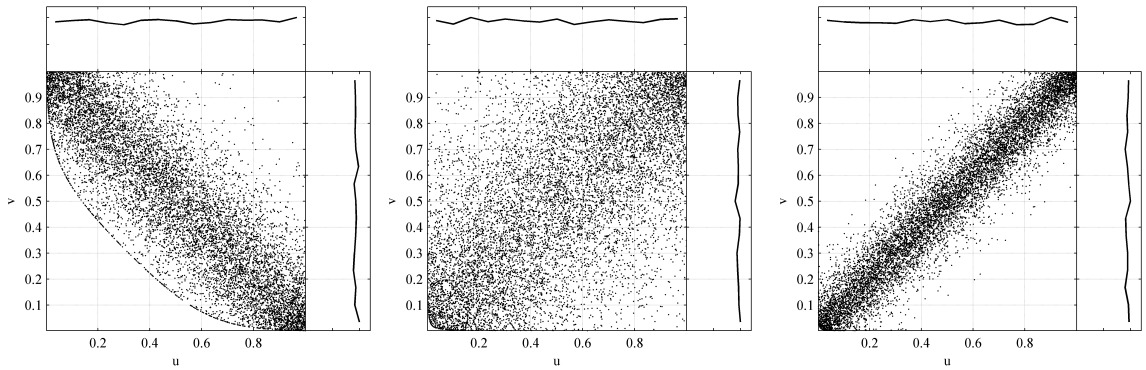

(a) θ = -10.0 (b) $\theta = 5.0$ (c) $\theta = 20.0$

Figure 12: Simulations of Frank copula with 10,000 points at various values of θ

4.3.3 Modeling and Simulation of Copulas

Modeling copulas through simulations is an important part of any problem which seeks to leverage the power of this theory to define dependencies between random variables. It is also essential to visualizing different copula families and identifying their unique properties in order to select the proper family and θ value for the problem at hand. There are multiple ways to visualize copulas, each with their own benefits and drawbacks which should be explored in detail. These procedures are beyond the scope of the current research plan, but are expounded upon in detail in Appendix 7.1.

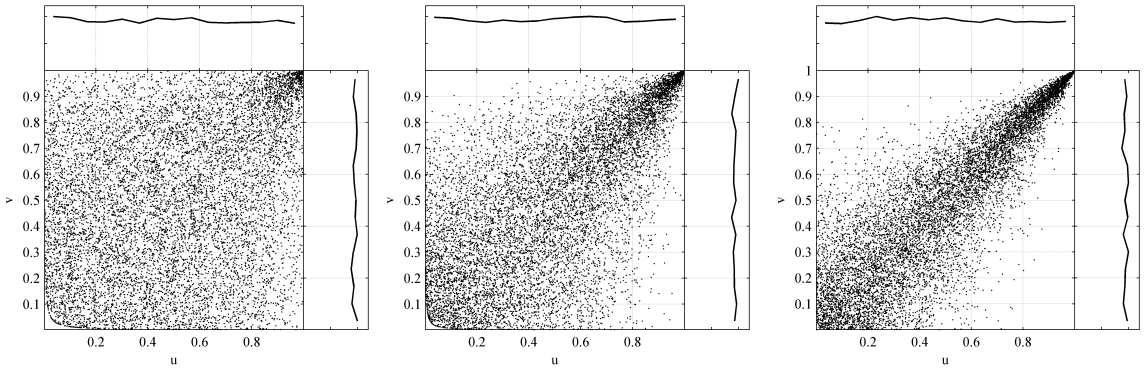

(a) $\theta = 1.5$ (b) $\theta = 3.0$ (c) $\theta = 5.0$

Figure 13: Simulations of Joe copula with 10,000 points at various values of θ

4.3.4 Copula Marginal Distributions

The marginal distributions of copulas are always uniform but this is usually not the case for input random variables in probabilistic assessments of complex systems. The desired marginal distribution to represent an input random variable to a probabilistic assessment can be obtained in many ways such as, elicitation from subject matter experts, matching historical trends, fitting to existing data sets, etc. Once a target marginal distribution is chosen to represent the input random variable in the probabilistic assessment, the copula can be mapped to it using the inversion method.

4.3.5 Inversion Method

A copula is defined in the $\mathbf{I}^n$ space for n standard uniform random variables. In practice the vast majority of non-deterministic systems analysis problems subscribe to other univariate distributions. It is therefore necessary to transform the standard uniform distribution to any other distribution such that the underlying dependence between standard uniform samples related by a copula is preserved. Such a transformation mechanism can be found in the *inversion method*, a well known approach in random number generation and vastly documented in the literature as seen in Refs. [223, 83, 34, 224]. The mathematical formulation and practical considerations are

discussed at length by Devroye [52]. The inversion method relates a standard uniform random variable u to the cumulative distribution function $F(x)$ of the random variable x as follows in Eq. (8)

$$F^{-1}(u) = \inf\{x : F(x) = u, 0 < u < 1\} \tag{8}$$

The function F is continuous on $\mathbf{R}$ and has an inverse F^{-1}. The proof for Eq. 8 is given as,

$$\Pr(F^{-1}(u) \leq x) \tag{9}$$

$$= \Pr(u \leq F(x)) = F(x) \tag{10}$$

A sample of random variable x with probability distribution function $f(x)$ and cumulative distribution function $F(x)$ can be readily generated with a standard uniform sample evaluated in the inverse distribution F^{-1}. Closed form analytical solutions for the inverse function do not always exist, so numerical approximations are necessary in some cases. The inversion method can be applied in reverse to create a standard uniform sample from any other randomly distributed sample for which the distribution function is known. A random variable sample can therefore be transformed to any other distribution using the standard uniform distribution as an intermediate state.

The flexibility to select any required marginal distribution pursuant of whatever subjective encoding method is desired, is central to developing the use of copulas for practical applications. The inversion method is applied to univariate samples separately and does not compromise the multivariate dependence structure predicated by a copula defined for said variables. Although the shape of the univariate distributions changes slightly with the implementation of the inversion method, as does the shape of the sample in the multivariate space, the sample correlation remains effectively invariant.

The inversion method is demonstrated using the generic exponential distribution which is distributed as follows:

$$\text{pdf: } f(x) = \lambda e^{-\lambda x}, x \geq 0 \tag{11}$$

$$\text{CDF: } f(x) = F(x) = 1 - e^{-\lambda x}, x \geq 0 \tag{12}$$

A uniformly distributed random variable U between 0 and 1 is generated in Fig 14.

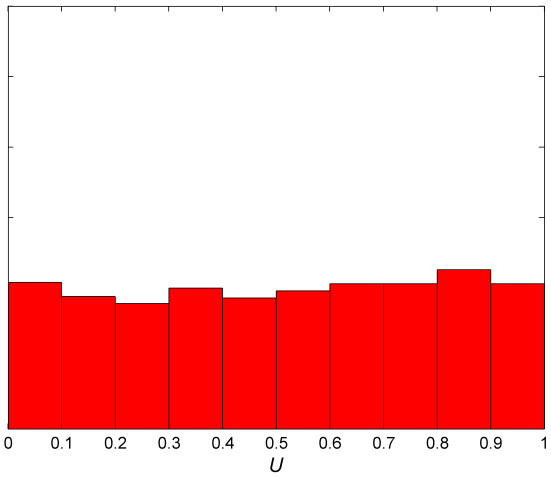

Figure 14: Uniform random variable $U(0, 1)$

Assuming $\lambda = 2$, the random variable U is sampled $n = 1,000$ times to plot the exponential distribution pdf and CDF through Eq. 11 and Eq. 12 respectively, as shown in Figs. 15a and 15b.

Using the inverse exponential cumulative distribution which exists in closed form (Eq. 13) the inverse function can be plotted by sampling the same uniform random variable U shown in Fig. 14. The resulting graph is expected to simply be a transformation of the exponential distribution CDF in the line $y = x$.

$$F^{-1}(x) = \frac{-ln(1-x)}{\lambda} \tag{13}$$

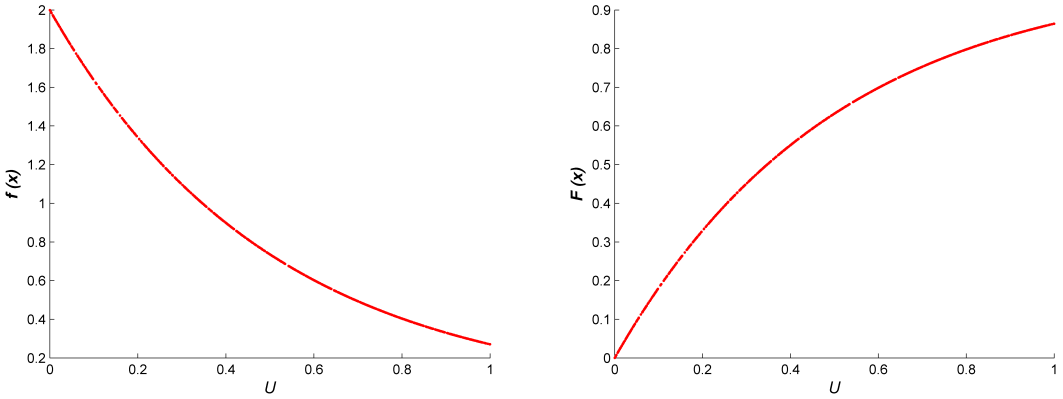

(a) Exponential distribution pdf (b) Exponential distribution CDF

Figure 15: Exponential distribution generated by sampling $U(0,1)$ assuming $\lambda = 2$

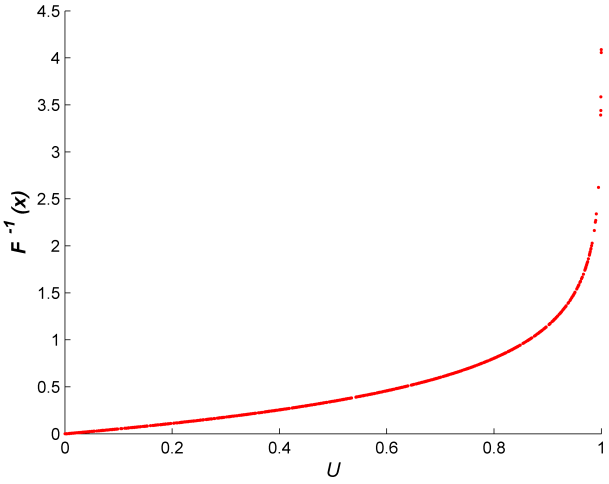

Figure 16: Exponential distribution inverse CDF generated by sampling $U(0,1)$

The inverse CDF is shown in Fig. 16 and appears as expected. However plotting the histogram of the inverse as shown in Fig. 17 reveals a trend which directly corresponds to the exponential distribution probability density function in Fig. 15a. It is possible to generate the pdf of the exponential distribution by supplying the inverse CDF of the exponential distribution with the uniform random variable U. This is because the inversion method relies on the exponential function's own inverse CDF to transform the uniform random variable into data corresponding to the exponential function. This method is particularly useful because it can be used with any function

for which the inverse cdf is known. In this manner the inversion method, via the inverse CDF of a distribution, F^{-1}, provides a link between any uniform random variable and the original distribution's pdf.

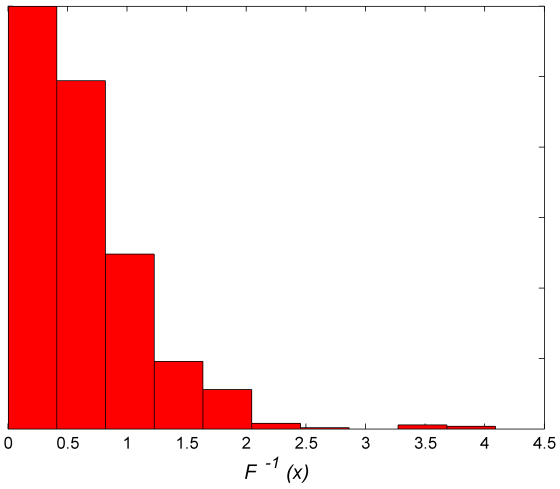

Figure 17: Histogram of the exponential distribution inverse CDF

Recall that by the inversion method any CDF and its inverse can be expressed using the uniform distribution in the following manner,

$$F(x) = u \tag{14}$$

$$F^{-1}(u) = x \tag{15}$$

The process can be taken a step further to retrieve back, via the inversion method, the original sample of values in the random variable U. Simply evaluate the CDF of the exponential function to the x values obtained in the histogram above following the similar but reversed formulation of the Inversion Method:

$$F^{-1}(x) = u \tag{16}$$

The only difference is that now the inverse CDF is actually the CDF of the exponential function. By doing this the exact same sample of U can be retrieved which this example was begun with as shown in Fig. 18.

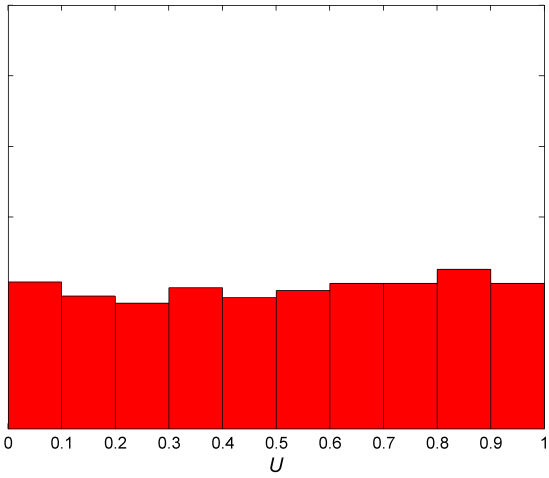

Figure 18: Starting uniform distribution of U retrieved back by applying original CDF to the x values of the inverse CDF

This example demonstrates how the exponential distribution can be obtained by using its inverse CDF via any uniform random variable distributed between 0 and 1. This process can be extended to relate uniform variables with probability distributions for any function whose inverse CDF is known. This example also illustrates how the process can be reversed by applying the CDF of the original function to return the exact uniform random variable used in the original inversion process.

4.3.6 Applications of Copulas

Copulas theory has been applied in several fields including demographic statistics, finance, and insurance risk analysis, among others. Some of these applications are reviewed to illustrate how copulas theory has been used outside the aerospace community.

Benzia et al. [16] tried to model test metrics of electronic devices used in the sensors and signals processing field. They recognized that dependencies existed between output parameters of the devices they wished to test, so they employed Archimedean copulas to model that dependence and used it to evaluate their devices on a large scale. In light of insufficient data to properly model their faulty imaging devices, a

parametric Clayton copula was fit to existing data in order to simulate larger samples augmenting the original one, which helped to attain greater accuracy in the predictive models they developed. In this way copulas were used to augment a particular trend of data and add statistical significance to models that captured that trend.

Rui and Pu [190] presented a convertible bond pricing and valuation approach based on copulas theory. They use four different types of copulas (Gumbel, Frank, Clayton, and normal) to measure the dependence between the factors that influence bond price. They argued in favor of copulas due to their greater sensitivity in capturing nonlinear dependencies relative to other techniques. They cited two main advantages when copulas are used in multivariate modeling, namely, that there is no restriction on the random variable marginal distribution and the ability to separate the dependence structure from the marginal distribution. They concluded that Archimedean copulas predict bond price better than the normal copula at various stock prices.

Huang et al. [84] showed how the inclusion of copulas in reliability models can improve the prediction of equipment lifetime. They formulate a reliability equation using the Gumbel-Hougaard copula. Weibull distributions were fit to two different failure modes of the equipment based on failure times from historical data. First, they calculated the Weibull marginal distribution parameters and used that to estimate reliability, taking the marginals as independent. Then they related the two failure modes using the Gumbel-Hougaard copula and estimated the reliability again. They concluded that the inclusion of the copula significantly improves the estimation of equipment lifetime and showed the shift in the reliability curve.

Noh et al. [157] combined a reliability based design optimization (RBDO) problem with copulas in the structural multidisciplinary optimization field. They related the design inputs using a Gaussian copula but transformed their marginal distributions to the copula space using two different techniques, the Rosenblatt and Nataf

transformations, and compared the RBDO results from each. They preferred the Nataf transformation because it requires less information to produce similar results. They also compared both of these methods to the independent inputs assumption and concluded that the dependent inputs significantly affected the RBDO results for structural design.

4.3.7 Selecting Copulas

Copulas are most useful in capturing dependencies when specific data is unavailable but there is a notional understanding of how the dependence structure should look. This is particularly relevant in the case of future aircraft technologies where technology impacts must be forecasted but dependencies between the impacts must be included because they are significant. Figures 10 - 13 show several copulas families at a few different values of correlation parameter θ. These are meant to give the reader an understanding of the types of relationships copulas can capture, but Nelsen provides a more detailed [155] listing of 22 different Archimedean copula families in his text. Each of these copula families has a continuous range of correlation parameter θ which significantly affects the dependence structure. Simulating all 22 copula families at various values of correlation parameter θ can produce a plethora of different types of dependencies. With so many different choices, it can be difficult for a new user of copulas to know where to begin. They will need some guidance to aid in finding the right copula family and θ value for their needs.

In Fig. 19, a CopulA Selection Tree called CAST, has been created to guide system analysts in identifying a copula family and θ value for their application by answering basic questions about the underlying relationship they wish to capture. The answers to these questions represent a low level understanding of the dependence structure upon which the use of copulas is predicated.

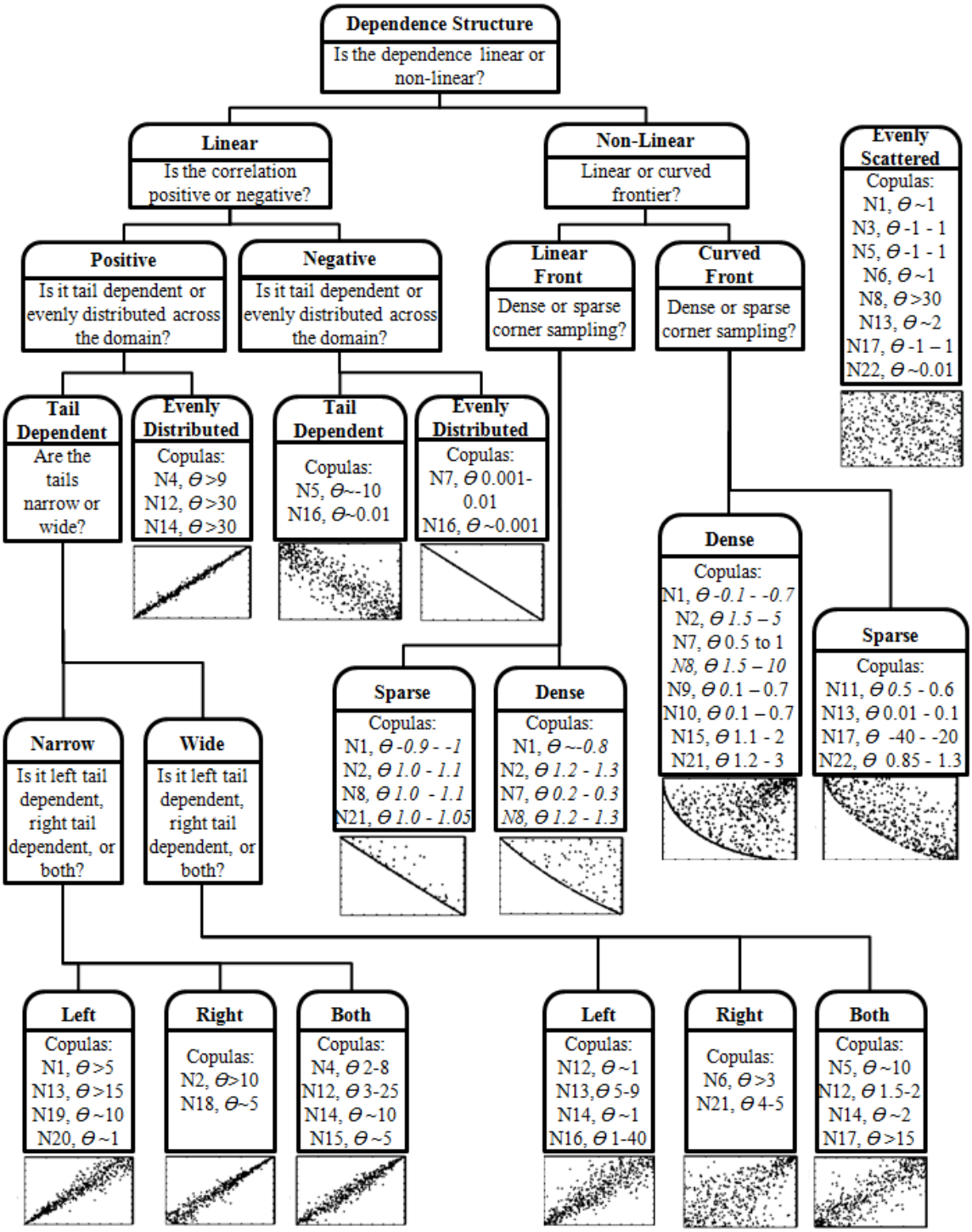

Figure 19: Archimedean CopulA Selection Tree (CAST)

CAST was created by first simulating and cataloging all the Archimedean copulas listed by Nelsen. During the cataloging process several distinct and pertinent

dependence structures arose across different copula families. Then copulas and theta values with similar types of dependence were organized into sets. By examining the sets it was found that this doesn't have to be a flat organization, but rather can be arranged into a structure based on general relationships between the sets. These relations form a hierarchical breakdown from broad to specific descriptions of the dependence structure properties captured in each set. This realization led to the development of a formal tree structure which starts with generic categorizations at the top and concludes with various sets of copulas in leaves that represent distinct categories of dependence structures. The copulas in the tree leaves represent initial categorizations that were subjectively assigned based on a visual assessment of the dependence structure shown by various copulas. Therefore, CAST is a subjectively created, encoding tool designed to convert the practitioner's qualitative knowledge of the desired underlying relationship into copula selections useful in their applications.

Before proceeding it is relevant to note a couple of points. There were three copula families in the Archimedean class that were not included in the simulation and cataloging process due to difficulties in properly modeling them. This difficulty was encountered with the N18, N19, and N20 copula families specifically because of the exponential functions present in their generator functions. Due to machine limitations in Matlab, the exponential function can't be evaluated to a distinct value at extremely low negative numbers. This limitation causes failures in the copula simulation algorithm and creates nonuniform marginal distributions which violates a key principle of copulas. This limitation was not encountered while simulating any other families in the Archimedean class. However, this limitation was overcome for these three copula families by examining their dependence structure in the work published by Armstrong [8], and using the same subjective cataloging process to place them in the appropriately leaves of the selection tree. Additionally, the copula selection tree (CAST) proposed here was formally published [254] to the aerospace

community as tool to aid practitioners in selecting copulas.

CAST begins with an overarching question about the dependence structure and whether it is linear or non-linear. The question is intended to be answered qualitatively based on the analyst's understanding. The structure of the tree is such that the answer to the first question is followed immediately by another series of questions that lead to distinct leaves of the tree. The final answer concludes in a subset of copulas and correlation parameter θ values that capture the analyst's desired dependence structure. Along the linear branch questions arise about positive or negative correlation in terms of whether the relationship between the variables tends to be directly proportional or inversely proportional. The next question is about the spread of the points and asks if they are evenly distributed along the linear trend or tightly concentrated on one/both ends such that propensity of one variable having an extreme value is closely linked to the other variable having a similarly extreme value, i.e., tail dependent. If tail dependence exists, is that dependence very sharp in the tail (narrow tail, low uncertainty) or is it moderate in the tail (wide tail, more uncertainty)? Then, the last question asks if this dependence is found in the left, right, or both tails and the tree concludes with the prescribed set of copulas and θ values. In the non-linear branch, copulas can form Pareto front type dependence structures which either have curved frontiers or linear frontiers. The next question asks whether the corner inside the frontier is highly sampled or sparsely sampled. Then, each leaf concludes with the recommended subset of copulas and θ values. The evenly scattered category near the top right is a subset of copula families that are not linear or nonlinear but rather provide a more space filling dependence structure. These copulas can be tuned to have a defined but low dependence, which corresponds with a high degree of uncertainty and could be useful when limited knowledge is known about the dependence structure or if independence must be enforced between random variables.

For convenience, CAST follows the same numerical listing as Nelsen [155, chap.

4] to identify copula families. Each final leaf of the selection tree includes a subset of copula families and approximate θ values. It is also accompanied by a notional graph to give the reader a visual understanding of the types of relationships described by that leaf. Fig. 19 is obviously not a comprehensive listing of all types of copulas since it focuses on the Archimedean class, but it does include all 22 of Nelsen's documented copulas. Some leaves of the tree may not appear as developed as others; for example, the linear-negative branch does not have as many options as the linear-positive branch. However, since all marginal distributions are uniformly distributed between 0 and 1, positively dependent copulas can be reoriented and employed for negative dependence structures. This can be done through intermediate mappings of the random variables by setting $u_{transformed} = 1 - u_{original}$ and $v_{transformed} = 1 - v_{original}$ as needed. In fact any of the copulas can be manipulated in this manner to match a particular dependence structure. CAST is not necessarily a conclusive tool but rather is intended to guide the novice practitioner to the desired set of families and correlation parameter θ values that are suitable to their needs. The system analyst is then encouraged to simulate, test, and adjust (through the correlation parameter θ and any appropriate transformations) those recommended copulas in the final leaf of the tree to settle upon the copula family and θ value which best meets their needs. In this sense, CAST can serve as a very useful tool to new users of copulas who are not familiar with the wide breadth of relationships readily available to copula users.

Copula research is continuing in the field of statistics [80, 55], and new families are being discovered through various transformations and higher order applications. As more copulas are discovered and infused, other leaves of the selection tree can become further developed and refined by ongoing research. Fig 19 represents a first iteration that will continue to evolve.

4.3.8 Research Question 1

Examining the selection tree leads to several observations. The first obvious point is that the tree was created using a subjective view of the available copula families, and is therefore not necessarily absolute. In order to add scientific rigor and further refine CAST, an effort will be made to demonstrate that this tree has an objective statistical repeatable underlying structure. This leads to the first research question.

Research Question 1

Can the proposed copula selection tree be shown to be consistent with objective statistics? Given an input vector of copula samples X, and a set of objective statistics S, can the groupings in tree T be reproduced?

Expectation 1

CAST is based on user intuition and visual inspection but also corresponds to a hierarchical relational structure that is reproducible and objective when using descriptive statistics

Research Question 1 (RQ1) and the corresponding expectation lead us to believe that some kind of underlying objective structure can be found in this copula selection tree. The expectation is not called a hypothesis because the assertion does not have enough specificity to be testable under the scientific method. As such further observations will be made and Research Question 1 will be broken down into smaller sub-questions.

The next observation is that the tree uses simple subjective questions for classification. Each question acts as a decision gate dividing the available set of copulas in the full Archimedean class into smaller and smaller subsets that correspond to the

properties evoked by the qualitative questions at each decision gate. This continues until the copulas are placed into leaves at the end of the selection tree. There are 10 decision gates throughout the tree (numbered 1-10) and a total of 14 leaves (lettered A-N) representing the various types of dependence structures available in the Archimedean class. These are shown in Fig. 20.

By answering these qualitative questions about a dependence structure, eventually a leaf of the tree will be reached. In this way the tree provides a subjectively assigned label for every copula that corresponds to the letter of the leaf that it belongs to. For example the N4,$\theta > 9$ copula belongs to leaf H and therefor has the label H. The

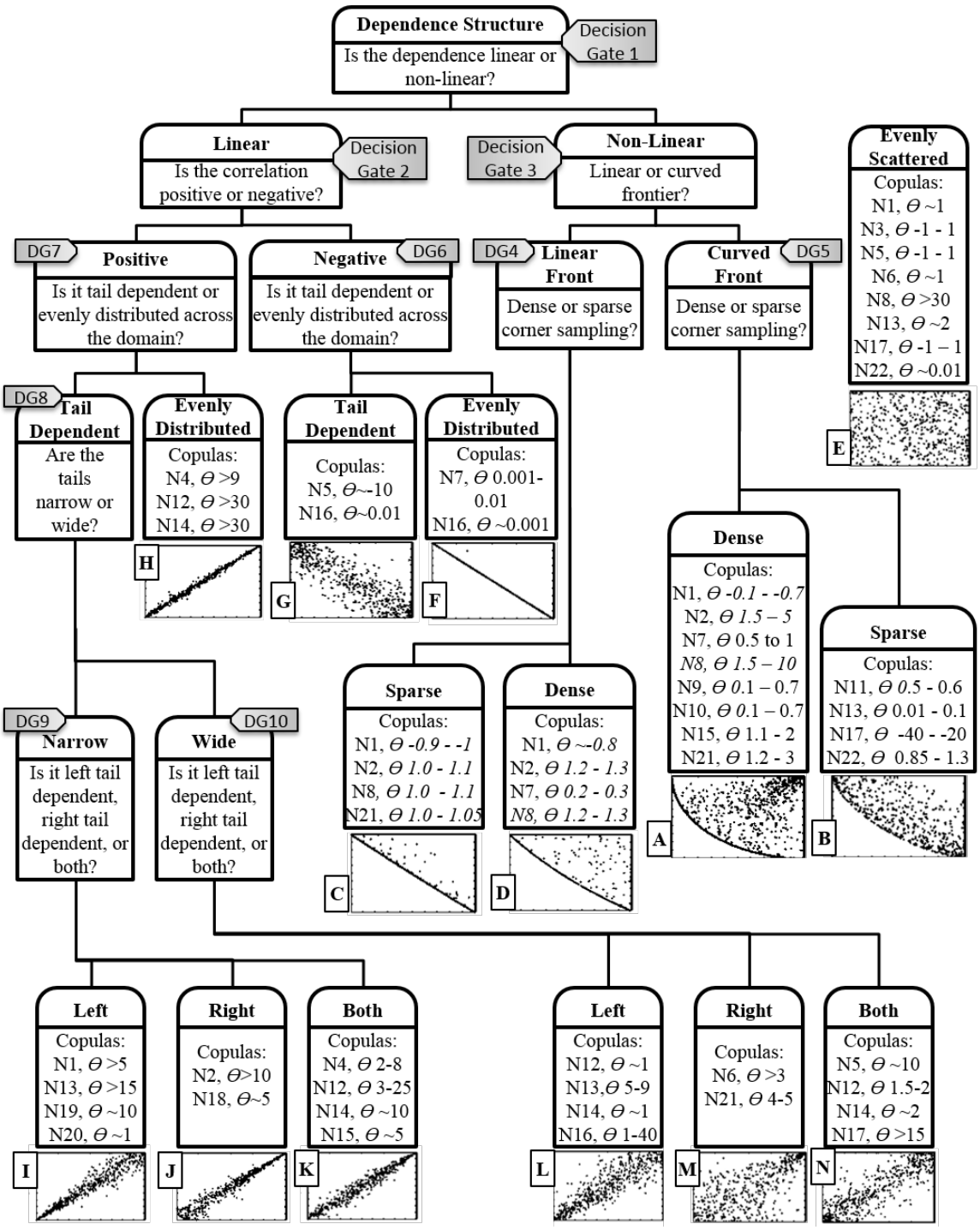

Figure 20: Archimedean CopulA Selection Tree (CAST) with labeled decision gates and leaves

N1,$\theta > 5$ copula is in leaf I and has the label I.

4.3.8.1 Research Question 1.1

Recognizing the various decision gates and labeled leaves in the tree, and knowing that RQ1 intends to replicate the copula groupings in each leaf using objective statistics leads to the first sub-research question.

Research Question 1.1

Are there objective repeatable statistics that can capture the subjective behaviors qualitatively assessed at each decision gate? Do such statistics exist and can they be used to make objective decisions about a dependence structure at each decision gate?

Expectation 1.1

Descriptive statistics can capture these behaviors and be used to make the decisions posed at each decision gate but not all of them exist. In addition to existing ones, some custom statistics will be needed to evaluate dependence structures at all the decision gates in the tree.

4.3.8.2 Research Question 1.2

The next observation is that the copulas in the tree only represent a subset of all the possible copulas in the Archimedean class. In fact the copulas and θ values depicted in the tree are those that represent fairly distinct dependence structures which are reflected in the categorization of the leaves. However θ is a continuous variable in its domain and there are many copula families, so there are many other copulas in the Archimedean class that may not fit into these defined categories. This leaves many of these fringe type copulas out of the selection tree and leads to the next sub-research question.

Research Question 1.2

What is the implication of fringe copulas which do not appear explicitly in CAST? Are these copulas simply to be ignored? If they were to be included, where do they belong?

Expectation 1.2

Fringe copulas exist but don't belong in CAST because their dependence structure is not distinct enough to be archetypal of a particular leaf.

4.3.8.3 Research Question 1.3

Another observation is that some leaves are subjectively speaking, close in the appearance of their dependence structures. Some of these similar leaves are only separated by one decision, like leaf M and leaf N. However there are others like leaf C and leaf F that have separated very early on in the tree structure but still appear somewhat similar. This causes concerns about the tree groupings and more importantly about whether or not these distinctions can be made objectively.

Research Question 1.3

Is there a better way to make these groupings to avoid similar looking leaves? What descriptive statistics exist that can be used to objectively differentiate between these similar looking leaves?

Expectation 1.3

The groupings have been made subjectively and can be refined. For similar tree leaves, a single descriptive statistic may not be sufficient to objectively differentiate between leaves, but a combination of statistics should be able to make the distinctions.

4.3.8.4 Research Question 1.4

The next observation is that the assignment of a particular copula family and θ value as being archetypal of a distinct behavior was done subjectively. Consequently, the exact range of θ values assigned to a leaf for a given copula family is open to subjective interpretation. This leads to some further sub-research questions.

Research Question 1.4

How can the label assignments of a particular copula and θ value be objectively verified? Does the range of θ need to expand, shrink, or shift entirely? At what point do the subjective estimates of θ become unreliable?

Expectation 1.4

The label assignments and θ values of each copula family will have to be evaluated individually and checked with objective statistics. The assignments and the ranges of θ will either meet or not meet the cut off value of the statistics which will verify their placement in CAST.

4.3.8.5 Research Question 1.5

The previous question raises some important concerns about the accuracy of the subjective label assignments. In addition to this, since copulas are probabilistic the repeatability of CAST should also be established. Although the proposed tree has been published to the aerospace community, if it is expected to be carried forward, the accuracy of the groupings and the repeatability of the tree should be verified in an objective manner. This leads to the final sub-research question.

Research Question 1.5

How can the groupings in the tree leaves be verified and validated in an objective and repeatable manner? How can it be demonstrated that this subjective model can be arrived upon by repeatable objective statistics?

Expectation 1.5

The groupings can be verified with repeatable objective statistics but this will require multiple instantiations of the copulas in the subjective tree.

Answering these research questions successfully will establish the underlying objective nature of the copula selection tree. The value of this effort will be to show that the proposed subjective decision tree is consistent with objective metrics that can measure different aspects of these dependence structures in order to repeatedly and accurately label each copula.

4.4 CopulA Selection Tree (CAST)

4.4.1 CAST Research Plan

A research plan was created to answer RQ1 and its associated sub-research questions. This plan is a general outline of steps and will need many additional details to answer all the research questions.

1. Create an objective model of the subjective copula selection tree
2. Train the objective model using an initial training set of copulas to accurately predict the groupings in the subjective tree leaves

3. Verify the model and validate its objective statistical values using a new instantiation of the training set and additional copulas

    (a) Include fringe copulas in the validation set that were not in the training set to determine their purpose

This effort will begin by constructing an objective model using descriptive statistics that can systematically answer all the qualitative questions at the decision gates in the tree. If each question is answered correctly, then the objective statistics will follow the same path through the tree as the subjective analyst and ultimately assign the copula being assessed the same label as the subjective process. If any of the objective statistics fail to exit a decision gate accurately, then the copula being assessed will take a different path through the decision tree and eventually end in a different leaf than the subjective process. This will result in the copula being mislabeled and not matching the subjective procedure's assignment. The model will be adequately prepared when an initial training set of copulas can be passed through and its predictive labeling completely matches those provided by the subjective analyst. The model should have zero error in its predictive labeling or get as close to it as possible.

If this can be achieved for the initial training set of copulas, then the objective model will have been verified, meaning that it can accurately label the copulas that its objective statistics were trained on. This is a key step in answering RQ1 and is analogous to Model Fit Error (MFE) in surrogate modeling. Any mislabeled copulas indicate that the model's objective statistics are failing to match the subjective analyst for those copulas and resulting in a non-zero MFE of the model. To improve the MFE the model's objective statistics must be refined so they can accurately label all the copulas in the training set. After verifying the objective model on the training set copulas, it must be validated using other copulas that are not from the training set. This can be thought of as Model Representation Error (MRE) from surrogate

modeling. If the model has good predictive capability for copulas out the training set, i.e. low MRE, then it will be validated as well.

CAST was created by simulating and cataloging all the different copula families in the Archimedean class at many values of θ. Several distinct and useful dependence structures became obvious across different copula families during the cataloging process. These dependence structures were subjectively assigned into groupings that would be useful to a system analyst for dependence modeling such as a left tail dependent group of copulas or a right tail dependent group of copulas. Each type of grouping is assigned to a leaf in the selection tree. The leaf groupings are representative of the archetypal dependence structures that exist in the Archimedean class of copulas and are created subjectively. The general relationships between the leaves were used to create the structure of the tree through a hierarchical breakdown from broad to specific descriptions of the dependence structure properties. Each level in the hierarchy is traversed through a decision gate that asks the user a qualitative question about the dependence structure they want to represent. Eventually the answers to these questions lead to a single leaf that is archetypal of their desired dependence structure and a subset of copula families that can simulate it. This research plan is intended to demonstrate that the hierarchical breakdown and assessment of copulas through the decision gates, and their assignment into each leaf, can be replicated with objective statistics. If successful, this will objectively prove that the copula families that were subjectively assigned to a leaf during the cataloging process, do in fact belong in that leaf. The archetypal dependence structures represented by each leaf were created and will remain subjective. This research plan will demonstrate that the assessment of copulas through the decision gates and their membership into each archetypal leaf can be done objectively using descriptive statistics.

4.4.2 Experimental Design

An important consideration in the experimental design is to ensure that the most amount of information is obtained from a minimum number of copula simulations. This is important because while the simulations themselves are computationally efficient to run, the subjective labeling process is manual and laborious. For each copula and its associated θ value, the dependence structure must be individually analyzed. It must be subjectively assessed through each decision gate by answering the series of qualitative questions until ultimately reaching a particular leaf. Then the copula is assigned to that leaf and its label is recorded for comparison to the objective model's predicted label. This process must be repeated for each and every copula in the training and validation sets, so that the performance of the model can be tested. For this reason it is efficient to answer RQ1 and its sub-research questions with as few copula simulations as possible.

4.4.3 Identify Candidate Metrics

There are many descriptive statistics in the literature that can be used to model the copula selection tree. The descriptive statistics will be used to measure the copulas so they can also be thought of as metrics. Since CAST has ten different decision gates which subjectively assess a unique feature of the dependence structure, the metrics should be identified corresponding to the qualitative decision gate they will be used to objectively mimic. Many different metrics were identified that can measure features of the dependence structure relevant to each decision gate. Some of these statistics were found in the literature and others were created as custom statistics in order to measure a key property of the dependence structure in each copula. Once the candidate metrics were identified for each decision gate, they were down selected to a usable amount of statistics based on a simple qualitative assessment.

The assessment involved four categories and each metric was given a High, Medium,

or Low ranking for each category. High is considered better than Low in all categories of this assessment. The first category is Currently Available in software packages. A High ranking would mean that it's already present and minimal effort will be needed to measure copulas with this metric while a Low ranking would indicate the opposite. The second category is Ease of Implementation, or how difficult it will be to code this statistic in a software package like Matlab. The third category is computational efficiency which measure relatively how long it will take to measure each copula with the metric. Finally the last category is the ability of a statistic to measure a distinct property relevant to that decision gate. These four criteria were used to judge all of the candidate metrics for each decision gate in order to down select the most useful ones to include in the objective model.

4.4.3.1 Decision Gate 1

Decision Gate (DG) 1 is depicted in Fig. 20 and asks whether the dependence structure is linear or nonlinear. There are several different potential statistics in the literature to measure linearity including some well-known correlation coefficients. Some additional custom statistics have also been proposed to aid in making the proper decision for each copula objectively. All of these statistics are listed in Table 2 with their ranking in each category and their associated symbol.

1. Pearson's ρ is a well known correlation coefficient from the literature [168]. It ranges from -1 to 1 and can measure linear or inverse correlation. For an x and y pair, it is calculated by

$$\rho = \frac{\sum_{i=1}^{n}(x_i - \bar{x})(y_i - \bar{y})}{\sqrt{\sum_{i=1}^{n}(x_i - \bar{x})^2}\sqrt{\sum_{i=1}^{n}(y_i - \bar{y})^2}} \tag{17}$$

   and a value close to 1 or -1 reflects either a positively or negatively correlated set. Values close to zero reflect low correlation and can indicate nonlinear behavior. Pearson's ρ will be used to objectively assess copulas at Decision Gate 1.

Table 2: Decision Gate 1 Candidate Metrics

Metric Name	Symbol	Ease of Implementation	Currently Available	Metric Computational Efficiency	Measure Property of this DG
1. Pearson's rho	ρ_p	Medium	High	High	Medium
2. Kendall's tau	τ_k	Medium	High	Low	Medium
3. Spearman's rho	ρ_s	Medium	High	Low	Medium
4. Covariance	cov	Medium	High	Low	Low
5. Avg Distance	$\bar{d}$	High	Low	High	High
6. Avg Inverse Distance	$\bar{d}^{-1}$	High	Low	High	High
7. Origin Corner Density	σ_o	High	Low	High	High
8. Pareto Frontier Point Density	ϕ	Medium	Low	Medium	High

2. Kendall's τ is a commonly used rank correlation coefficient in the literature [106]. It also ranges from -1 to 1 and can measure both linear or inverse correlation. It is calculated using the number of concordant τ_c and discordant pairs τ_d as follows

$$\tau = \frac{\tau_c - \tau_d}{\frac{1}{2}n(n-1)} \tag{18}$$

and values close to -1 or 1 indicate high correlation. When its value is close to zero this metric typically indicates low correlation and nonlinear behavior. Kendall's τ will be used to objectively assess copulas at Decision Gate 1.

3. Spearman's ρ is an established rank correlation coefficient in the literature [221]. Ranging from -1 to 1, it can measure both negative and positive correlations. It is calculated by

$$\rho = \frac{\sum_{i=1}^{n}(X_i - \bar{X})(Y_i - \bar{Y})}{\sqrt{\sum_{i=1}^{n}(X_i - \bar{X})^2}\sqrt{\sum_{i=1}^{n}(Y_i - \bar{Y})^2}} \tag{19}$$

and values near zero indicate low correlation and the potential for nonlinear behavior. Spearman's ρ will be used to objectively assess copulas at Decision Gate 1.

4. Covariance (cov) is a measure of how much an x and y pair will change together. If an increase in x corresponds to an increase in y and vice verse for decreases, the the variables change together and the covariance is positive. However, if a decrease in x corresponds to an increase in y, or vice versa, and the variables change in opposite directions, then the covariance will be negative. The magnitude of the covariance is not as easily interpreted but its normalized version is Pearson's ρ whose magnitude is easily relatable to the strength of the correlation. Due to this property of covariance, it will not be as useful in assessing copulas at Decision Gate 1 and will not be used.

5. Avg Distance ($\bar{d}$) is a custom metric created specifically to measure the spread of points off of the imaginary line $y = x$. This spread is calculated by first computing the absolute value of the vertical distance of every point above or below the line $y = x$. Then the Pythagorean theorem is applied to find the perpendicular distance of each point off of the line $y = x$. The perpendicular distance is then summed and divided by the total number of points to find an average perpendicular distance, or spread of points off of the line $y = x$. If the Avg Distance is low, it indicates high positive correlation and linearity but if it is high then it indicates low correlation and possible nonlinear behavior. Avg Distance ($\bar{d}$) will be used to objectively assess copulas at Decision Gate 1.

6. Avg Inverse Distance ($\bar{d}^{-1}$) is a custom metric created specifically to measure the spread of points off of the imaginary line $y = -x + 1$. This spread is calculated by first computing the absolute value of the vertical distance of every point above or below the line $y = -x + 1$. Then the Pythagorean theorem is applied to find the perpendicular distance of each point off of the line $y = -x + 1$. The perpendicular distance is then summed and divided by the total number of points to find an average perpendicular distance, or spread off of the line $y = -x+1$. If the Avg Inverse Distance is low, it indicates high negative correlation and linearity but if it is high then it indicates low correlation and possible nonlinear behavior. Avg Inverse Distance ($\bar{d}^{-1}$) will be used to objectively assess copulas at Decision Gate 1.

7. Origin Corner Density (σ_o) is a custom metric that measures the density of points in the square area formed by the origin, the line $x = 0.4$, and the line $y = 0.4$. The metric counts the points in this imaginary square and normalizes them by the total number of points. The metric can theoretically take on values from 0 to 1, and can be used to identify nonlinear behavior if there are no points

at all near the origin. Origin Corner Density (σ_o) will be used to objectively assess copulas at Decision Gate 1.

8. Pareto Frontier Point Density (ϕ) is a custom metric measuring the number of points on the Pareto frontier. It is calculated by isolating the Pareto frontier points and summing them all. The sum is then normalized by the total number of points. The metric can theoretically take on values from 0 to 1, and can be used to identify nonlinear behavior if there are a high proportion of points on the frontier instead of being more evenly spread out. Pareto Frontier Point Density (ϕ) will be used to objectively assess copulas at Decision Gate 1.

4.4.3.2 Decision Gate 2

Decision Gate 2 is depicted in Fig. 20 and examines all copulas that are determined to be linear by decision gate 1. Decision gate 2 tries to determine whether the linear copulas are positively of negatively correlated. Several of the established correlation coefficients from the literature can be used to make this determination based on their signs. All of these statistics are listed in Table 3 with their ranking in each category and their associated symbol.

1. Pearson's ρ was described in decision gate 1 and can be used to determine positive or negative correlation based on its sign. It will take on positive sign for positive correlations and a negative sign for negative correlations. Pearson's ρ will be used to objectively assess copulas at Decision Gate 2.

2. Kendall's τ was described in decision gate 1 and can also be used to determine positive or negative correlation based on its sign. Positive correlation will have positive sign and negative correlations will have negative sign. Kendall's τ will be used to objectively assess copulas at Decision Gate 2.

3. Spearman's ρ was described in decision gate 1 and can be used to determine

Table 3: Decision Gate 2 Candidate Metrics

Metric Name	Symbol	Ease of Implementation	Currently Available	Metric Computational Efficiency	Measure Property of this DG
1. Pearson's rho	ρ_p	Medium	High	High	Medium
2. Kendall's tau	τ_k	Medium	High	Low	Medium
3. Spearman's rho	ρ_s	Medium	High	Low	Medium
4. Covariance	cov	Medium	High	Low	Medium

positive or negative correlation based on its sign. It will take on positive sign for positive correlations and a negative sign for negative correlations. Spearman's ρ will be used to objectively assess copulas at Decision Gate 2.

4. Covariance (cov) was described in decision gate 1 and can also be used to determine positive or negative correlation based on its sign. Positive correlation will have positive sign and negative correlations will have negative sign. It will be used to objectively assess copulas at Decision Gate 2.

4.4.3.3 Decision Gate 3

Decision Gate 3 is depicted in Fig. 20 and examines all copulas that are determined to be nonlinear by decision gate 1. Decision Gate 2 tries to determine whether the nonlinear copulas have a curved or linear Pareto frontier, or are simply just evenly scattered throughput the space. Determining these features will require tailored metrics that examine the Pareto frontier points of these nonlinear copulas. All of these

Table 4: Decision Gate 3 Candidate Metrics

Metric Name	Symbol	Ease of Implementation	Currently Available	Metric Computational Efficiency	Measure Property of this DG
1. Avg Pareto Inverse Distance	$\bar{d}_{\phi}^{-1}$	Medium	Low	Medium	High
2. Pareto Frontier Point Density	ϕ	Medium	Low	Medium	High
3. Avg Inverse Distance	$\bar{d}^{-1}$	High	Low	High	High

custom statistics are listed in Table 4 with their ranking in each category and their associated symbol.

1. Avg Pareto Inverse Distance ($\bar{d}_{\phi}^{-1}$) is a custom metric that measures the distance of only the Pareto frontier points off of the imaginary line $y = -x + 1$. First the Pareto frontier points are isolated and operated on, ignoring the other points in the joint distribution. Then the spread is calculated by first computing the absolute value of the vertical distance of every point above or below the line $y = -x + 1$. Then the Pythagorean theorem is applied to find the perpendicular distance of the Pareto frontier points off of the line $y = -x + 1$. The perpendicular distance is then summed and divided by the total number of Pareto frontier points to find an average perpendicular distance, or spread off of the line $y = -x + 1$. If the Avg Pareto Inverse Distance is low, it indicates a linear Pareto frontier but if its very high, it indicates potential for random scatter of points. An intermediate value indicates a curved Pareto frontier.

Avg Pareto Inverse Distance ($\bar{d}_{\phi}^{-1}$) will be used to objectively assess copulas at Decision Gate 3.

2. Pareto Frontier Point Density (ϕ) was described in decision gate 1 and can be used to determine the number of points on the Pareto frontier and thereby indicate how filled it is. This can be used to aid in determining if the frontier is curved or linear based on how tightly packed the points on the frontier are. Pareto Frontier Point Density (ϕ) will be used to objectively assess copulas at Decision Gate 3.

3. Avg Inverse Distance ($\bar{d}^{-1}$) was described in Decision Gate 1 and can be used to assess nonlinear copulas to determine how curved or linear all the points in the space are. This can his can be used to aid in determining if the frontier is curved or linear. Avg Inverse Distance ($\bar{d}^{-1}$) will be used to objectively assess copulas at Decision Gate 3.

4.4.3.4 Decision Gate 4

Decision Gate 4 is depicted in Fig. 20 and asks whether the linear frontier copulas identified by Decision Gate 3 have sparse or dense Pareto corner density. The Pareto corner is the corner of the distribution behind the Pareto frontier which can be sparsely or densely sampled by different copulas. Decision Gate 4 attempts to use density based statistics to objectively make this delineation for each copula. All of these statistics are presented in Table 5 with their ranking in each category and their associated symbol.

1. Lower Density (σ_{Low}) is a custom metric that measures the total number of points in the lower third of the joint distribution between the lines $x = 0$ and the line $x = 0.3333$. It counts the total number of points with coordinates such that $x < 0.3333$ and sums them. If there are a high number of points in the

Table 5: Decision Gate 4 Candidate Metrics

Metric Name	Symbol	Ease of Implementation	Currently Available	Metric Computational Efficiency	Measure Property of this DG
1. Lower Density	σ_{Low}	High	Low	High	Medium
2. Middle Density	σ_{Mid}	High	Low	High	Medium
3. Upper Density	σ_{Upp}	High	Low	High	Medium
4. Pareto Corner Density	σ_{ϕ}	Medium	Low	Medium	High
5. Pareto Frontier Point Density	ϕ	Medium	Low	Medium	High

lower and middle parts of the space, then there will be less points remaining to populate the upper region where the Pareto corner is, giving an indication of the Pareto corner density. Due to the superiority of other custom metrics to directly measure the density in the Pareto corner, Lower Density (σ_{Low}) will not be directly used to assess copulas at Decision Gate 4.

2. Middle Density (σ_{Mid}) is a custom metric that measures the total number of points in the middle third of the joint distribution between the lines $x = .3333$ and the line $x = 0.6666$. It counts the total number of points with coordinates such that $x > 0.3333$ and $x < 0.6666$. Then it sums them and records the value. If there are a high number of points in the lower and middle parts of the space, then there will be less points remaining to populate the upper region where the Pareto corner is, giving an indication of the Pareto corner density. Due to the superiority of other custom metrics to directly measure the density in the Pareto corner, Middle Density (σ_{Mid}) will not be directly used to assess copulas at Decision Gate 4.

3. Upper Density (σ_{Upp}) is a custom metric that measures the total number of points in the upper third of the joint distribution between the lines $x = .6666$ and the line $x = 1$. It counts the total number of points with coordinates such that $x > 0.6666$ and sums them. If there are a low number of points in the upper part of the space, then there will few points populating the Pareto corner which exists in the upper region, giving an indication of the Pareto corner density. Upper Density (σ_{Upp}) will be used to objectively assess copulas at Decision Gate 4.

4. Pareto Corner Density (σ_{ϕ}) is a custom metric that measures the density of points in the square area behind the Pareto frontier. This is called the Pareto corner and is formed by the lines $x = 0.6666$, $x = 1$, and the lines $y = 0.6666$,

$y = 1$. It counts the total number of points with coordinates such that $x > 0.6666$ and $y > 0.6666$. Then it sums them and normalizes by the total number of points. This metric provides a direct evaluation of the number of points in the Pareto corner and can theoretically take on values from 0 to 1. Values closer to zero indicate sparse corner sampling while values significantly higher than zero indicate a densely populated Pareto corner. Pareto Corner Density (σ_ϕ) will be used to objectively assess copulas at Decision Gate 4.

5. Pareto Frontier Point Density (ϕ) was described in Decision Gate 1 and can be used to determine the number of points on the Pareto frontier. This gives an indication of how many points remain behind the Pareto frontier that can potentially populate the Pareto corner. This can be used to decide how dense the Pareto corner is. Pareto Frontier Point Density (ϕ) will be used to objectively assess copulas at Decision Gate 4.

4.4.3.5 Decision Gate 5

Decision Gate 5 is depicted in Fig. 20 and asks whether the curved frontier copulas identified by Decision Gate 3 have sparse or dense Pareto corner density. The Pareto corner is the corner of the distribution behind the Pareto frontier which can be sparsely or densely sampled by different copulas. Similar to Decision Gate 4, Decision Gate 5 attempts to use density based statistics to objectively make this delineation for each copula. All of these statistics are presented in Table 6 with their ranking in each category and their associated symbol.

1. Lower Density (σ_{Low}) was described in Decision Gate 4 and can be used to determine the number of points in the lower third of the joint distribution. If there are a high number of points in the lower and middle parts of the space, then there will be less points remaining to populate the upper region where the Pareto corner is, giving an indication of the Pareto corner density. Due to

Table 6: Decision Gate 5 Candidate Metrics

Metric Name	Symbol	Ease of Implementation	Currently Available	Metric Computational Efficiency	Measure Property of this DG
1. Lower Density	σ_{Low}	High	Low	High	Medium
2. Middle Density	σ_{Mid}	High	Low	High	Medium
3. Upper Density	σ_{Upp}	High	Low	High	Medium
4. Pareto Corner Density	σ_{ϕ}	Medium	Low	Medium	High
5. Pareto Frontier Point Density	ϕ	Medium	Low	Medium	High

the superiority of other custom metrics to directly measure the density in the Pareto corner, Lower Density (σ_{Low}) will not be directly used to assess copulas at Decision Gate 5.

2. Middle Density (σ_{Mid}) was described in Decision Gate 4 and can be used to determine the number of points in the middle third of the joint distribution. If there are a high number of points in the lower and middle parts of the space, then there will be less points remaining to populate the upper region where the Pareto corner is, giving an indication of the Pareto corner density. Due to the superiority of other custom metrics to directly measure the density in the Pareto corner, Middle Density (σ_{Mid}) will not be directly used to assess copulas at Decision Gate 5.

3. Upper Density (σ_{Upp}) was described in Decision Gate 4 and can be used to determine the number of points in the lower third of the joint distribution. If there are a low number of points in the upper part of the space, then there will few points populating the Pareto corner which exists in the upper region, giving an indication of the Pareto corner density. Upper Density (σ_{Upp}) will be used to objectively assess copulas at Decision Gate 5.

4. Pareto Corner Density (σ_{ϕ}) was described in Decision Gate 4 and provides a direct evaluation of the number of points in the Pareto corner and can theoretically take on values from 0 to 1. Values closer to zero indicate sparse corner sampling while values significantly higher than zero indicate a densely populated Pareto corner. Pareto Corner Density (σ_{ϕ}) will be used to objectively assess copulas at Decision Gate 5.

5. Pareto Frontier Point Density (ϕ) was described in Decision Gate 1 and can be used to determine the number of points on the Pareto frontier. This gives an

indication of how many points remain behind the Pareto frontier that can potentially populate the Pareto corner. This can be used to decide how dense the Pareto corner is. Pareto Frontier Point Density (ϕ) will be used to objectively assess copulas at Decision Gate 5.

4.4.3.6 Decision Gate 6

Decision Gate 6 is depicted in Fig. 20 and asks whether the negative linear copulas identified by Decision Gate 2 are tail dependent or evenly distributed. Tail dependent copulas tend to have clustering with higher concentrations in small areas at one or both ends of the joint distribution. Evenly distributed copulas do not exhibit this clustering behavior but maintain roughly uniform sampling thorough the dependence structure. Decision Gate 6 attempts to make this distinction using metrics that detect the spread of the points in the joint distribution. All of these statistics are presented in Table 7 with their ranking in each category and their associated symbol.

1. Avg Inverse Distance ($\bar{d}^{-1}$) was described in Decision Gate 1 and can be used to assess inversely linear copulas to determine the average spread of points in the entire space. This can be used to determine if clustering is present when the metric has a low value. Avg Inverse Distance will be used to objectively assess copulas at Decision Gate 6.

2. Avg Inverse Lower Distance ($\bar{d}^{-1}_{Low}$) is a custom metric that measures the spread of the points in the lower third of the joint distribution off of the imaginary line $y = -x+1$. This is calculated in the same manner as Avg Inverse Distance ($\bar{d}^{-1}$), except it focuses only on the points in the lower third of the joint distribution between the lines $x = 0$ and the line $x = 0.3333$. The metric isolates all points with coordinates such that $x < 0.3333$ and then computes the absolute value of the vertical distance of these points above or below the line $y = -x + 1$. Then the Pythagorean theorem is applied to find the perpendicular distance

Table 7: Decision Gate 6 Candidate Metrics

Metric Name	Symbol	Ease of Implementation	Currently Available	Metric Computational Efficiency	Measure Property of this DG
1. Avg Inverse Distance	$\bar{d}^{-1}$	High	Low	High	High
2. Avg Inverse Lower Distance	$\bar{d}^{-1}_{Low}$	High	Low	High	High
3. Avg Inverse Middle Distance	$\bar{d}^{-1}_{Mid}$	High	Low	High	High
4. Avg Inverse Upper Distance	$\bar{d}^{-1}_{Upp}$	High	Low	High	High
5. Quantile Exceedance Probability	Θ	Low	Low	Low	High

of these points off of the line $y = -x + 1$. The perpendicular distance is then summed and divided by the total number of points in the lower third of the joint distribution to find an average perpendicular distance, or spread off of the line $y = -x + 1$ in the lower region of the space. If Avg Inverse Lower Distance ($\bar{d}^{-1}_{Low}$), Avg Inverse Middle Distance ($\bar{d}^{-1}_{Mid}$), and Avg Inverse Upper Distance ($\bar{d}^{-1}_{Upp}$) all have similar values, this can indicate that the points in the entire space are evenly distributed. However, if there is a disparity in their values, this can indicate some sort of tail dependence. Avg Inverse Lower Distance ($\bar{d}^{-1}_{Low}$) will be used to objectively assess copulas at Decision Gate 6.

3. Avg Inverse Middle Distance ($\bar{d}^{-1}_{Mid}$) is a custom metric that measures the spread of the points in the middle third of the joint distribution off of the imaginary line $y = -x + 1$. This is calculated in the same manner as Avg Inverse Distance ($\bar{d}^{-1}$), except it focuses only on the points in the middle third of the joint distribution between the lines $x = 0.3333$ and the line $x = 0.6666$. The metric isolates all points with coordinates such that $x > 0.3333$ and $x < 0.6666$, and then computes the absolute value of the vertical distance of these points above or below the line $y = -x + 1$. Then the Pythagorean theorem is applied to find the perpendicular distance of these points off of the line $y = -x + 1$. The perpendicular distance is then summed and divided by the total number of points in the middle third of the joint distribution to find an average perpendicular distance, or spread off of the line $y = -x + 1$ in the middle region of the space. If Avg Inverse Lower Distance ($\bar{d}^{-1}_{Low}$), Avg Inverse Middle Distance ($\bar{d}^{-1}_{Mid}$), and Avg Inverse Upper Distance ($\bar{d}^{-1}_{Upp}$) all have similar values, this can indicate that the points in the entire space are evenly distributed. However, if there is a disparity in their values, this can indicate some sort of tail dependence. Avg Inverse Middle Distance ($\bar{d}^{-1}_{Mid}$) will be used to objectively assess copulas at Decision Gate 6.

4. Avg Inverse Upper Distance ($\bar{d}^{-1}_{Upp}$) is a custom metric that measures the spread of the points in the upper third of the joint distribution off of the imaginary line $y = -x+1$. This is calculated in the same manner as Avg Inverse Distance ($\bar{d}^{-1}$), except it focuses only on the points in the upper third of the joint distribution between the lines $x = 0.6666$ and the line $x = 1$. The metric isolates all points with coordinates such that $x > 0.6666$, and then computes the absolute value of the vertical distance of these points above or below the line $y = -x + 1$. Then the Pythagorean theorem is applied to find the perpendicular distance of these points off of the line $y = -x + 1$. The perpendicular distance is then summed and divided by the total number of points in the upper third of the joint distribution to find an average perpendicular distance, or spread off of the line $y = -x+1$ in the upper region of the space. If Avg Inverse Lower Distance ($\bar{d}^{-1}_{Low}$), Avg Inverse Middle Distance ($\bar{d}^{-1}_{Mid}$), and Avg Inverse Upper Distance ($\bar{d}^{-1}_{Upp}$) all have similar values, this can indicate that the points in the entire space are evenly distributed. However, if there is a disparity in their values, this can indicate some sort of tail dependence. Avg Inverse Upper Distance ($\bar{d}^{-1}_{Upp}$) will be used to objectively assess copulas at Decision Gate 6.

5. Quantile Exceedance Probability (Θ) is an existing metric in the literature that measures the strength of dependence between two random variables using a limiting conditional probability in the extreme values of those variables. For example, when measuring upper tail dependence, the quantile exceedance probability examines the probability that a random variable exceeds a particular quantile value given that the other random variable also exceeds the same quantile value. Since this is the upper tail dependence, the limit is then taken as the quantile value approaches unity. Lower tail dependence is essentially the same but symmetrically opposite and evaluated in the limit of the quantile value approaching

zero. Further details regarding the calculation of quantile exceedance probabilities can be found in the text by McNeil et. al. [145]. Calculating the conditional probability can become difficult if the copula does not have a closed form, which is the case for several of the copula families simulated in this work. The quantile exceedance probability (Θ) can immediately reveal the degree of tail dependence in a copula but due to its difficulty in implementation for some Archimedean copulas, it will not be used to objectively assess copulas at Decision Gate 6.

4.4.3.7 Decision Gate 7

Decision Gate 7 is depicted in Fig. 20 and asks whether the linear copulas identified by Decision Gate 2 are tail dependent or evenly distributed. Tail dependent copulas tend to have clustering with higher concentrations in small areas at one or both ends of the joint distribution. Evenly distributed copulas do not exhibit this clustering behavior but maintain roughly uniform sampling thorough the dependence structure. Similar to Decision Gate 6, Decision Gate 7 attempts to make this distinction using metrics that detect the spread of the points in the joint distribution. All of these statistics are presented in Table 8 with their ranking in each category and their associated symbol.

1. Avg Distance ($\bar{d}$) was described in Decision Gate 1 and can be used to assess linear copulas to determine the average spread of points in the entire space. This can be used to determine if clustering is present when the metric has a low value. Avg Distance ($\bar{d}$) will be used to objectively assess copulas at Decision Gate 7.

2. Avg Lower Distance ($\bar{d}_{Low}$) is a custom metric that measures the spread of the points in the lower third of the joint distribution off of the imaginary line $y = x$. This is calculated in the same manner as Avg Distance ($\bar{d}$), except it focuses only on the points in the lower third of the joint distribution between the lines $x = 0$ and the line $x = 0.3333$. The metric isolates all points with coordinates

Table 8: Decision Gate 7 Candidate Metrics

Metric Name	Symbol	Ease of Implementation	Currently Available	Metric Computational Efficiency	Measure Property of this DG
1. Avg Distance	$\bar{d}$	High	Low	High	High
2. Avg Lower Distance	$\bar{d}_{Low}$	High	Low	High	High
3. Avg Middle Distance	$\bar{d}_{Mid}$	High	Low	High	High
4. Avg Upper Distance	$\bar{d}_{Upp}$	High	Low	High	High
5. Quantile Exceedance Probability	Θ	Low	Low	Low	High
6. Evenness Distribution	ε	High	Low	High	Medium

such that $x < 0.3333$ and then computes the absolute value of the vertical distance of these points above or below the line $y = x$. Then the Pythagorean theorem is applied to find the perpendicular distance of these points off of the line $y = x$. The perpendicular distance is then summed and divided by the total number of points in the lower third of the joint distribution to find an average perpendicular distance, or spread of the off of the line $y = x$ in the lower region of the space. If Avg Lower Distance ($\bar{d}_{Low}$), Avg Middle Distance ($\bar{d}_{Mid}$), and Avg Upper Distance ($\bar{d}_{Upp}$) all have similar values, this can indicate that the points in the entire space are evenly distributed. However, if there is a disparity in their values, this can indicate some sort of tail dependence. Avg Lower Distance ($\bar{d}_{Low}$) will be used to objectively assess copulas at Decision Gate 7.

3. Avg Middle Distance ($\bar{d}_{Mid}$) is a custom metric that measures the spread of the points in the middle third of the joint distribution off of the imaginary line $y = x$. This is calculated in the same manner as Avg Distance ($\bar{d}$), except it focuses only on the points in the middle third of the joint distribution between the lines $x = 0.3333$ and the line $x = 0.6666$. The metric isolates all points with coordinates such that $x > 0.3333$ and $x < 0.6666$, and then computes the absolute value of the vertical distance of these points above or below the line $y = x$. Then the Pythagorean theorem is applied to find the perpendicular distance of these points off of the line $y = x$. The perpendicular distance is then summed and divided by the total number of points in the middle third of the joint distribution to find an average perpendicular distance, or spread of the off of the line $y = x$ in the middle region of the space. If Avg Lower Distance ($\bar{d}_{Low}$), Avg Middle Distance ($\bar{d}_{Mid}$), and Avg Upper Distance ($\bar{d}_{Upp}$) all have similar values, this can indicate that the points in the entire space are evenly distributed. However, if there is a disparity in their values, this can

indicate some sort of tail dependence. Avg Middle Distance ($\bar{d}_{Mid}$) will be used to objectively assess copulas at Decision Gate 7.

4. Avg Upper Distance ($\bar{d}_{Upp}$) is a custom metric that measures the spread of the points in the upper third of the joint distribution off of the imaginary line $y = x$. This is calculated in the same manner as Avg Distance ($\bar{d}$), except it focuses only on the points in the upper third of the joint distribution between the lines $x = 0.6666$ and the line $x = 1$. The metric isolates all points with coordinates such that $x > 0.6666$, and then computes the absolute value of the vertical distance of these points above or below the line $y = x$. Then the Pythagorean theorem is applied to find the perpendicular distance of these points off of the line $y = x$. The perpendicular distance is then summed and divided by the total number of points in the upper third of the joint distribution to find an average perpendicular distance, or spread off of the line $y = x$ in the upper region of the space. If Avg Lower Distance ($\bar{d}_{Low}$), Avg Middle Distance ($\bar{d}_{Mid}$), and Avg Upper Distance ($\bar{d}_{Upp}$) all have similar values, this can indicate that the points in the entire space are evenly distributed. However, if there is a disparity in their values, this can indicate some sort of tail dependence. Avg Upper Distance ($\bar{d}_{Upp}$) will be used to objectively assess copulas at Decision Gate 7.

5. Quantile Exceedance Probability (Θ) was described in Decision Gate 6 and can be used to directly assess the degree of dependence in the tails of the joint distribution. However, due to the difficulty in calculating this metric for copulas that don't have closed form, as is the case for some of the copulas simulated in this work, this metric will not be used to objectively assess copulas at Decision Gate 7.

6. Evenness Distribution (ε) is a custom metric based on several custom metrics

also described in Decision Gate 7. It attempts to quantify the difference between the overall Avg Distance ($\bar{d}$) and the average distances specific to each third of the space, and then summing those three differences. Essentially it tires to quantify how different the spread in any one third of the space is from the spread in the overall space, and then sum those differences. If the sum is close to zero, then the differences are low and the points are likely evenly distributed. However, if the sum is non-zero then this could indicate some type of tail dependence. Evenness Distribution (ε) will be used to objectively assess copulas at Decision Gate 7.

4.4.3.8 Decision Gate 8

Decision Gate 8 is depicted in Fig. 20 and asks whether the tail dependent copulas identified by Decision Gate 7 have narrow or wide tails. Narrow tail copulas appear to converge to a point in the corner of the tail while wide tail copulas maintain greater spread at the tail end of the space. Decision Gate 8 attempt to use a combination of spread and density statistics to delineate between narrow and wide tail copulas. All of these statistics are presented in Table 9 with their ranking in each category and their associated symbol.

1. Lower Density (σ_{Low}) was described in Decision Gate 4 and can be used to determine the number of points in the lower third of the joint distribution. If the tails are narrow there will be many points clumped in them relative to the middle third, potentially leading to a higher point density in the upper and lower regions of the space. In this way narrowness of the tails could be assessed, but other metrics can discern the spread of points in the tails more directly so Lower Density (σ_{Low}) will not be directly used to assess copulas at Decision Gate 8.

2. Middle Density (σ_{Mid}) was described in Decision Gate 4 and can be used to

Table 9: Decision Gate 8 Candidate Metrics

Metric Name	Symbol	Ease of Implementation	Currently Available	Metric Computational Efficiency	Measure Property of this DG
1. Lower Density	σ_{Low}	High	Low	High	Medium
2. Middle Density	σ_{Mid}	High	Low	High	Medium
3. Upper Density	σ_{Upp}	High	Low	High	Medium
4. Avg Lower Distance	$\bar{d}_{Low}$	High	Low	High	High
5. Avg Middle Distance	$\bar{d}_{Mid}$	High	Low	High	High
6. Avg Upper Distance	$\bar{d}_{Upp}$	High	Low	High	High

determine the number of points in the middle third of the joint distribution. If the tails are narrow there will be many points clumped in them relative to the middle third, potentially leading to a higher point density in the upper and lower regions of the space. In this way narrowness of the tails could be assessed, but other metrics can discern the spread of points in the tails more directly so Middle Density (σ_{Mid}) will not be directly used to assess copulas at Decision Gate 8.

3. Upper Density (σ_{Upp}) was described in Decision Gate 4 and can be used to determine the number of points in the lower third of the joint distribution. If the tails are narrow there will be many points clumped in them relative to the middle third, potentially leading to a higher point density in the upper and lower regions of the space. In this way narrowness of the tails could be assessed, but other metrics can discern the spread of points in the tails more directly so Upper Density (σ_{Upp}) will not be used to objectively assess copulas at Decision Gate 8.

4. Avg Lower Distance ($\bar{d}_{Low}$) was described in Decision Gate 7 and can be used to determine the spread of points in the lower third of the space. If the spread is relatively low compared to the middle or upper thirds, this indicates the lower tail is narrow. In this way it can be determined if the right tail is narrow or not. Avg Lower Distance ($\bar{d}_{Low}$) will be used to objectively assess copulas at Decision Gate 8.

5. Avg Middle Distance ($\bar{d}_{Mid}$) was described in Decision Gate 7 and can be used to determine the spread of points in the middle third of the space. If the spread is relatively high compared to the upper or lower thirds, this indicates that one or both of the tails are narrow. Avg Middle Distance ($\bar{d}_{Mid}$) will be used to objectively assess copulas at Decision Gate 7.

6. Avg Upper Distance ($\bar{d}_{Upp}$) was described in Decision Gate 7 and can be used to determine the spread of points in the upper third of the space. If the spread is relatively low compared to the middle or lower thirds, this indicates the upper tail is narrow. In this way it can be determined if the left tail is narrow or not. Avg Upper Distance ($\bar{d}_{Upp}$) will be used to objectively assess copulas at Decision Gate 7.

4.4.3.9 Decision Gate 9

Decision Gate 9 is depicted in Fig. 20 and asks whether the narrow tail dependent copulas identified by Decision Gate 8 are left tail dependent, right tail dependent, or both tail dependent. Left (lower) tail dependent copulas have smaller spread in the left tail relative to the middle region and right (upper) tail. Right (upper) tail dependent copulas have smaller spread in the right tail relative to the middle region and left (lower) tail. Both tail dependent copulas have smaller spread in the both the upper (right) and lower (left) tails relative to the middle region of the space. Decision Gate 9 will attempt to use a combination of spread and tail dependence statistics to identify all three types of tail dependence simultaneously. All of these statistics are presented in Table 10 with their ranking in each category and their associated symbol.

1. Avg Distance ($\bar{d}$) was described in Decision Gate 1 and can be used to assess the spread of the points in the overall space. A comparison of this value with the spread in the tails can be used to determine the type of tail dependence in these copulas. Avg Distance ($\bar{d}$) will be used to objectively assess copulas at Decision Gate 9.

2. Avg Lower Distance ($\bar{d}_{Low}$) was described in Decision Gate 7 and can be used to determine the spread of points in the lower third of the space. If the spread is relatively low compared to the middle or upper thirds, this indicates at least left tail dependence, and possibly both tail dependence depending on the behavior

Table 10: Decision Gate 9 Candidate Metrics

Metric Name	Symbol	Ease of Implementation	Currently Available	Metric Computational Efficiency	Measure Property of this DG
1. Avg Distance	$\bar{d}$	High	Low	High	High
2. Avg Lower Distance	$\bar{d}_{Low}$	High	Low	High	High
3. Avg Middle Distance	$\bar{d}_{Mid}$	High	Low	High	High
4. Avg Upper Distance	$\bar{d}_{Upp}$	High	Low	High	High
5. Quantile Exceedance Probability	Θ	Low	Low	Low	High
6. Upper to Lower Ratio	υ	High	Low	High	High

in the middle and upper regions. In this way the type of dependence can be discerned. Avg Lower Distance ($\bar{d}_{Low}$) will be used to objectively assess copulas at Decision Gate 9.

3. Avg Middle Distance ($\bar{d}_{Mid}$) was described in Decision Gate 7 and can be used to determine the spread of points in the middle third of the space. If the spread is relatively high compared to the upper or lower thirds, this indicates left or right tail dependence depending on which region has lower spread. It could also indicate both tail dependence if both the upper and lower regions have less spread than the middle region. Avg Middle Distance ($\bar{d}_{Mid}$) will be used to objectively assess copulas at Decision Gate 9.

4. Avg Upper Distance ($\bar{d}_{Upp}$) was described in Decision Gate 7 and can be used to determine the spread of points in the upper third of the space. If the spread is relatively low compared to the middle or lower thirds, this indicates at least right tail dependence, and possibly both tail dependence depending on the behavior in the middle and lower regions. In this way the type of dependence can be identified. Avg Upper Distance ($\bar{d}_{Upp}$) will be used to objectively assess copulas at Decision Gate 9.

5. Quantile Exceedance Probability (Θ) was described in Decision Gate 6 and can be used to directly assess the degree of dependence in the tails of the joint distribution, thereby revealing the type of tail dependence as well. However, due to the difficulty in calculating this metric for copulas that don't have closed form, as is the case for some of the copulas simulated in this work, this metric will not be used to objectively assess copulas at Decision Gate 9.

6. Upper to Lower Ratio (υ) is a custom metric based on several custom metrics also used in Decision Gate 9. It attempts to quantify a comparison of the spread in the upper (right) tail to that of the lower (left) tail. It is measured by dividing

the Avg Upper Distance ($\bar{d}_{Upp}$) by the Avg Lower Distance ($\bar{d}_{Low}$). If this ratio is high it indicates that copula has left tail dependence. If the ratio is low it indicates that copula has right tail dependence. If the ratio has a relatively middle value it indicates both tail dependence. In this way all three types of dependence can be simultaneously determined by this metric. Upper to Lower Ratio (υ) will be used to objectively assess copulas at Decision Gate 9.

4.4.3.10 Decision Gate 10

Decision Gate 10 is depicted in Fig. 20 and asks whether the wide tail dependent copulas identified by Decision Gate 8 are left tail dependent, right tail dependent, or both tail dependent. Left (lower) tail dependent copulas have smaller spread in the left tail relative to the middle region and right (upper) tail. Right (upper) tail dependent copulas have smaller spread in the right tail relative to the middle region and left (lower) tail. Both tail dependent copulas have smaller spread in the both the upper (right) and lower (left) tails relative to the middle region of the space. Similar to Decision Gate 9, Decision Gate 10 will attempt to use a combination of spread and tail dependence statistics to identify all three types of tail dependence simultaneously. All of these statistics are presented in Table 11 with their ranking in each category and their associated symbol.

1. Avg Distance ($\bar{d}$) was described in Decision Gate 1 and can be used to assess the spread of the points in the overall space. A comparison of this value with the spread in the tails can be used to determine the type of tail dependence in these copulas. Avg Distance ($\bar{d}$) will be used to objectively assess copulas at Decision Gate 10.

2. Avg Lower Distance ($\bar{d}_{Low}$) was described in Decision Gate 7 and can be used to determine the spread of points in the lower third of the space. If the spread is relatively low compared to the middle or upper thirds, this indicates at least left

Table 11: Decision Gate 10 Candidate Metrics

Metric Name	Symbol	Ease of Implementation	Currently Available	Metric Computational Efficiency	Measure Property of this DG
1. Avg Distance	$\bar{d}$	High	Low	High	High
2. Avg Lower Distance	$\bar{d}_{Low}$	High	Low	High	High
3. Avg Middle Distance	$\bar{d}_{Mid}$	High	Low	High	High
4. Avg Upper Distance	$\bar{d}_{Upp}$	High	Low	High	High
5. Quantile Exceedance Probability	Θ	Low	Low	Low	High
6. Upper to Lower Ratio	υ	High	Low	High	High

tail dependence, and possibly both tail dependence depending on the behavior in the middle and upper regions. In this way the type of dependence can be discerned. Avg Lower Distance ($\bar{d}_{Low}$) will be used to objectively assess copulas at Decision Gate 10.

3. Avg Middle Distance ($\bar{d}_{Mid}$) was described in Decision Gate 7 and can be used to determine the spread of points in the middle third of the space. If the spread is relatively high compared to the upper or lower thirds, this indicates left or right tail dependence depending on which region has lower spread. It could also indicate both tail dependence if both the upper and lower regions have less spread than the middle region. Avg Middle Distance ($\bar{d}_{Mid}$) will be used to objectively assess copulas at Decision Gate 10.

4. Avg Upper Distance ($\bar{d}_{Upp}$) was described in Decision Gate 7 and can be used to determine the spread of points in the upper third of the space. If the spread is relatively low compared to the middle or lower thirds, this indicates at least right tail dependence, and possibly both tail dependence depending on the behavior in the middle and lower regions. In this way the type of dependence can be identified. Avg Upper Distance ($\bar{d}_{Upp}$) will be used to objectively assess copulas at Decision Gate 10.

5. Quantile Exceedance Probability (Θ) was described in Decision Gate 6 and can be used to directly assess the degree of dependence in the tails of the joint distribution, thereby revealing the type of tail dependence as well. However, due to the difficulty in calculating this metric for copulas that don't have closed form, as is the case for some of the copulas simulated in this work, this metric will not be used to objectively assess copulas at Decision Gate 10.

6. Upper to Lower Ratio (υ) is a custom metric based on several custom metrics also used in Decision Gate 10. It attempts to quantify a comparison of the

spread in the upper (right) tail to that of the lower (left) tail. It is measured by dividing the Avg Upper Distance ($\bar{d}_{Upp}$) by the Avg Lower Distance ($\bar{d}_{Low}$). If this ratio is high it indicates that copula has left tail dependence. If the ratio is low it indicates that copula has right tail dependence. If the ratio has a relatively middle value it indicates both tail dependence. In this way all three types of dependence can be simultaneously determined by this metric. Upper to Lower Ratio (υ) will be used to objectively assess copulas at Decision Gate 10.

4.4.3.11 Decision Gate Metrics

Several different objective metrics have been identified for each Decision Gate. Using the High, Medium, and Low qualitative assessment, each of these descriptive statistics was down selected to form the most useful set to assess copulas at each Decision Gate based on the features most relevant to the Decision Gate. This down selection helps to answer Research Question 1.1. Objective repeatable statistics do exist that can capture the subjective behaviors qualitatively assessed at each decision gate. However, it remains to be tested how well these metrics will perform in assessing copulas through the entire copula selection tree.

4.4.4 Copulas Training Set

The overarching research question attempts to determine if the copula selection tree is consistent with objective statistics. These objective metrics have been selected but they're accuracy has not been verified. CAST is a subjective tool to identify copulas that produce relevant dependence structures for practitioners. Using objective statistics to replicate this subjective tool is essentially creating a model or surrogate of CAST. Models aim to reproduce the same result as the phenomena they are imitating, yet they all have some degree of error. The objective statistics and decision gates are trying to reproduce, in an objective manner, the same copula groupings that

are included in the subjective copula selection tree. Any copulas that the objective statistics do not assign to the same groupings can be thought of as model error. In order to reduce the model error, a training set of copulas will be created to improve the predictive capacity of the chosen metrics at each decision gate.

The copulas in the leaves of Fig. 20 were assigned to their current groupings by a subjective cataloging process. The training set of copulas is created directly from this initial version of CAST. Each copula and theta value in all the leaves represents a member of the training set. Some copulas had ranges or open intervals for their θ values, so each one was individually added to the training set to ensure all the copulas and their subjectively made leaf assignments were included. For example, if the copula selection tree showed a leaf with copula N14, $\theta = 12$, then the training set includes one observation of N14θ12. If the selection tree showed a leaf with an open interval like N14, $\theta > 12$, the training set has only one observation of this copula which corresponds to the start of the open interval, N14θ12. If the selection tree showed a leaf with a specific range like N14, $\theta = 10 - 12$, the training set has only two observations corresponding to the upper and lower limits of the θ range, N14θ10 and N14θ12. Each copula and theta value in Fig. 20 was recorded and added to the training set in this manner. The training set of copulas had 86 different copulas at the end of this process. The training set also recorded the subjectively assigned label (leaf) for each of these copulas, which is also shown in Fig. 20.

4.4.5 Measuring the Training Set

All the copulas in the training set are simulated and then measured using the objective statistics chosen for each decision gate. The statistical values of these metrics is recorded and saved as each copula is simulated in Matlab. The values of these statistics are used to determine how each copula passes through the decision gates and then ultimately which label it is assigned.

4.4.6 Baseline Objective Tree

A baseline objective tree is created using the training set of copulas and the vector of objective metrics chosen for each decision gate. The objective metrics are laid over the decision gates in the subjective selection tree in Fig. 20, replacing the qualitative questions of each decision gate with objective statistics. Instead of a qualitative answer determining how a copula proceeds through a decision gate, the objective metric value will now make this delineation. The threshold values of the objective metrics will need to be identified through the training process. If a copula has a metric value above or below the threshold that will determine the group it is directed to after the current decision gate. The baseline objective tree now consists of the training set copulas taken from the original copula selection tree in Fig. 20, and the objective metrics which can be used to decide membership at each decision gate by dividing the copulas into two different branches at each gate until the final leaves are reached. However, the objective metrics cannot predict membership until the threshold values of each metric are identified for all the decision gates.

4.4.7 Metric Threshold Values

Determining the threshold values of these objective metrics that can accurately predict membership of the copulas at each decision gate is a difficult task. All of the copulas entering a decision gate must be isolated and then they must be separated into the subgroups they will be directed to after the decision gate. Then each group must be analyzed to determine what metric values belong to each subgroup to identify a proper threshold for distinguishing the subgroups. This process must be repeated for all ten decision gates. Due to the difficulty in performing this task manually, machine learning techniques are used to find the threshold values.

There are many different types of machine learning algorithms. Hierarchical clustering methods are a popular class of machine learning algorithms. They are broadly

categorized into agglomerative and divisive clustering techniques. K-means clustering, a divisive partitional algorithm popularized by its simplicity, seemed like a natural fit for this problem because its objective was to divide the original data set into K groups based on the properties of the members in the data set. CAST had 14 different groups (leaves) and appropriate objective statistics to classify the copulas into those groupings. However, clustering based techniques did not produce good results because they consider all of the objective statistics simultaneously when creating the groupings. This is not appropriate for replicating the selection tree groupings because all of the metrics are not relevant at every single decision gate. For example, Pareto Frontier Point Density (ϕ) is not a relevant statistic for Decision Gate 8 which is trying to determine whether the linear copulas have narrow or wide tails. Considering all the objective statistics simultaneously in this manner, as clustering techniques do, inputs irrelevant noise to the algorithm leading to poor results.

4.4.8 Discriminant Analysis

Discriminant analysis is a machine learning technique that can be applied in stages and only uses the variables given to it at each stage. It does not need all the available information at once like clustering to form groupings. In addition, it can be applied independently to each decision gate one at a time, which can help avoid unnecessary noise metrics in the discrimination process. Discriminant analysis uses patterns and features to separate two or more classes of outcomes. It predicts membership in a group based on observed values of continuous variables. Discriminant analysis is already available in jmp software and only requires the factors to use for classification at the decision gate of interest and the actual subjective labels that the decision gate will apply to the copulas. The classification factors are continuous variables known as covariates. The algorithm calculates the multivariate mean, or centroid, of the actual groups using the covariates. Then using the Mahalanobis distance

(refer to Ref. [134] for further details) of each observation from the centroid of each group, it predicts the probabilty that the observation belongs to each group. Each observation's membership is assigned to the group with the highest probability. Then this is compared with the subjective assignment made by the decision maker for each observation to determine the total number of misclassified observations from the discriminant analysis process.

In this case the observations are the simulated copulas in the training set. The covariates are the objective metrics that are used to measure distinct features of the copulas. Based on the metrics chosen, the discriminant analysis will try to predict the group in which each copula belongs. Each decision node of the subjective tree has 2 or more outcomes, directing the copulas to a different node until they are filtered into a leaf. The discriminant analysis will try to predict the membership of the copulas at each decision node, based on the measured values of the metrics for each copula. In JMP software, the discriminant analysis process also provides a scatterplot matrix of the chosen covariates plotting all the observations and the normal probability contours of the predicted groupings. This plot provides a simple way to identify the threshold value of each covariate that maximizes the distance between each group.

The discriminant analysis process is applied to each decision gate individually. It takes in all the copulas entering that decision gate and predicts each copula's subgroup membership as it leaves the decision gate using the objective metrics relevant to that decision gate. The discriminant analysis process not only gives the predicted subgroups for each copula based on the covariates, but it also provides threshold values of the classification factors at which to cutoff membership between groupings. As part of the training process of the objective model, the prediction accuracy at each decision gate is improved by testing different individual objective metrics and combinations of metrics to use as classification factors. The metric or combination of metrics yielding the least misclassified predictions and highest probability of correct

prediction will be chosen for each decision gate. This process is repeated for all ten decision gate to arrive at the best set of covariates for each decision gate, and their corresponding threshold values.

4.4.8.1 Decision Gate 1

Decision Gate 1 is the input to the copula selection tree and receives all the copulas in the training set. Decision Gate 1 determines if the input samples of copulas are linear or nonlinear. The objective metrics available to the discriminant analysis algorithm are Pearson's ρ, Kendall's τ, Spearman's ρ, Avg Distance ($\bar{d}$), Avg Inverse Distance ($\bar{d}^{-1}$), Origin Corner Density (σ_o), and Pareto Frontier Point Density (ϕ). Multiple experiments are run using these metrics to test how well they can discriminate each copula observation and match its subjective assignment. Initially individual metrics are tested on their own. However, this gives high mislabeling results. For example, Fig. 21 shows the discriminant analysis results of Pearson's ρ as the only covariate.

This experiment gives 12 mislabeled copulas so the next metric, Kendall's τ is used in the second experiment as a covariate to see if it can act as a better discriminant. The experiment results are shown in Fig. 22.

This experiment gives 9 mislabeled copulas which is an improvement over Pearson's ρ by itself. The next experiment uses Spearman's ρ as the only discriminant and its results are shown in Fig. 23.

This experiment gives 12 mislabeled copulas which is worse than Kendall's τ. Kendall's τ is the best covariate up so far. Since none of the existing metrics was able to predict the copulas with complete accuracy, the discriminant analysis process will now test custom metrics. The next experiment is with Avg Distance ($\bar{d}$) and its results are shown in Fig. 24.

This experiment gives 6 mislabeled copulas which is better than Kendall's τ. The first custom metric performs better than all the existing metrics tested so far. The

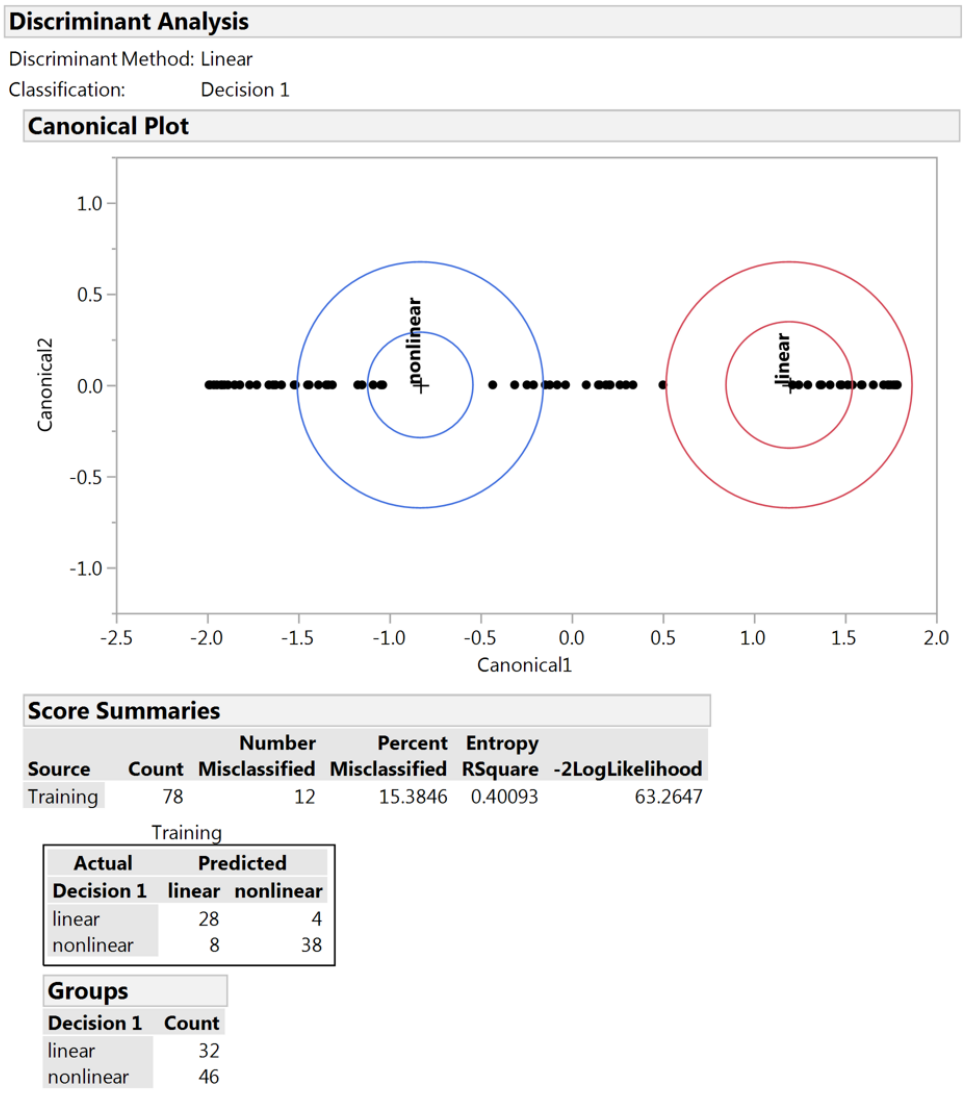

Figure 21: Discriminant analysis with Pearson's ρ

next experiment is with Avg Inverse Distance ($\bar{d}^{-1}$) and its results are shown in Fig. 25.

This experiment gives 17 mislabeled copulas which is the worst performing individual covariate yet. It should not be used on its own as a discriminant for this decision gate. The next experiment is with Origin Corner Density (σ_o) and its results are shown in Fig. 26.

This experiment gives 9 mislabeled copulas. The final single covariate experiment

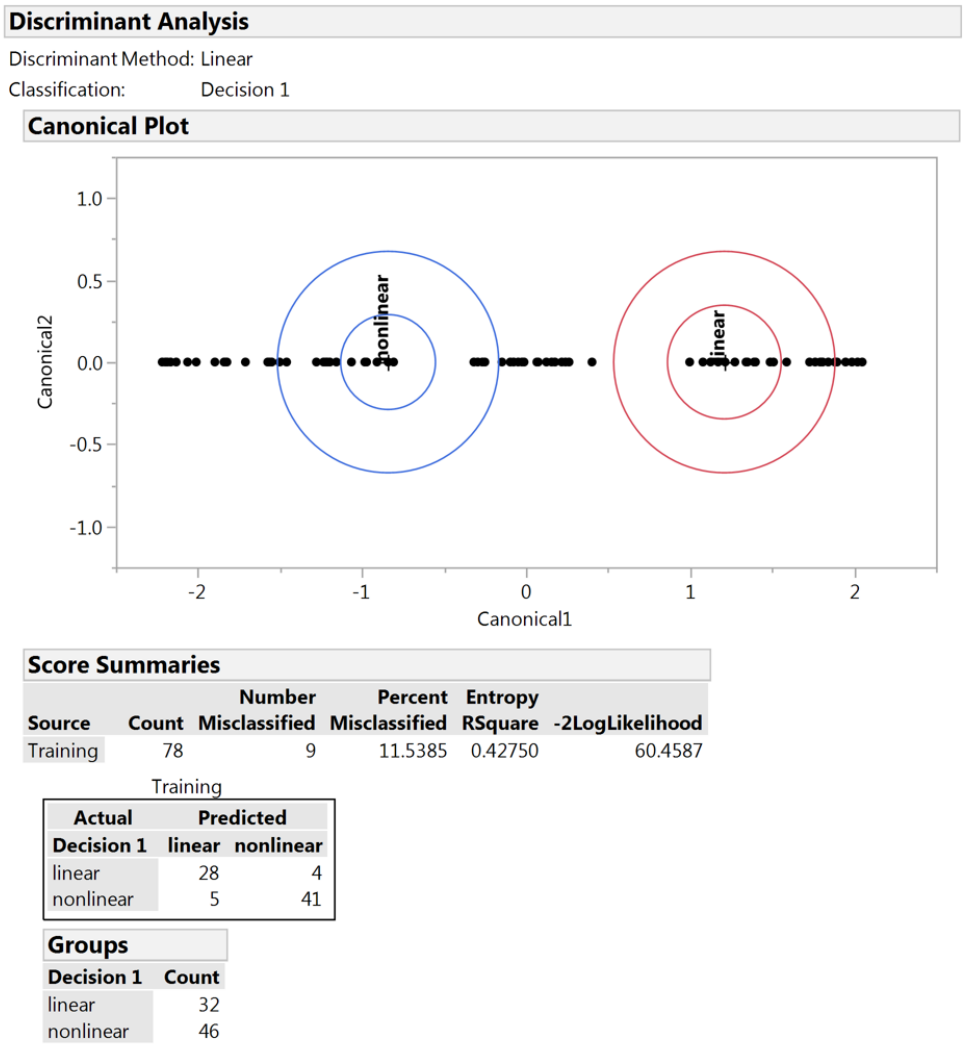

Figure 22: Discriminant analysis at Decision Gate 1 with Kendall's τ

is with Pareto Frontier Point Density (ϕ) and its results are shown in Fig. 27.

This experiment gives 26 mislabeled copulas reflecting a very poor individual discriminant for this decision gate. Since none of the objective metrics were satisfactory discriminators on their own, further experiments will be conducted using combinations of objective metrics to find the group resulting in the fewest possible mislabeled copulas. The first combination of metrics is all of the existing metrics as covariates combining Pearson's ρ, Kendall's τ, and Spearman's ρ. The results are shown in Fig. 28.

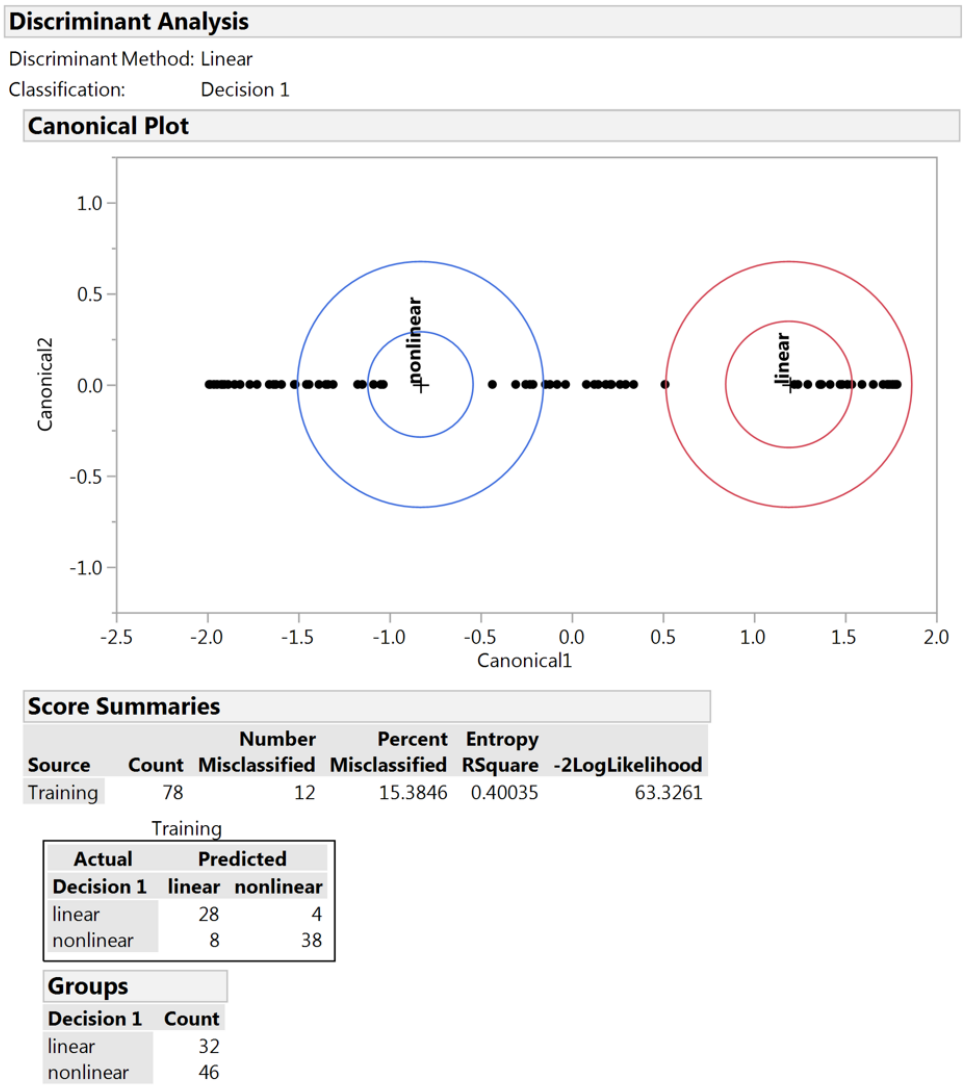

Figure 23: Discriminant analysis at Decision Gate 1 with Spearman's ρ

This first combination of existing metrics gives 9 mislabeled copulas. This is better than some of the individual covariates by themselves, but still not satisfactory. The next combination of metrics is all of the custom metrics combined; Avg Distance ($\bar{d}$), Avg Inverse Distance ($\bar{d}^{-1}$), Origin Corner Density (σ_o), and Pareto Frontier Point Density (ϕ). The results are shown in Fig. 29.

This combination of metrics utilizing all the custom metrics resulted in 0 mislabeled copulas. This experiment yielded the best results for the input set of copulas and indicates that the training set can be predicted through Decision Gate 1 with

Discriminant Analysis

Discriminant Method: Linear

Classification: Decision 1

Canonical Plot

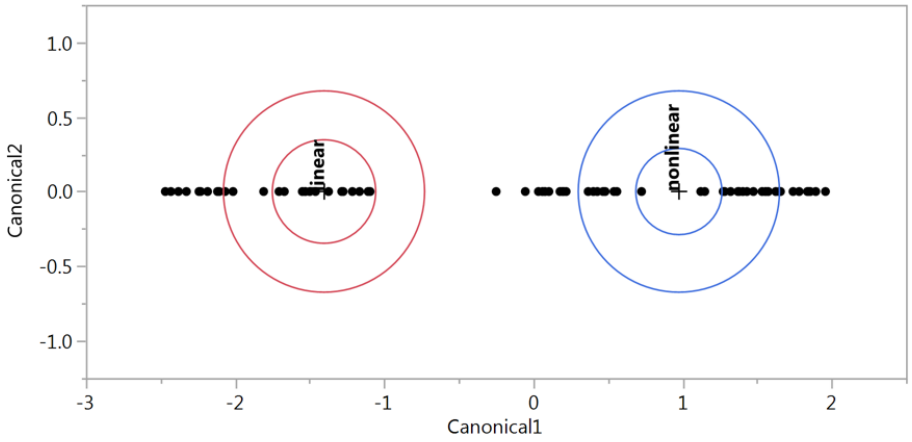

Score Summaries

Source	Count	Number Misclassified	Percent Misclassified	Entropy RSquare	-2LogLikelihood
Training	78	6	7.69231	0.46857	56.1213

Training

Actual Decision 1	Predicted linear	Predicted nonlinear
linear	28	4
nonlinear	2	44

Groups

Decision 1	Count
linear	32
nonlinear	46

Figure 24: Discriminant analysis at Decision Gate 1 with Avg Distance ($\bar{d}$)

100% accuracy using these objective metrics. These metrics and their threshold values are recorded and saved to construct the objective model of CAST. Training the objective model to pass through this decision gate with perfect accuracy on the input set copulas is an important first step in demonstrating that the subjective assigned membership of each copula is consistent with objective metrics. The output subgroups from Decision Gate 1 are labeled as linear or nonlinear and are passed to Decision Gate 2 and Decision Gate 3. There the set of copulas input to those decision gates will be analyzed to identify the combination of objective metrics that can best predict the membership of copulas passing through that decision gate.

Discriminant Analysis

Discriminant Method: Linear

Classification: Decision 1

Canonical Plot

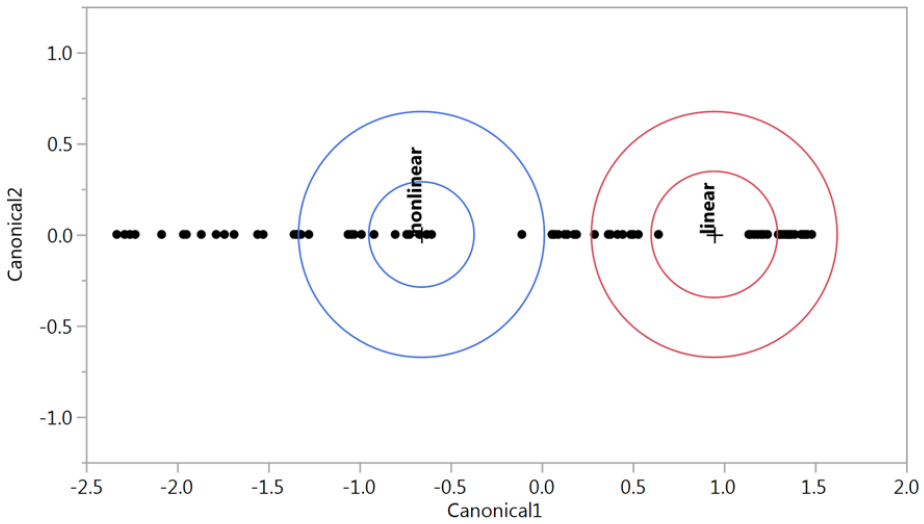

Score Summaries

Source	Count	Number Misclassified	Percent Misclassified	Entropy RSquare	-2LogLikelihood
Training	78	17	21.7949	0.31779	72.0439

Training

Actual Decision 1	Predicted linear	Predicted nonlinear
linear	28	4
nonlinear	13	33

Groups

Decision 1	Count
linear	32
nonlinear	46

Figure 25: Discriminant analysis at Decision Gate 1 with Avg Inverse Distance ($\bar{d}^{-1}$)

This discriminant analysis process is repeated at Decision Gate 2 and 3, and all the other decision gates in CAST to identify the ideal set of covariates that can replicate the answer to the qualitative question asked at each decision gate. The discriminant analysis reports for all of the tested combinations of covariates at Decision Gate 1 are presented in this section. The discriminant analysis reports for the remaining nine decision gates are provided in Appendix 7.2.

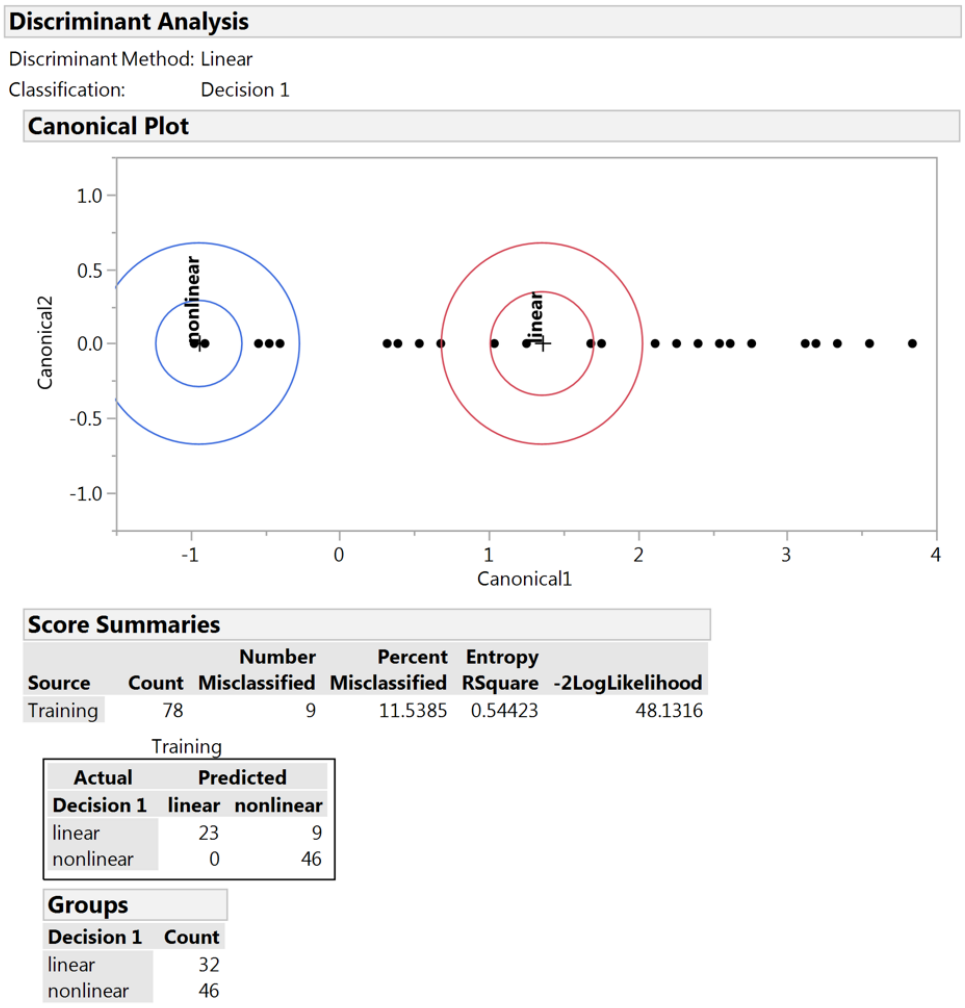

Figure 26: Discriminant analysis at Decision Gate 1 with Origin Corner Density (σ_o)

4.4.8.2 Decision Gate Covariates

The covariate or combination of covariates yielding the least misclassified predictions and highest probability of correct prediction for each decision gate will depend on the copulas input to the decision gate. If the copula observation's subjective assignment is updated during the training process, this will affect the prediction accuracy for a given set of covariates at a decision gate. It will also affect the threshold values of the corresponding objective metrics identified during the discriminant analysis process. The best set of covariates for each decision gate and their associated threshold values

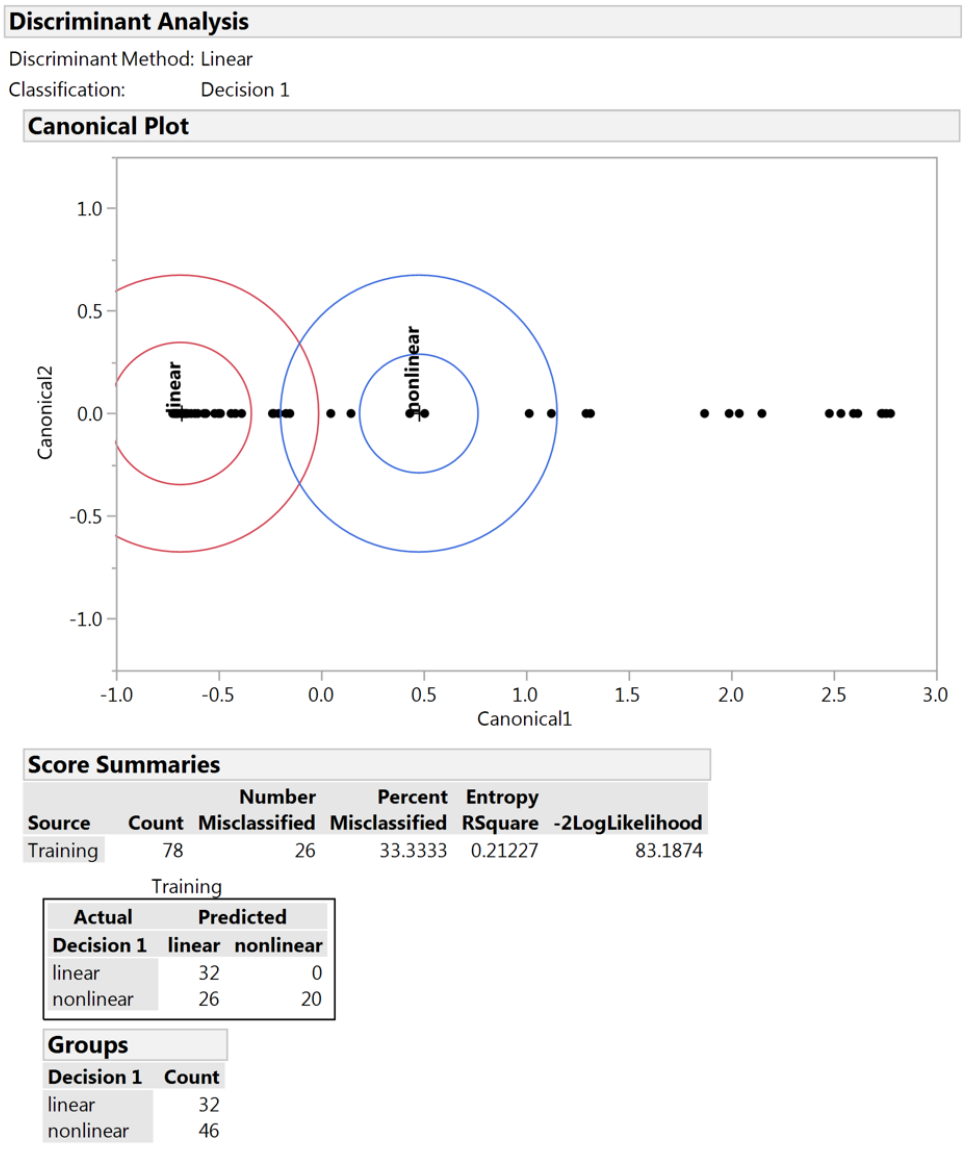

Figure 27: Discriminant analysis at Decision Gate 1 with Pareto Frontier Point Density (ϕ)

will evolve as the sample of copulas in the training set changes during the training of the objective tree. The final set of covariates at each decision gate and their threshold values will be fixed at the end of the training process.

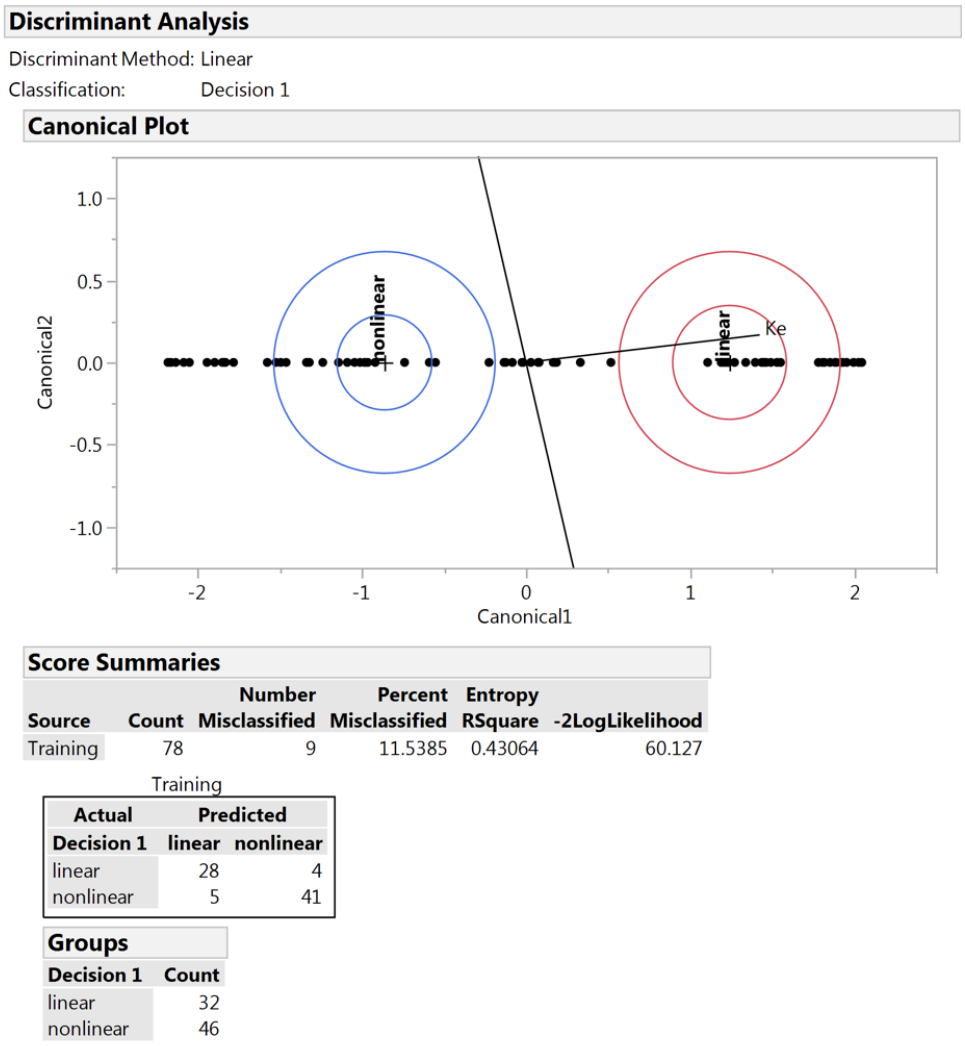

Figure 28: Discriminant analysis at Decision Gate 1 with Pearson's ρ, Kendall's τ, and Spearman's ρ

4.4.9 Training the Objective Selection Tree

A baseline objective tree has been created using the training set of copulas and the objective metrics identified earlier. Discriminant analysis is chosen as the most appropriate machine learning technique for objectively predicting membership at each decision gate using different classification factors that will be tested as part of the training process. The goal of the training process is to be able to create an objective selection tree that can predict the groupings of all copulas in the training set with

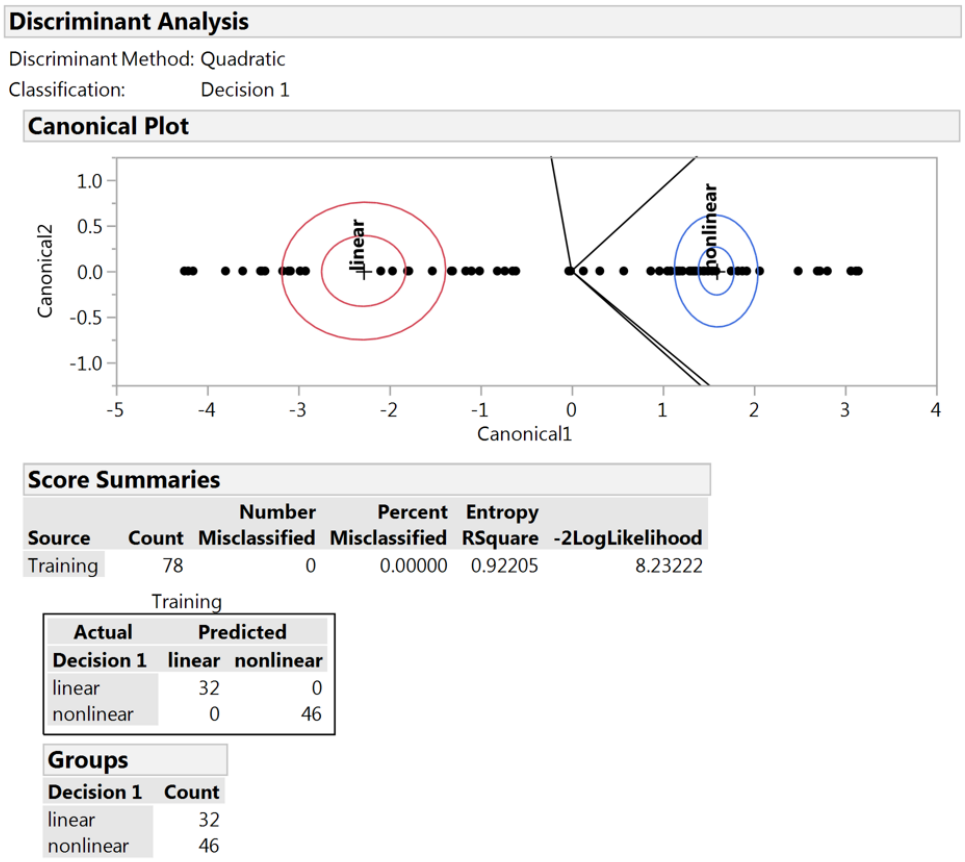

Figure 29: Discriminant analysis at Decision Gate 1 with Avg Distance ($\bar{d}$), Avg Inverse Distance ($\bar{d}^{-1}$), Origin Corner Density (σ_o), and Pareto Frontier Point Density (ϕ)

100% accuracy relative to their subjective assignments. Currently the objective model has error in its predictive capability on the training set, or model fit error. This can be improved upon by finding better combinations of covariates at each decision gate in the discriminant analysis process or changing the copulas in the training set. Finding better combinations of covariates is akin to increasing the complexity of the surrogate model to improve its predictive capabilty. Changing the copulas in the training set is similar to removing outliers or failed cases from the observations the surrogate is trained on.

The training process will reveal the accuracy of the subjective assignments proposed in Fig. 20. Some of the subjective assignments have wider ranges of θ then they

should in order to belong to a particular leaf. Recall that the leaves of the subjectively created selection tree are intended to be archetypal of a particular dependence structure. For this reason the training process based on objective metrics may reveal that the θ ranges for some copulas may need to be narrowed or shifted. It could also show that some copulas families do not belong to a certain leaf at all and that the subjective assignment should be refined in order to improve the prediction accuracy of the objective model. Then the improved set of copulas in the training set are sent back to the discriminant analysis process to see if a new combination of objective covariates can better predict the refined subjective assignments.

Essentially the training of the objective model is an iterative process depicted in Fig. 30, with two degrees of freedom. The first degree of freedom is to change the copulas in the training set by adjusting their θ values or by changing the copula families in the leaves by refining their subjective assignments. This degree of freedom is altered while locking the second degree of freedom in the training process which is the combination of covariates at each decision gate. Then a Matlab script is used to measure the number of mislabeled copulas in the training set based on the adjusted copulas in the training set and the locked covariates at each decision gate. Then the first degree of freedom is locked by freezing the copulas in the training set. This set of copulas is passed to the discriminant analysis process and the second degree of freedom is unlocked. The discriminant analysis process uses the updated set of input copulas in the training set and attempts to improve its prediction accuracy by altering the combinations of covariates used to forecast membership through each decision gate. It finds the combination of covariates that yields the least number of misclassified copulas and highest probability of correct membership for each decision gate. All the mislabeled copulas are counted and identified at the end of the discriminant analysis process. Now the second degree of freedom is locked by freezing the combination of covariates at each decision gate. Then the process begins a new iteration by

unlocking the first degree of freedom. This iterative training process converges when the objective model can predict the entire training set of copulas with 100% accuracy and there is zero model fit error.

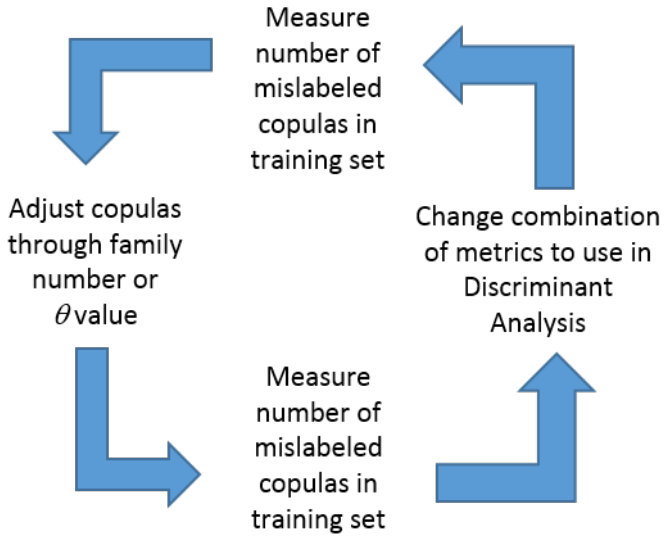

Figure 30: Iterative Objective Tree Training Process

4.4.10 Training Challenges

While executing the preliminary loops of the iterative training process in Fig. 30, it became clear that the initial subjective tree proposed in Fig. 20 could be improved upon. The improvements came as a result of overcoming challenges encountered during the early phases of the training process but their solutions yielded insights into the selection tree structure and helped to answer specific research questions posed earlier.

In some instances the subjective assignment of where a copula belongs was made incorrectly because of how the distribution of points was interpreted by the decision maker. In these instances the copulas in the tree leaf were not actually representative of the archetypal feature displayed by that leaf. For example, the N7θ0.001 copula has a distribution appearing like that of leaf F in Fig. 20. However this type of distribution is not archetypal of an evenly distributed, negatively dependent, linear

copula. An even distribution would have an uniform spread of points along the inverse diagonal, whereas this distribution is more of a perfectly straight inverse line with a couple of points in the upper triangle section above the diagonal. In reality the N7θ0.001 copula is more representative of leaf C, a nonlinear dependence structure with a linear Pareto frontier and sparse corner sampling. That is why even though the subjective assignment for this copulas was leaf F, the objective metrics kept predicting its membership in leaf C through the discriminant analysis. Examining this issue revealed that the ideal, evenly distributed, negative dependent, linear copula should have a different distribution from that which is shown in leaf F. This realization resulted in a replacement of the visualization used to represent the archetypal dependence structure depicted by leaf F in the final copula selection tree. It also became clear that the N7θ0.001 copula does not ideally represent the archetypal dependence structure desired in leaf F or leaf C, and so even though it is placed in leaf C by the discriminant analysis process, it was still removed from the training set. This increased the prediction accuracy of the discriminant analysis process. Overcoming this challenge helped to improve the understanding of the archetypal dependence structure in leaf F and aided in improving the credibility of the copula selection tree as a whole. This also answers Research Question 1.3 which asks whether the tree groupings can be improved to avoid similar looking leaves and if objective statistics exist that can differentiate these leaves. The groupings can be improved by adjusting copulas that were subjectively assigned to leaves whose properties they are not archetypal of reflecting. Even though leaves may appear similar, the discriminant analysis process can still identify when a copula is in the wrong leaf because it is based on objective statistics. The objective statistics for each leaf have been identified in the decision gate immediately preceding the leaf. In this case leaf C and leaf F actually split from each other at Decision Gate 1, so the relevant objective statistics for differentiating them are Avg Distance, Avg Inverse Distance, Origin Corner Density,

and Pareto Frontier Point Density.

Another challenge was that the full range of θ values for some copulas in the proposed subjective tree (Fig. 20) was too wide to be consistently labeled correctly by the discriminant analysis process. Examples of this include copulas from leaf K such as N4θ2$-$8 and N12θ3$-$25. Some of these θ ranges include fringe copulas that do not accurately represent the distinct dependence structure that a particular leaf was meant to capture. The θ range was refined to only those copulas which were archetypal of the distinct dependence structure desired for that leaf, and which the objective metrics could accurately and consistently predict through the discriminant analysis process. In some cases this was done by shifting the θ range, in others it was done by narrowing it. In the case of leaf K, the copula families were refined to N4$\theta 6 - 10$ and N12$\theta 5 - 7$. This answers Research Question 1.4 which asks how the subjectively labeled θ values can be objectively verified and at what point the subjective estimates of θ become unreliable. The θ ranges of each family can be verified through the objective metrics used in the discriminant analysis process. If it can objectively and accurately predict a copula's leaf, then that θ value belongs in the given leaf. The subjective estimates of θ become unreliable when the discriminant analysis can not consistently predict membership for that θ value accurately. These θ values are not included as being archetypal of a particular leaf's dependence structure and are removed from the training set. Overcoming this challenge increased the robustness and predictive capability of the objective copula selection tree while improving its overall credibility.

Following the iterative process depicted in Fig. 30 repeatedly, finally yielded a training set of copulas and a combination of covariates that predicted them with 100% accuracy. The results of this lengthy training process are shown in Fig. 31.

The objective selection tree uses descriptive statistics to accurately classify every copula in the training set. At the completion of the training process, there were 78

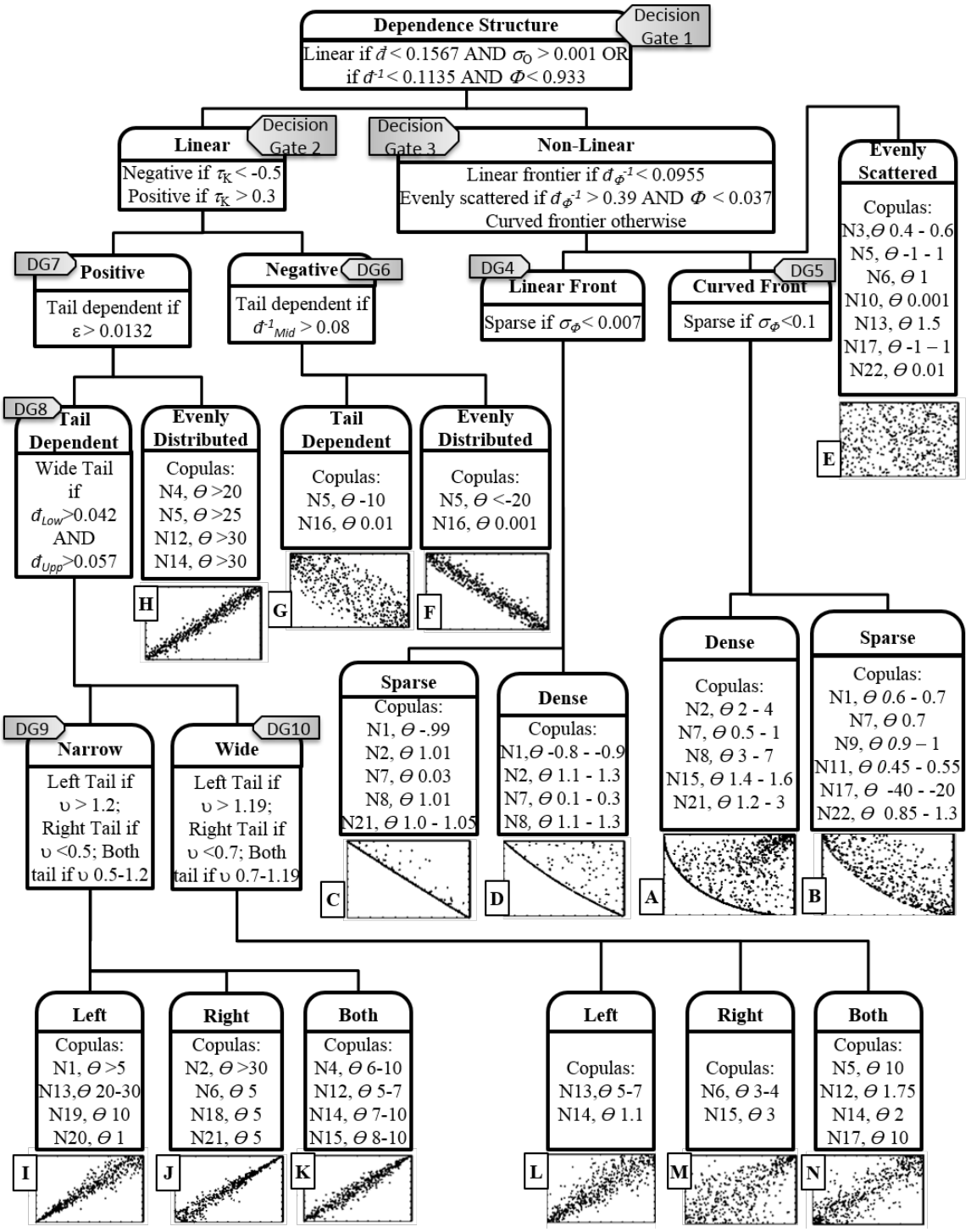

Figure 31: Archimedean CopulA Selection Tree (CAST) based on objective metrics

copulas in the leaves of the selection tree. Each one has been verified to be archetypal of the dependence structure of the leaf to which it belongs. This confirms that the

objective metrics can predict the groupings of all copulas in the training set. Next this objective model is validated against copulas beyond those in the training set.

4.4.11 Validating the Objective Selection Tree

In response surface methodology a surrogate model is validated by calculating its model representation error. This metric is used to check how well the model performs on data points that it was not trained on. In a similar way, the objective copula selection tree will be validated against copulas that are outside the range of θ values it was trained on. It will also contain new instantiations of the same copulas it was trained on because copulas are probabilistic in nature.

The analogy for model fit error and model representation error is useful to understand how this objective tree model is created, trained, and validated. However, the analogy has a shortcoming because in the traditional response surface methodology the data points used to train the surrogate model are deterministic. If a surrogate model is recreated using the same settings and training points, it will be identical to the original surrogate. However, copulas are probabilistic so when two different instantiations of a copula are created, using the same copula family and θ value, its joint distributions will not be identical. The overall dependence structure will be similar but the points will not be in the exact same place due to the stochasticity in the sampling process. Consequently it is necessary to ensure that different instantiations of the same copula give relatively constant values of the metrics to ensure repeatability. If there are a low number of points in a copula sample, the metrics measuring the joint distribution will not be stable and repeatability will be poor. However, if the number of points is high and more typical of probabilistic studies (on the order of hundreds to thousands), then the metrics will be relatively constant. Any variation of the objective metrics due to the probabilistic nature of copulas is either captured within the metrics decision tolerance or is insignificant enough that

a new instantiation of the same copula won't be mislabeled in the training set. The biggest factor to ensure repeatability is to maintain a high number of points in the copula distribution that gives stable values of the objective metrics. After running many simulations on various Archimedean copula families and tracking the desired objective metrics, this was determined to be about 1,500 points for each simulation.

All of the 78 copulas from the final iteration of the training set are designated as test type 1. A new instantiation of each of these copulas will be created using the same copula family and θ value. These 78 repeated copulas are designated as test type 2. The validation set also include copulas that have θ values inside the range of those in the training set, but not explicitly included in the training set. For example, if the training set hypothetically included the copula N14, $\theta 10 - 12$ (Test type 1), then the validation set will include a copula inside that θ range, e.g., N14, $\theta 11$. These copulas are designated as test type 3. Finally, the validation set also includes copulas that have θ values outside the range of those in the training set. For example, if the training set hypothetically included the copula N14, $\theta 10 - 12$ (Test type 1), then the validation set will include a copula outside that θ range, e.g., N14, $\theta 15$. These copulas are designated as test type 4. Test type 4 copulas are extrapolations for the model and are not expected to be predicted well by the objective metrics. Most of these copulas were removed during the initial training process of the objective model as they are not archetypal of a particular dependence structure found in any of the selection tree leaves. However, these fringe copulas do exist mathematically and investigating them through the selection tree will help reveal their purpose.

4.4.12 Validation Set Hypotheses

A formal hypothesis should be 100% tractable and verifiable, it should be directly supported by experiments, and it should have a low likelihood of being achieved by chance or other factors beyond the experiment [66]. With these factors in mind, four

hypotheses are formulated for each test type of copulas in the validation set.

1. Hypothesis 1.1: Copulas of test type 1 will be predicted with 100% accuracy by the objective copula selection tree

2. Hypothesis 1.2: Copulas of test type 2 will be predicted with 100% accuracy by the objective copula selection tree

3. Hypothesis 1.3: Copulas of test type 3 will be predicted with 100% accuracy by the objective copula selection tree

4. Hypothesis 1.4: Copulas of test type 4 will be predicted with greater than 75% accuracy by the objective copula selection tree

Hypothesis 1.1 is expected because it was a stated requirement from the training process of the objective model that each copula in the training set be predicted with 100% accuracy. Hypothesis 1.2 is a reasonable expectation if the objective model is repeatable on the probabilistic copulas. This hypothesis will be verified if there are enough points in the copula samples for the objective metrics to be relatively stationary between different instantiations. Hypothesis 1.3 should also be expected since these θ values are inside the range of test type 1 which are required to be 100% accurate. Hypothesis 1.4 is made on copulas that the model is not expected to predict well and so has been given a degree of error tolerance. The 25% and 75% limits are standard quartiles used in measuring error distributions. The 75% quartile is used here because the objective model is trained to be very accurate on copulas within its θ ranges and it is expected to handle some degree of extrapolation decently well.

4.4.13 Objective Copula Selection Tree Results

All of these hypotheses were tested with a single experiment which ran all of the validation set copulas through a script to compare their subjective leaves with the

Table 12: Objective Copula Selection Tree Experimental Results

Copula Test Type	Amount of this Type	Correct	Incorrect	Accuracy Hypothesis	Accuracy Actual
1	78	78	0	100%	100%
2	78	78	0	100%	100%
3	37	37	0	100%	100%
4	68	58	10	>75%	85%

objective selection tree's label assignment. The results of the experiment are shown in Table 12.

The training set, test type 1 copulas, did have 100% accuracy as expected. The overall validation set (test types 2, 3, and 4) had 95% accuracy and only 10 mislabeled copulas in all. These ten copulas were all test type 4 and outside the range of θ values that the objective tree was trained for. The objective selection tree shows excellent predictive capability for test types 1, 2, and 3. For test type 4 copulas, which the model had to extrapolate on to predict, the objective tree had good performance and verified the hypothesis.

This proves the objective model can predict well outside the ranges that it was trained on but this is not required of it. The errors represent fringe copulas which are not archetypal of distinct dependence structures that are useful to practitioners. Even though many were predicted correctly by the objective model (58 out of 68), this only indicates that the values of their objective metrics were within the tolerances

allowed by the discriminant analysis process at each decision gate. This answers Research Question 1.2 which asks what are the implications of fringe copulas and where do they belong in the objective selection tree. While they may exist mathematically, their correct prediction by the objective model does not imply that they are archetypal of the distinct dependence structures that a practitioner would like to use when incorporating a relationship between two random variables in a probabilistic assessment.

Predicting test type 2 copulas with 100% accuracy helps to answer the final research question of this section (Research Question 1.5) which asks how the tree groupings can be validated in a repeatable manner and how the subjective copula selection tree can be arrived upon by repeatable objective statistics. In total there are 261 different copulas in the training and validation sets, and in large part they were all predicted very well by the objective model. The overall accuracy of this exercise provides an objective and repeatable validation of the groupings in the tree leaves through a statistical representation that is consistent with the final form of the subjective tree shown in Fig. 32. The objective model that corresponds to Fig. 32 is given in Fig. 31 along with the objective descriptive statistics at each decision gate and their threshold values. The key difference between these two figures is simply what the decisions are based on at each decision gate. In Fig. 32 they are based on subjective answers to qualitative questions, and in Fig. 31 they are based on objective measurable statistics.

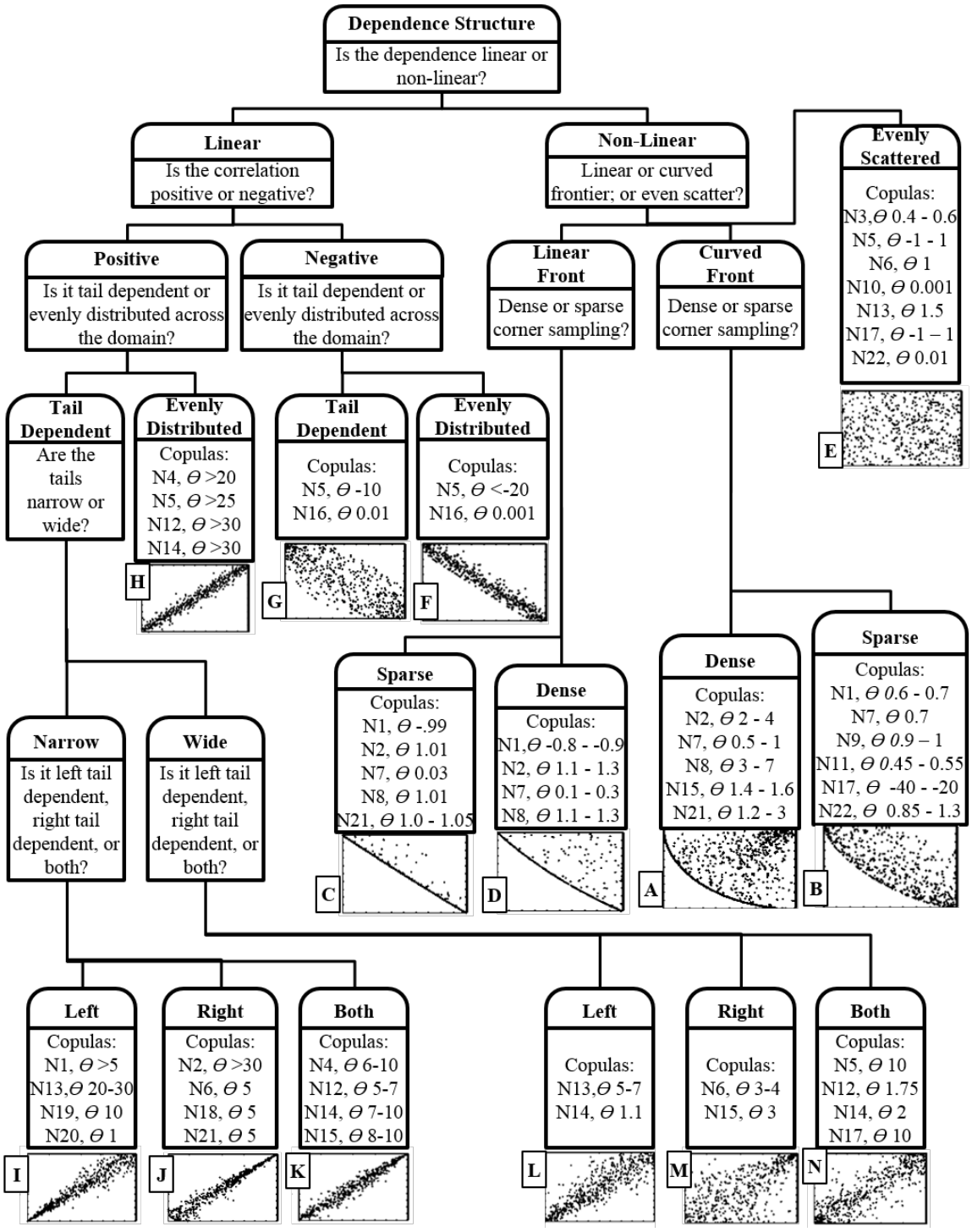

Figure 32: Archimedean CopulA Selection Tree (CAST) with objectively verified and validated copula groupings

4.4.14 Research Question 2

Reviewing copula applications in other fields provides an understanding of how they are used and what kind of effect they can have. The next question is how can they be applied and what kind of effect will they have in aerospace applications, particularity for aircraft technology assessment problems. This leads to Research Question 2.

Research Question 2

What is the quantified effect of using copulas in aircraft technology assessment? What types of applications are they suited for and how does that affect their impact?

Expectation 2

Copulas will have a significant effect on the variance of the output distribution relative to independent simulations. The amount of change will vary depending on the application and variables chosen for dependence with the copula.

Research Question 2 is also answered with an expectation because it must be further reduced to developed a testable hypothesis. The effect of using copulas will be different between applications and depends on a multitude of factors including which random variables are related with the copula, what their marginal distributions are, how much of an effect those variables have on the response, etc. In the interest of demonstrating copulas for technology assessment it is important to illustrate the specific ways that these relationships can exist between random variables and how copulas can be used to capture them. Drawing from personal experience and the literature, three different real world applications will be tested to examine couplings that exist between technology impact factors. The experiment for all three will be

similar in that they will be executed using the same canonical airplane performance problem employing the Breguet range equation. The technologies will be applied to a baseline aircraft to create an improvement in range. Each of the three technology applications will demonstrate a different way to capture an existing coupling between technology impact factors. The experiment will be used to quantify the difference in the output when coupling is treated as independent and when it is captured by a copula.

4.4.14.1 Research Question 2.1

The first research subquestion is directed at examining a coupling that exists when a single technology is used. The coupling between its benefit and penalty to the aircraft system is considered.

Research Question 2.1
What is the quantified effect of using a copula to relate a benefit and a penalty within a single technology?
Hypothesis 2.1
The quantified effect of using copulas in a single technology will be a 10% reduction of output pdf standard deviation with a mean shift of less than 5% relative to independent case

4.4.14.2 Research Question 2.2

The second research subquestion examines the coupling across two different technologies that happen to impact the same technology impact factor.

Research Question 2.2

What is the quantified effect of using a copula to relate the same technology impact factor across two different technologies?

Hypothesis 2.2

The quantified effect of using copulas across two different technologies will be a 10% reduction of output pdf standard deviation with a mean shift of less than 5% relative to independent case

4.4.14.3 Research Question 2.3

The third research subquestion considers the potential coupling between a design parameter and a technology impact factor.

Research Question 2.3

What is the quantified effect of using a copula to relate a technology impact factor with a design parameter?

Hypothesis 2.3

The quantified effect of using copulas between a technology impact factor and a design parameter will be a 15% reduction of output pdf standard deviation with a mean shift of less than 5% relative to independent case

All three of these research subquestions will be answered using the same experiment, by using three different applications of a canonical airplane performance problem. The assumptions and formulation of the canonical problem are described at

length in the following section. The specific technologies used in each application, their marginal distribution parameters, and the copulas used to capture the proposed couplings are also discussed in detail. The proposed simulations and experiments were actually performed in advance to increase confidence in the method. As such, preliminary results for each application are also included in the next section. These results and their implications will be discussed in greater detail during future work.

4.5 Formulation and Implementation of the Canonical Problem

A representative canonical problem is formulated and implemented to illustrate the use of copulas in aircraft performance analysis and design subject to uncertain technology benefits. In doing so a quantitative characterization of how probabilistic results change with the use of copulas is illustrated, thus providing a measure of the potential value added by copulas to the aerospace domain. These applications are meant to demonstrate where dependencies may exist in the aerospace domain and how copulas can be used to capture them. While this canonical problem will obviously not cover all the potential applications in the vast field of aerospace engineering, it will be sufficient to give the systems analyst an understanding of how copulas can probabilistically capture a dependence structure and better represent the uncertainty in any problem.

Technologies of interest are modeled by way of performance benefits and degradations at the subsystem level where the effects are approximately known. Intermediate impact factors in the performance model capture these effects and propagate them to aircraft mission-level measures of performance. By treating impact factors as random variables, the performance model is effectively made probabilistic with respect to the technology impacts.

The canonical problem centers about the estimation of mission range for a 300 passenger twin aisle commercial airliner for which various technology improvement

options exist. This vehicle is modeled to be representative of aircraft in the current fleet with respect to configuration, technology level, and mission performance. It assumes a wing area of 4,200 ft^2 and a wing span of 196 ft, yielding an effective aspect ratio of 9.13 after correcting for wing glove area on the order of 313 ft^2. It is further assumed that the entire cruise is realized at 39,000 ft, Mach 0.84. Weight and other assumptions are detailed throughout this section.

The mission range is estimated using the Breguet equation in a numerical integration approach so as to allow for variations in lift to drag ratio and specific fuel consumption throughout cruise. The interval of instantaneous weight values between the start of cruise W_0 and end of the cruise W_1 is broken down uniformly into n intervals. For each interval j, W_i^j and W_f^j respectively denote the initial and final weights, so that

$$W_i^j > W_f^j \ \forall \ j \tag{20}$$

$$W_i^j - W_f^j = c \ \forall \ j \tag{21}$$

$$W_0 - W_1 = W_i^{j=1} - W_f^{j=n} \tag{22}$$

$$= \sum_{j=1}^{n} W_i^j - W_f^j \tag{23}$$

A sufficiently large number n of correspondingly smaller intervals ensures adequate approximation of the numerical approach to the analytical solution, while balancing against acceptable computational runtime. A routine involving weights, aerodynamics, and propulsion analysis leading up to the Breguet equation is recursively executed, once for each weight value segment, to estimate the corresponding range for the j^{th} cruise segment as follows:

$$R^j = \frac{V}{TSFC}\frac{L}{D} log\left(\frac{W_i^j}{W_f^j}\right) \tag{24}$$

For simplicity fuel consumption for taxi out, takeoff, climb, descent, reserves, and taxi in are assumed constant and are estimated as shown in Table 13. This assumption

implies that the considerable majority of the aircraft's fuel consumption occurs during the cruise phase, and assumed technology improvements are only reflected in cruise range estimates. The total mission fuel weight is also fixed based on the estimated fuel capacity allowance, allowing range to vary as a function of V, $TSFC$, and L/D. The payload weight is estimated for 300 passengers at 180 lb per passenger plus 30 lb baggage.

Accordingly, weight values for the start of cruise W_0 and end of the cruise W_1 are calculated by

$$W_0 = W_{Ramp} - W_{TaxiOut} - W_{Takeoff} - W_{Climb}; \tag{25}$$

$$W_1 = W_{Oper} + W_{Payload} + W_{Descent} + W_{Reserves} + W_{TaxiIn}; \tag{26}$$

Level flight conditions at a constant Mach number are used for the entire cruise phase so that lift must be equal to weight and thrust must be equal to drag at all times. Thus, for each cruise segment the required lift coefficient can be estimated from its fundamental definition as follows:

$$C_L = W_i/(qS); \tag{27}$$

Drag is estimated in typical fashion as

$$D = C_D qS \tag{28}$$

where the drag coefficient is handled as the sum of lift dependent and lift induced contributions

$$C_D = C_{D,0} + C_{D,i} \tag{29}$$

Lift independent drag is approximated as

$$C_{D,0} = \frac{S_{wet}}{S} C_{fe} \tag{30}$$

Table 13: Weight assumptions for component and mission segment fuel consumption

Weight Group	Value [lb]
W_{Empty}	257,839
W_{Misc}	19,946
W_{Oper}	$W_{Empty} + W_{Misc}$
$W_{Payload}$	62,210
W_{Fuel}	215,697
W_{Ramp}	$W_{Oper} + W_{Payload} + W_{Fuel}$
$W_{TaxiOut}$	453
$W_{Takeoff}$	1,179
W_{Climb}	10,270
$W_{Descent}$	3,341
$W_{Reserves}$	20,231
W_{TaxiIn}	251

where S_{wet} is the wetted area of the aircraft. The ratio of S_{wet} to S is approximated from empirical data and supporting relationships as presented by Anderson, [6] Ch. 2.9. C_{fe} is the equivalent skin friction coefficient that is a function of Reynolds number based on the mean chord length. Approximation of C_{fe} follows empirical relationships by Anderson, [6] Ch. 2.9 following earlier data published in the work by Jobe[96]. Induced drag is estimated by

$$C_{D,i} = k\ C_L^2 \tag{31}$$

The constant k is in turn approximated based on Prandtl's lifting line theory for a high aspect ratio straight wing as

$$k = \frac{1}{\pi e AR} \tag{32}$$

The span efficiency factor e is also calculated from lifting line theory as a function of the parameter δ

$$e = \frac{1}{1+\delta} \tag{33}$$

which is in turn a function of the aspect ratio and taper ratio as illustrated by Anderson, [6] p. 110.

The equality condition for thrust and drag provides a known value of thrust with which fuel consumption may be estimated. To this avail, an engine deck constructed in prior efforts [203, 205] for a turbofan engine representative of those found in the current fleet of 300-passenger commercial airliners. The engine is an axial flow twin-shaft turbofan that achieves an overall pressure ratio of 40 with a bypass ratio of 9, and yields a maximum static thrust of 94,000 lbs at sea level. Thrust and thrust specific fuel consumption (TSFC) contours at maximum power code are shown in Fig. 33 as representative figures of engine performance.

The engine deck provides thrust and TSFC values for prescribed combinations of

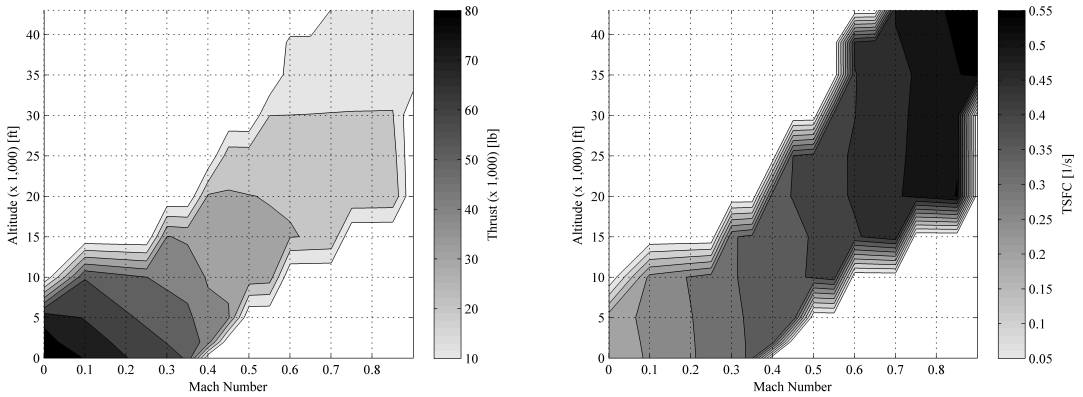

(a) Thrust (b) TSFC

Figure 33: Thrust and TSFC for Mach number and altitude

altitude, Mach number, and power code. The engine deck is arranged as a three-dimensional array on which 3-dimensional interpolation operations are readily implemented. One array has thrust values for corresponding values of altitude, Mach number, and power code along each of the three dimensions of the array. A second array is constructed with TSFC values in the same manner. The thrust array is used to determine the power code PC_j that yields the required thrust (T=D) for a known cruise altitude and Mach number. The aircraft has two engines for this calculation. The TSFC array is used to determine fuel consumption for the known cruise altitude, Mach number, and power code PC_j.

Given the formulation and accompanying assumptions discussed in this section, a nominal range of 7,170 nmi is estimated which is commensurate with existing large twin aisle aircraft in the 300-passenger capacity class. Variations of this nominal value result from the introduction of improvements or degradations in prescribed technology impact areas. For the canonical problem in this work, technology improvement areas typical of recent systems analysis and technology assessment efforts in aeronautics for commercial transport aircraft are adopted. The canonical problem considers weight reduction benefits for major airframe components and structural weight groups achieved through new materials and manufacturing processes. Weight degradations

are also considered as potential weight penalties incurred by other variations. This effect with a technology impact factor t_{WE} on empty weight is modeled so that W_{Empty} in Table 13 is adjusted as

$$W_{Empty} = W_{Empty,nominal}\ (t_{W_{Empty}});\ \text{where } W_{Empty,nominal} = 257,839 \tag{34}$$

Potential benefits and degradations are considered in overall aerodynamic characteristics and this effect is modeled with factors on lift independent and lift induced components of drag. Equation 29 is thus recast as

$$C_D = C_{D,0}\ (t_{C_{D,0}}) + C_{D,i}\ (t_{C_{D,i}}) \tag{35}$$

Lastly, engine performance improvements and degradations are manifested as changes in TSFC. The engine deck array for TSFC is uniformly scaled with an impact factor t_{TSFC} so that TSFC values are scaled accordingly for given values of altitude, Mach number, and power code.

$$TSFC = TSFC_{nominal}\ (t_{TSFC}) \tag{36}$$

TSFC is scaled using the technology impact factor t_{TSFC} through Eq. 36 to incorporate changes specified by relevant technology impact factor distributions. The engine deck array for thrust is not changed, thus assuming that technology impacts allow for the same thrust to be attained throughout the flight envelope prescribed by the engine deck, albeit at a greater or lesser fuel expense.

Technology impact factors in this problem setup are defined for the domain [0, ∞) and normalized at 1 to represent nominal conditions, namely no technology impacts. Values in the interval [0,1) imply reductions of the corresponding performance parameter with the extreme case at 0, and values in the interval (1, ∞) imply increments.

For this canonical problem, technologies pursuant of current aeronautical research and development efforts are considered as documented in published literature. The

identification of technology impact factors and the definition of corresponding distributions follow from our judgment and interpretation of relevant published work. All technology impacts are triangular distributed, a methodological choice popular in subjective encoding applications such as this one because they are readily defined by only three parameters that are intuitive and easily understood: minimum, most likely (mode), and maximum value.

Three different technology impact applications are demonstrated for copulas. The first application considers a single advanced wing technology, Hybrid Laminar Flow Control (Technology 1, T1). This technology features benefits and penalties including skin friction drag reduction, engine horsepower extraction, and additional system weight. Although these impacts are certainly related to one another, their relationship is not fully known or quantified. Copulas are used to describe these relationships and examine the resulting effect on estimate distributions for mission range relative to those assuming independent impact factors. The second application considers two different technologies with effects on the same impact factor: HLFC and Wing Riblets (Technology 2, T2), both featuring the same primary impact on skin friction drag reduction. A dependence structure in the contributions of the two technologies toward this impact factor is established to account for the nonlinear addition of the two contributions. A third application considers the Advanced Aerodynamic Wing (Technology 3, T3) and the allowances it provides with respect to wing weight and the corresponding selection of aspect ratio as a fundamental wing design parameter. Copulas are used to capture the aforementioned dependence structure, noting that in this third application the design decision over aspect ratio is effectively modeled as a random variable coupled with uncertain wing properties.

In the interest of keeping with the simplicity of the canonical problem and isolating the effect of copulas in the probabilistic evaluation, the aircraft are not reoptimized nor redesigned with the simulated implementation of technologies. Accordingly the

first and second applications are commensurate with retrofitting an existing aircraft or developing a variant with the technologies in question. Similarly, the third application may be interpreted as the assessment of a new aircraft variant with a redesigned and more technologically advanced wing but with no other changes in the airframe.

At this point, it is worth reminding ourselves when the use of copulas is prudent and when it is not. When a connection between two variables is very well known and can be predicted with very little uncertainty, a deterministic relationship is best. This includes relationships for which the physical processes are well understood and predictive models have been verified and validated over many years. In these types of relationships, introducing a copula will artificially and unnecessarily increase uncertainty, a step that should be reasonably avoided. On the opposite extreme of the spectrum is the situation in which absolutely no information is known about the relationship between two variables. The presence of one does not have any effect on the other, or the effect is completely unknown. Introducing a copula in this situation would reduce the uncertainty, but the reduction would be arbitrary and not based on any known or estimated relation. As a result, the reduction in the variation of the response would not be justified, and a copula should not be used. However, most engineering problems are not of this nature. Many engineering applications fall under the category in which engineering judgment can state that some relationship between two variables does exist and perhaps can be qualitatively assessed, but the degree of uncertainty in the relation is either unknown or difficult to quantify. This is where copulas can fill an important gap and help systems analysts to incorporate and understand the effect of uncertainty in design problems.

4.5.1 Copulas in a Single Aerodynamic Wing Technology

4.5.1.1 Application 1 Formulation

The first application considers the impacts of a single technology and how their relationship can be quantified to more accurately predict aircraft performance. Technology 1 (T1) is wing Hybrid Laminar Flow Control (HLFC) in which passive mechanisms such as shaping and surface finishing (commonly referred to as Natural Laminar Flow) are combined with Active Flow Control in the form of suction or blowing to tailor boundary behavior. The principal aim of this technology is to preserve laminarity of the boundary layer and delay the onset of turbulence transition. The local effect is a reduction in skin friction drag. HLFC suction can be provided in a number of ways, one of which is a vacuum pump driven by the engine accessory gearbox. This vacuum is extended from the engine driven pump to the wing and distributed along the leading edge. The pump, vacuum piping, and supporting structure impose a weight penalty on the aircraft. Testing conducted by NASA has shown that this technology can offer skin friction drag reduction of approximately 10% or more depending upon the percentage of the wing observing laminar flow [101, 100, 69, 201]. These studies have also shown that benefits increase with greater aircraft size and range [101]. To achieve this amount of skin friction drag reduction, a certain amount of engine horsepower extraction is required for the vacuum system pump. Pump sizing is highly dependent on the altitude at which the HLFC system will be used. At lower altitudes, the ambient pressure is higher, requiring the pump to work harder to exhaust the ingested flow back into the air stream, thus increasing its sizing requirement [201]. Depending on the amount of laminar flow desired over the wing, the size of the wing, and the lowest desired operating altitude, the HLFC pump horsepower extraction can be on the order of 200 horsepower [201, 69]. The horsepower extraction will result in a higher TSFC required for the same amount of thrust produced since the engine turbine will have to provide more work to drive the additional load of the vacuum

pump. From engine thermodynamic cycle equations as shown by Hill and Peterson [81] one can estimate an additional 0.5% increase in TSFC for the noted horsepower extraction requirement. This technology will impose a weight penalty on the aircraft empty weight, the prediction of which involves uncertainty due to the complexity of integration within the aircraft system as a lack of sufficient empirical data. Implementation work and testing on a modest set of technology demonstrators has shown that with structural redesign and advanced materials HLFC suction piping can be developed to be approximately the same weight as current structures and not impose a significant penalty on the airframe [201]. While this may represent one extreme of the possible weight penalty caused by HLFC, it implies the most significant portion of the weight penalty will be due to the vacuum pump itself, which is dependent on the amount of horsepower extraction required. A more conservative estimate would still include a weight penalty for more than just the vacuum pump, also accounting for likely changes in structure and piping weight. While the additional weight of the HLFC system can be accounted for anywhere in the aircraft empty weight at the discretion of the designer, due to its similarity with pneumatic systems, technologists have accounted for the vacuum pump weight, piping, and supporting structure with a nearly 80% increase in the air conditioning subsystem weight. This figure is still dependent upon a variety of factors including the size of the wing and the percentage of the wing for which laminar flow is desired. This increase in the air conditioning subsystem weight translates to an increase in the aircraft empty weight following basic sizing trends provided by Roskam [188]. While the trends in this text are based on historical data, they do show how aircraft have historically evolved over time and can serve as a useful starting point for estimating how aircraft may be sized in the future. Following these references, one can estimate an increase in empty weight on the order of 1% from the addition of the HLFC technology.

The main benefit of applying the HLFC technology is a reduction in $C_{D,0}$, applied

in this problem through the technology impact factor $t_{CD,0}$ using Eq. 35. The key penalties of this technology are the increase in the empty weight and TSFC, which are modeled through the technology impact factors $t_{W_{Empty}}$ and t_{TSFC} via Eqs. 34 and 36. These penalties are both dependent upon the amount of horsepower extraction required. Using the technology references mentioned previously, linear relationships are generated that can be applied over random variable distributions to relate horsepower extraction to TSFC, and horsepower extraction to empty weight, for our notional aircraft at constant cruise conditions. As horsepower extraction changes linear relationships will yield corresponding values for t_{TSFC} and $t_{W_{Empty}}$ technology impact factors. The estimated effect on $C_{D,0}$, $HP_{extraction}$,W_{Empty}, and TSFC due to HLFC have been obtained from the technology and sizing references mentioned previously. Triangular distributions were defined by the authors in collaboration with systems analysts familiar with this technology by providing minimum, maximum, and most likely values. The parameters of each triangular distribution used to model this technology are provided in Table 14. The technology impact factors consistently use the same univariate distributions as specified by parameters in Table 14 for all simulations in application 1. Joint distributions will change according to the specified dependence structure in each simulation, while the univariate distributions (shown as marginal distributions) remain fixed.

4.5.1.2 Application 1 Simulations

In this application, three uncertainty dependence structures are simulated to examine the relationship between technology impact factors and their impact on predicted aircraft performance. First, the status quo is considered in which the technology impact factors are independent, and this is used as the baseline for comparison with copula defined relationships in subsequent simulations. In this initial simulation, $t_{C_{D,0}}$ and

Table 14: Triangular distribution parameters for Hybrid Laminar Flow Control technology

Technology Variable	Technology Impact Factor	Minimum Value	Mode Value	Max Value
$C_{D,0}$	$t_{C_{D,0}}$	0.88	0.92	0.97
Horsepower Extraction (hp)	N/A	79	217	375
W_{Empty}	$t_{W_{Empty}}$	1.007	1.012	1.017
TSFC	t_{TSFC}	1.002	1.006	1.01

$HP_{extraction}$ are not dependent, and $t_{W_{Empty}}$ and t_{TSFC} are known through deterministic linear relationships with $HP_{extraction}$. The joint distribution of the technology impact factors is shown in Figs. 35a and 36a. These figures include probability density contours to highlight features of the pairwise joint distribution topology in the random variable space.

The second simulation of application 1 represents the first non-independent case in which a copula is employed to dictate the dependence structure between technology impact factors, following algorithms specified by Nelsen [154, chap. 4]. An underlying relationship exists between skin friction drag and $HP_{extraction}$ such that as $HP_{extraction}$ increases we expect to see greater reductions in skin friction drag. While there is still much uncertainty, in this relationship it is reasonable to expect an inversely proportional relationship between $HP_{extraction}$ and $t_{C_{D,0}}$. In other words, greater reductions in $C_{D,0}$ occur with greater weight penalties. There is also no conclusive reason to narrow the distribution at the tails so they will be left wide to include more uncertainty. Whenever there is not enough knowledge to incorporate a specific trend, it is best to choose a copula that has greater spread and more uncertainty.

This basic understanding can be used to navigate the copula selection tree in Fig.

32. This process is depicted in Fig. 34 where the green lines indicate the path taken to arrive at a leaf with a representative copula family for the desired dependence structure.

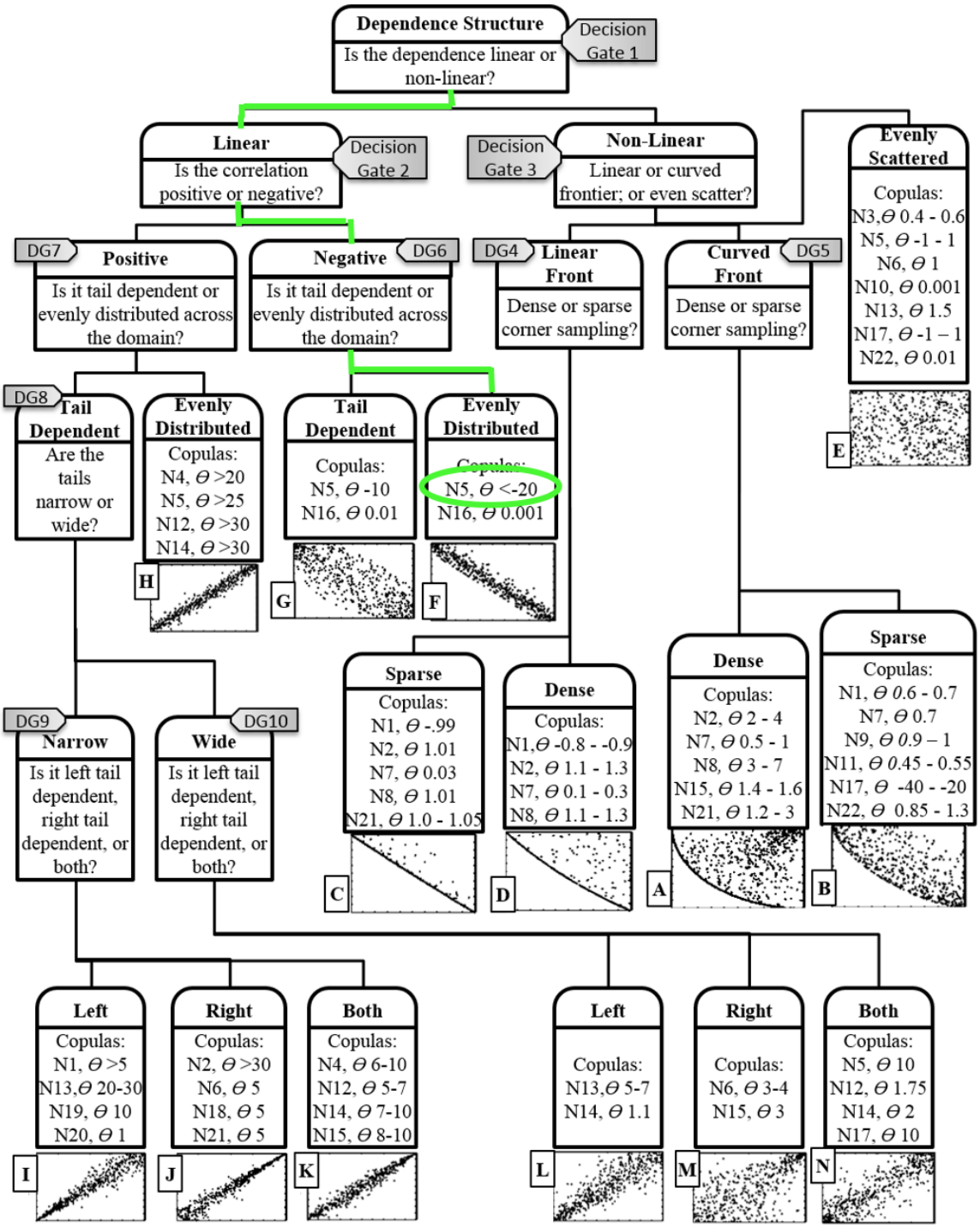

Figure 34: Copula Selection Tree with Path Highlighted for Choosing Copula Family in Application 1

Decision Gate 1 asks whether the dependence structure is linear or nonlinear and the answer is linear since it is known that the relationship is inversely proportional. This directs the user to Decision Gate 2 which asks whether the relationship is negative or positive. The answer is negative since the relationship is inversely proportional. This sends the user to Decision Gate 6 which asks if the relationship is tail dependent or evenly distributed. Since there is no reason to suspect tail dependence for this application, the evenly distributed answer is used. This directs the user to Leaf F of the selection tree where they can select from copula families N5 or N16 at the given values of θ. Since θ is a continuous variable, these θ values can be adjusted to match the user's desired degree of dependence. The copula selection tree in Fig. 34 helps the user determine that this uncertain relationship is well captured using a N5 (Frank family in Table 1) copula with θ = -15 between $HP_{extraction}$ and the technology impact factors $t_{C_{D,0}}$. This relationship will also be mirrored by the deterministic linear mappings to the technology impact factors t_{TSFC} and $t_{W_{Empty}}$, which will also preserve this dependence.

After identifying the proper copula family and θ value, the next step is to use the inversion method to convert the copula's standard uniform marginal distributions into the distributions that represent the random variables of this application. The random variables for application 1 have been specified with triangular distributions as reported in Table 14. The inversion method converts the copula's standard uniform marginal distributions into these specific triangular distributions for use in this application. The N5 copula creates a dependence structure between the triangular distributions that more accurately describes the tradeoff between the improvement in skin friction drag (decreasing $t_{C_{D,0}}$) and the corresponding increases in empty weight (increasing $t_{W_{Empty}}$) and TSFC (increasing t_{TSFC}) due to the additional $HP_{extraction}$. The joint distribution specified by the N5 copula is plotted in Figs. 35b and 36b. Both of these figures demonstrate that while the joint distributions have changed between

the independent and non-independent cases, the univariate marginal distributions of each technology impact factor have not been altered by the copula.

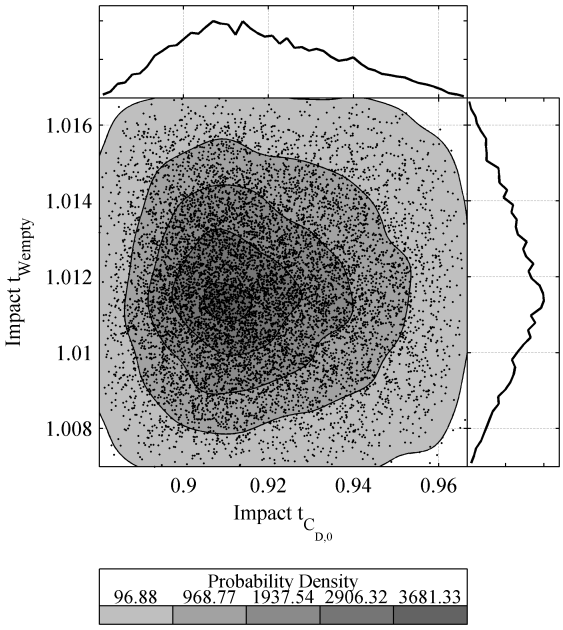

(a) Independent, 10,000 points

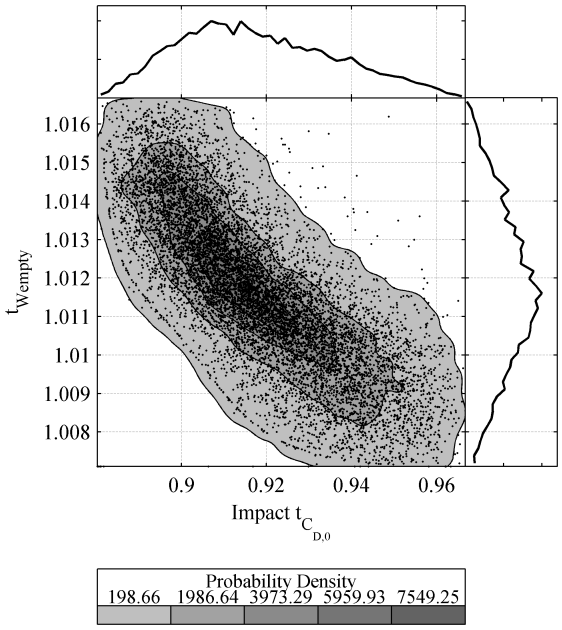

(b) Frank copula, θ = -15, 10,000 points

Figure 35: Joint distributions of $t_{C_{D,0}}$ and $t_{W_{Empty}}$

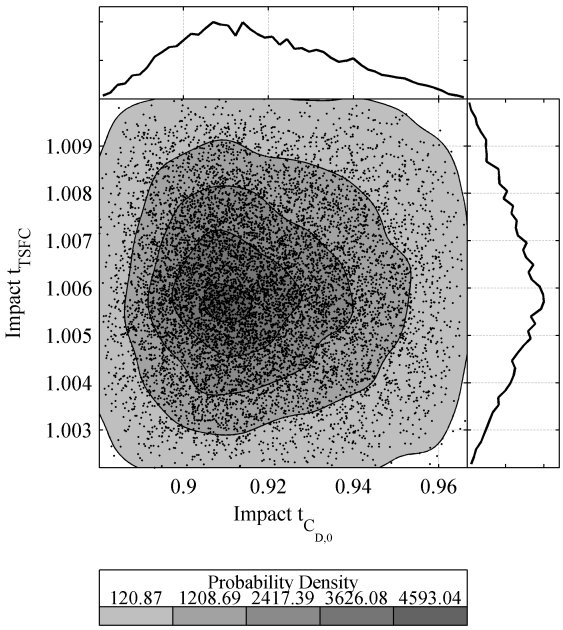

(a) Independent, 10,000 points

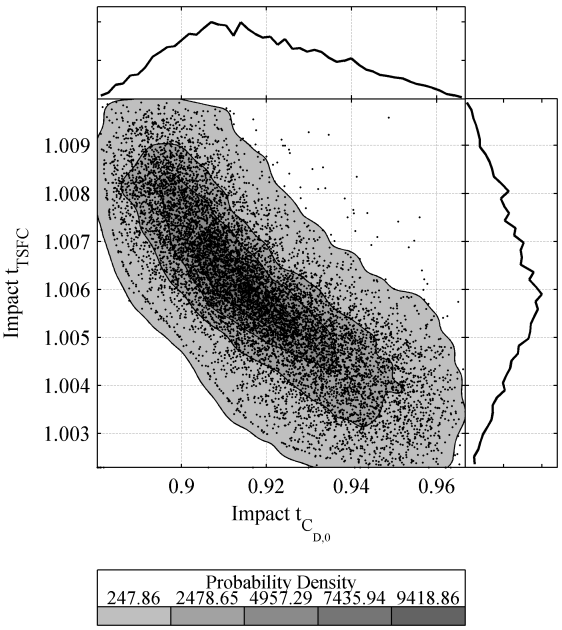

(b) Frank copula, θ = -15, 10,000 points

Figure 36: Joint distributions of $t_{C_{D,0}}$ and t_{TSFC}

As discussed earlier, the application of copulas requires engineering judgment and is predicated on some understanding of the underlying relationships. The third simulation delves into the importance and implications of this condition. The relationship between $HP_{extraction}$ and $t_{W_{Empty}}$ developed for this work is an extension of empirical data trends for existing air conditioning subsystems sizing. Although presented as a deterministic relationship, its interpretation should be that of a rough estimate or "rule of thumb" for low-order estimates in conceptual design sizing. In reality, there is some uncertainty in this relationship that is captured by replacing the deterministic relationship with a copula for $HP_{extraction}$ and $t_{W_{Empty}}$ random variables. The assumed deterministic linear relationship between $HP_{extraction}$ and $t_{W_{Empty}}$ used in the previous two simulations for this technology application is shown in Fig. 37a. The positive dependence used to replace it is shown in Fig. 37b and is modeled as a Frank copula with $\theta = 5$. Once again, it is obvious that, while the bivariate distribution has changed between the deterministic and non-deterministic cases (Figs. 37a and 37b), the univariate marginal distributions of both variables remains unchanged.

In general, one can formulate this application with the three impact factors $t_{C_{D,0}}$, $t_{W_{Empty}}$, and t_{TSFC} by establishing the dependence structure in nine possible ways. Each dependence structure is a combination of the three bivariate relationships, each defined as independent, probabilistically related with a copula, or deterministically related.

4.5.1.3 Application 1 Results

The first simulation assumed independent relationships to serve as a baseline for comparison for the second and third simulations in which the dependence structure for random variables is introduced with copulas. As expected, the use of copulas to relate the technology impact factors yields a change in the resulting distribution for the aircraft range. Figure 38 shows the empirical probability density functions (pdf)

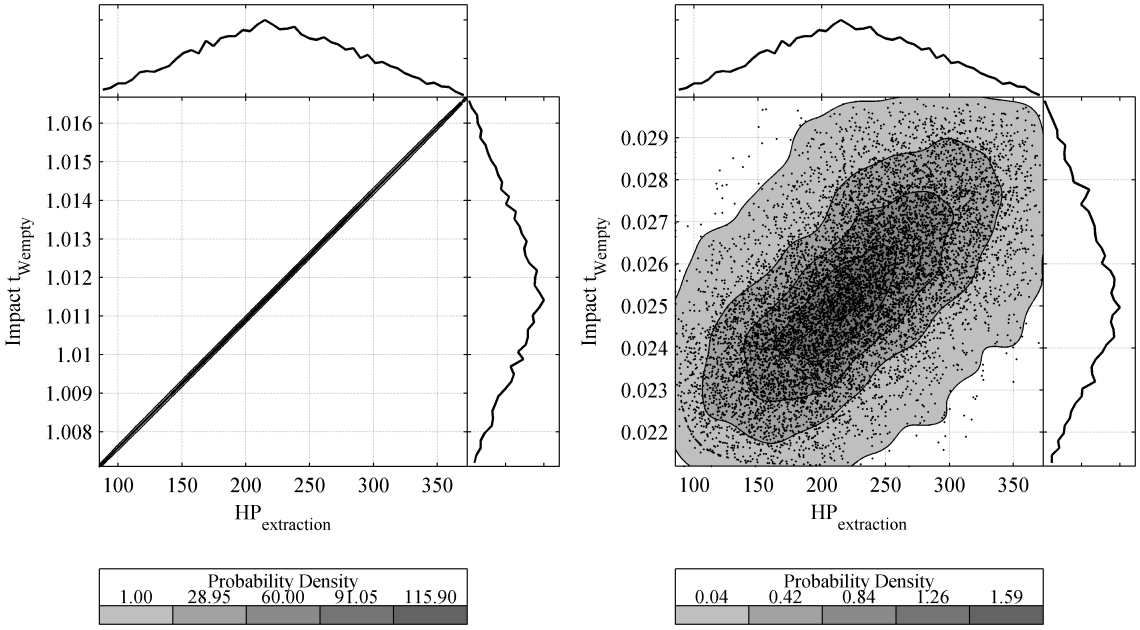

(a) Deterministic, for simulations 1 and 2 (b) Frank Copula for simulation 3, $\theta = 5$

Figure 37: Joint distributions for $HP_{extraction}$ and $t_{W_{Empty}}$, 10,000 points

of the first two simulations, comparing the results of the independent case to that of the copula dependent case.

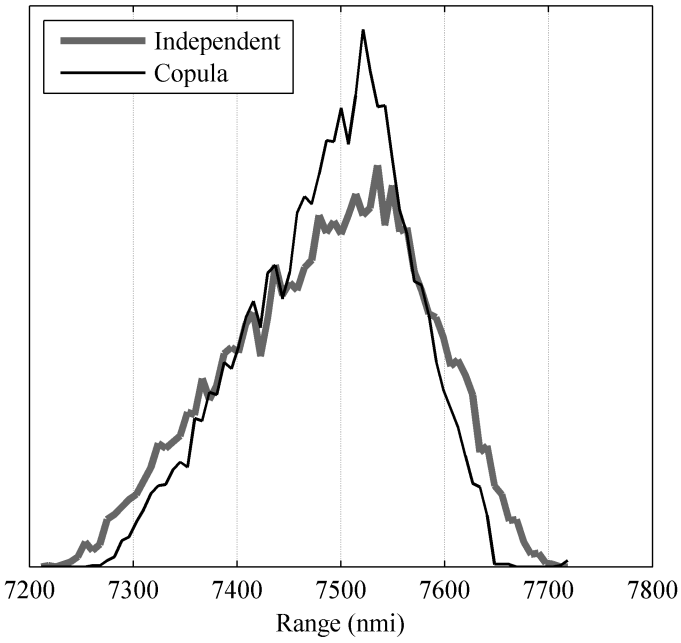

Figure 38: Empirical pdf of range subject to independent and Frank copula related technology impact factors

The probability density function (pdf) distributions in Fig. 38 for the first and second simulations of this application immediately reveal a difference in variance, with the distribution resulting from independent random variables having greater uncertainty than its copula-related counterpart. Table 15 shows the empirical pdf distribution parameters for application 1 and as expected, the mean does not shift because the input univariate distributions are exactly the same in both simulations. The copula 1 empirical pdf has a smaller variance than the independent case because the copula is avoiding certain regions of the bivariate space. By changing the dependence of the input distributions, certain combinations have been removed and can no longer be sampled from the joint distribution. If these removed combinations would have resulted in extreme values of the transfer function distribution, then the variance would decrease; if they would have resulted in more middle values, then the variance would increase. In this case, the combinations omitted by the copula would have resulted in extreme values of the aircraft range distribution, and so the uncertainty would decrease as reported in Table 15. Additionally, the copula omitted combinations at the extremes of the joint distribution are now being sampled closer to the middle of the bivariate space. This will result in more centered values of the transfer function, which yield a higher peak about the mean. Together, these two effects will compound to decrease the standard deviation of the copula dependent pdf.

This is also reflected in the difference between the tails of the empirical pdfs. The area between the two empirical pdfs in the right tail corresponds to the empty region in the lower left corner of Figs. 35b and 36b representing high-benefit and low-penalty combinations that are reasonably assumed to be extremely unlikely. Conversely the area between the two empirical pdfs in the left tail corresponds to the empty region in the upper right corner of Figs. 35b and 36b representing low-benefit and high-penalty combinations that are also assumed to be extremely unlikely. This may remove some high impact technology combinations but it is justified based on our

engineering judgment. The use of copulas should always be based upon knowledge of underlying relationships. The copula has removed parts of the bivariate space to better represent the engineering knowledge of the relationship between variables. If one subscribes to these assumptions and accepts the copula as a reasonable relational mechanism for the benefit and penalty impact factors, then it follows that the use of the copula better represents the uncertainty of this technology that would otherwise be overestimated as illustrated by these results.

The total aircraft range for all three simulations is given in the first data column of Table 15. This table also gives the average improvement in range over the nominal aircraft range (7,170 nmi.) provided by the inclusion of the technology. The HLFC technology does make a noteworthy improvement to the range ($\sim$317 nmi.) across all three simulations in this application as shown by the second column of data in Table 15. However, our focus in this work is not necessarily on the benefit provided by the technologies but rather on the reduction of uncertainty in the estimation of aircraft performance by using copulas. It is important to note that any comparisons of uncertainty to the aircraft range should be made relative to the additional range provided by the technology and not to the total aircraft range since the technology alone is the source of uncertainty in this canonical problem. The uncertainty in this application was a direct result of the addition of the HLFC technology, modeled by the probabilistic technology impact factors. A common way to measure that uncertainty is through the standard deviation of the range distribution, which is given by the third column of data in Table 15. The independent simulation gives us a baseline value of the uncertainty in the estimation of range. The two copula simulations were performed to see how the uncertainty could be better represented using existing knowledge to capture the relationship between the probabilistic technology impact factors. To better understand the effect of using a copula on the uncertainty, one can

make a comparison of the standard deviations as shown in Eq. (37),

$$\sigma_{reduction} = \frac{\sigma_{independent} - \sigma_{copula}}{\sigma_{independent}} \tag{37}$$

This simple relation provides a quantified measure of how much the uncertainty can be reduced by using copulas in this application. This has been recorded for both copula simulations in the fourth data column of Table 15. The addition of the HLFC technology has improved the average range (an additional ∼317 nmi.) for the independent and copula simulations, but the value of the copula is in the accuracy with which this improvement can be estimated. In the copula 1 and copula 2 simulations, the the added range from the HLFC technology can be predicted with 17% and 15% less uncertainty, respectively, over the independent simulation, by way of the standard deviation. While the copula does not reduce the physical uncertainty associated with the technology, it demonstrates how the independent simulation was overestimating the uncertainty in this application. The use of the copula selection tree in Fig. 32 to better represent the joint distribution paired with the inversion method to seamlessly transform univariate marginal distributions, together, is what allows for the improved representation of uncertainty in this application.

The significance of the change in uncertainty is also readily apparent in the comparison of the empirical cumulative distribution functions (CDFs) of each case, shown in Fig. 39. CDFs are known to be less noisy than pdfs so they typically lend themselves better to individual comparisons. Reinforcing this notion is the fact that many statistics exist in the literature for the comparison of two samples, and these are applied to cumulative distributions functions. These statistical techniques include the Kolmogorov−Smirnov test [120, 216] and the Cramer−von Mises test [45, 243, 7] which are well documented in probability and statistics literature. The null hypotheses for both methods is that the two samples being tested are drawn from the same distribution. The test statistics of both methods can be used to characterize the difference between the CDFs of each simulation. The Kolmogorov−Smirnov test statistic

is particularly simple to understand and represents the value of the maximum difference between the two sample empirical CDFs. It can assume values between 0 and 1 where 0 indicates no difference between the two distributions, and 1 indicates the maximum difference between two distributions. The Cramer−von Mises test statistic is a sum of the squared difference of the two empirical CDF distributions and provides a better representation of the difference between the two curves along the full range of their values rather than just the maximum difference at one point. This statistic assumes values between 0 and infinity where 0 indicates no difference. The first column in Table 16 gives the values of the Kolmogorov−Smirnov and Cramer−von Mises test statistics for the comparison of simulations 1 and 2. Both statistics indicate a significant difference between the two empirical CDFs.

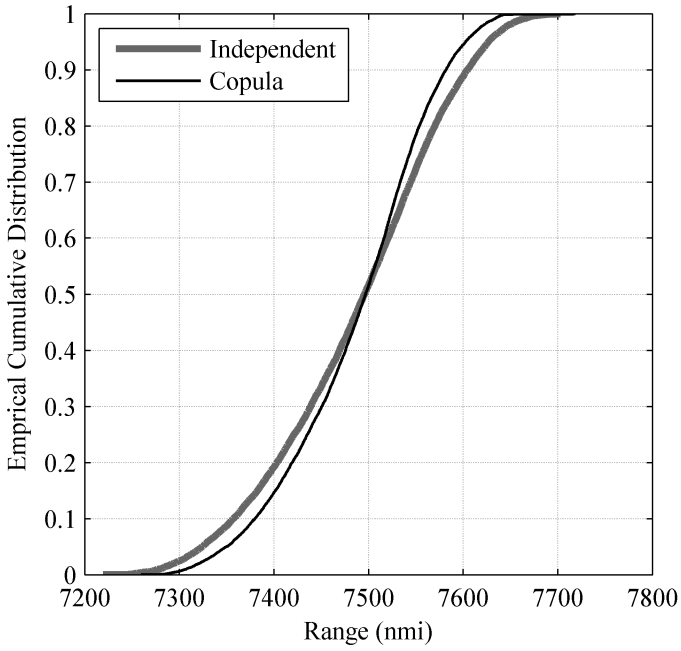

Figure 39: Empirical cumulative distribution for range subject to independent and Frank copula dependent technology impact factors

The third simulation in application 1 maintained the settings used in the second simulation except for introducing a second Frank copula (copula 2) to replace the deterministic relationship assumed between $HP_{extraction}$ and the technology impact

Table 15: Application 1 empirical pdf distribution parameters

Application 1 Distributions	Total Range mean (nmi)	Range Improvement mean (nmi)	Range Improvement Standard Deviation σ (nmi)	Standard Deviation Reduction
Independent pdf (Simulation 1)	7487.4	317.4	92.8	N/A
Copula 1 pdf (Simulation 2)	7486.5	316.5	76.8	17.2%
Copula 2 pdf (Simulation 3)	7487.0	317.0	78.5	15.4%

Table 16: Application 1 empirical CDF comparisons

Test Statistic	Independent vs Copula 1	Independent vs Copula 2	Copula 1 vs Copula 2
Kolmogorov−Smirnov	0.070	0.058	0.012
Cramer−von Mises	7.8	5.8	0.18

factor $t_{W_{Empty}}$. Since the deterministic relationship includes no uncertainty, the probabilistic bivariate dependence introduced by this second copula should increase the variance compared to simulation 2 (copula 1). However, a reduction in uncertainty is still expected relative to simulation 1, which assumes complete independence. Figure 40 shows the pdf distribution for this third simulation and also includes the pdf distributions from the first two simulations for comparison. Table 15 shows that, as expected, the standard deviation of the empirical pdf for the third simulation is higher than the second simulation and lower than that of the first simulation. In general a higher valued peak of a pdf curve indicates a greater likelihood of the mode, and typically less variance for most typical distributions with moderate kurtosis. Indeed, the results of the first simulation with independent impacts features the lowest peak and greatest spread, the second simulation (copula 1) should have the highest peak and smallest spread due to its dependent random variables and deterministic relation between $HP_{extraction}$ and $t_{W_{Empty}}$, and the third simulation that employs only copula dependent assumptions should have a peak in between these two. Figure 40 supports this hypothesis for the three empirical pdf distributions. This helps to answer Research question 2 for this application.

Figure 41 gives the CDF distribution of the third simulation and also includes the empirical CDF distributions from the first two simulations for comparison. The level of uncertainty has increased in simulation 3 relative to simulation 2, but it is

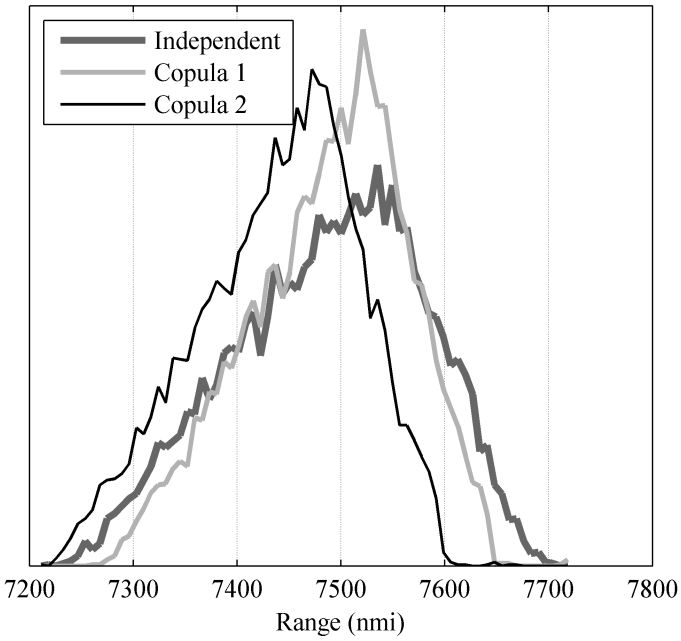

Figure 40: Empirical pdf of range subject to independent and Frank copula dependent technology impact factors

still less than that of simulation 1. The copula 2 curve should lie in between the independent and copula 1 curve, which is shown in Fig. 41. The copula 2 curve in this figure matches very closely to copula 1, which shows that using the copula to better represent the deterministic assumption between $HP_{extraction}$ and W_{Empty} did not have a significant effect. This can be explained by the relatively small range of values for W_{Empty} and the weak effect of W_{Empty} on the system level response, which is not as significant as other variables such as $C_{D,0}$. This points to the importance of using copulas to relate variables that are significant drivers of the response.

The second column of Table 16 gives the Kolmogorov−Smirnov and Cramer−von Mises test statistics for simulations 1 and 3. As expected, there is a significant difference in both the test statistics, but their values are lower than the comparison of simulations 1 and 2. The third column of Table 16 provides the CDF test statistics for the comparison of the copula 1 and copula 2 curves in Fig. 41. While these values may be small relative to the other comparisons, it is important to note that

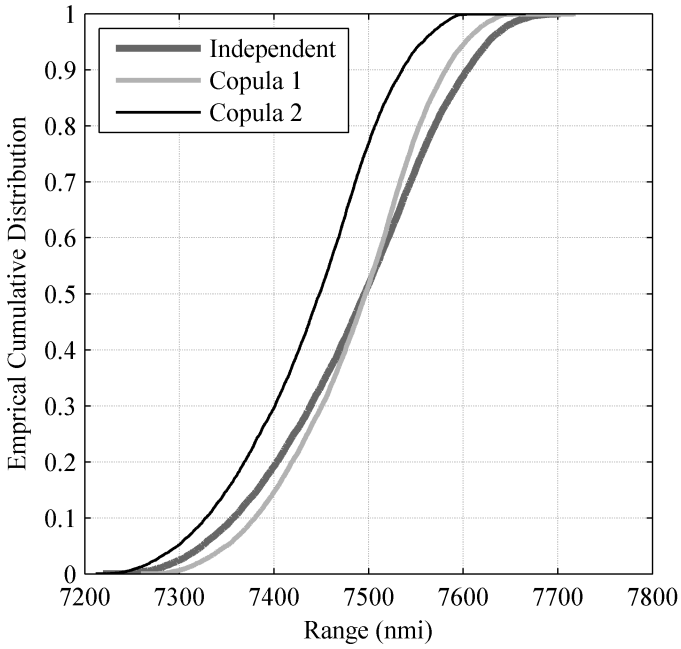

Figure 41: Empirical cumulative distribution for range subject to independent and Frank copula dependent technology impact factors

the difference between these curves is still measurable and quantifiable using these CDF test statistics. A subjective or qualitative assessment would surely be very difficult, supporting the use of quantitative measures for benchmarking assessments as the one discussed here. Collectively, these results illustrate how knowledge about the underlying relationships between technology impact factors in application 1 can be suitably captured and propagated to system level results.

4.5.2 Copulas Across Two Aerodynamic Wing Technologies

4.5.2.1 Application 2 Formulation

Application 2 examines the effect of dependence between the same impacts across two different technologies. This application assumes that both advanced technologies are compatible and can be applied to the aircraft wing concurrently. The uncertainty lies in the amount of benefit that can be gained by simultaneously applying both technologies. The technology impact factor used across both technologies is $t_{C_{D,0}}$. The first technology (T1) is the same technology used in application 1, and will

be modeled using the settings of the first simulation in application 1. The second technology, Wing Riblets (T2), is directed at increasing the range of the aircraft by reducing the skin friction drag of the wing. Riblets are a passive technology applied to the surface of the wing in the shape of very small v-shaped grooves that create spanwise viscous forces that act on the turbulent boundary layer to reduce drag. These grooves have heights and spacing on the order of the turbulent wall streak and burst dimensions and allow the local streamline near the surface of the wing to remain laminar [247]. Testing has shown a 2-3% decrease in total airplane drag, which is modeled through the lift-independent drag factor [242, 229]. Several aggressive estimates have predicted even greater drag reduction using riblets on the order of 5-8% [247, 246]. It has been shown that the weight penalty due to the addition of the riblets is marginal when the grooves are etched into the existing paint or polymer material on the surface of the wing. This will require regular maintenance and replacement, or the effectiveness of the drag reduction will be reduced. It has also been indicated that the effectiveness of the riblets varies greatly with the incidence angle of the streamline to the applied grooves. The drag reduction is highest at zero incidence angle, but as the angle of attack increases, the passive riblets technology loses effectiveness [229]. Since the canonical problem only examines the cruise segment of flight and assumes steady level flight conditions, reduction in the effectiveness of the riblets technology due to varying incidence angle is not modeled.

The key benefit of the riblets technology (T2) is a decrease in $C_{D,0}$ applied in this a problem with a conservative estimate on the order of 2% skin friction drag reduction. Triangular distribution parameters for the technology impact factor $t_{C_{D,0}}$ are summarized in Table 17 and were defined by the authors in collaboration with systems analysts familiar with this technology. The $t_{C_{D,0}}$ technology impact factor for T1 will consistently use the same marginal distribution parameters specified in Table 14 for all simulations; however, the joint distributions will change according to

Table 17: Triangular distribution parameters for Wing Riblets technology (T2)

Technology Variable	Technology Impact Factor	Minimum Value	Mode Value	Max Value
$C_{D,0}$	$t_{C_{D,0}}$	0.965	0.980	0.994

the specified dependence structure in each simulation.

4.5.2.2 Application 2 Simulations

Application 2 uses two different simulations to examine the effect of correlating the same technology impact factor across two different technologies. Similar to application 1, an independent simulation and a copula dependent simulation are conducted. In both simulations, the $t_{C_{D,0}}$ technology impact factors for T1 and T2 will be be sampled from their respective distributions given in Tables 14 and 17. The samples will then be combined, and the total $t_{C_{D,0}}$ representing the aggregate effect of both technologies on skin friction drag will be used in the canonical problem via Eq. 35. In both simulations, all non-drag related impact factors of T1 (provided in Table 14) will assume the same settings as the first simulation of application 1 (independent relationships). This will ensure there is no prior dependence structure present in the modeling of T1 and the results will strictly be a reflection of the dependence structure applied by copulas in application 2. The independent bivariate distribution for simulation 1 is simple to visualize and is given in Fig. 42a.

It is unlikely that the presence of one technology in this application will have no effect on the other. Conservative accounting from technologists familiar with both technologies indicates that the maximum individual benefit of both technologies will likely not be obtained due to diminishing returns, but rather that the interaction will eventually reduce the benefits of each. In essence, this represents a topology of the bivariate random shape akin to a bivariate Pareto tradeoff frontier. This low-level

qualitative understanding can be used to answer the questions of the copula selection tree in Fig. 19 to determine that this feature is well modeled by the Clayton family of copulas. Therefore, the second simulation relates the $t_{C_{D,0}}$ technology impact factors for T1 and T2 using a Clayton copula with θ = -0.6. This copula will create a dependence structure in the bivariate distribution of the two $t_{C_{D,0}}$ technology impact factors, which more adequately captures the expected interaction between the technologies when they are concurrently implemented. This copula dependent bivariate distribution is shown in Fig. 42b.

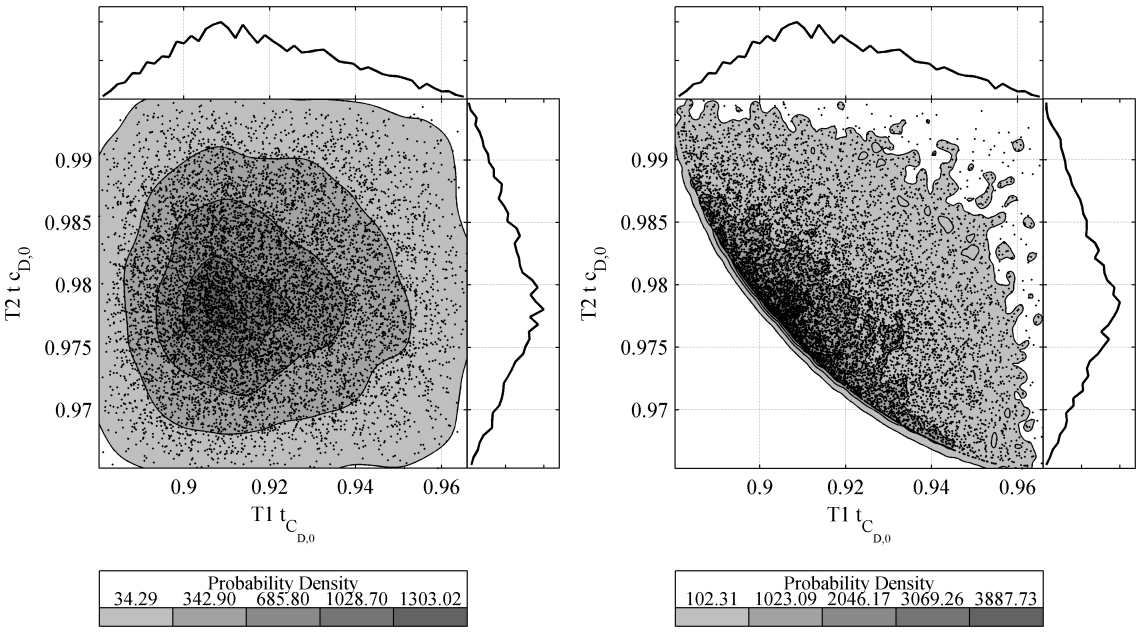

(a) Independent, 10,000 points (b) Clayton Copula, θ = -0.6, 10,000 points

Figure 42: Joint distributions of Hybrid Laminar Flow Control (T1) $t_{C_{D,0}}$ and Wing Riblets (T2) $t_{C_{D,0}}$

The bivariate distributions have changed between the independent and non-independent cases (Figs. 42a and 42b), but the univariate distributions of both variables remains unaltered by the copula. The aircraft range for the second simulation is recalculated using the copula dependence and compared with the first simulation.

4.5.2.3 Application 2 Results

The empirical pdf curves of both simulations are shown in Fig. 43, which illustrates the reduction in uncertainty by employing the Clayton copula. Figure 43 shows a higher peak with a greater concentration of samples centered about the mode for the copula dependent pdf and more variation in the independent simulation pdf. Table 18 also shows a reduced standard deviation for the copula dependent pdf in the third data column, reflecting a decrease in the uncertainty for this simulation. This is because the range distribution no longer has some of the extreme combinations that are reflected in the wider tails of the independent simulation pdf since the copula has omitted them. Fig. 42b shows the empty region in the lower left corner of bivariate distribution which is no longer sampled due to the copula dependence structure. This region of maximum benefit from both technologies which will likely not be obtainable, and is also reflected in the shrinking tails of the copula dependent empirical pdf shown in Fig. 43. This is particularly seen in the right tail of the empirical pdf distribution that shrinks to remove the more uncertain and overly optimistic values of range in the independent distribution.

The total aircraft range for both simulations is given in the first data column of Table 18. This application uses two advanced technologies, resulting in an even greater improvement in the range ($\sim$420 nmi.) over the baseline value for both simulations, as indicated in the second column of data in Table 18. The independent simulation provides a baseline value of the uncertainty associated with the estimation of range due to the addition of these two technologies. The copula simulation is conducted to determine how much that uncertainty can be reduced by incorporating existing engineering knowledge about the relationship between the technology impact factors. Using Eq. (37), the uncertainty as measured by the standard deviation of the range distributions, is reduced by almost 18% in the copula simulation. This helps to answer Research question 2 for this application.

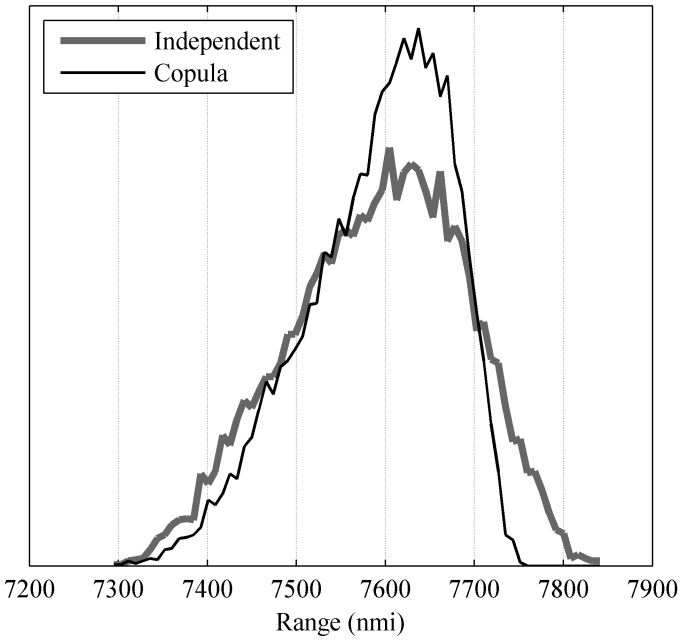

Figure 43: Empirical pdf of range subject to independent and Clayton copula dependent technology 1 $t_{C_{D,0}}$ and technology 2 $t_{C_{D,0}}$

Figure 44 gives the empirical CDF distributions of these two simulations. There is a significant shift in the copula CDF from the independent CDF, particularly at the higher values of range. This difference at higher values also reflects the overly optimistic values of range that were removed by the copula dependence structure (shown in Fig. 42b) to reduce the uncertainty. The variation between the two CDFs is quantified by the the Kolmogorov−Smirnov and Cramer−von Mises test statistics in Table 19.

Table 18: Application 2 empirical pdf distribution parameters

Application 2 Distributions	Total Range mean (nmi)	Range Improvement mean (nmi)	Range Improvement Standard Deviation σ (nmi)	Standard Deviation Reduction
Independent pdf (Simulation 1)	7,589.7	419.7	98.7	N/A
Copula pdf (Simulation 2)	7,590.3	420.3	81.1	17.8%

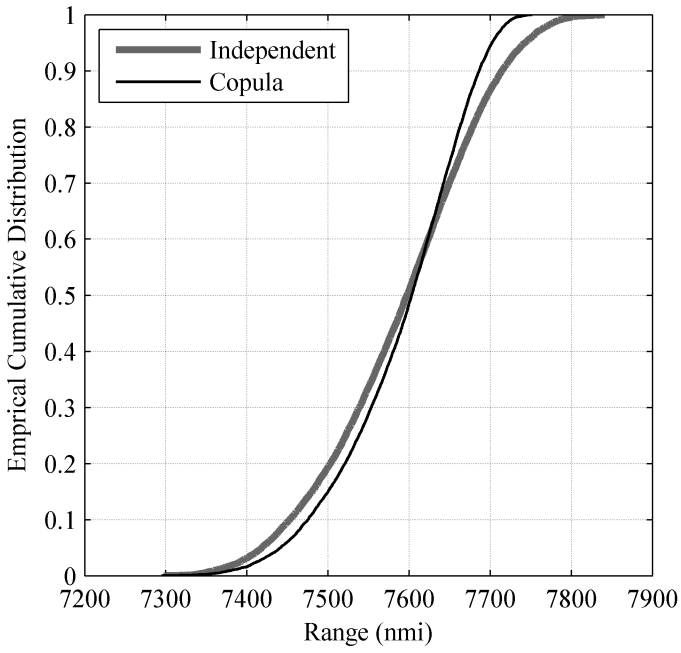

Figure 44: Empirical cumulative distribution for range subject to independent and Clayton copula dependent technology 1 $t_{C_{D,0}}$ and technology 2 $t_{C_{D,0}}$

Table 19: Application 2 empirical CDF comparisons

Test Statistic	Independent CDF vs Copula CDF
Kolmogorov−Smirnov	0.083
Cramer−von Mises	9.7

Both statistics show that CDFs from the two simulations are substantially different from each other. This change in the distribution of the aircraft range is found to be strongly driven by the significant effect that $C_{D,0}$ imparts on the estimation of mission range, and therefore is also driven by the underlying dependence structure associated with $C_{D,0}$ contributions.

4.5.3 Copulas With a Wing Design Variable

4.5.3.1 Application 3 Formulation

Application 3 relates a technology impact factor to a wing design parameter, aspect ratio. The advanced technology in this application is called Advanced Aerodynamic Wing and represents the recent advances in wing design that are characterized by an increased aspect ratio driven by the availability of stronger and cheaper materials [10, 90]. Increasing the aspect ratio has been a continuing trend over several decades and is expected to continue as greater technological advances are made [90]. Increasing the aspect ratio reduces induced drag, which reduces fuel burn and extends the aircraft range. As aspect ratio increases, the wing span also increases. The wing bending moment and associated loads generally increase rapidly with increasing wing span, which necessitates additional structure at the wing root [32, 107]. This structure adds a weight penalty that must be overcome by the benefits in drag reduction to justify choosing the increased aspect ratio. The uncertainty lies in the amount of additional

Table 20: Triangular distribution parameters for Advanced Aerodynamic Wing

Technology Variable	Technology Impact Factor	Minimum Value	Mode Value	Max Value
Aspect Ratio	N/A	10.5	11	13
W_{Empty}	$t_{W_{Empty}}$	1.043	1.054	1.117

structure required to support the bending loads associated with the increased wing span for a given structural technology. Technologists and references of next-generation vehicles have indicated an estimated 5% increase in the empty weight due to an increase in the aspect ratio on the order of 11 [107, 90, 22, 23].

The key benefit of increasing the aspect ratio design variable is seen in this problem via Eqs. 31 and 32. The main penalty of this technology is the increased empty weight, which will be modeled using the technology impact factor $t_{W_{Empty}}$. Using the literature and subject matter expert (SME) input, the authors defined the triangular distributions for the aspect ratio and $t_{W_{Empty}}$, which are summarized in Table 20. As the aspect ratio changes, the aircraft will not be re-optimized for this design variable change. The wing area remains constant as the span increases. The wing sees the benefit of the reduced induced drag and the penalty of the increased empty weight, but the aircraft as a whole is not re-sized. This results in a fixed aircraft for the probabilistic assessment so that a valid comparison of range can be made between each combination of the sampled aspect ratio and weight penalty, subject only to the variation in the Advanced Aerodynamic Wing technology. The aspect ratio and the $t_{W_{Empty}}$ technology impact factor consistently employ the same univariate distributions specified in Table 20 for all simulations; however, the joint distribution changes according to the specified dependence structure of each simulation.

4.5.3.2 Application 3 Simulations

An independent and a copula dependent simulation are performed to examine the effects of design variable dependencies. Both simulations sample the aspect ratio and the $t_{W_{Empty}}$ technology impact factor from the prescribed distributions in Table 20. The sampled aspect ratio replaces the baseline aspect ratio in our canonical problem, and the sampled $t_{W_{Empty}}$ is applied through Eq. 34. The independent simulation is given in Fig. 45a.

The literature indicates that a weight penalty will be incurred as the aspect ratio increases. The uncertainty lies in specifying how much that weight penalty will be, and this uncertainty increases at higher aspect ratios. This requires a positively correlated relationship between the aspect ratio and the $t_{W_{Empty}}$ technology impact factor, and a wider spread in the joint distribution at high aspect ratios to represent the greater uncertainty there, i.e., a left tail dependency. Again, by applying this basic qualitative knowledge to the copula selection tree in Fig. 19, it is quickly determined that this relationship is well described using Nelsen's 13th copula (N13) with a $\theta = 7$. This copula creates a dependence structure in the bivariate distribution that is more representative of the current understanding of the uncertainty associated with this technology. This copula dependent bivariate distribution is shown in Fig. 45b.

As the bivariate distributions change between the independent and non-independent cases (Figs. 45a and 45b), the univariate marginals of both variables remains unaltered by the copula. The aircraft range for the second simulation is recalculated using the uncertainty dependence provided by the copula and compared with the results from the first simulation of this application.

4.5.3.3 Application 3 Results

The results of the first independent simulation and the copula simulation are shown in Fig. 46. The empirical pdf distributions show how much the uncertainty has been

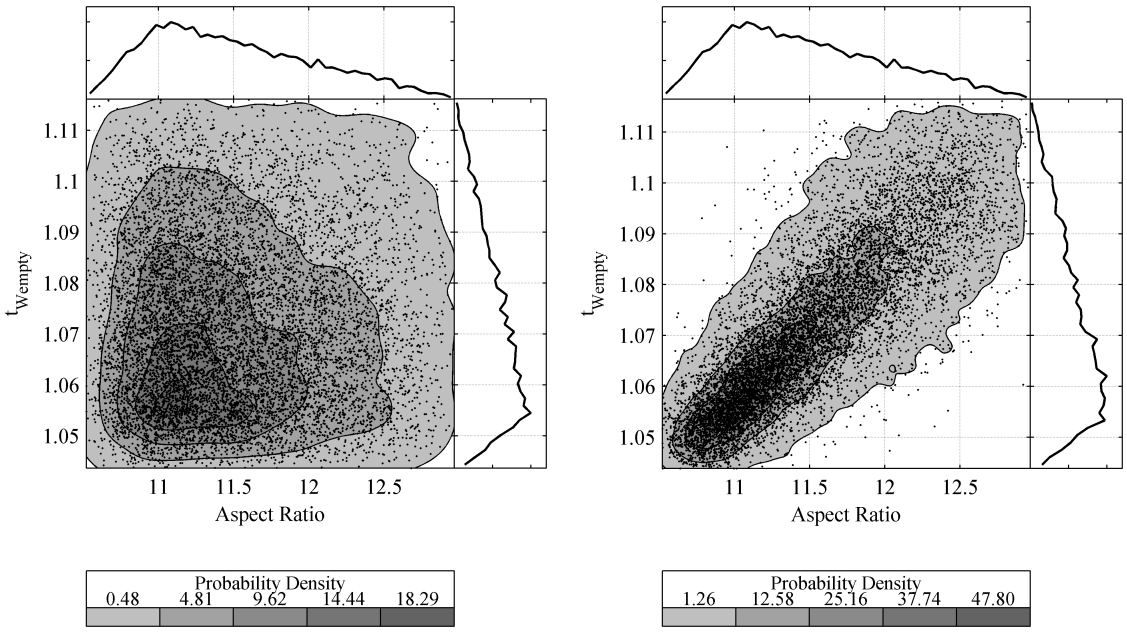

(a) Independent joint distribution, 10,000 points

(b) N13 copula distribution, $\theta = 7$, 10,000 points

Figure 45: Joint distributions of aspect ratio and $t_{W_{Empty}}$

reduced by using the N13 copula dependence in the second simulation. The copula pdf distribution in Fig. 46 shows a higher peak that is more centered about its mode and has less variation than the independent distribution. The shrinking tails of the copula dependent pdf, relative to the independent pdf, correspond to those combinations of high benefit (high aspect ratio) and low weight penalty (low $t_{W_{Empty}}$) and low benefit and high penalty shown in the empty regions of Fig. 45b. These combinations are unlikely to be used in design and contribute uncertainty to the estimation of range in the independent simulation, which is easily removed with the N13 copula.

Table 21 shows a reduced standard deviation for the copula dependent pdf, reflecting a decrease in the uncertainty for this simulation by removing certain regions of the bivariate distribution with the copula. However, Table 21 shows the highest variance in its simulations compared to all previous applications (Tables 15 and 18), which suggests that dependencies using design parameters can have greater uncertainty associated with them than those that simply relate technology impacts.

The total aircraft range for both simulations is given in the first data column of Table 21. This application uses a technology that is applied through a design variable yielding an average improvement in range of ∼192 nmi. over the baseline value for both simulations, as indicated in the second column of data in Table 18. The independent simulation gives a reference value of the uncertainty associated with the estimation of the range brought by the application of this technology. The copula simulation assesses how much that uncertainty can be reduced by capturing existing engineering knowledge about the relationship between the technology impact factor and the design variable. Using Eq. (37), the uncertainty as measured by the standard deviation of the range distributions, is reduced by 31% in the copula simulation. This helps to answer Research question 2 for this application.

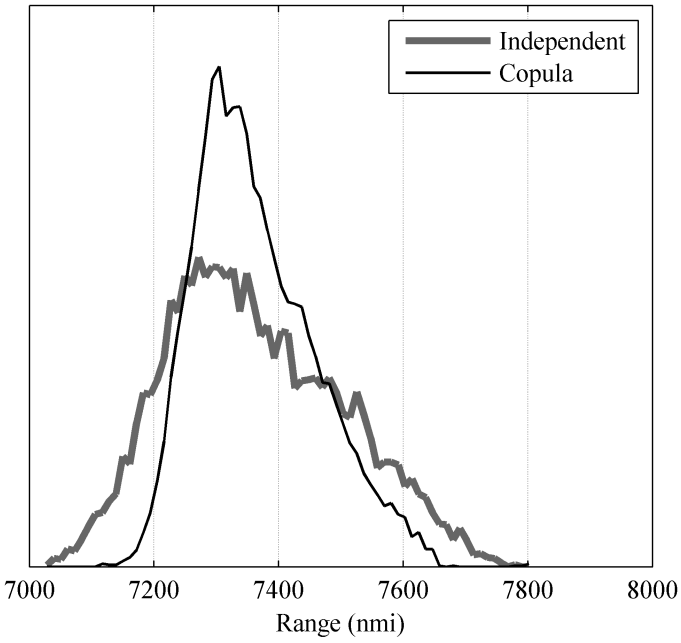

Figure 46: Empirical pdf of range subject to independent and N13 copula dependent aspect ratio and $t_{W_{Empty}}$

Table 21: Application 3 empirical pdf distribution parameters

Application 1 Distributions	Total Range mean (nmi)	Range Improvement mean (nmi)	Range Improvement Standard Deviation σ (nmi)	Standard Deviation Reduction
Independent pdf (Simulation 1)	7,361.9	191.9	140.1	N/A
Copula pdf (Simulation 2)	7,362.6	192.6	96.1	31.4%

Figure 47 gives the empirical CDF distributions of these two simulations. There is a substantial change in the copula CDF from the independent CDF, at both higher and lower values of range. The difference between the two CDFs is quantified by the the Kolmogorov−Smirnov and Cramer−von Mises test statistics in Table 22.

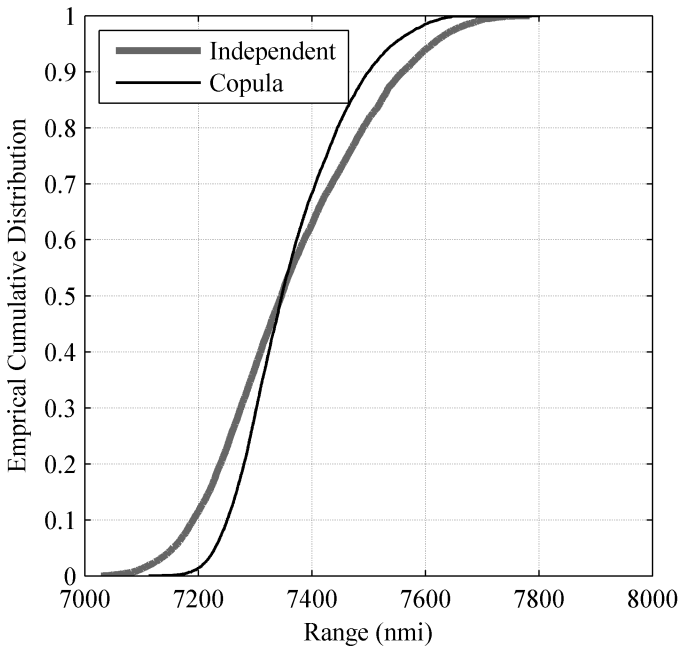

Figure 47: Empirical cumulative distribution for range subject to independent and N13 copula dependent aspect ratio and $t_{W_{Empty}}$

The statistics show that CDFs from the two simulations are different and in fact are even more different from each other than either of the first copula simulation statistics from applications 1 and 2 (Tables 16 and 19). This indicates that correlating design variables with impact factors can have an even greater effect on the system response than just dependencies within a technology or across technologies. Of course the change in the response is also highly dependent upon which random variables are

Table 22: Application 3 empirical CDF comparisons

Test Statistic	Independent CDF vs Copula CDF
Kolmogorov−Smirnov	0.141
Cramer−von Mises	32.5

related and how much they contribute to the variation of the response. The change in the response is both a function of the copula dependence and how significant a random variable is to the response.

4.5.3.4 Consequences of Copulas

The results of all three applications have illustrated how copulas can propagate forecasted information about dependencies between random variables in order to improve the variance in system level responses. These applications all focused on real technologies that are currently being pursued in the aviation industry and about whom there is a great deal of uncertainty in their impacts and their dependencies. These applications have shown that copulas can probabilistically represent this uncertainty in a manner that incorporates qualitative information from subject matter experts via the copula selection tree (Fig. 32). They also demonstrate that significant improvements in the variance of the system level responses can be obtained by propagating dependencies with copulas through the probabilistic assessment. In contrast, ignoring these important dependencies can lead to misrepresentation of the uncertainty on system level metrics which will affect the technology selection problem on the output side of the probabilistic assessment. This will affect the decision maker's selection decision for future technologies and potentially lead to improper technology investment decisions. These decisions have implications that can take decades to reveal themselves and cost billions of dollars. They can shape the future of major companies and that of the industry as whole. Any blunders in investment decisions at this level due to poor representation of uncertainty associated with future technologies can be irrecoverable. It is critical that tools like copula theory and CAST are provided to the decision maker so that they can make proper technology investment decisions based on accurate representations of the technology uncertainty.

CHAPTER V

UTILITY THEORY BASED DECISION ANALYSIS AND SELECTION

5.1 Probabilistic Assessment Results

Modern probabilistic assessments generally create an abundance of output data. The hope is that this data will help a decision maker glean useful information leading to an optimal decision. Much of this data is created to represent and reflect the uncertainty in the response metrics due to the uncertainty in the input variables. In the aircraft technology selection problem motivating this work, the probabilistic assessment uses probability distributions over technology impact factors and design variables in order to quantify the uncertainty on aircraft system level responses. The system level responses are related to the uncertain input variables by physics based design equations. Each technology portfolio (or technology package) represents a baseline aircraft with a unique set of future technologies applied to it. This unique technology package has probability distributions showing its performance and uncertainty for each response of interest. This information should be considered as a whole for each technology package when making a selection between competing alternatives.

A recent approach to handling this type of problem was made by way of multiobjective stochastic optimization in order to identify superior designs in the large combinatorial space of technology solutions [94]. The optimization procedure is a genetic algorithm operating on the deterministic values of the technology package's performance to seek out a Pareto frontier of technology solutions in the objective space. While this procedure does not actually make a selection, it does help to significantly reduce the number of available options to only Pareto optimal solutions.

However, the procedure operates on deterministic performance estimates and does not use probabilistic assessment data to incorporate the uncertainty in achieving the estimated performance values. Selecting an optimal technology package will obviously require consideration of the performance over multiple responses, but it will also need to incorporate the uncertainty associated with these future technologies and how the decision maker values those aspects of the technology package. Even with only a few different alternatives, considering these factors simultaneously makes it difficult to make any selection, much less an optimal one. With hundreds or thousands of Pareto-optimal technology packages to choose from the problem becomes intractable, so there is a need to approach this challenge with a rapid technique that is logical and axiomatic. Essentially this is a complex decision making problem under uncertainty; so both decision making and uncertainty are investigated in the context of design.

5.1.1 Decision Making

While the interpretation of engineering design as a decision making process is relatively new, decision making and decision theory have been studied for almost 250 years [77]. Decision theory was originally created to study why people were unsatisfied with the decision they made [236]. Unaided decision makers made irrational, suboptimal choices inconsistent with their own beliefs, especially when they were subject to complex tradeoffs and uncertainty [103, 245]. Therefore, decision theory was created upon a set of "axioms of rational behavior" [244] to support the decision maker in making optimal choices. Many different methods exist for engineering decision making but not all are axiomatically valid. Popular methods such as Analytical Hierarchy Process, Weighted Sum of Product Attributes, Euclidean Distance to Ideal, and Taguchi Loss Function have all received some level of criticism for being fundamentally flawed or failing to meet axiomatic principles of proper decision making (Ref. [78, 43]. The literature also indicates that decision making under uncertainty

should adhere to logical, objective, and axiomatic principles which yield consistent and repeatable rankings of alternatives. These are formed using mathematical models that capture a decision maker's preferences. This preference function based on rational axioms is known as "utility" [236]. The formulation of utility for decision making under uncertainty is often credited to von Neumann and Morgenstern (1944) [244]. To remain consistent with the literature, it will also be referred to as von Neumann-Morgenstern (vN-M) utility theory, or simply utility theory, in this work but the author would like to note that this notion of utility as a decision making tool under uncertainty was originally proposed by Frank Ramsey in his essay entitled "Truth and Probability" (1926) [179]. As engineering design has become more and more thought of as a decision making process (Refs. [239, 196, 156, 76]), utility has become further established as the key parameter upon which to base these decisions.

5.1.2 Uncertainty

The topic of uncertainty is well documented in the literature and is broadly categorized under aleatory (irreducible) uncertainty and epistemic (reducible) uncertainty. Many sources of uncertainty exist under these categories including inherent uncertainty, statistical uncertainty, model uncertainty, measurement uncertainty, human error, and others depending on the application. There has been interesting discussion on whether uncertainty truly exists initiated by Laplace in 1814 where he predicted that if the precise initial conditions of every particle in the universe were known at one time, then everything in the future could be predicted from that knowledge. This concept is known as Laplace's demon and conflicts with another famous uncertainty principle postulated by Werner Heisenberg in 1927. The Heisenberg uncertainty principle claims that physically speaking the location and velocity of an electron cannot both be known simultaneously, pointing to a continuous form of aleatory uncertainty. The philosophical significance of uncertainty labels and forms has been debated in

the literature (Ref. [118]). There is an interesting notion that perhaps the names given to uncertainty are not as important as what the practical implication of that uncertainty is. More specifically, naming an uncertainty type is significant only if it "renders possible engineering decisions to allocate resources to reduce the uncertainty before making design decisions" [75]. This attitude is adopted here with an aim to ensure that uncertainty quantification from probabilistic assessments are actually utilized in a structured manner to make engineering decisions.

5.2 Utility Theory

5.2.1 History and Axioms

The earliest references to utility theory date back to the 17th century and the founding of probability theory. In 1654 Pascal and de Fermat [166] were the first to establish the notion of utility by computing expectations of monetary value gambled over dice throws. Following this cost theory became the prevailing way to measure value and make choices. However, in 1713 Nicolas Bernoulli proposed the St. Petersburg paradox [20] showcasing a notional casino game with infinite expected value to demonstrate flaws in the expected cost approach. The paradox shows that even if a notional game has infinite expected value, a rational person will not play the game forever. In 1738 Daniel Bernoulli solved the paradox by introducing the concept of marginal utility [18]. This explains that as wealth increases, the value of each additional unit of wealth decreases and eventually a rational person will stop playing the game even if it has infinite expected value. This led to the log utility, or diminishing marginal utility of wealth and is a function of the gambler's total wealth and the cost to enter the game. He also proposed the idea that the same amount of money can have different worth to different people, implying that the relationship between monetary value and utility is subjective [73]. This practical and useful conclusion is the foundation upon which modern forms of utility are based.

In 1944 von Neumann and Morgenstern formalized utility as a decision theory based on several axioms in their seminal text, Theory of Games and Economic Behavior [244]. In order to incorporate uncertainty and risk, they built their formulation of utility on a notional lottery and several logical axioms. The vN-M lottery (Fig. 48) and the six axioms are well summarized in Ref. [77]. The vN-M lottery has multiple outcomes and the more preferable outcomes have higher utility. The vN-M utility axioms describe a rational decision maker always seeking to maximize their utility and how they interpret chance outcomes in a lottery.

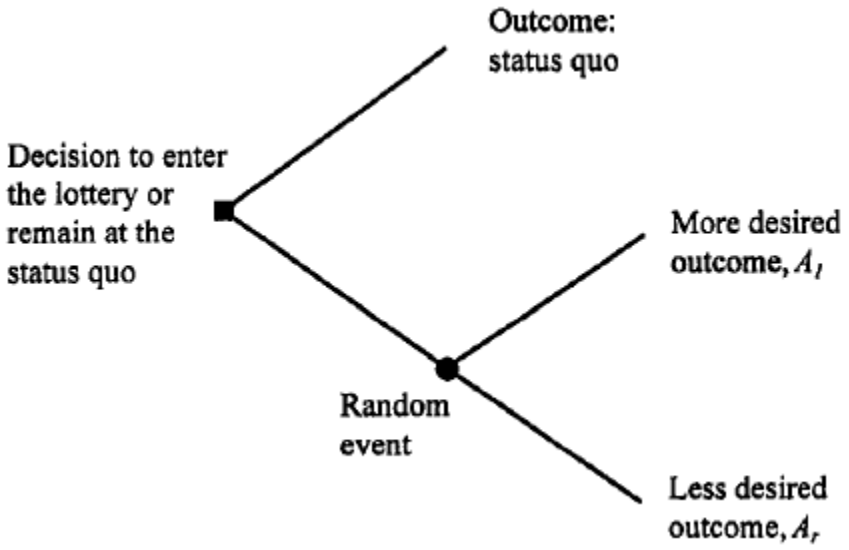

Figure 48: von Neumann-Morgenstern Lottery

1. All outcomes of a vN-M lottery can be ordered in terms of the decision maker's preferences, and that ordering is transitive allowing for rational decision making

2. Any compound lottery, (one whose outcome is another lottery) can be reduced to a simple lottery that has among its outcomes all the outcomes of the compound lottery with the associated probabilities of their occurrence

3. If the outcomes of a lottery, $A_1, A_2, ..., A_n$, are ordered from most desired to least desired, then there exists a number p, $0 < p < 1$, such that one is indifferent

between an outcome A_i, $1 < i < n$, and the lottery A_1 at probability p and A_n at probability $p - 1$. This assures the continuity of preferences between outcomes A_1 and A_n

4. For any lottery adhering to continuity (Axiom 3), with p specified, there exists a certainty outcome that can be substituted for A_i, and the preferences of the decision maker will remain unchanged. The result is that any lottery can be reduced to an equivalent lottery that contains only the outcomes A_1 and A_n

5. The decision maker's preferences and indifferences among lotteries is transitive, ensuring that rational preferences exist among lotteries

6. Given two lotteries, each with only two identical outcomes, differing only in the probabilities of the outcomes, the lottery in which the probability of the more desired outcome is higher is the preferred lottery. This ensures rational preference of the decision maker

This framework establishes utility as a measure that can be used to evaluate uncertain outcomes. It also suggests that utility is tailored to each decision maker individually and is highly subjective while monetary value is not. With this context, a somewhat philosophical, yet understandable definition of utility offered in the text by W. Smart (1891) is "the importance which a good possesses as generally capable of ministering to the well being of a subject." [215]. The encompassing measure of utility over value is further illustrated as he states, ""value is the calculation-form of utility", an expression which will be appreciated if we realize how impossible it is to estimate the utility of a harvest, yet how easy to calculate its amount and its price." He summarizes the distinction simply by stating, "while value reflects utility, the mirror is too small to hold all the picture." This narrative helps to underscore the role of the decision maker's attitudes and preferences in giving rise to their individual utility function.

5.2.2 Decision Makers

Decision makers can be a group of stakeholders or a single rational individual. This distinction is important to note because the methods for determining their utilities are different. Arrow's Impossibility Theorem [9] states that axiomatized rational decision making is not possible for groups unless all the members of the group agree to act like an individual, for example by following the wishes and preferences of a dictator. Bedford [15] further postulates that in groups without strong consensus, even the use of multicriteria decision analysis (MCDA) in itself won't generate that consensus. When there are groups of decision makers, basic utility theory fundamentals do not apply because individuals in groups tend to have different preferences violating some axioms of utility theory, such as being able to make consistent decisions. In such cases a separate branch of utility theory is currently evolving which tries to survey individuals in a group and determine their preferences to form an aggregate utility function. This approach uses techniques like Structured Expert Judgment, Stakeholder Preference Elicitation, and probabilistic inversion which are discussed further by Cooke [43] and Bedford [15]. These techniques are notably useful when there is a scarcity of empirical data and to allow for a diversity of viewpoints.

Random Utility Theory is another technique for groups of decision makers often applied in transportation optimization schemes (Cascetta 2009 [31]) and social choice models (Soufiani 2012 [219]). Cascetta describes Random Utility Theory as, "the richest and by far the most widely used theoretical paradigm for modeling transport-related choices and more generally, choices among discrete alternatives." Its basic assumptions include that the choice set may differ according to the decision-maker, that each decision-maker assigns to each alternative in their choice set a perceived utility or "attractiveness" and selects the alternative that maximizes this utility, the utility assigned to each choice alternative depends on a number of measurable characteristics that are relative to the alternative and the decision maker, and lastly that

because the utility assigned by decision maker to each alternative is not known with certainty, the utility must be represented in general by a random variable. Further detailed discussion on this technique is available in the literature (Refs. [136, 31]).

In this thesis it is assumed that the decision maker is a single rational individual adhering to the axioms of vN-M utility theory. The decision makers may also be a group of individuals, but they will have the same consistent preferences such that they can be treated theoretically as a single decision maker.

5.2.3 Lotteries

Lotteries are often used to explain key ideas in utility theory. A lottery, or gamble, is simply a probability distribution over a known, finite set of outcomes. A simple probability distribution, p on a set of outcomes, A is specified by:

1. a finite subset of A, called the support of p
2. for each $A \in support(p)$, a number $p(x) > 0$, with $\sum_{A \in support(p)} p(x) = 1$.

A simple example of discrete distribution of probability on a set of states is a coin toss. Suppose on a single toss of a fair coin, if it comes up heads you get \$100, if it comes up tails you get \$0. In this case the probability of heads, p, is 0.5 and the probability of tails, $1 - p$ is 0.5 and the outcomes are $A = \{\$0, \$100\}$. In simple lotteries the outcomes are certain but other variations of lotteries exist such as compound lotteries where the outcomes themselves are simple lotteries.

5.2.4 Using Utility Theory

In general, utility theory is most useful in problems where a decision maker is trying to select between multiple alternatives, that each have a performance quantified by metrics or attributes. The value of each attribute is not exactly known, but the decision maker is able to assign probabilities to the various outcomes that might occur. How should the decision maker proceed?

The answer is provided by Keeney and Raiffa in their formative text on utility theory [105]. "If an appropriate utility is assigned to each possible consequence and the expected utility of each alternative is calculated, then the best course of action is the alternative with the highest expected utility." Utility theory has changed over time and there are different ways to calculate utility, but the general statement implies that utility theory is a powerful method for making decisions with uncertainty using rational preferences. It allows a decision maker to capture the risk associated with a particular alternative based on their preferences in order to select between a set of options. Hazelrigg [77] stated that utility theory is essential in these problems because "we are not trying to make a compromise between objectives but rather we are seeking to maximize value". In the future aircraft technology selection problem, utility theory can help make an optimal selection that incorporates preferences and uncertainty to maximize value for a rational decision maker.

Keeney and Raiffa pose the following decision making problem to help the decision maker understand the need for utility theory and explain why in some cases even mean, variance, or expected value methods are not sufficient to consistently make a decision. The selection problem is to choose one action from the following alternatives:

Outcome A_1 - earn \$100,000 for sure

Outcome A_2 - earn \$200,000 or \$0, each with a probability of 0.5

Outcome A_3 - earn \$1,000,000 with probability 0.1 or \$0 with probability 0.9

Outcome A_4 - earn \$200,000 with probability 0.9 or lose \$800,000 with probability 0.1

They point out that for all of these acts the expected value is the same, \$100,000, so that is not helpful for making a decision. Outcome A_1 is obviously appealing compared to A_2 because it involves no uncertainty, but since uncertainty usually exists in most real problems, a method is needed to rank order alternatives that includes uncertainty. Variance may seem like a good criterion but outcomes A_3 and A_4 both

have the same expected value and variance, so even the combination of these would still yield indifference between the alternatives. This simple example points to the need for a better alternative criterion which the authors indicate as the maximization of the expected utility.

5.2.5 Expected Utility in Lotteries

In 1954 Savage authored an important text laying the foundations of modern decision theory called The Foundations of Statistics [198]. In this work he represents the preferences of a rational individual with expected utility. He further proves that there is one and only one set of subjective probabilities over the attributes of the problem and a unique utility function over the states of the subject such that if outcome A_1 is preferred by the subject over act outcome A_2, then the expected utility of A_1 is greater than the expected utility of A_2. The literature has repeatedly indicated that expected utility is the appropriate tool for decision making under uncertainty [105, 77, 214], but how can one calculate expected utility? Before proceeding it is useful to recall two ideas central to expected utility.

The "Bernoulli utility function" refers to a decision-maker's utility over wealth because it was Bernoulli who originally proposed the idea that people's internal, subjective value for an amount of money was not necessarily equal to the physical value of that money. This part of utility incorporates the decision maker's preferences and risk attitudes. The term von Neumann-Morgenstern utility function refers to a decision-maker's utility over lotteries or gambles. This part of utility expresses how utility incorporates probabilities of outcomes over which the decision maker has no control. Both of these concepts are well illustrated in a simple example.

It is often the case in real world situations, that one may not act to maximize the expected value of their monetary savings. If the decision maker possesses \$100 in total savings, they may be hesitant to risk the entire sum for a small chance at

winning \$1000. Presume a lottery with a 15% chance of winning \$1000 and a 85% chance of winning \$0. The expected value of the lottery is:

$$E(L) = 15\%(\$1000) + 85\%(\$0) = \$150 \tag{38}$$

The expected value of the lottery is still greater than the \$100 the decision maker currently has, but many would still not enter this lottery. This conflicts with basic cost theory where decision makers should act to maximize expected value. However, if the decision maker is vN-M rational, this behavior is already captured in their utility function, U, in terms of their risk attitude. This is because for most people the expected utility of this lottery is less the utility of the \$100 in total savings they currently have for certain. This can be expressed mathematically as:

$$E(U(L)) = 15\%u(\$1000) + 85\%u(\$0) < u(\$150) \tag{39}$$

This concept of evaluating a lottery based on its expected utility is an important one that will be applied in this thesis. The inequality in Eqn. 39 is likely true for most risk averse decision makers due to the high likelihood of getting \$0, but it is not true for all decision makers. Each vN-M rational decision maker has their own utility function, which is used to evaluate their preferences over competing alternatives.

5.2.6 von Neumann-Morgenstern Utility Functions

A utility function with the following expected utility form is called a von Neumann-Morgenstern (vN-M) expected utility function. Let A denote a finite set of outcomes, and let n be number of outcomes. The utility U is an expected utility if there is an assignment of numbers $(u_1, ..., u_n)$ to the n outcomes such that for every simple lottery L, we have

$$U(L) = \sum p(A_i)u(A_i) \tag{40}$$

The expected utility of every simple lottery over these outcomes is given by the utility of each outcome multiplied by the probability the lottery assigns to it, summed over all possible outcomes. The resulting utility function (which takes a simple lottery L as an argument and returns its expected utility) is the vN-M expected utility function. This formulation of the vN-M expected utility is so powerful it has been stated that, "subject to the six axioms of vN-M utility (i.e., rational decision making), not only does the expected utility theorem provide a valid utility measure (that is, a valid measure for rank ordering design alternatives), it is the only valid measure. All other measures are wrong (or equivalent)" [77].

5.3 Single Attribute Utility Theory

5.3.1 Assessing Single Attribute Utility functions

Utility is a relative concept to each decision maker, not an absolute one. It builds on expected cost theory by allowing for nonlinear relationship between monetary value and utility. The challenge lies in assigning utility values and encoding this relationship. The best technique for doing this depends on the decision maker and the context of the problem. In general there are five basic steps in this process [105]:

1. Preparing for the assessment
2. Identifying the relevant qualitative characteristics
3. Specifying quantitative restrictions
4. Choosing a utility function
5. Checking for consistency

There are many different procedures and variations of techniques for eliciting utility functions [152, 49, 13, 199] from decision makers due to the numerous ways of carrying out each of these five steps. In fact, Keeney and Raiffa [105] state that, "the

assessment of utility functions is as much of an art as it is a science, and, therefore, no single set of rules can be laid down that invariably result in a utility function." From this it can be understood that the utility assessment procedure is adaptable to the given problem and the available resources. This is an important revelation that will be applied in this thesis to create a utility function assessment method for the future aircraft technology selection problem.

The first step in the procedure ensures that the analyst and decision maker are on the same page, that they both understand the attribute outcomes, orientation of scales, etc. It should be pointed out to the decisions maker that the process is meant to capture their subjective feelings and hence there no right or wrong answers. In fact, one purpose behind this process is to make a decision maker reflect on their preferences and gain a better understanding of their own problem by assessing how they value attributes of the problem. Note that from this section onward the notation used thus far for notional outcomes, A_i on an attribute A, will change to x_i on attribute X for single attribute, and x_i, y_i, z_i on attributes X, Y, Z for multiple attributes. This is done for ease of understanding as the discussion transitions from single to multiple attribute utility theory in the succeeding sections.

5.3.1.1 Risk Attitudes of Decision Makers

The second step in assessing utility functions identifies properties of the decision maker like their risk attitudes and whether the utility function is monotonic or not. In utility theory, risk attitudes are reflected in the shape of utility functions. A decision maker's feelings towards taking chances (e.g., entering a lottery) will determine how their utility function looks.

If a decision maker is asked to choose between receiving a particular outcome for sure or entering a lottery and assume its inherent risk, and they always choose the certain outcome over the lottery, they would be risk averse. This is because they

prefer the certain outcome over assuming the risk involved in the lottery. Another way to understand this concept is to examine the lottery in terms of utility. Since a risk averse decision maker always prefers a certain outcome over a lottery with the same expected value, it means that their utility for the certain outcome, is always greater than the expected utility of the lottery. The lack of willingness to take the risk of the lottery implies that this decision maker's utility function is concave. Keeney and Raiffa [105] provide a proof of this statement, but it suffices here to understand that concave utility functions (e.g., $u(x) = ln(2x)$) indicate that the decision maker is risk averse. This is illustrated by the green curve in Fig. 49 [174].

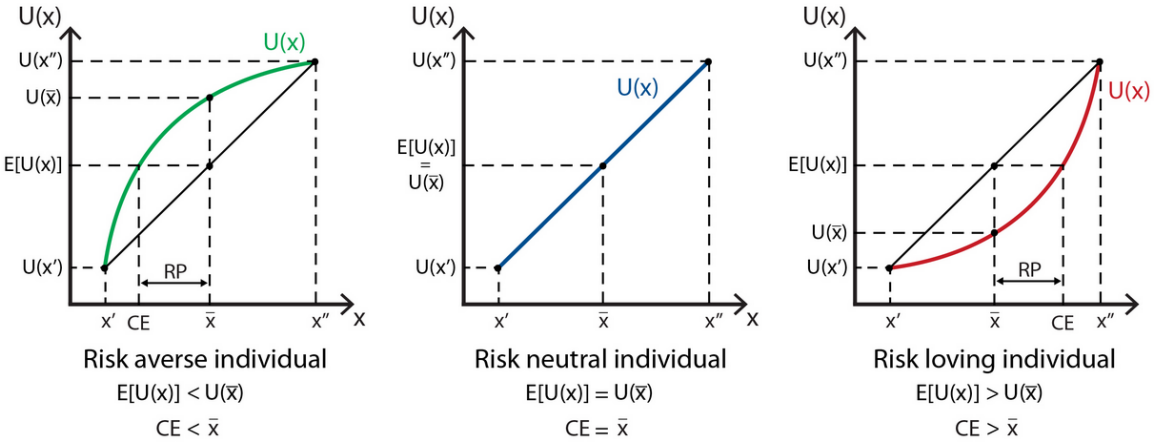

Figure 49: Risk Attitudes in Utility Functions

The opposite of a risk averse decision maker is a risk prone (risk loving) decision maker. This is a decision maker who always prefers the risk of a lottery to the expected value of that lottery. Their utility of the certain value is always less than the expected utility of the lottery. The willingness of this decision maker to always enter the lottery implies that their utility function is convex. A proof for this statement is also provided by Keeney and Raiffa [105], but here it is sufficient to understand that convex utility functions (e.g., $u(x) = 2x^2$)) belong to risk prone decision makers. This is illustrated by the red curve in Fig. 49.

Risk neutral decision makers are indifferent towards choosing between a certain

value for sure and entering a lottery with the same expected value. For them, the utility of the certain value is equal to the expected utility of the lottery. These decision makers have linear utility functions, e.g., $u(x) = 2x$. This is illustrated by the blue line in Fig. 49.

Monotonic utility functions are either continuously increasing or decreasing. The sign of their slope does not change. The formulation of risk in utility functions and the concept of monotonicity are both further expounded upon in Appendix 7.3.

The third step in assessing utility functions is to fix some quantitative points on the utility function. Based on the possible outcomes in a problem, the decision maker can create a utility scale by choosing a minimum and maximum point relative to two of the outcomes in their set. These generally correspond to the lowest and highest outcome in a set, but this does not have to be the case, especially if more importance is placed on some intermediate outcome in the set. For example, if there is a target value in the set, then the decision maker can choose to assign that the maximum utility, and then have utility decrease for outcomes after the target value has been met. This notion will be useful in the aircraft technology selection problem where specific goals exist in each attribute.

After setting the minimum and maximum utility points the remaining outcomes can be assessed relative to these two defined utilities. If $x_1, x_2, ..., x_n$ are possible outcomes, x^* is the most desirable outcome, and x^0 is the least desirable outcome, then the a common utility scale to use is $u(x^*) = 1$ and $u(x^0) = 0$. The remaining outcomes can be assigned a utility value by asking the standard lottery question between x^* and x^0 for a given outcome x_i. At which probability p is a decision maker indifferent between entering a lottery with probability p of getting x^* and probability $1 - p$ of getting x^0, or getting the outcome x_i for certain? The answer, i.e., the probability p, is the utility of x_i [73]. The utility of each outcome can be assessed in this way using Eqn. 70.

$$u(x_i) = pu(x^*) + (1-p)u(x^0) \tag{41}$$

This direct assessment technique can be difficult to complete in cases where there are many outcomes. In those cases it is recommended to assess the utilities of a few different points directly, and then fit a generic utility function curve to these assessed points. The shape and functional form of the curve is based in large part on the decision maker's attitude towards risk.

5.3.1.2 Certainty Equivalent

The certainty equivalent is a basic concept in utility theory and has different uses including the assessment of utility functions. Formally stated, the certainty equivalent of a lottery is an amount x, such that the decision maker is indifferent between choosing the lottery outcome and the amount x for certain. It is formulated in a similar manner as the standard lottery question used to directly assess utilities for every outcome x_i, except that instead of trying to identify a probability p over lottery outcomes, the certainty equivalent seeks to identify the outcome value x that has the same utility as a lottery with known outcomes and probabilities. For example, given the 50-50 lottery between x^* and x^0 in Eqn. 42,

$$u(x_{0.5}) = 0.5 * u(x^*) + 0.5 * u(x^0) \tag{42}$$

the outcome x at which the decision maker is indifferent between taking x for certain (100% probabilty) and entering the lottery, is the certainty equivalent for this lottery. When the certainty equivalent is determined by comparing to a lottery that has 0 and 1 as utility outcomes, the certainty equivalent has a utility equal to 0.5.

It is useful to note that the certainty equivalent will take on a single unique value for monotonic utility functions. The mathematical formulation and other details about the certainty equivalent are expounded upon in Appendix 7.3.

In practice assessing utilities for every outcome can be arduous for decision makers. Instead, a general strategy is to set a minimum and a maximum utility point at utility equals 0 and 1 respectively, then identify a few different certainty equivalent points along the utility function, and finally fit a known utility functional form through these points. The first certainty equivalent ($x_{0.5}$) is identified by the lottery in Eqn. 42. The next two certainty equivalents that are generally calculated are $x_{0.25}$ and $x_{0.75}$. They are found using the newly obtained midpoint utility outcome $x_{0.25}$ as expressed in Eqns 43-44.

$$u(x_{0.25}) = 0.5 * u(x_{0.5}) + 0.5 * u(x^0) \tag{43}$$

$$u(x_{0.75}) = 0.5 * u(x^*) + 0.5 * u(x_{0.5}) \tag{44}$$

The three certainty equivalent points and the minimum and maximum utility points yield five different points along the utility function. The fourth step in assessing utility functions is to fit a generic curve through these points. While any appropriate functional form can be applied, the exponential function is commonly used due to its monotonic and curved nature that can easily represent various risk attitudes. For example, in general a risk averse decision maker's utility points can be fit using a function of the form in Eqn. 45

$$u(x) = -b * exp^{-cx} \tag{45}$$

A risk prone decision maker's utility points can be fit using a function of the form in Eqn. 46

$$u(x) = b * exp^{-cx} \tag{46}$$

A risk prone decision maker's utility points can be fit using a function of the form in Eqn. 47

$$u(x) = b * x + c \tag{47}$$

Consistency checks are an important final step in assessing utility functions to detect errors in the decision makers utility function. An error implies that the assessed utility function does not represent the true preferences of the decision maker. Any utility values that seem strange or do not adhere to the assumed functional form well can be checked. A second check is to ask the decision maker their preference between any lottery and any outcome, or between two lotteries. In both cases, whatever the decision maker prefers must have higher expected utility to be consistent. Another check described by Keeney and Raiffa [105], involves asking a set of circular preference questions that can actually help a decision maker straighten out their own preferences, which is particularly helpful in complex decision problems. In these situations the need for real consistency checks is even more important.

5.3.2 Research Question 3

This review has covered many different topics within utility theory. An important observation from this review is that expected utility is the appropriate measure to make comparisons between lotteries. The expected utility of a lottery on an attribute X is written as

$$E(U(X)) = \sum_{i=1}^{n} p(x_i)u(x_i) \tag{48}$$

where $p(x_i)$ is the probability of outcome x_i occurring and $u(x_i)$ is the utility of that outcome for a given decision maker. Research Question 3 asks how this important concept can be applied to the future aircraft technology selection problem.

Research Question 3

How can the concept of expected utility be applied to evaluate and make comparisons between technology packages?

Postulate 3

Applying utility theory to this context, each solution in the n-dimensional objective space can be treated as a lottery whose expected utility can be used to make a preference ranking

This research question will not be tested with a contingent statement and an experiment because it asks how something can be done, instead of questioning the particular state of a variable. Since that is not a formally testable hypothesis, the answer for Research Question 3 is formulated as a postulate that will be demonstrated and explained.

5.3.3 Formulation of the Aircraft Technology Selection Problem with Single Attribute Utility Theory

Interpreting the aircraft technology selection problem in the context of utility theory using Eqn. 48 immediately brings to light the fact that this is a two part problem. The first part is the evaluation of the probabilities reflecting the uncertainty over the outcomes. Each technology package has a probability distribution over a given attribute indicating its performance in that attribute and the uncertainty associated with that attribute. Recall that a lottery is simply a probability distribution over a known, finite set of outcomes. Recognizing that a technology package's performance in a given attribute is provided by a probability distribution over a finite set of outcomes, it can be stated that each *technology package* is in fact a *lottery* over the given attribute. Then by computing the expected utilities of the lotteries, it is possible

to compare and tradeoff different technology packages (Fig. 50) using vN-M utility theory.

Figure 50: Notional Technology Packages as Lotteries

The second part of the problem is the assessment of a decision maker's utility over these outcomes. A decision maker must subjectively specify how they view each of the outcomes in the lottery. These two aspects of the problem represent distinct roles between separate stakeholders that should not be mixed. The role of the technologist is to evaluate the uncertainty associated with the technology package and specify through a probabilistic assessment, the probability distribution over the attribute of interest. The role of the decision maker is to rationally specify their utility preferences over the uncertain outcomes from the probabilistic assessment. These two roles should be executed independently and then brought together via Eqn. 48 to calculate the expected utility of a technology package (lottery). Then repeat this process for every technology package under consideration. The expected utility provides a single metric to axiomatically rank order all the technology packages in a manner that is traceable, repeatable, and rationally consistent with the decision maker's preferences.

5.3.4 Environmental Design Space (EDS)

In order to demonstrate the answer to Research Question 3, aircraft vehicle assessments must be performed on different technology packages to obtain the uncertainty associated with them. That uncertainty will be converted into probabilities that can be used to form lotteries representing the technology packages. This information can be obtained from the Environmental Design Space (EDS) [114] which is powerful physics-based tool used to assess the performance of current and future aircraft. It

can also model the improvements in performance by technology infusion into these aircraft with respect to the goals outlined in Fig. 1. The capabilities of EDS make it invaluable in generating realistic technology portfolios and very relevant to the aircraft technology selection problem.

EDS is a tool developed by Georgia Tech's Aerospace Systems Design Laboratory (ASDL) for the U.S. Federal Aviation Administration's Office of Environment and Energy (FAA/AEE) as part of a comprehensive suite of software tools that allows for a thorough assessment of the environmental effects of aviation [114]. EDS provides the capability to generate an integrated analysis of aircraft performance, source noise, and exhaust emissions at the aircraft level for potential future aircraft designs under different policy and technological scenarios. The integrated analysis enables the assessment of the interdependencies and associated trade-offs between aircraft performance, noise, and emissions in a transparent and traceable manner. EDS is a physics-based, integrated, multidisciplinary modeling and simulation environment which seamlessly combines core modules originally developed by NASA, coupled with design rules and logic along with user defined engine and airframe design parameters to create aircraft designs [109].

The EDS environment contains four phases with respect to a single vehicle that are shown in Fig 51 (Ref. [108]). Phase 1 begins with the initialization steps, which establishes the different modes and options for running EDS and determines the settings of all the design variables. These design variables can include hundreds of different engine, aerodynamic, weight, and geometry settings. Phase 2 is the vehicle design phase which performs the necessary engine cycle analysis and sizes the engine and airframe. Details on the modules within EDS and how they operate can be found in Refs. [42, 68, 132, 133, 161, 238, 202]. The aircraft is fixed at the end of this phase. Phase 3 is the vehicle performance evaluation phase. In this phase all desired performance evaluations are conducted including gaseous emissions, noise

certification, takeoff and landing performance evaluations, and fuel burn for off-design points on a payload-range chart [158] [258, 259]. Phase 4 is the output data phase where all desired data is compiled into user-specified summary files.

EDS models technology infusion using a series of additive or multiplicative factors at various levels of the analysis. These factors collectively encompass the technology design space defined by first formally collecting technology data in terms of its quantitative impacts and interactions with other potential technologies. The technology data is then formally recorded in a Technology Interaction Matrix (TIM) and a Technology Compatibility Matrix (TCM) respectively. These matrices provide both traceability and transparency to the technology modeling and auditing process. Technology information may be gathered from publicly available literature, including peer reviewed publications, and subject matter experts, either at NASA or in industry. It is important to note that technology impacts are modeled at the component level and allowed to propagate through the EDS modeling and simulation environment in order to determine their aircraft-level benefits, rather than modeling a technology as a simple improvement in a given performance metric[110].

5.3.5 Implementation of Single Attribute Utility Theory in the Aircraft Technology Selection Problem

The implementation of this method will capitalize on existing work performed for NASA's Environmentally Responsible Aviation (ERA) project which is described in detail by Refs. [203, 204, 205]. That work leveraged the EDS environment to create an ERA Dashboard using surrogate models that rapidly replicate the analyses performed within EDS. The ERA Dashboard (Fig. 52 [203]) allows for quick and efficient generation of technology packages to examine the performance and tradeoffs between various future technologies at the vehicle and fleet level. The ERA Dashboard also uses its surrogate models to perform a Monte Carlo simulation on SME

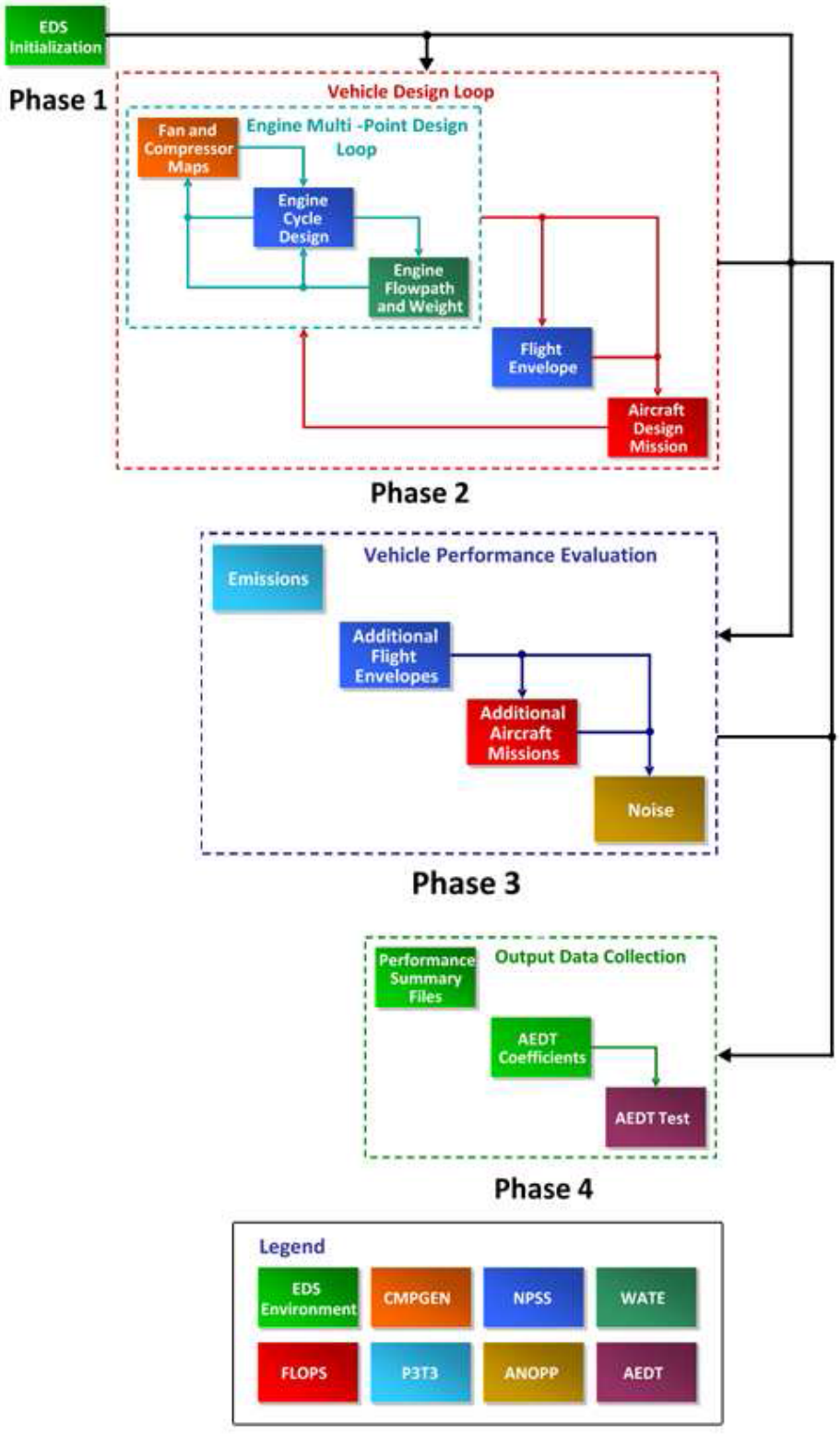

Figure 51: Flowchart of Information and Modules in EDS

(subject matter experts) encoded uncertainty distributions for the input random variables, to rapidly conduct a probabilistic assessment on any technology package. The result of the assessment are probability distributions quantifying the performance and uncertainty of the technology package on the attributes of interest. Three notional technology packages will be considered for evaluation and ranking using a single attribute vN-M utility function. The attribute under consideration for each technology package is percent fuel burn (FB) reduction over a reference baseline vehicle. The baseline vehicle represents a reference 300 passenger, 1995 technology level aircraft, similar to that used in Research Question 2. Various combinations of advanced future technologies, each representing a technology package, are applied to this baseline aircraft resulting in unique distributions of %FB reduction over the baseline aircraft. In general, higher values of %FB reduction are more desirable as this indicates greater improvement in fuel efficiency over the baseline aircraft.

Figure 52: NASA Environmentally Responsible Aviation (ERA) Technology Dashboard

Three technology packages are chosen from the Pareto frontier of technology solutions (red colored points in the top right of Fig. 52) shown by the ERA Dashboard.

The Pareto frontier of solutions was identified using the multiobjective stochastic optimization genetic algorithm described in Ref. [94] that operated on the deterministic values of each technology package's attributes. The Pareto frontier represents 1,500 different non-dominated technology solutions and the decision maker is left to find a way to choose between them. While the ERA Dashboard can conduct probabilistic assessments for any selected technology solution on an ad hoc basis, it can't use that information to create a preference based, axiomatic ranking of the technology solutions. All of the 1,500 deterministically identified technology solutions on the Pareto frontier appear equal to it. Using expected utility to incorporate the uncertainty information and the decision maker's preferences, it will be shown that this is not true and that utility theory can provide an axiomatic ranking between Pareto frontier technology solutions. For the sake of clarity and traceability this expected utility formulation will be implemented using three distinct technology packages on the Pareto frontier. The three selected technology packages correspond to unique portfolios of technology combinations that achieve low %FB reduction (Technology Package 1), high %FB reduction (Technology Package 2), and medium %FB reduction (Technology Package 3) over the baseline aircraft. Their probability distributions are reported from the ERA Dashboard as depicted in Fig. 53.

Each value under the histograms in Fig. 53 represents a possible outcome in the attribute of interest, %FB reduction over the baseline aircraft. The histogram bars give a sense of how likely each outcome will be, but they do not directly provide the probabilities over the outcomes which are needed in the expected utility formulation. In order to obtain that, the data is transferred to Matlab where a numerical histogram is created and normalized by the total number of points. Each bar represents an interval of continuous outcomes in the lottery, e.g., 49 to 49.5 %FB reduction. The area under each bar of the normalized histogram is calculated and stored. This area represents the probability of an outcome occurring between 49 to 49.5 %FB reduction.

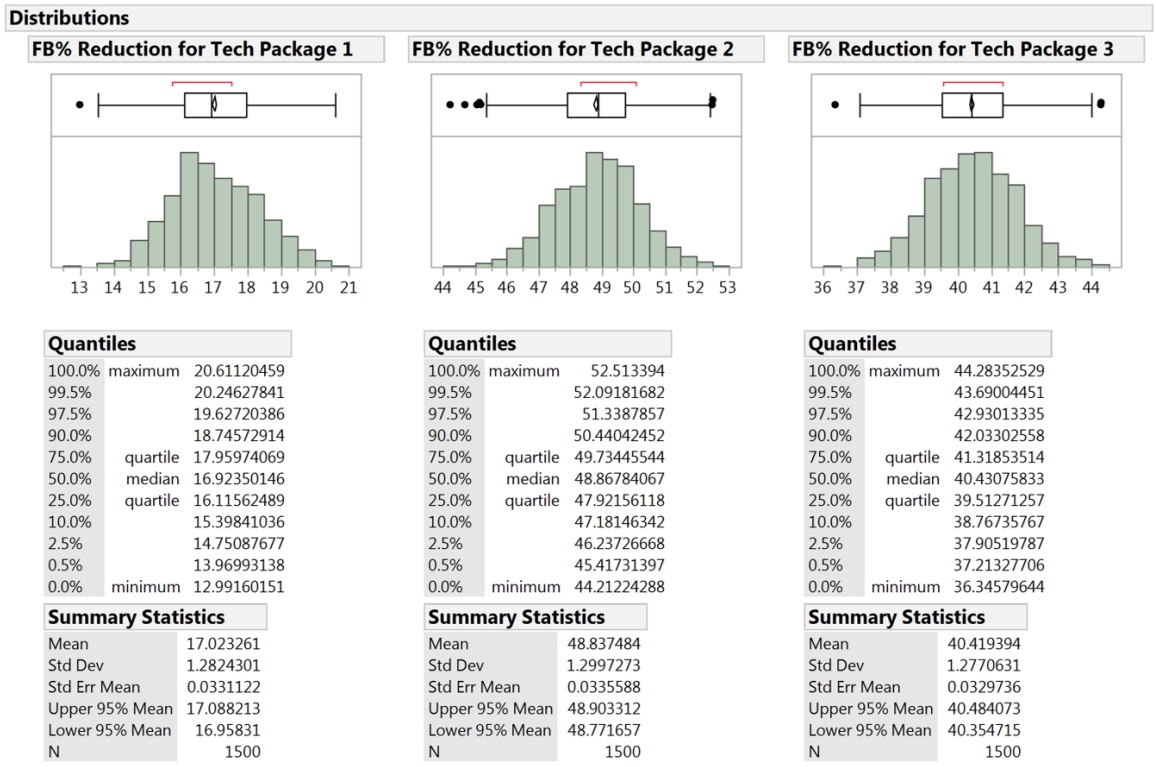

Figure 53: %FB reduction over baseline aircraft for Technology Packages 1, 2, and 3

The sum of all the areas under each bar is one. In order to map a probability value to a single lottery outcome, the midpoint of the interval is identified and used as the discrete lottery outcome, which would be 49.25% FB reduction in this example. This converts the continuous intervals to discrete occurrences which can be interpreted as outcomes of a lottery. The probability over that interval (49 to 49.5 %FB reduction) is assigned to this discrete midpoint value (49.25% FB reduction). The number of intervals is increased numerically such that the error in this approximation is small. The smaller the interval, the more accurate the probability distribution. There is a tradeoff between decreasing interval size and increasing run time but this was resolved by running a sensitivity study and choosing an interval size that gave satisfactory run time while ensuring that the error in the approximation was 1% or less. Obtaining these probabilities over the finite set of outcomes is the first part of the expected utility formulation and is conducted by the technologist.

The second part of the expected utility formulation is to elicit the decision maker's preferences over these discrete lottery outcomes. The procedure for doing this is described in Sec. 5.3.1 where Eqns. 42-44 can be used to fit an exponential or linear utility function (Eqns. 45-47) based on the decision maker's preferences and risk attitudes. This utility function does not have to be monotonic, particularly if their is a target value that is exceeded by the range of outcomes. Exceeding a target value in a particular attribute could mean excess resources have been applied in an unprofitable area of the attribute. It would have been cheaper to simply meet the goal than to exceed it. In this scenario the outcome matching the target value is assigned utility equal to one and utility decreases after the target value is exceeded. In Ref. [105, Sec 4.8.4] Keeney and Raiffa describe how to handle nonmonotonic utility functions. Essentially they suggest a piecewise interval approach to constructing the utility function as two separate, monotonic, utility functions that joined at the target value to produce an overall nonmonotonic utility function.

For the sake of clarity and traceability in this implementation of the expected utility formulation, the utility function for a simple risk neutral decision maker is used. Their utility function is anchored at zero for 0% FB reduction (lower end of attribute range) and at one for 55% FB reduction (upper end of attribute range). The utility function is assessed so that it is encompassing of all possible outcome values in the range of the attribute. This ensures that the utility function will only have to be elicited from a particular decision maker once. The same utility function can be used to calculate the expected utility of all technology package lotteries under consideration (assuming the decision maker's preferences do not change). The three probability distributions for technology packages 1, 2, and 3 and the notional decision maker's risk neutral utility function over them are given in Fig. 54.

Using the probability distributions over the outcomes and the decision maker's assessed utility function, the expected utility of each lottery can be found by Eqn.

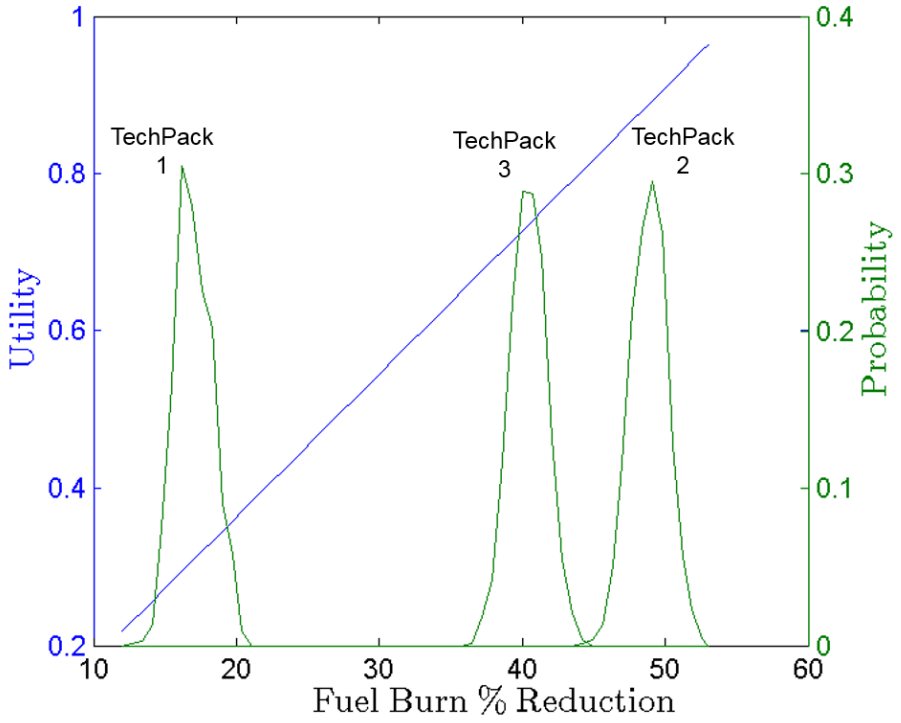

Figure 54: Technology package 1, 2, and 3 probability distributions (right axis) and risk neutral utility function (left axis)

49.

$$E(U(FB)) = \sum_{i=1}^{n} p(FB_i)u(FB_i) \tag{49}$$

The exact value of the expected utility is equal to the integral over the continuous probability distributions times their utility, but in this numerical simulation a summation will be calculated over many small intervals to approximate this integral. The intervals are the same ones used to approximate the probability distribution earlier and are chosen such that the error in calculating the expected utility of the technology package lottery is less than 1%.

5.3.6 Single Attribute Utility Theory Results

The product of the utility function and the probability distribution, or the utility scaled probabilities, provides a traceable way of quickly visualizing how a decision

maker values each outcome. The summation of all of these products gives the expected utility of the lottery as stated in Eqn. 49. This is visualized for the single attribute technology packages in Fig. 55.

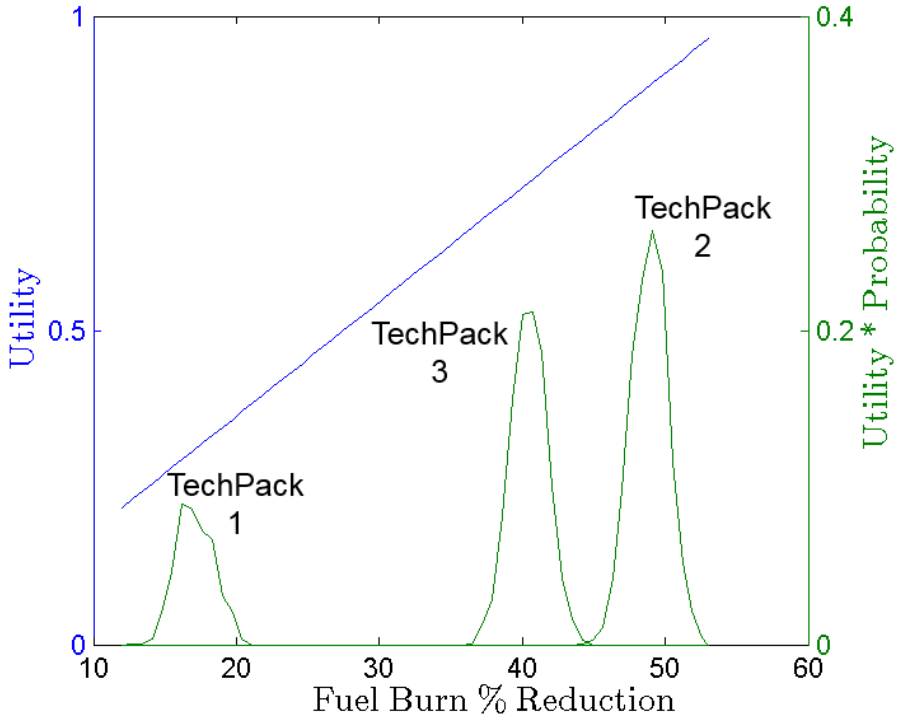

Figure 55: Utility scaled probabilities of technology packages 1, 2, and 3 (right axis) and risk neutral utility function (left axis)

Fig. 55 provides traceability to the selection process and shows why the outcomes of one lottery may be preferred over the outcomes of another, based on the utility function of the decision maker. The lottery representing technology package 1 will not perform well because the decision maker has low utility for lower values of %FB reduction. The lottery representing technology package 3 is most preferred because it has outcomes whose utilities are highly valued by the decision maker. In this way it is clear which technology package lottery is most preferred by the decision maker even before the summation in Eqn. 49 is performed to quantify the expected utility of each technology package lottery.

The results for the expected utility assessment for all three technology packages

Table 23: Single Attribute Expected Utility Results

Technology Package	Package Description	Expected Utility	Ranking
Tech Package 1	Low %FB reduction	0.30	3
Tech Package 2	High %FB reduction	0.88	1
Tech Package 3	Med %FB reduction	0.73	2

are summarized in Table 23.

Table 23 shows that the three technology packages under consideration can be rank ordered by their expected utilities. This ranking is consistent with the probability distributions in Fig. 54. Technology package 1 has probabilities distributed over the lowest range of outcomes and should have a low expected utility. Technology package 2 has probabilities distributed over the highest range of outcomes and should have a high expected utility. Technology package 3 has probabilities distributed in the middle of the range but closer to technology package 2, so it should have an expected utility between technology package 1 and technology package 2, but closer to technology package 2. The utility function is linear and so it gives more importance to higher values of FB %reduction. This is also consistent with the results in Table 23. This answers Research Question 3 by demonstrating how technology packages can be rank ordered in a logical, repeatable, axiomatic fashion via expected utility, that is not only consistent with the decision maker's preferences, but is also traceable back to the utility of the probability distributions of each technology package lottery.

This capability can be used to evaluate and rank all of the technology solutions on the Pareto frontier that were previously considered to be equal, by using expected utility to incorporate the uncertainty information and the decision maker's preferences into a structured and axiomatic metric. The results in this section for single attribute utility were intended to be simple to demonstrate the expected utility framework. The ranking and selection process quickly becomes nontrivial as the number of lotteries increase, when the probability distributions have different variances, when the decision maker's utility function is more complex, and as the number of attributes increases. In those cases, it is critical to rely on the axiomatic foundations of utility theory to produce a consistent and logical ranking of the technology package lotteries.

5.3.7 Aggregating the Single Attribute Functions

This process has been demonstrated for a single attribute expected utility function using %FB reduction. Other attributes like aircraft noise margin (above a reference limit) or emissions quantified by %NOx reduction over a baseline are also worth consideration at the conceptual design level [35, 203]. These attributes can be assessed for expected utility in a similar manner. However, the aircraft technology selection problem has multiple simultaneously competing attributes. A utility formulation is needed that can assess expected utility over multiple attributes simultaneously. There are multiple methods in the literature for multicriteria decision making but many are not based on axiomatic fundamentals like utility theory. Stakeholder Preference Elicitation (Ref. [43]) and Random Utility theory (Refs. [31, 136, 219]) are suited to incorporate utility theory over multiple attributes but are designed for multiple decision makers, which is beyond the scope of this work. Multiattribute Utility Theory (Ref. [15, 105]) is intended for a single rational decision maker and can be used to find expected utility over multiple attributes simultaneously. Extending the concept of expected utility from a single attribute to multiple attributes is expressed

mathematically by Eqn. 50.

$$E(U(X,Y,Z)) = \sum_{i=j=k=1}^{n} p(x_i, y_j, z_k)u(x_i, y_j, z_k) \tag{50}$$

Expected utility functions for two and three attributes consistent with the form of Eqn. 50 will be investigated and demonstrated in the succeeding sections. It is recognized that while theoretically possible, the extension of these methods beyond three attributes will be difficult. In cases where this is needed, it is recommended to conduct sensitivity tests to identify the number of critical attributes in the decision making process, explore the technique of conditional preferential independence (Ref. [14]), or apply random variable based utility theory (Refs. [31, 43, 136, 219]). Another possibility is to consider dimension reduction techniques like principal component analysis and factor analysis to identify the most important attributes in the problem (Ref [99, 92]. Once identified, the two or three attribute procedures investigated here may be applied.

5.4 Multiattribute Utility Theory

5.4.1 Multiattribute Utility Theory Introduction

Multiattribute Utility Theory (MAUT) is an aggregation technique for single attribute utility functions of a decision maker. When more than one attribute of a problem is relevant to the decision maker, multiattribute utility (MAU) theory can facilitate proper decision making. It is a somewhat old theory from the 1950's and requires rigid assumptions of independence between the attributes, which can make it difficult to use in some applications. The most important concept which dictates the form of the multiattribute utility function is that of utility independence.

5.4.2 Forms of Attribute Independence in Utility Analysis

Various types of independence conditions exist between attributes in multiattribute utility analysis and they dictate the specific form of the MAU function that will

be used. The first type is utility independence, a key concept explained by Keeney and Raiffa [105] that examines the relationship between the attributes in terms of their utility. Utility independence is similar to probabilistic independence in multivariate probability theory. Attribute is utility independent of attribute Y when conditional preferences for lotteries on X given a specific outcome y do not depend on the particular level of y. Thurston (Ref. [236]) provides another description for utility independence, saying that X is utility independent of Y if the degree of risk aversion in outcomes on attribute X remains constant regardless of the value of Y. The attributes are mutually utility independent, when each attribute is utility independent of the other. In this case use the multilinear form (Ref. [105, Sec 5.4]) of the multiattribute utility function. Preferential independence exists when the rank order of outcomes on one attribute X does not depend on the outcome value of the second attribute Y. Thurston (Ref. [236]) explains preferential independence with a simple example between two attributes, cost X and weight Y. "If (50 pounds, \$100) is preferred to (40 pounds, \$100) and (50 pounds, \$80) is preferred to (40 pounds, \$80) then weight is preferentially independent of cost." When attributes X and Y are both utility and preferentially independent, the multiplicative form of the multiattribute utility function is used. The remaining aggregation form is the additive form which requires additive independence between the attributes. Keeney and Raiffa explain that "attributes X and Y are additive independent if the paired preference comparison of any two lotteries defined by two joint probability distributions, depends only on their marginal probability distributions." (Ref. [105, Sec 5.3]) In this case the additive multiattribute utility function is appropriate.

5.4.2.1 Multiplicative Utility Function

The multiplicative multiattribute utility function is explained in Ref. [105, Sec 5.4.3] and it is given in Eqn. 51 [236].

$$U(\mathbf{X}) = 1/K \left[\left[\prod \left(K k_i U(x_i) + 1 \right) \right] - 1 \right] \tag{51}$$

where K is a normalizing constant such that utility of the vector of attributes $\mathbf{X}$ scales from 0-1. k_i represents the single attritbute utitlity function scaled from 0-1. This multiplicative form is used when the attributes are preferential independent and utility independent.

5.4.2.2 Additive Utility Function

The additive utility function is the most restrictive multiattribute utility function. It requires preferential, utility, and additive independence conditions to be met in order to be used. It uses two positive scaling constants to sum the contributions of the two attributes to find the total utility. Its form is given in Ref. [105, Sec 5.3] by Eqn. 52

$$U(X, Y) = k_X u(x) + k_Y u(y) \tag{52}$$

The attributes X and Y are additive independent if the paired preference comparison of any two lotteries, or the joint probability distribution of X and Y, depend only on the marginal probability distributions.

5.4.2.3 Multilinear Utility Function

When Y and Z are mutually utility independent of one another, their multiattribtue utility function is of the multilinear form. This functional form is more complex than the additive form because it takes into account the interactions between the decision makers preferences over X and Y. Its form is given Ref. [105] by Eqn. 53

$$U(X, Y) = k_X u(x) + k_Y u(y) + k_{XY} u_X(x) u_Y(y) \tag{53}$$

The multilinear form adds the interaction term constant k_{XY} to capture the underlying behavior between X and Y. This form is applicable when attribute Y is

utility independent of attribute X, and attribute X is utility independent of attribute Y. The constants in these multiattribute equations are found by solving systems of equations which are based on known conditions in the utility function space. Some of these conditions depend on how the utility function is created such as specifying the lowest and highest value of utility. Other equations are formed using the certainty equivalent. The expected utility of a lottery can be difficult to interpret physically for a decision maker, so it is often easier to understand this situation by thinking of the equivalent certain consequence. When this is quantified by the decision maker, it can provide another useful equation to solve for the constants in their multiattribute utility function. This procedure is outlined in a good teaching example by Keeney and Raiffa in Ref. [105, Sec 5.10].

5.4.2.4 Implications of Attribute Independence

It is important to discuss the difference between attribute independence in utility analysis and in engineering design, as these are distinct concepts with different implications. Attribute independence in engineering design refers to the relationship between design decisions and objectives in the design configuration as postulated by Suh [227]. Meeting the conditions of attribute independence in engineering design allows a designer to make independent improvements in one objective without any losses in the other objectives. However, meeting attribute independence conditions in utility analysis does not enable the designer in the same way at all. Attribute independence conditions in utility analysis like utility independence and preferential independence exist only in the relationships between preferences over each objective. Meeting these independence conditions simply enables a decision maker to aggregate their single attribute utility functions using the standard forms in Eqns. 51 - 53. Thurston (Ref. [236]) indicates that if independence conditions in utility analysis are not met, it does not imply that utility analysis theory is invalid. Instead it simply

means that the standard forms in Eqns. 51 - 53 cannot be assumed and therefore the assessment of the multiattribute utility function is far more difficult. In fact Thurston [236] states that "The difficulty is the combinatorial explosion of required preference statements, and the complexity of the resulting functional form." The additional preference questions must be asked because the preference decisions and degree of risk aversion between the attributes changes with respect to one another. In these cases assuming a standard multiattribute utility form would be invalid and a misrepresentation of the decision makers utility.

Cooke (Ref. [43]) claims that it is difficult to bring rational methods to bear on real world problems because of the poor assumptions used in decision analysis and the wide spread use of flawed decision making tools. He contends that the assumption of independence conditions on preferences between attributes by using standard forms of MAUT (Eqns. 51 - 53) without verification is a common problem. He proposes the following example to illustrate: "The following preference pattern is eminently reasonable, yet inconsistent with the MAUT axioms:

a. If unemployment is low and pollution is high, Prefer: Close a dirty factory, to Keep dirty factory open

b. If unemployment is high and pollution is low, Prefer: Keep the dirty factory open to Close the dirty factory."

He argues that MAUT assumes the preference relationship between criteria is constant across the range of attributes. However, if a decision maker were asked, "If a policy A raised pollution by X but decreased unemployment by Y relative to policy B, would you choose A or B? The above example shows that the rate at which a subject trades off may depend on values of pollution and unemployment for policy B." He concludes from this that there are many scenarios where independence conditions for utility analysis will not hold and MAUT should not be used without verification, particularly when complex systems and tradeoffs are involved.

This review of MAUT brings to light that it is not suitable to assume the standard MAUT forms (Eqns. 51 - 53) for the future aircraft technology selection problem which certainly involves complex tradeoffs between design attributes. Then the real challenge lies in assessing the multiattribute utility function for a decision maker without assuming the independence conditions between the attributes. A simple solution to this challenge will be demonstrated for the two attribute utility functions and then a more complex and robust method will be introduced for the three attribute utility function.

5.4.3 Research Question 4

This leads to the final research question which asks how the decision maker's utility function can be identified in a valid and axiomatic manner so that Eqn. 50 can be used to find the expected utility of technology solutions in a multiobjective space under uncertainty.

Research Question 4

How can the multiattribute utility function for a decision maker be assessed in the aircraft technology selection problem without assuming the restrictive conditions of attribute preference independence in MAUT?

Postulate 4

A multiattribute utility function can be fit using a surrogate model to known utility points in the attribute objective space without making any independence assumptions between the attributes.

This research question will not be tested with a contingent statement. As this question is not prone to a formally testable hypothesis, the answer for Research

Question 4 is formulated as a postulate that will be demonstrated. The multiattribute probability distributions will have to be obtained and combined with the multiattribute utility function in order to calculate the multiattribute expected utility in Eqn. 50.

5.5 Two Attribute Utility

5.5.1 Two Attribute Utility Formulation

The aircraft technology selection problem with two attribute utility theory is similar in formulation to the single attribute process, except that an additional attribute is present. This has implications to both the probability distribution part of the problem and utility function part. On the probability distribution part, the joint probability distribution over both attributes must be considered and used to calculate joint probabilities of two attributes taking on distinct values at the same time. The more challenging task is the formulation of the multiattribute utility function without using the MAUT standard forms (Eqns. 51 - 53) that are invalid for this problem.

5.5.2 Two Attribute Utility Implementation

The same three notional technology packages from the single attribute utility implementation are used in the two attribute case. The first attribute is obviously the %FB reduction over the baseline. The second attribute of interest in the aircraft technology selection problem is noise margin, measured in decibels, over the Stage IV regulatory limit [35, 203]. Higher noise margin (NM) values are more desirable for this attribute as they indicate a quieter aircraft. The %FB reduction uncertainty distributions are the same as the single attribute case shown in Fig. 53. The three selected technology packages correspond to unique portfolios of technology combinations that achieve low %FB reduction and high NM (Technology Package 1), high %FB reduction and low NM (Technology Package 2), and medium %FB reduction and medium NM (Technology Package 3) over the baseline aircraft. The NM uncertainty distributions for

the same three technology packages as the single attribute case are shown in Fig. 56.

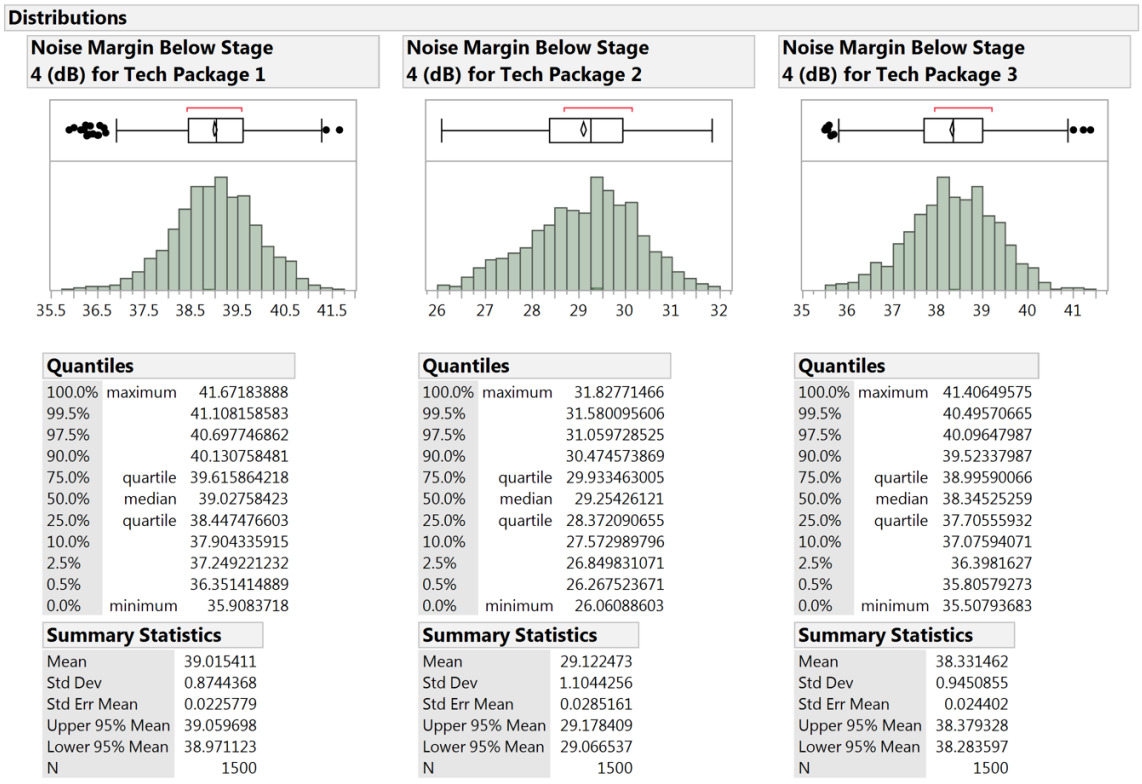

Figure 56: Noise Margin Below Stage 4 (dB) for Technology Packages 1, 2, and 3

The histogram data in Fig. 56 must be combined with the data in the histograms shown in Fig. 53 to compute joint probabilities of pairwise outcomes across both attributes. Combining the two sets of histogram data in Matlab creates a joint probability grid as shown in Figs. 57, 58, 59 for technology packages 1, 2, and 3 respectively. Normalizing the vertical bars on the grid by the total number of points means that every bar on the grid represents a joint probability value over the interval formed by each square. A similar process to the single attribute case is followed to convert the continuous intervals into discrete outcomes whose probability corresponds to the height of the bar above a given square. The midpoint of each square is identified using outcome values on each attribute, essentially assigning two coordinates to each square interval. That coordinate pair is a unique outcome whose probability of occurring is taken from the bar above it. The sum of all the vertical probability bars

in each technology package lottery is one.

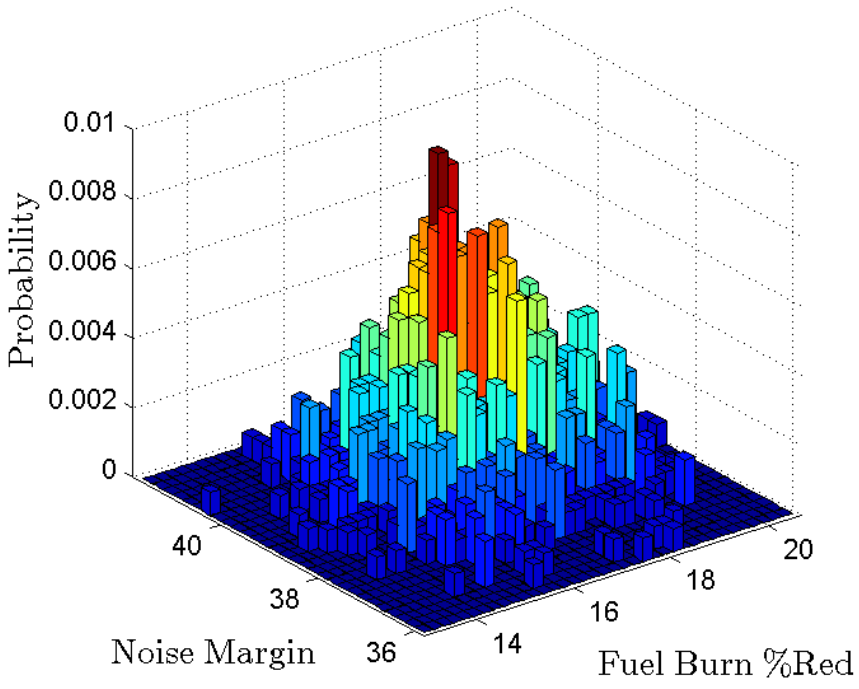

Figure 57: Joint probability grid of NM and %FB Red attributes for Technology Package 1

It is useful to visualize these individual lotteries and their associated probabilities in the same graph to see how they relate to one another and where they exist in the two attribute objective space. This is shown in Fig. 60.

The vertical bars in Fig. 60 give an indication of where the highest probability outcomes will occur in each two attribute lottery. The highest bars in each lottery (all colored dark red) have the same probability value (0.008 in this case) even though technology package 1 may appear higher due to the projection created by the plotting software. This fulfills the role of the technologist by providing the two attribute expected utility formulation with a set of outcomes and probability values for each of those outcomes.

The second part of the problem is to obtain the decision maker's two attribute utility function in order to evaluate utilities for all the outcomes in the two attribute

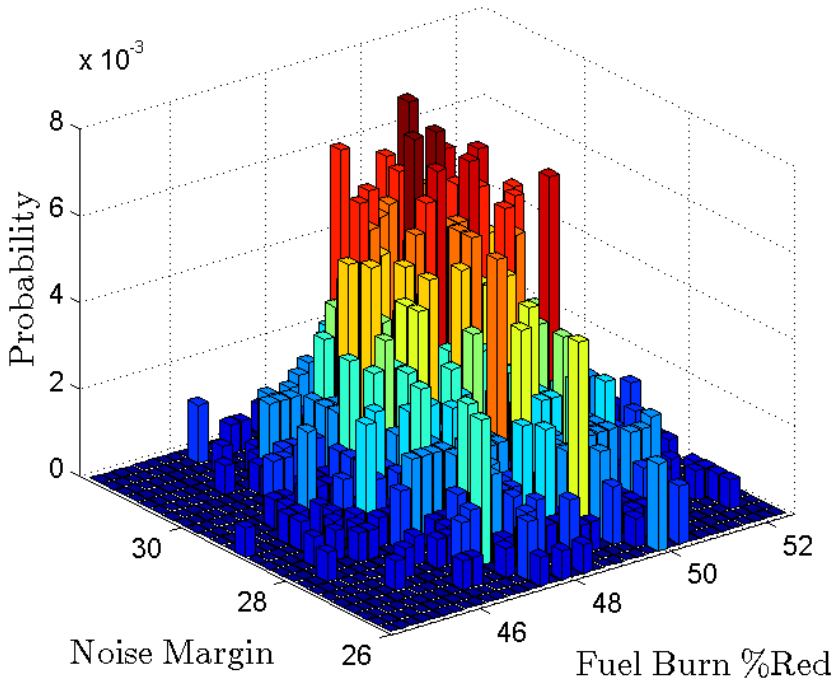

Figure 58: Joint probability grid of NM and %FB Red attributes for Technology Package 2

lottery. In the single attribute case standard functional forms (Eqns. 45-47) were available reflecting various risk attitudes of the decision maker. A risk neutral form (Eqn. 47) was applied for clarity and tractability. Since the standard MAUT functional forms cannot be used here, a simple approach is to leverage known information about the utility values over the two attribute objective space. This information is that the utility is equal to zero at the two attribute coordinate corresponding to (0 %FB red, 0 NM) and that utility equals one at the two attribute coordinate corresponding to (60 %FB red, 50 NM) the upper end of both attributes. The maximum values are extended compared to the single attribute case in order to accommodate all possible technology packages on the Pareto frontier. Using these two fixed points and assuming the decision maker has a risk neutral attitude, a linear interpolation between these points can be used to assess any utility for any outcome in between these two end points. This method makes no assumptions about the independence

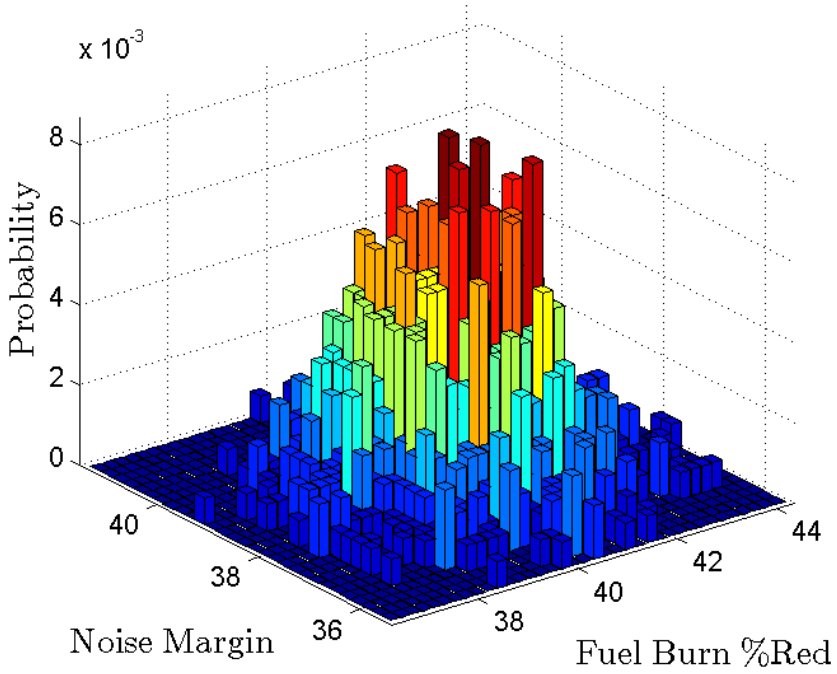

Figure 59: Joint probability grid of NM and %FB Red attributes for Technology Package 3

conditions between the attributes and provides a rapid way to assess utility of the outcomes in the three technology package lotteries for a risk neutral decision maker. The linear interpolated two attribute utility surface for the risk neutral decision maker is shown in Fig. 61.

The linear interpolation method of obtaining the utility function assumes the decision maker is risk neutral as seen in Fig. 61. Another strategy that avoids this assumption is created. The basic idea is to leverage on known utility points inside the space that are strategically chosen and some additional points on the boundaries of the space to form the basis for fitting a model to the underlying utility function. A response surface equation (Ref. [153]) is chosen to represent the multiattribute utility function due to their flexibility and ease of implementation.

Similar to the single attribute utility function elicitation, the process begins by setting the minimum and maximum utility points in the space which are known to

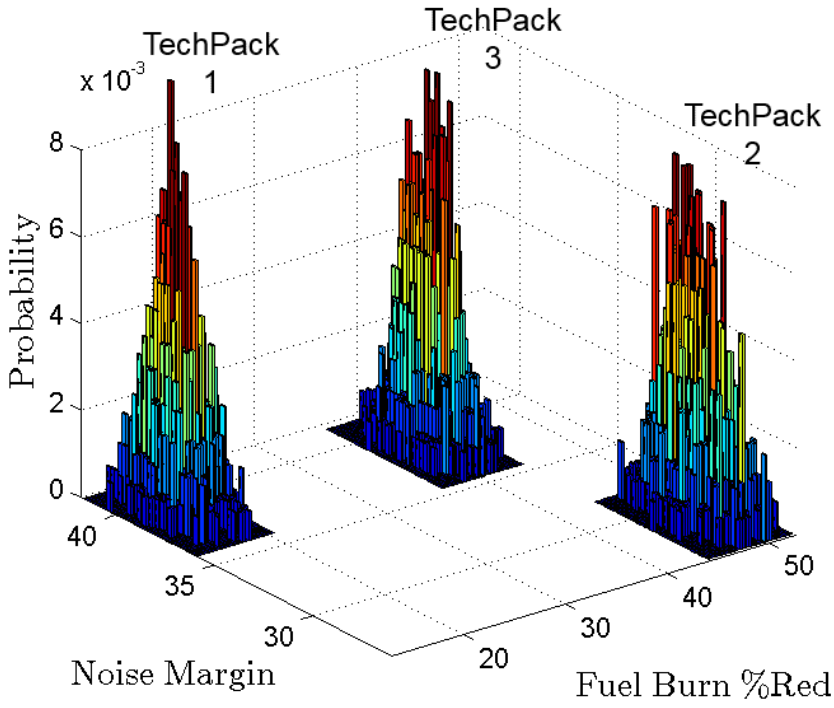

Figure 60: Joint probability grid of NM and %FB Red attributes for all three technology package lotteries

the decision maker. Utility is zero at the origin of the space where the (%FB, NM) coordinates are equal to (0,0). The utility is 1 at the diagonally opposite corner of the cube where the (%FB, NM) coordinates are equal to (60,50). These two utility 0 and 1 points are joined by an imaginary diagonal line through the multiattribute space in Fig. 62.

Recall that the certainty equivalent at utility equals 0.5 was assessed on a 50-50 lottery between the minimum and maximum utility points. This is given in Eqn. 42 for a single attribute and is extended in Eqn. 54 for two attributes.

$$u(x_{0.5}, y_{0.5}) = 0.5 * u(x^*, y^*) + 0.5 * u(x^0, y^0) \tag{54}$$

By Eqn. 54 the certainty equivalent point in this space can be identified for a given decision maker. This point is denoted as $CE_{0.5}$ and is found to be at the coordinate

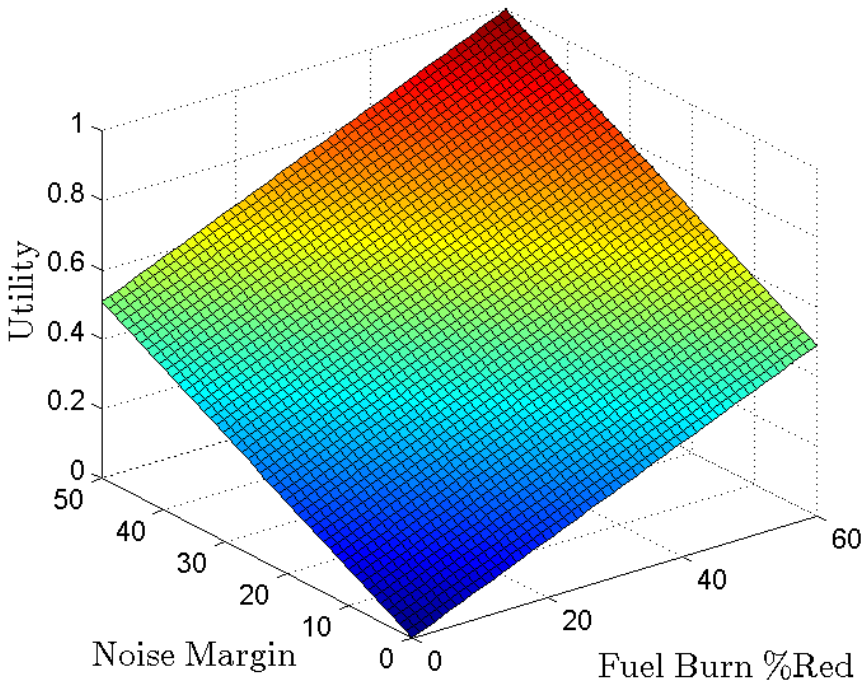

Figure 61: Two attribute linear interpolated utility function surface of a risk neutral decision maker

point (%FB, NM) $\rightarrow$ (22.5, 17.5) for a real decision maker familiar with the aircraft technology selection problem and the two attribute objective space. The $CE_{0.5}$ is added to the two attribute objective space as a known utility point in Fig. 63 (blue dot).

There are two corner points and one center point for which utility values have been assigned. The $CE_{0.5}$ center point is now leveraged to encode another point near the boundary of the two attribute objective space, that also has utility equals 0.5. In order to have equal utility the decision maker must be indifferent between the new point and the $CE_{0.5}$ center point. A general strategy has been created in this work to identify such a point. Perform a projection to a boundary of the space by zeroing one attribute, and then moving in the direction of most rapid improvement for the other attribute, while asking the decision maker indifference questions about points along this path to identify a point of equal utility. This strategy maintains positioning

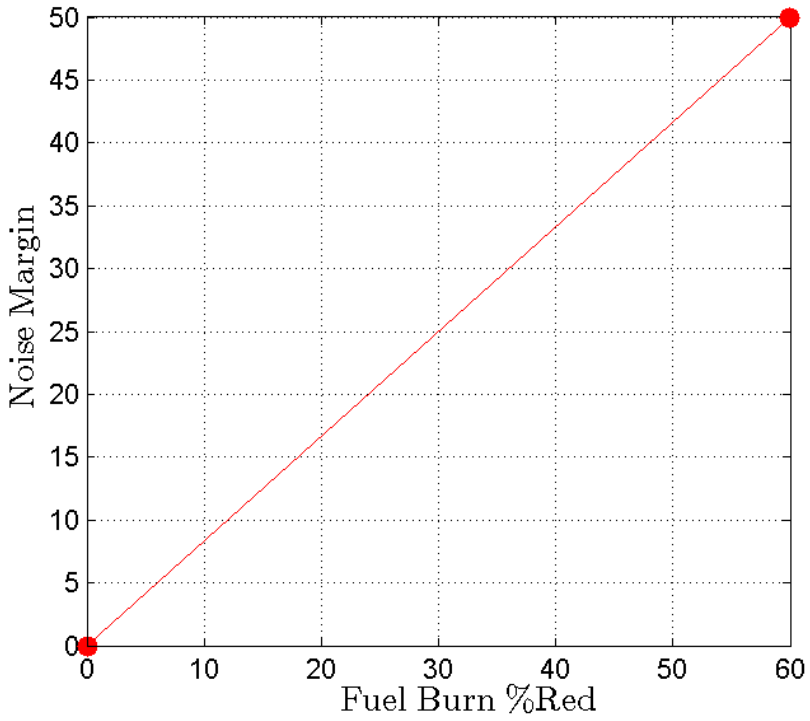

Figure 62: Two attribute objective space with utility 0 and 1 points identified and joined by diagonal line

along the boundary of the objective space and rapidly elicits a point that is useful for fitting a response surface model. This is demonstrated by starting out with the blue $CE_{0.5}$ center point whose coordinates are (%FB, NM) $\rightarrow$ (22.5, 17.5) and performing a projection to the NM axis by zeroing out the %FB attribute. This is shown in Fig. 64 (blue arrow).

At this new green point (%FB, NM) $\rightarrow$ (0, 17.5), query the decision maker if they are indifferent between choosing the green point or the blue $CE_{0.5}$ center point. The answer should obviously favor the blue $CE_{0.5}$ center point, so improve the green point by moving in the direction of greatest improvement along this axis (keep %FB=0). The strategy from single attribute utility encoding of certainty equivalents is borrowed upon by setting the current point as the new minimum and the corner point of the objective space in the direction of greatest improvement as the new maximum, and bisecting the distance in between to arrive at the next point where the decision

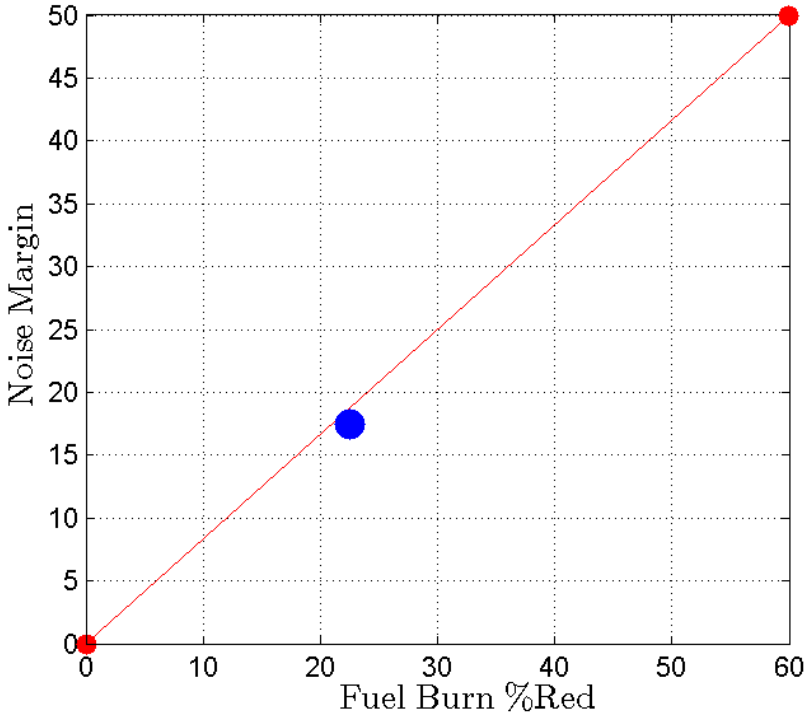

Figure 63: Two attribute objective space with blue dot for $CE_{0.5}$

maker is queried. This kind of optimal path movement is also found in numerical optimization techniques (Ref. [241]) like golden section rule and the bisection method. These concepts are shown in Fig. 65 where the blue dashed line is the direction of greatest improvement along this axis of the objective space and the green point represent the bisected point between the corner and the original 2D projection point.

The coordinates of the green point are now (%FB, NM) $\rightarrow$ (0, 34), and here the decision maker is once again asked if they are indifferent between this point and the blue $CE_{0.5}$ center point. If they are indifferent, then this green point represents the utility equals 0.5 point on this boundary of the two attribute space. If they prefer the green point to the blue $CE_{0.5}$ center point, then reverse direction and perform another bisection that reduces their utility for the green point until an indifference point is located on this boundary. If they still prefer the blue $CE_{0.5}$ center point over the green point, then there are two options. The analyst can continue in the

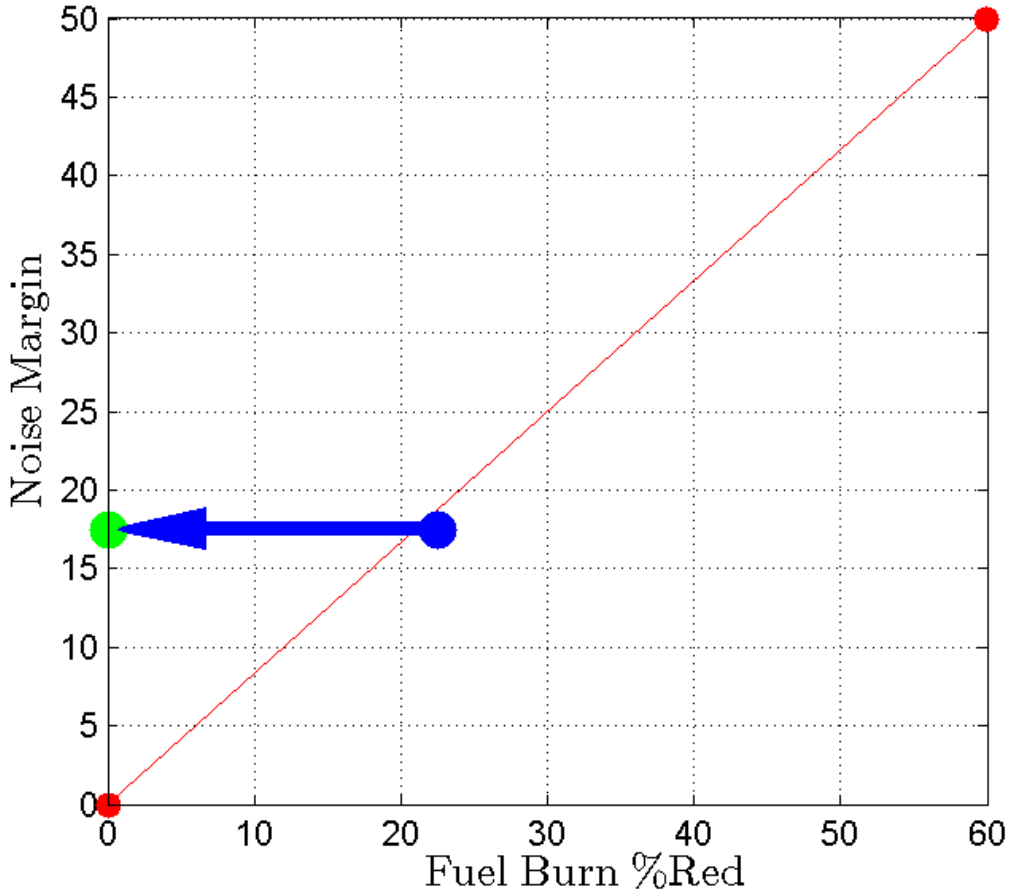

Figure 64: Projection to NM axis by zeroing %FB reduction attribute

direction of greatest improvement and perform another bisection that increases the decision maker's utility for the green point. However, if there is no point along this path for which the decision maker will feel indifferent, the second option is jump directly to the corner point and query the decision maker there as shown in Fig. 66 (blue arrow).

The coordinates of the green point are now (%FB, NM) $\rightarrow$ (0, 50), and here the decision maker is once again asked if they are indifferent between this point and the blue $CE_{0.5}$ center point. If they are indifferent then this green point represents the utility equals 0.5 point at this corner of the two attribute space. If they prefer the green point to the blue $CE_{0.5}$ center point, then reverse direction and perform another

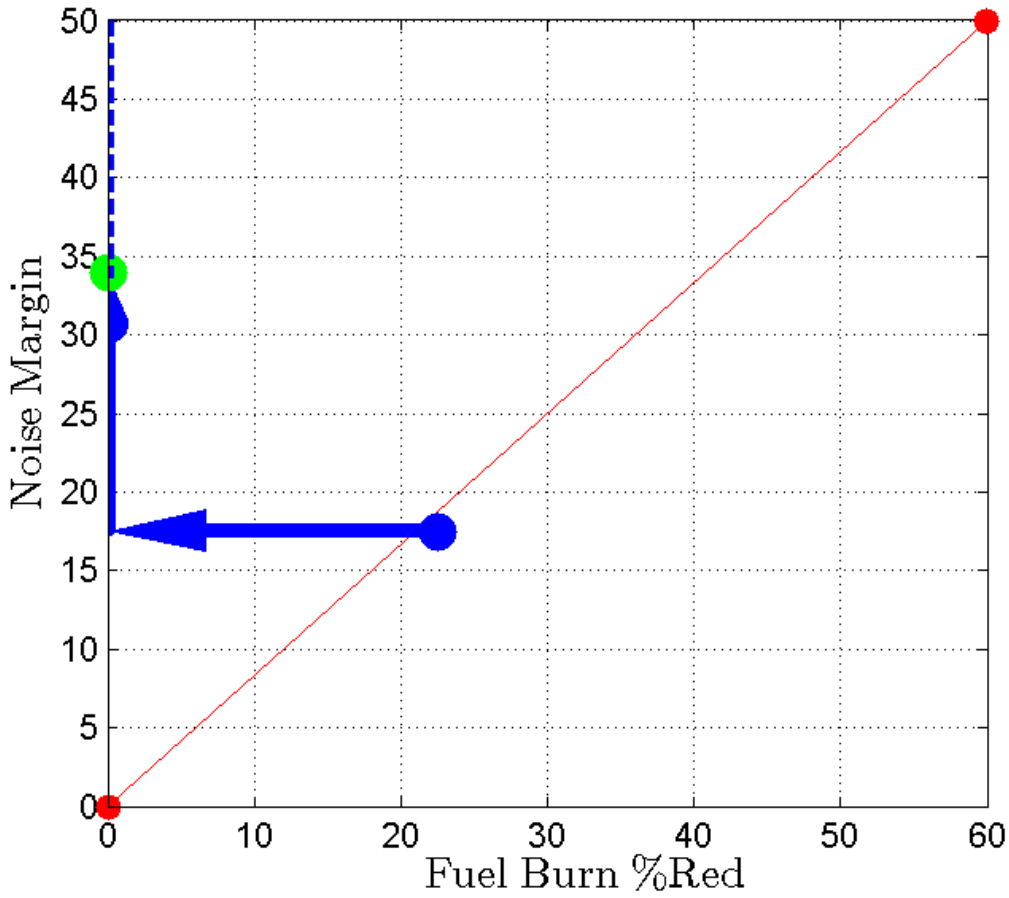

Figure 65: Direction of most rapid improvement along the NM axis and the bisected query point (green)

bisection that reduces their utility for the green point until an indifference point is located on this axis. If they still prefer the blue $CE_{0.5}$ center point over the green point, then the only remaining direction of improvement is along the %FB attribute. Perform a bisection along the edge of the cube where NM is fixed at its maximum value, and %FB is increasing until a point of indifference is located for the decision maker. This new direction of improvement along the upper edge of the two-attribute space is shown in Fig. 66 by the blue dashed line. The green point represents a new bisected point between the corner and the maximum %FB level of the blue $CE_{0.5}$ center point.

The coordinates of the green point are now (%FB, NM) $\rightarrow$ (11, 50), and here the

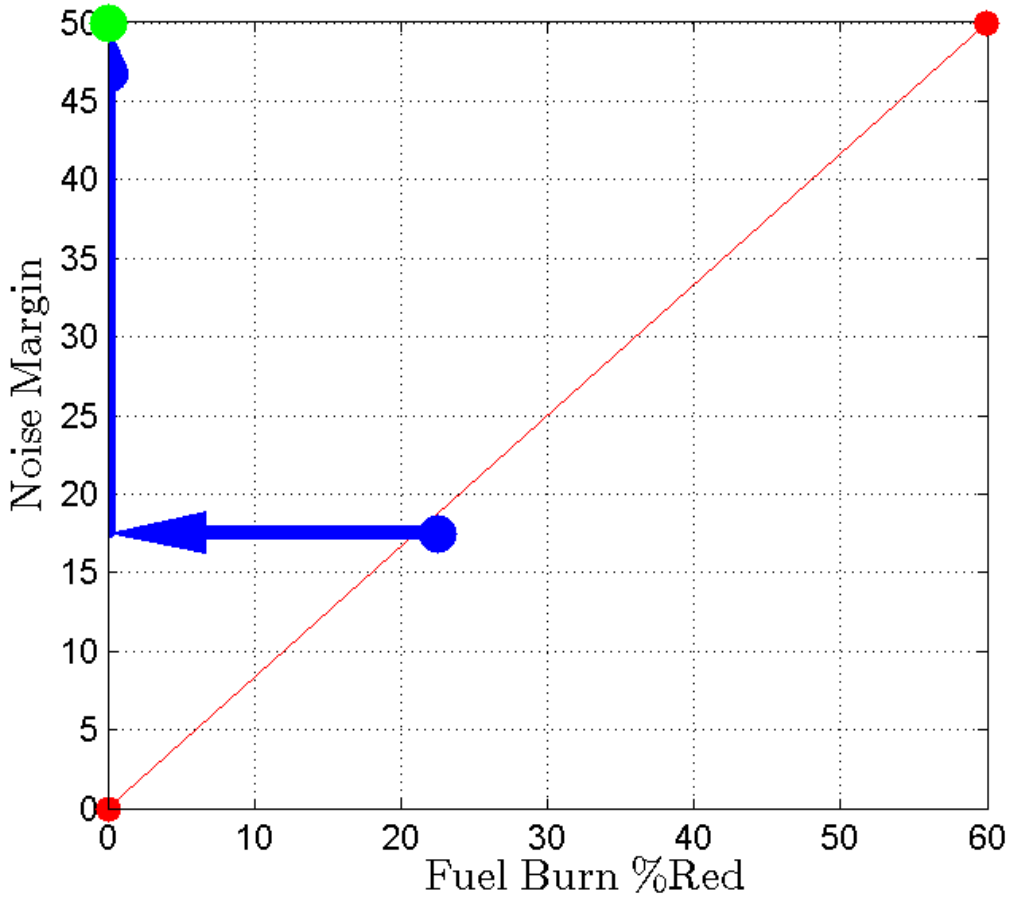

Figure 66: Advance to corner point along direction of most rapid improvement along NM axis

decision maker is once again asked if they are indifferent between this point and the blue $CE_{0.5}$ center point. If they are indifferent then this green point represents the utility equals 0.5 point along this edge of the two attribute space. If they prefer the green point to the blue $CE_{0.5}$ center point, then reverse direction and perform a bisection that reduces their utility for the green point until an indifference point is located on this edge. If they still prefer the blue $CE_{0.5}$ center point over the green point, then perform another bisection that increases their utility for the green point until an indifference point is located on this edge. Once the indifference point is located, record this coordinate as the $\%FB_{u=0.5}$ indifference point because it was located by first setting the %FB attribute to zero. A similar procedure is then repeated to identify

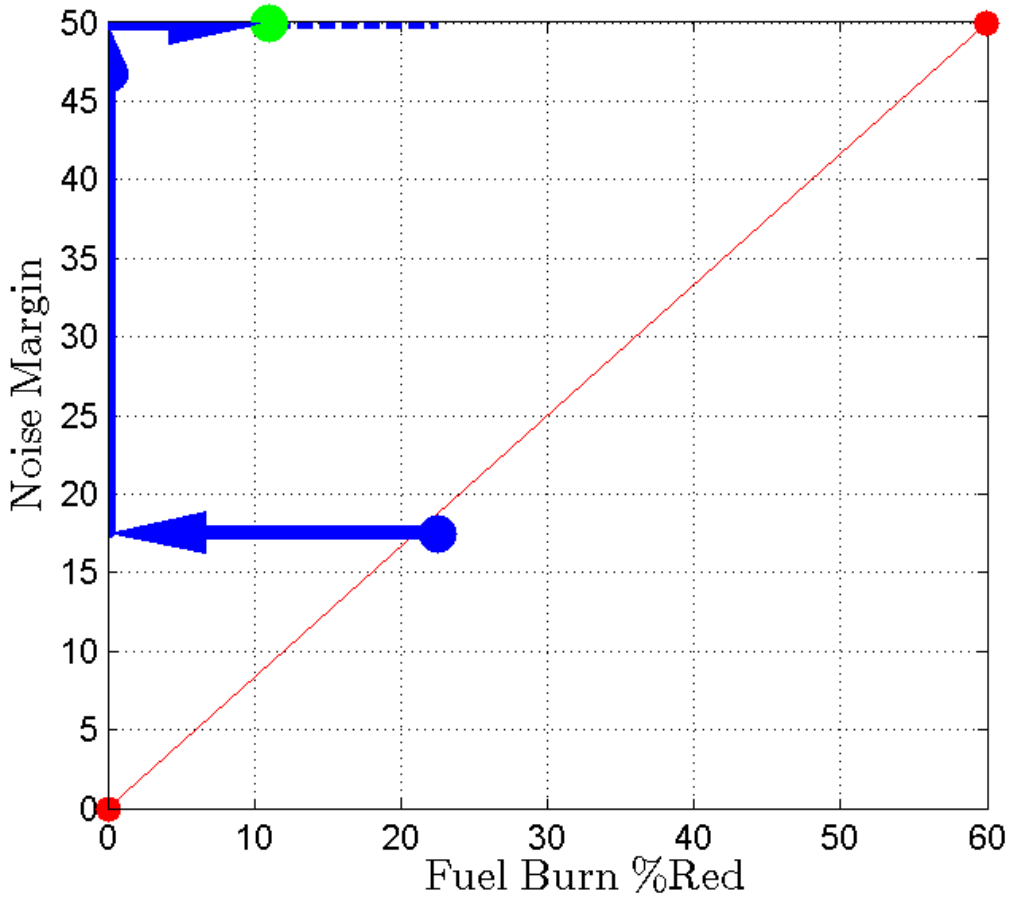

Figure 67: Advance to bisected point along the edge of two objective space in the direction of %FB improvement

the $NM_{u=0.5}$ indifference point. The procedure for obtaining this indifference point begins at the blue $CE_{0.5}$ center point, the only difference is that NM will be set to zero to find the $NM_{u=0.5}$ indifference point. This procedure is executed with the real decision maker interviewed to obtain the blue $CE_{0.5}$ center point earlier. The results of the interview process are recorded in Table 24.

The blue $CE_{0.5}$ center point and the two indifference points ($\%FB_{u=0.5}$ and $NM_{u=0.5}$) are shown in Fig. 68.

These points can be used to approximate a $u(\%FB, NM) = 0.5$ iso-utility contour by linearly joining the points. This is shown in Fig. 69.

The $u(\%FB, NM) = 0.5$ iso-utility contour is created by eliciting a center point

Table 24: Interview results of decision maker's 5 elicited data points

Description	%FB attribute coordinate	NM attribute coordinate	Utility value
Minimum utility point (origin)	0	0	0
Maximum utility point	1	1	1
$CE_{0.5}$ center point	22.5	17.5	0.5
$\%FB_{u=0.5}$ indifference point	20	50	0.5
$NM_{u=0.5}$ indifference point	30	0	0.5

and two edge points from the decision maker. As Table 24 shows, there are now five known utility points in the three attribute objective space. Currently two corner points, two edge points, and a center point are known in the three attribute objective space. Without additional utility points, the response surface fit would be poor.

When assessing single attribute utility functions, the general procedure is to set a minimum and a maximum utility point at utility equals 0 and 1 respectively, identify three different certainty equivalent (using Eqns 42-44.) points along the utility function, and finally fit a known utility functional form to those points. Eqns. 43-44 help to identify two extra utility values along the single attribute outcomes. This concept is extended to multiple attributes to identify additional utility data points in the two attribute objective space. Eqns. 55-56 can be used to identify two more certainty equivalent points along the red diagonal line that represents the backbone of the underlying multiattribute utility function.

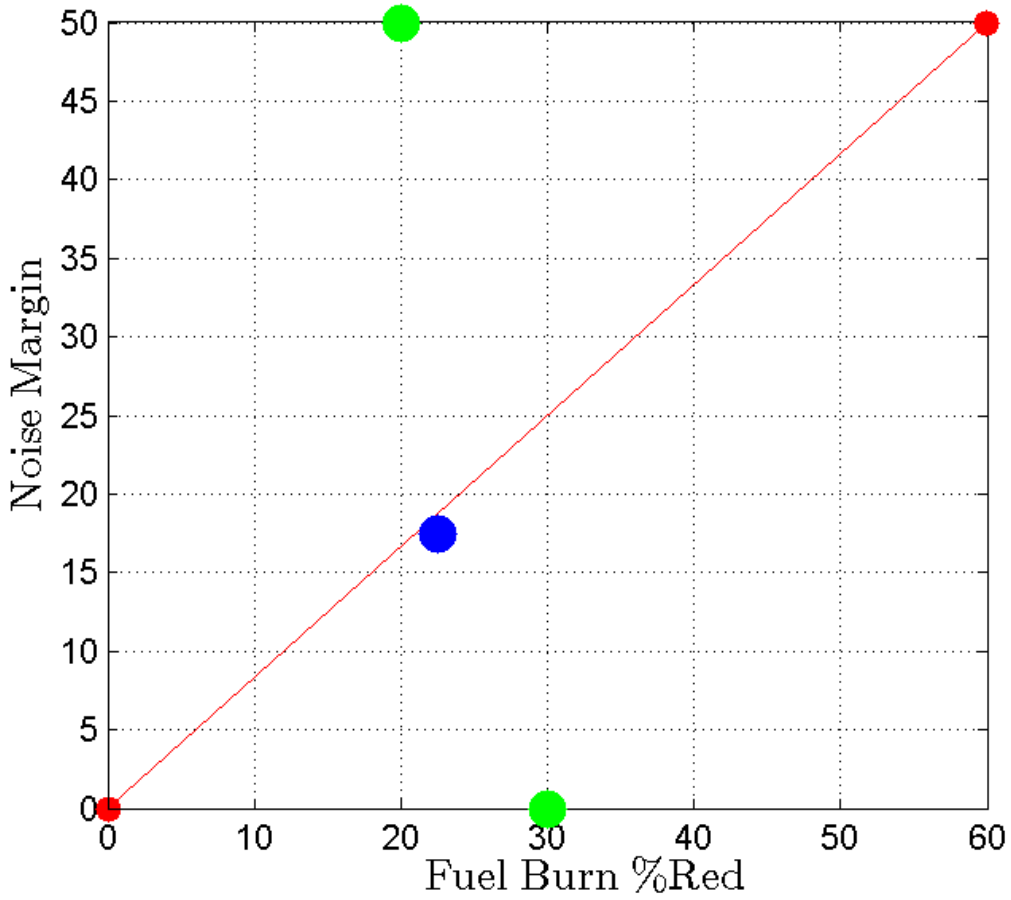

Figure 68: The blue $CE_{0.5}$ center point and two green indifference points for $\%FB_{u=0.5}$ and $NM_{u=0.5}$

$$u(x_{0.25}, y_{0.25}) = 0.5 * u(x_{0.5}, y_{0.5}) + 0.5 * u(x^0, y^0) \tag{55}$$

$$u(x_{0.75}, y_{0.75}) = 0.5 * u(x^*, y^*) + 0.5 * u(x_{0.5}, y_{0.5}) \tag{56}$$

Querying the decision maker and using the $CE_{0.5}$ certainty equivalent as an intermediate minimum/maximum as shown in Eqns. 55-56 identifies the $CE_{0.25}$ and $CE_{0.75}$ certainty equivalent points. These points are depicted in Fig. 70 and reported in Table 25.

The blue points in Fig. 70 are the $CE_{0.5}$, $CE_{0.25}$, and $CE_{0.75}$ certainty equivalent

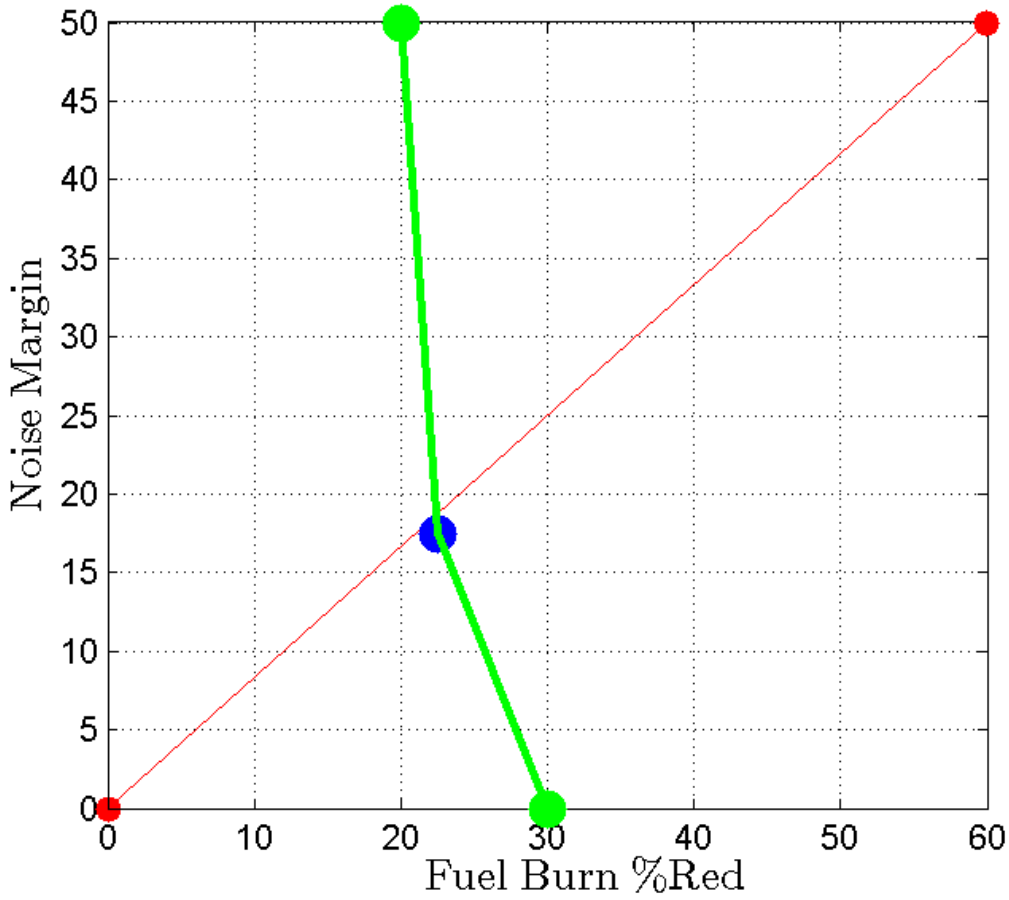

Figure 69: $u(\%FB, NM) = 0.5$ iso-utility contour of underlying multiattribute utility function

points. The two indifference points $\%FB_{u=0.5}$ and $NM_{u=0.5}$ were elicited using the procedure described earlier to identify points of indifference relative to the $CE_{0.5}$ certainty equivalent point. The same procedure can be repeated for the $CE_{0.25}$, and $CE_{0.75}$ certainty equivalent points to identify the the two indifference points $\%FB_{u=0.25}$ and $NM_{u=0.25}$ associated with the $CE_{0.25}$ certainty equivalent and the two indifference points $\%FB_{u=0.75}$ and $NM_{u=0.75}$ associated with the $CE_{0.75}$ certainty equivalent. The decision maker's responses for these interview questions are given in Table 25.

The decision maker's $CE_{0.25}$ certainty equivalent and two indifference points ($\%FB_{u=0.25}$ and $NM_{u=0.25}$) can be used to approximate a $u(\%FB, NM) = 0.25$ iso-utility contour.

Table 25: Interview results of decision maker's 11 elicited data points

Description	%FB attribute coordinate	NM attribute coordinate	Utility value
Minimum utility point (origin)	0	0	0
Maximum utility point	1	1	1
$CE_{0.5}$ center point	22.5	17.5	0.5
$\%FB_{u=0.5}$ indifference point	20	50	0.5
$NM_{u=0.5}$ indifference point	30	0	0.5
$CE_{0.25}$ center point	6	5	0.25
$\%FB_{u=0.25}$ indifference point	2	17.5	0.25
$NM_{u=0.25}$ indifference point	22.5	2	0.25
$CE_{0.75}$ center point	35	30	0.75
$\%FB_{u=0.75}$ indifference point	30	50	0.75
$NM_{u=0.75}$ indifference point	60	17.5	0.75

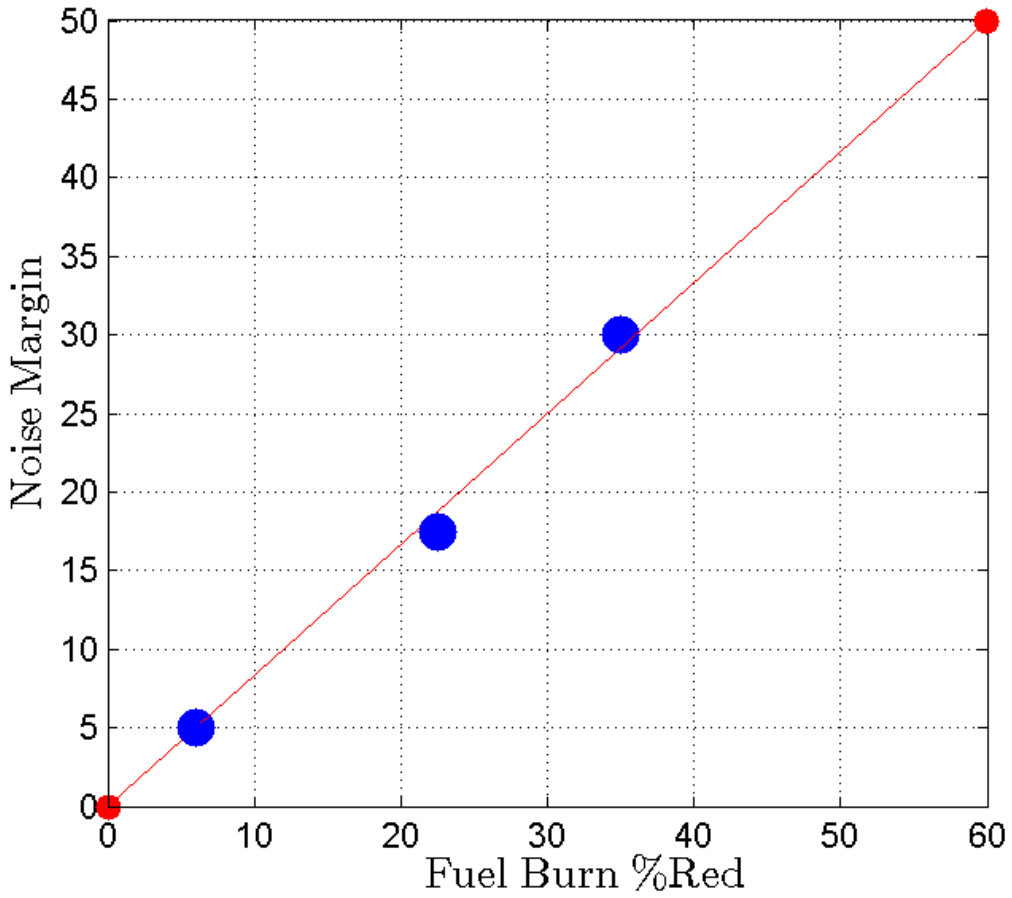

Figure 70: The $CE_{0.5}$, $CE_{0.25}$, and $CE_{0.75}$ certainty equivalent points

The same can be done with the $CE_{0.75}$ certainty equivalent its associated two indifference points ($\%FB_{u=0.75}$ and $NM_{u=0.75}$) to approximate the $u(\%FB, NM) = 0.75$ iso-utility contour. The contours are shown in Fig. 71.

The utility points reported in Table 25 represent 11 distinct data points in the two attribute objective space. These points are used to fit a response surface that approximates the decision maker's multiattribute utility function. A second order response surface equation was used to fit the data. This multiattribute utility function is shown in Fig. 72.

After obtaining the multiattribute utility function, consistency checks were performed with the decision maker to verify the elicited points and the fitted utility

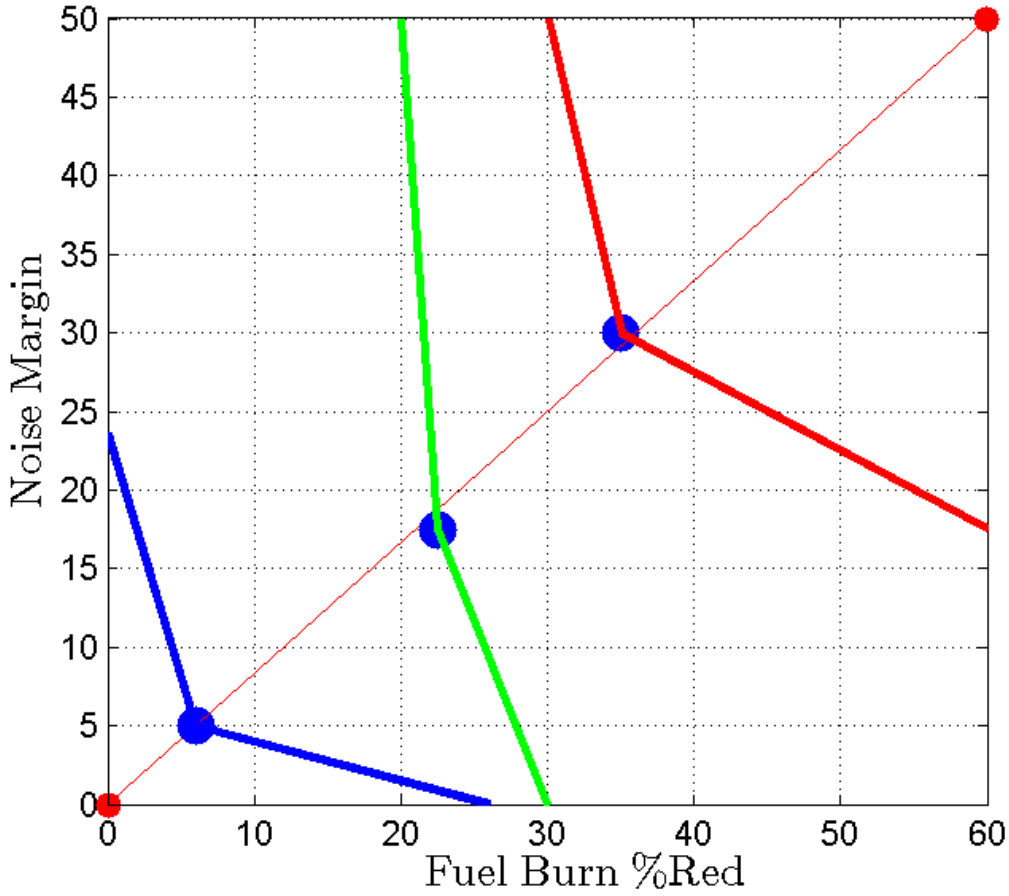

Figure 71: The $u(\%FB, NM) = 0.5$, $u(\%FB, NM) = 0.25$, $u(\%FB, NM) = 0.75$ iso-utility contours of underlying multiattribute utility function

function. The multiattribute utility function was found to match the decision maker's preferences and is used to calculate the expected utility of the three technology packages under consideration.

5.5.3 Multiattribute ENcoding of Utility (MENU) Method in Two Attributes

This process to elicit a decision maker's utility function is termed MENU, or the Multiattribute ENcoding of Utility method. It makes no assumptions about the independence conditions between the attributes and provides a structured and strategic method to elicit utility data from the decision maker. The MENU method does not

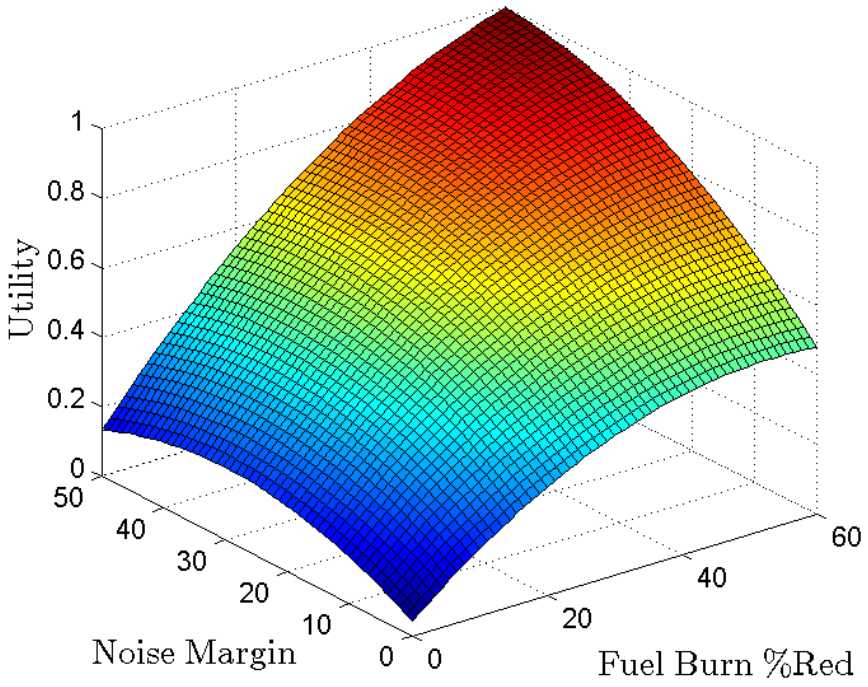

Figure 72: Multiattribute utility function surface elicited from a decision maker over the two objective space

limit the risk profile of the decision maker. Their risk attitudes arise organically through the elicitation of the certainty equivalents and indifference points. This procedure maintains the axiomatic principles of utility theory and does not rely on the presumed forms of MAUT which are not always applicable. This answers the last Research Question 4 which asked how the multiattribute utility function for a decision maker could be assessed without assuming the attribute independence conditions of MAUT. The MENU method demonstrates this by eliciting utility values directly from the decision maker in the two attribute objective space and using a response surface equation to represent the underlying multiattribute utility function. While effective for two attributes, this technique is shown to be extensible to three attributes later in this work.

Using the probability distributions over the outcomes of each technology package and the two different decision maker utility functions (linear interpolated in Fig. 61

and MENU assessed in Fig. 72), two different expected utilities for each lottery (technology package) can be found by Eqn. 57.

$$E(U(FB, NM)) = \sum_{i=1}^{n} p(FB_i, NM_i)u(FB_i, NM_i) \tag{57}$$

The exact value of the expected utility is equal to the double integral over the continuous probability distributions times their utilities, but in this numerical simulation a summation will be calculated over many small interval squares to approximate this integral. The intervals are the same ones used to approximate the probability distributions and are chosen such that the error in calculating the expected utility of the technology package lottery is less than 1%.

5.5.4 Two Attribute Utility Results

The product of the utility function and the probability distribution, or the utility scaled probabilities, provides a traceable way of quickly visualizing how a decision maker values each outcome. The summation of all of these products gives the expected utility of the lottery as stated in Eqn. 57. This will obviously change based on which utility function is used. The utility scaled probabilities for the linearly interpolated utility function (shown in Fig. 61) are visualized in Fig. 73.

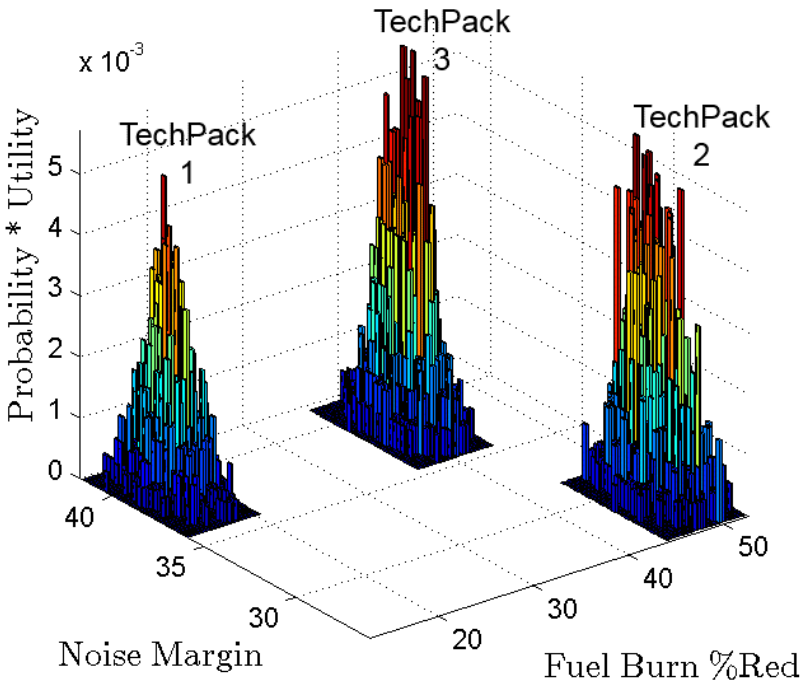

Figure 73: Utility scaled probabilities of technology packages 1, 2, and 3 for the linearly interpolated utility function over the two attribute objective space

The utility scaled probabilities for the utility function assessed using the MENU method (shown in Fig. 72) are visualized in Fig. 74.

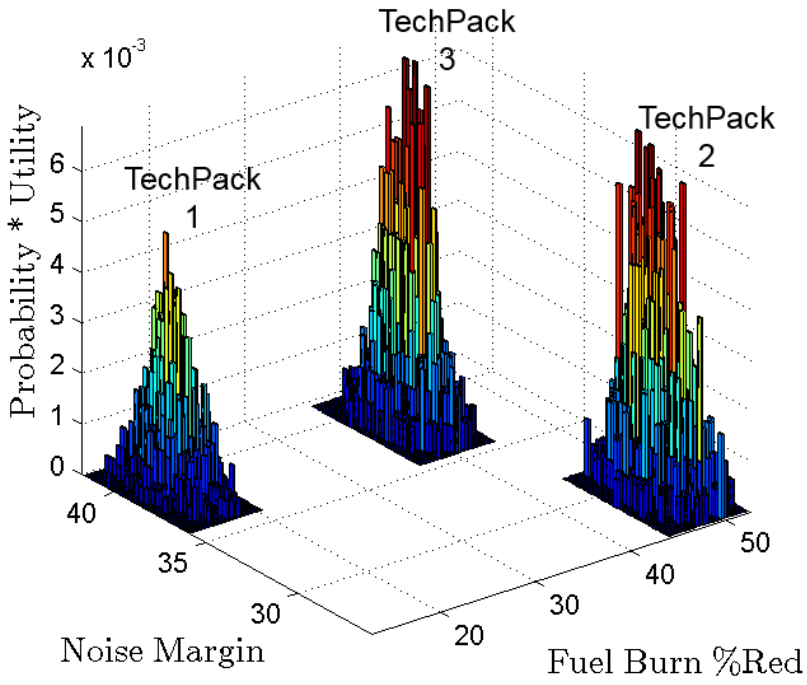

Figure 74: Utility scaled probabilities of technology packages 1, 2, and 3 for the MENU assessed utility function over the two attribute objective space

The MENU method captures the risk profile and attribute preferences of the decision maker. Incorporating these aspects into the utility function provides the expected utility framework with a better representation of the decision maker's values which will affect the ranking and selection process.

Fig. 73 and Fig. 74 provide traceability to the selection process and show why the outcomes of one lottery may be preferred over the outcomes of another, based on the utility function of the decision maker. In this way it is clear which technology package lottery is most preferred by the decision maker even before the summation in Eqn. 57 is performed to quantify the expected utility of each technology package lottery.

The results for the expected utility assessment for all three technology packages are summarized in Table 26.

Table 26 shows that the three technology packages under consideration can be rank

Table 26: Two Attribute Expected Utility Results

Technology Package	Package Description	Linear Interpolated Expected Utility	Linear Interpolated Ranking	MENU Assessed Expected Utility	MENU Assessed Ranking
Tech Package 1	Low %FB reduction and high Noise Margin	0.53	3	0.52	3
Tech Package 2	High %FB reduction and low Noise Margin	0.70	2	0.85	1
Tech Package 3	Med %FB reduction and med Noise Margin	0.72	1	0.83	2

ordered by their expected utilities. This ranking changes depending on the utility function used. For the linear interpolated utility function, the ranking is consistent with the probability distributions in Figs. 57, 58, 59 for technology packages 1, 2, and 3 respectively. The utility function equally gives more importance to higher values of %FB reduction and Noise Margin. However, the MENU assessed utility function captures the decision maker's preferences over the attributes and their risk profile and so its ranking change relative to the linear interpolated method. This decision maker has a preference for %FB reduction and so the MENU assessed utility function ranks Tech Package 2 (High %FB reduction and low Noise Margin) higher than Tech Package 3. This indicates the value of including decision maker preferences in the aircraft technology selection problem and highlights the two-attribute MENU method as a new technique for doing so. This also demonstrates how technology packages can be rank ordered in a logical, repeatable, axiomatic fashion that is not only consistent with the decision maker's preferences, but is also traceable back to the utility scaled probability distributions of each technology package lottery. This capability can be used to evaluate and axiomatically rank order all two attribute technology solutions on the Pareto frontier that were previously considered to be equal.

5.6 Three Attribute Utility

5.6.1 Three Attribute Utility Formulation

The aircraft technology selection problem with three attribute utility theory is similar in formulation to the two attribute process, except that an additional attribute is present. This has affects on both the probability distribution part of the problem and utility function portion. On the probability distribution part, the joint probability distribution over all three attributes must be considered and used to calculate joint probabilities of three attributes simultaneously taking on distinct values. The more challenging task is obviously the formulation of the multiattribute utility function

without using the MAUT standard forms (Eqns. 51 - 53) that are not useful for this problem.

5.6.2 Three Attribute Utility Implementation

The same three notional technology packages from the two attribute utility implementation are used in the three attribute case. The first and second attributes are %FB reduction over the baseline and noise margin, measured in decibels, over the Stage IV regulatory limit [35, 203]. The third attribute of interest in the aircraft technology selection problem is emissions reduction, measured as % Nitrogen Oxides (%NOx) reduction over the baseline aircraft. Higher (%NOx) reduction values are more desirable for this attribute as they indicate a less pollutant aircraft. The %FB reduction and noise margin uncertainty distributions are the same as the two attribute case shown in Figs. 53 and 56. The three selected technology packages correspond to unique portfolios of technology combinations that achieve low %FB reduction, high NM, and medium %NOx reduction (Technology Package 1); high %FB reduction, low NM, and high %NOx reduction (Technology Package 2); and medium %FB reduction, medium NM, and low %NOx reduction (Technology Package 3) over the baseline aircraft. The %NOx reduction uncertainty distributions for the same three technology packages as the two attribute case are shown in Fig. 75.

The histogram data in Fig. 75 must be combined with the data in the histograms shown in Figs. 53 and 56 to compute joint probabilities of outcomes across three attributes. Combining the three sets of histogram data in Matlab creates a joint probability cube. This large cube over the entire three attribute objective space is divided into smaller interval cubes. The density of points in each cube represents the likelihood that a three attribute lottery outcome corresponding to that interval cube will occur. Normalizing the smaller interval cubes by the total number of points means that every smaller interval cube contains a number of points that have been

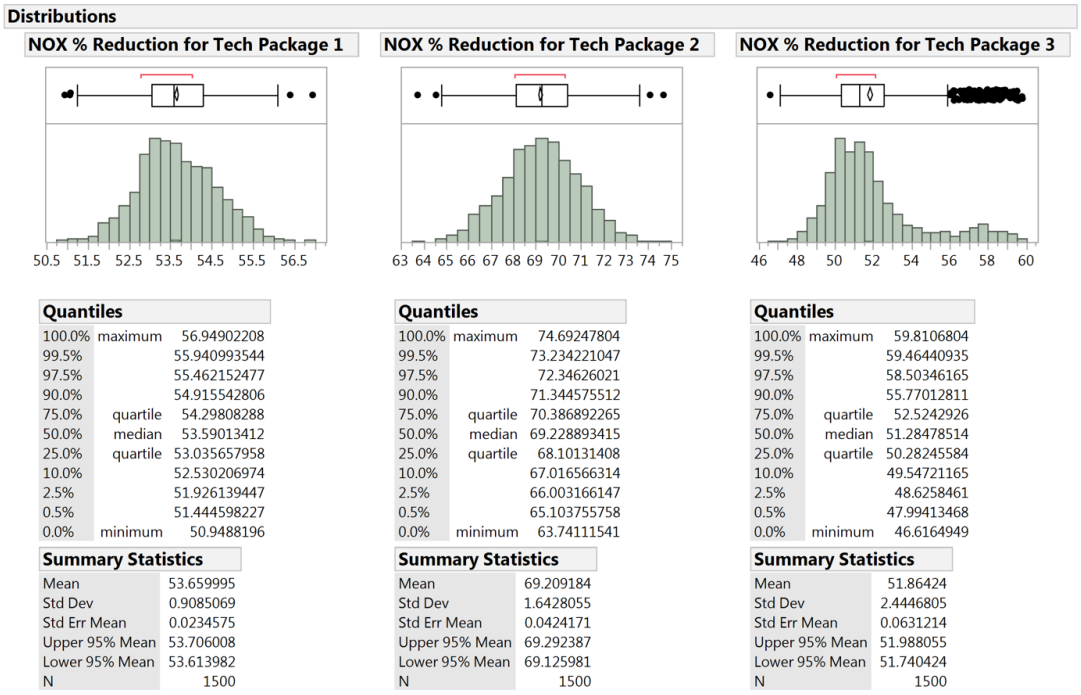

Figure 75: %NOx reduction over the baseline aircraft for Technology Packages 1, 2, and 3

normalized to yield the joint probability value over the interval formed by a given cube. A similar process to the two attribute case is followed to convert the continuous intervals into discrete outcomes whose probability corresponds to the density of points in each interval cube. The edge of each cube is identified using the outcome values on each attribute, essentially assigning three coordinates to each interval cube. That coordinate triple is a unique outcome whose probability of occurring is taken from the density of points in the interval cube. The sum of all the interval cubes is one. This fulfills the role of the technologist by supplying the three attribute expected utility formulation with a set of triple outcomes and probability values for each of those outcomes.

Due to the three dimensional nature of this application, the fourth dimension of probability density is harder to visualize. However normal contour ellipsoids can be used to gain an understanding of the spread of points in each technology package and view where each technology package exists in the objective space relative to one

another. This is shown with two views of the same three technology packages in Figs. 76 and 77.

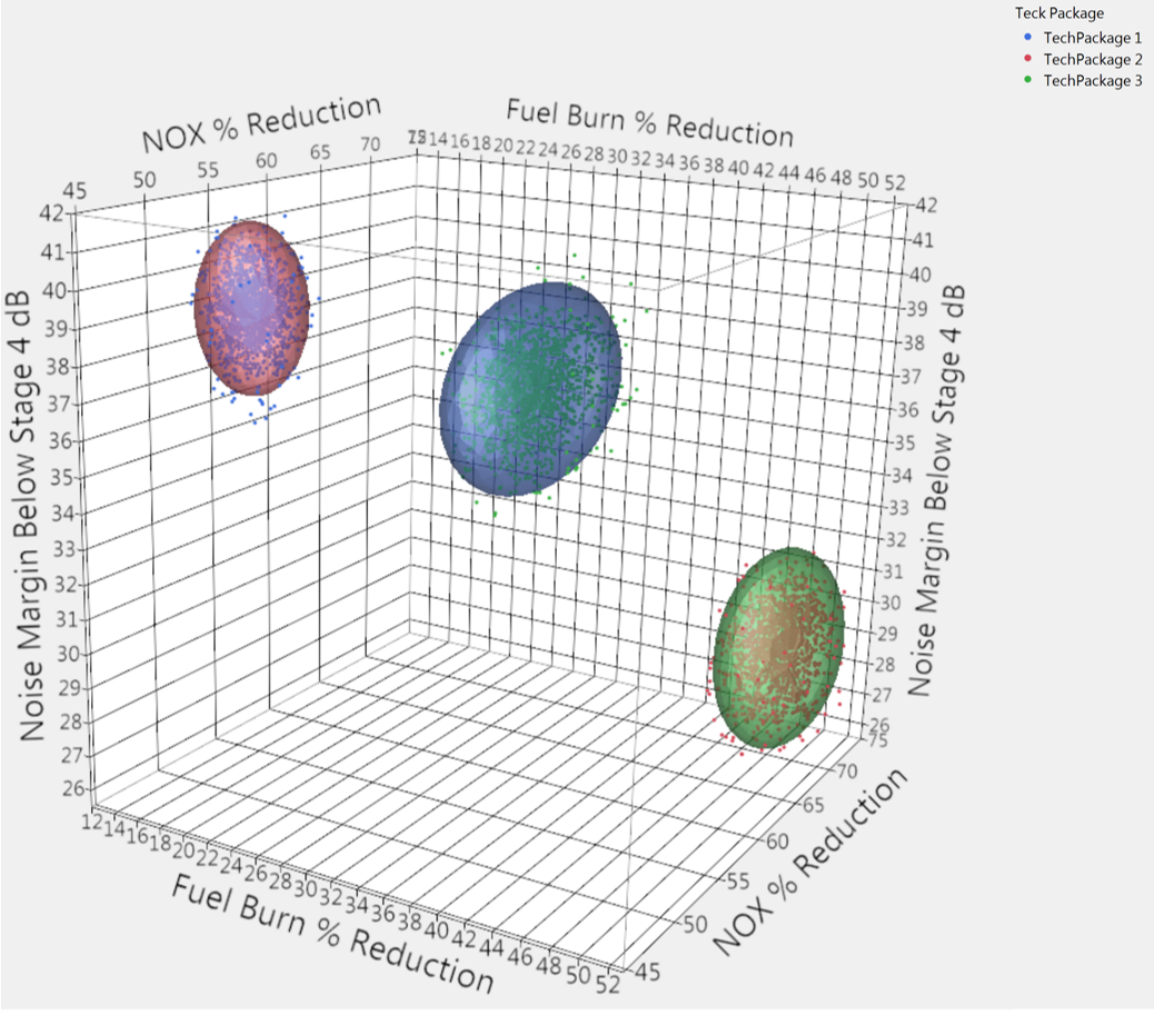

Figure 76: Normal contour ellipsoids for the joint distributions of %FB Red, NM, and %NOx Red attributes for all three technology packages, view 1

The second part of the problem is to obtain the decision maker's three attribute utility function in order to evaluate utilities for all the outcomes in the three attribute lottery. In the single attribute case standard functional forms (Eqns. 45-47) were available reflecting various risk attitudes of the decision maker. In the two attribute case a linear interpolation method was an option and the two-attribute MENU method was another. Due to the complexity added by the third attribute, MENU is the most suitable method but it must be extended to three attributes. Examining

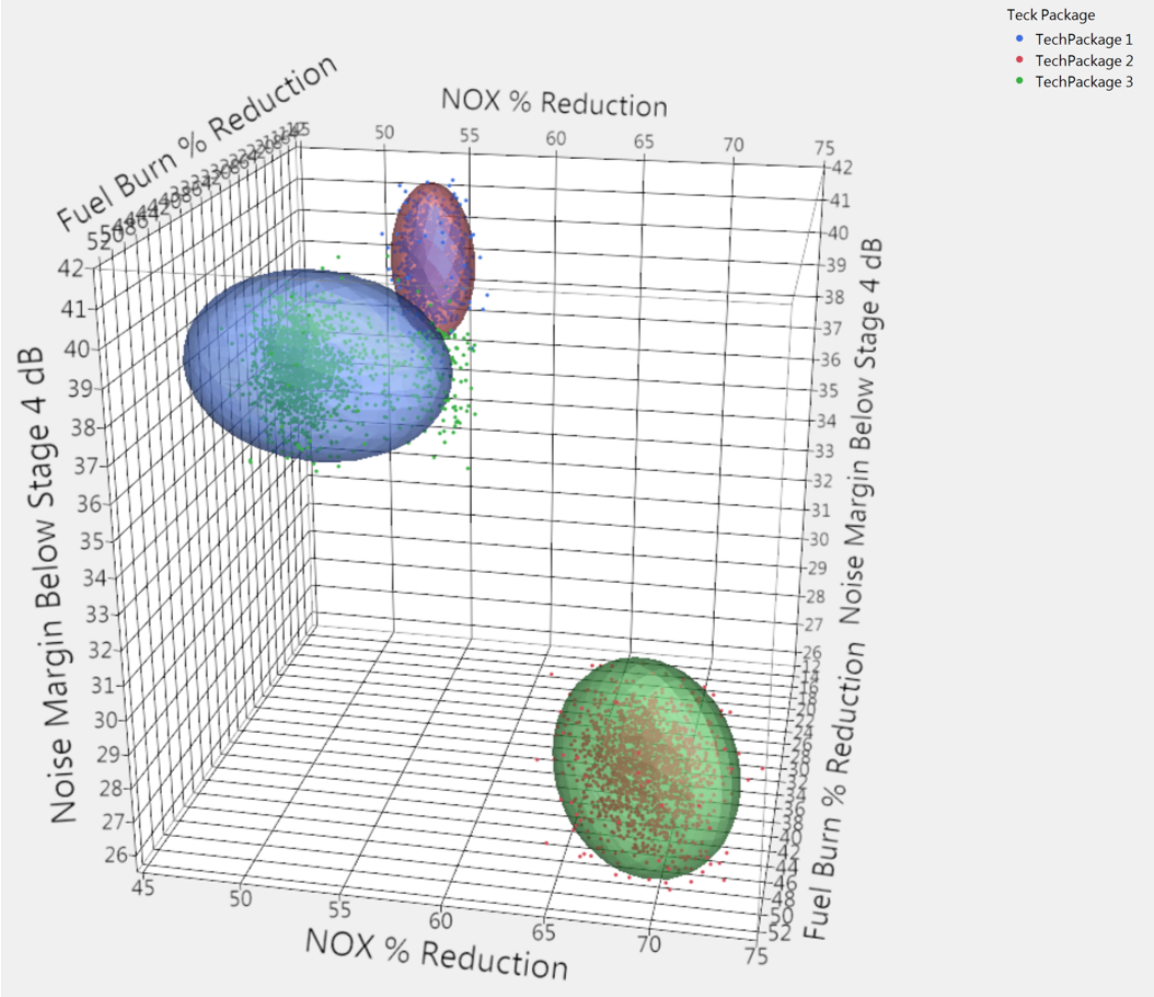

Figure 77: Normal contour ellipsoids for the joint distributions of %FB Red, NM, and %NOx Red attributes for all three technology packages, view 2

Figs. 76 and 77 shows that objective space is a cube, which contains an underlying function that can be quantified at points within the cube. The strategy is to leverage on some points inside the space that are strategically chosen (certainty equivalents) and some additional points on the boundaries of the space (indifference points), which form the basis for fitting a model to the underlying function. A response surface equation (Ref. [153]) is chosen to represent the multiattribute utility function due to their flexibility and ease of implementation. This can well approximate the utility function which is nominally already an approximation in the single attribute elicitation case. This process strategically extends this notion to three attributes, following the earlier

advice of Keeney and Raiffa [105] to adapt the utility assessment procedure to the context of the given problem.

The difficulty is in how to assess values of utility inside the three attribute cube. The simplest place to begin are the points where utility is equal to zero and one. Utility is zero at the origin of the cube where the (%FB, NM, %NOx) coordinates are equal to (0,0,0). The utility is 1 at the diagonally opposite corner of the cube where the (%FB, NM, %NOx) coordinates are equal to (60,50,95). These two utility 0 and 1 points are joined by an imaginary diagonal line through the three attribute space in Fig. 78.

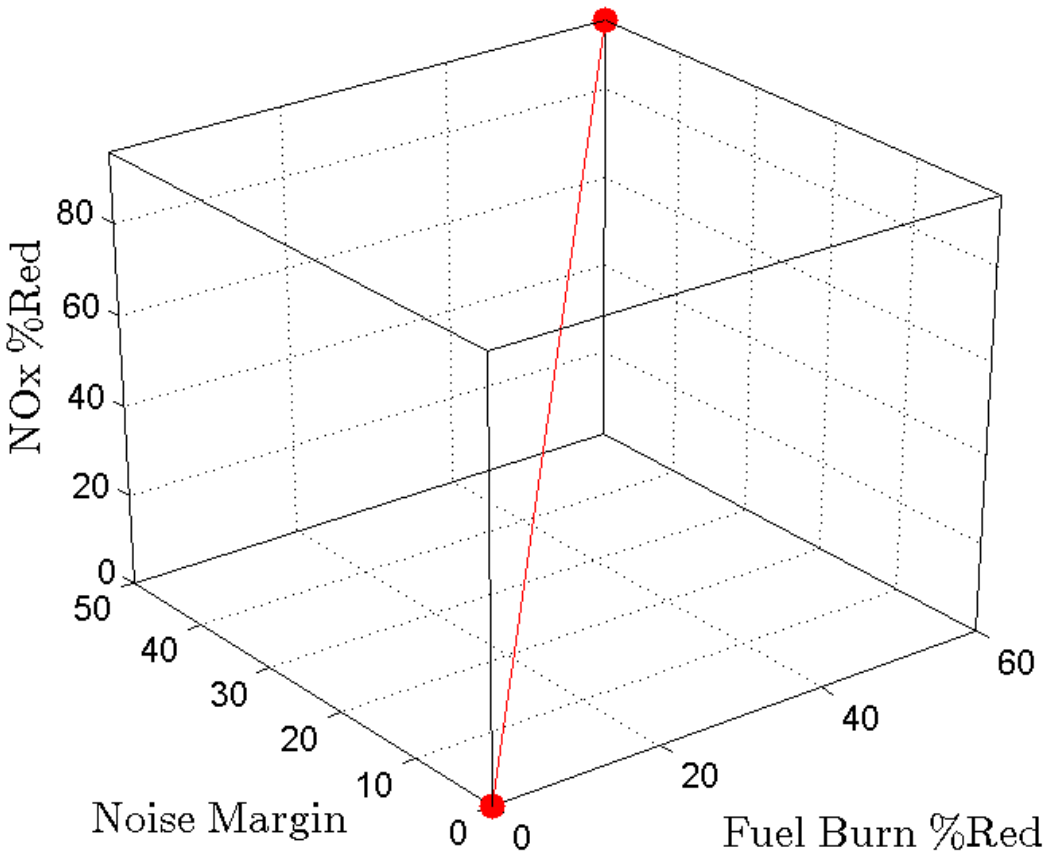

Figure 78: Three attribute objective space with utility 0 and 1 points circled and linked by diagonal line

This diagonal line represents the backbone upon which the underlying utility

function is assessed. Recall that the certainty equivalent at utility equals 0.5 was assessed on a 50-50 lottery between the minimum and maximum utility points. This is given in Eqn. 42 for a single attribute and is extended in Eqn. 58 for three attributes.

$$u(x_{0.5}, y_{0.5}, z_{0.5}) = 0.5 * u(x^*, y^*, z^*) + 0.5 * u(x^0, y^0, z^0) \tag{58}$$

By Eqn. 58 the certainty equivalent point in this cube can be identified for a given decision maker. This point is denoted as $CE_{0.5}$ and is found to be at the triple coordinate point (%FB, NM, %NOx) $\rightarrow$ (22.5, 17.5, 37.5) for a real decision maker familiar with the aircraft technology selection problem and the three attribute objective space. The $CE_{0.5}$ is added to the three attribute objective space as a known utility point in Fig. 79 (blue dot).

There are two corner points and one center point for which utility values have been assigned. The $CE_{0.5}$ center point is now leveraged to encode another point near the boundary of the three attribute objective space, preferably a corner or edge point, that also has utility equals 0.5. In order to have equal utility for this decision maker, the decision maker must be indifferent between the new point and the $CE_{0.5}$ center point. A general strategy has been created in this work to identify such a point. Perform a 2D projection to a face by zeroing out one attribute, and then moving in the direction of most rapid improvement for the remaining attributes, along the face of the three attribute space, while asking the decision maker indifference questions about points along this path to identify a point of equal utility. This strategy maintains positioning along the boundaries of the objective space and will rapidly elicit a point that is efficient for fitting a response surface model. This is demonstrated by starting out with the blue $CE_{0.5}$ center point whose coordinates are (%FB, NM, %NOx) $\rightarrow$ (22.5, 17.5, 37.5) and performing a 2D projection to the NM-%NOx plane by zeroing out the %FB attribute. This is shown in Fig. 80 (blue arrow).

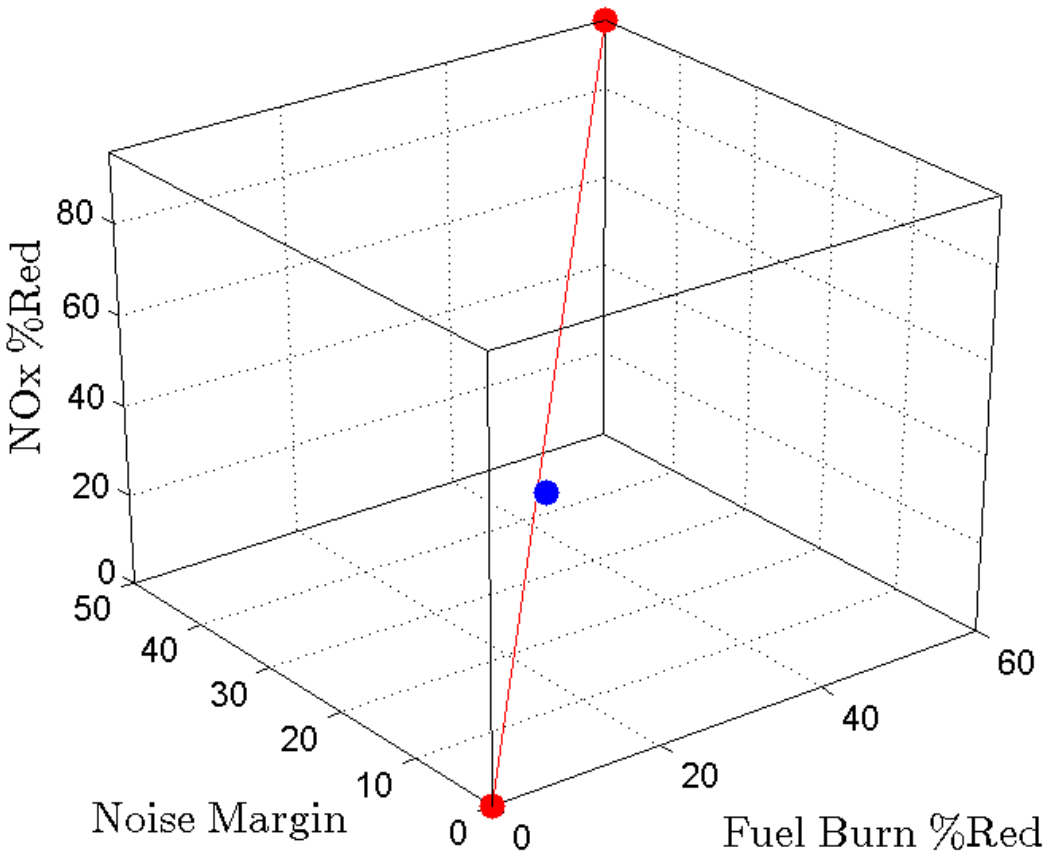

Figure 79: Three attribute objective space with blue dot for $CE_{0.5}$

At this new green point (%FB, NM, %NOx) $\rightarrow$ (0, 17.5, 37.5), query the decision maker if they are indifferent between choosing the green point or the blue $CE_{0.5}$ center point. The answer should obviously favor the blue $CE_{0.5}$ center point, so improve the green point by moving in the direction of greatest improvement on this face (keep %FB=0). The strategy from single attribute utility encoding of certainty equivalents is borrowed upon by setting the current point as the new minimum and the corner point of the objective space in the direction of greatest improvement as the new maximum, and bisecting the distance in between to arrive at the next point where the decision maker is queried. This kind of optimal path movement is also found in numerical optimization techniques (Ref. [241]) like golden section rule and

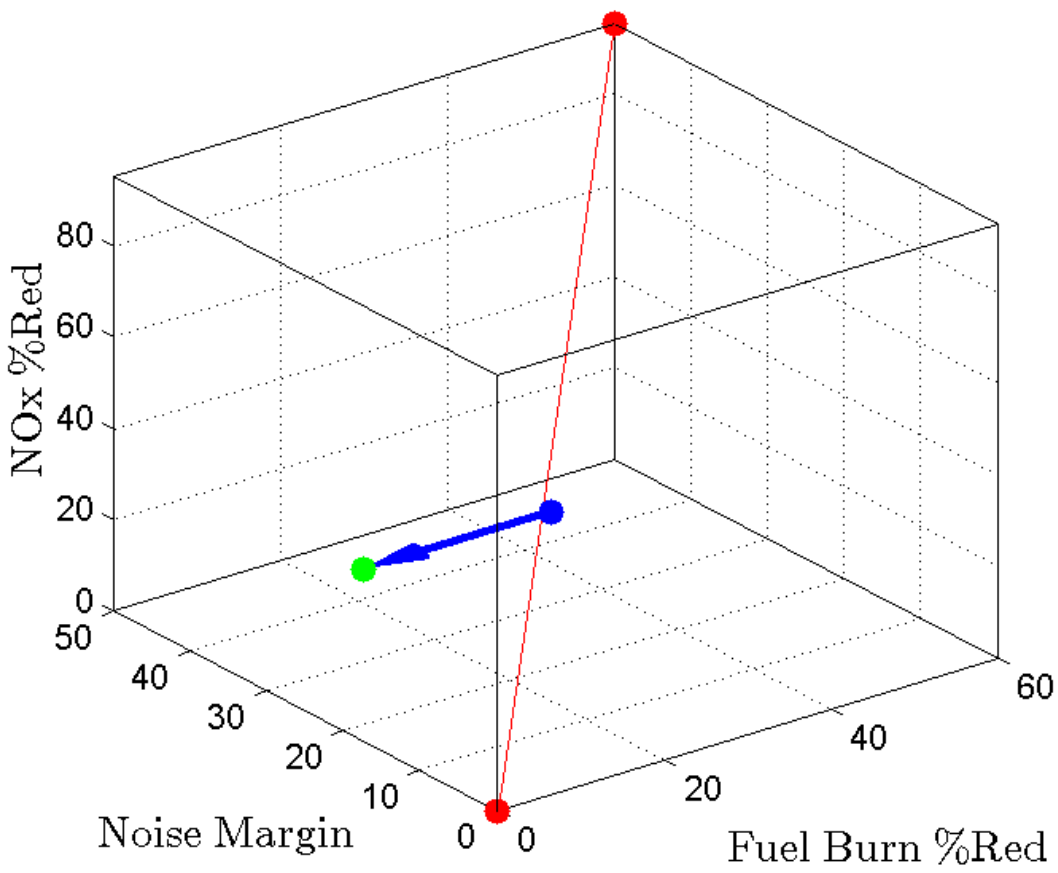

Figure 80: 2D projection to NM-%NOx face by zeroing %FB attribute

the bisection method. These concepts are shown in Fig. 81 where the blue dashed line is the direction of greatest improvement along this face of the objective space and the green point represent the bisected point between the corner and the original 2D projection point.

The coordinates of the green point are now (%FB, NM, %NOx) $\rightarrow$ (0, 34, 66), and here the decision maker is once again asked if they are indifferent between this point and the blue $CE_{0.5}$ center point. If they are indifferent, then this green point represents the utility equals 0.5 point on this face of the three attribute space. If they prefer the green point to the blue $CE_{0.5}$ center point, then reverse direction and perform another bisection that reduces their utility for the green point until an

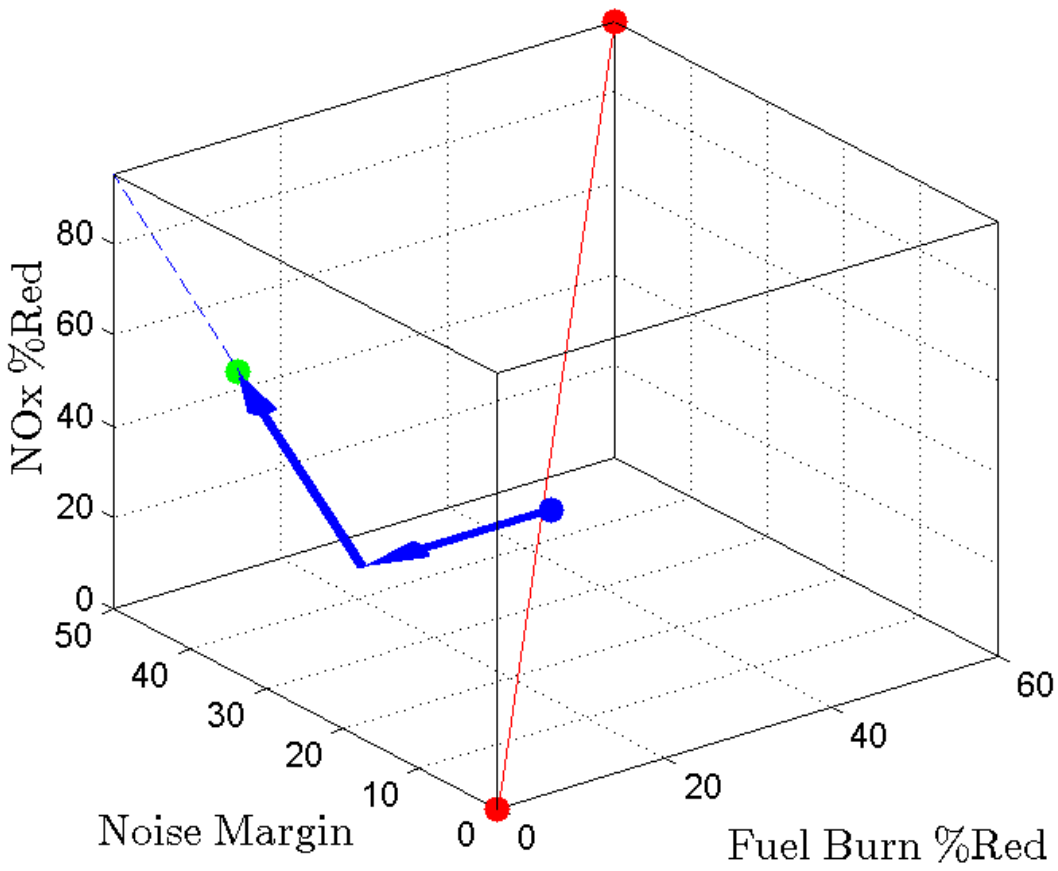

Figure 81: Direction of most rapid improvement on NM-%NOx face and bisected query point (green)

indifference point is located on this face. If they still prefer the blue $CE_{0.5}$ center point over the green point, then there are two options. The analyst can continue in the direction of greatest improvement and perform another bisection that increases the decision maker's utility for the green point. However, if there is no point along this path for which the decision maker will feel indifferent, the second option is jump directly to the corner point and query the decision maker there as shown in Fig. 82 (blue arrow).

The coordinates of the green point are now (%FB, NM, %NOx) $\rightarrow$ (0, 50, 95), and here the decision maker is once again asked if they are indifferent between this point and the blue $CE_{0.5}$ center point. If they are indifferent then this green point

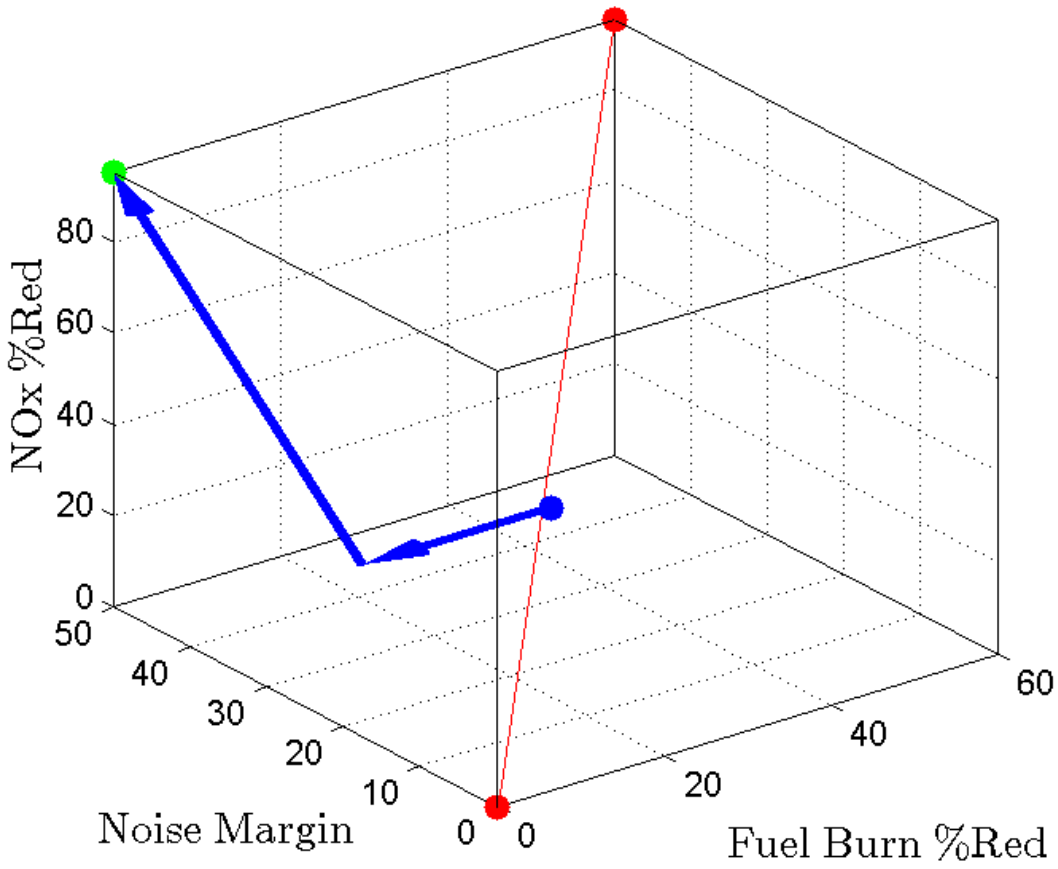

Figure 82: Advance to corner point along direction of most rapid improvement on NM-%NOx face

represents the utility equals 0.5 point at this corner of the three attribute space. If they prefer the green point to the blue $CE_{0.5}$ center point, then reverse direction and perform another bisection that reduces their utility for the green point until an indifference point is located on this face. If they still prefer the blue $CE_{0.5}$ center point over the green point, then the only remaining direction of improvement is along the %FB attribute. Perform a bisection along the edge of the cube where NM and %NOx are fixed at their maximum values, and %FB is increasing until a point of indifference is located for the decision maker. This new direction of improvement along the edge of the three-attribute space is shown in Fig. 82 by the blue dashed line. The green point represents a new bisected point between the corner and the

maximum %FB level of the blue $CE_{0.5}$ center point.

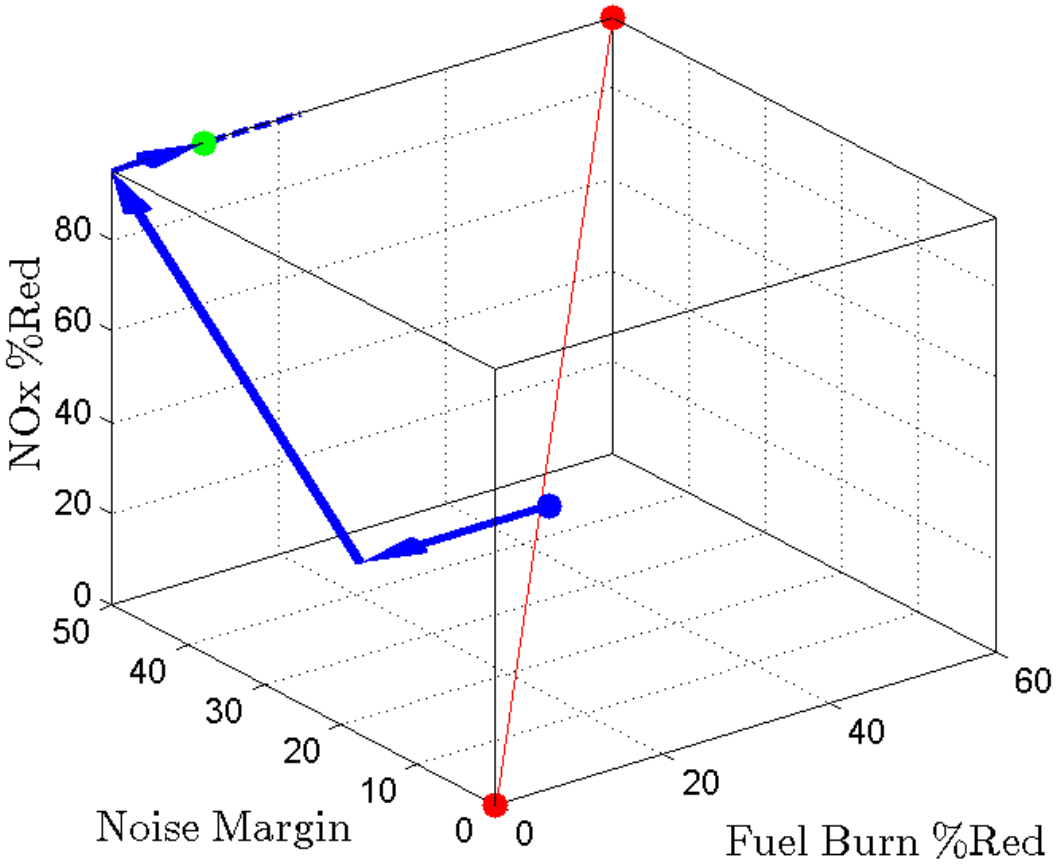

Figure 83: Advance to bisected point on edge of objective space along direction of %FB improvement

The coordinates of the green point are now (%FB, NM, %NOx) $\rightarrow$ (11, 50, 95), and here the decision maker is once again asked if they are indifferent between this point and the blue $CE_{0.5}$ center point. If they are indifferent then this green point represents the utility equals 0.5 point on this edge of the three attribute space. If they prefer the green point to the blue $CE_{0.5}$ center point, then reverse direction and perform a bisection that reduces their utility for the green point until an indifference point is located on this edge. If they still prefer the blue $CE_{0.5}$ center point over the green point, then perform another bisection that increases their utility for the green point until an indifference point is located on this edge. Once the indifference point

Table 27: Interview results of decision maker's 6 elicited data points

Description	%FB attribute coordinate	NM attribute coordinate	%NOx attribute coordinate	Utility value
Minimum utility point (origin)	0	0	0	0
Maximum utility point	1	1	1	1
$CE_{0.5}$ center point	22.5	17.5	37.5	0.5
$\%FB_{u=0.5}$ indifference point	20	50	95	0.5
$NM_{u=0.5}$ indifference point	30	0	45	0.5
$\%NOx_{u=0.5}$ indifference point	60	50	25	0.5

is located, record this coordinate triple as the $\%FB_{u=0.5}$ indifference point because it was located by first setting the %FB attribute to zero. A similar procedure is then repeated to identify the $NM_{u=0.5}$ and $\%NOx_{u=0.5}$ indifference points. The procedure for obtaining both of these indifference points will begin at the blue $CE_{0.5}$ center point, the only difference is that NM will be set to zero to find the $NM_{u=0.5}$ indifference point and %NOx will be set to zero to find the $\%NOx_{u=0.5}$ indifference point. This procedure is executed with the real decision maker interviewed to obtain the blue $CE_{0.5}$ center point earlier. The results of the interview process are recorded in Table 27.

The blue $CE_{0.5}$ center point and the three indifference points ($\%FB_{u=0.5}$, $NM_{u=0.5}$, and $\%NOx_{u=0.5}$) can be used to approximate a $u(\%FB, NM, \%NOx) = 0.5$ iso-utility

surface by joining the points with simplices. This is shown in Fig. 84.

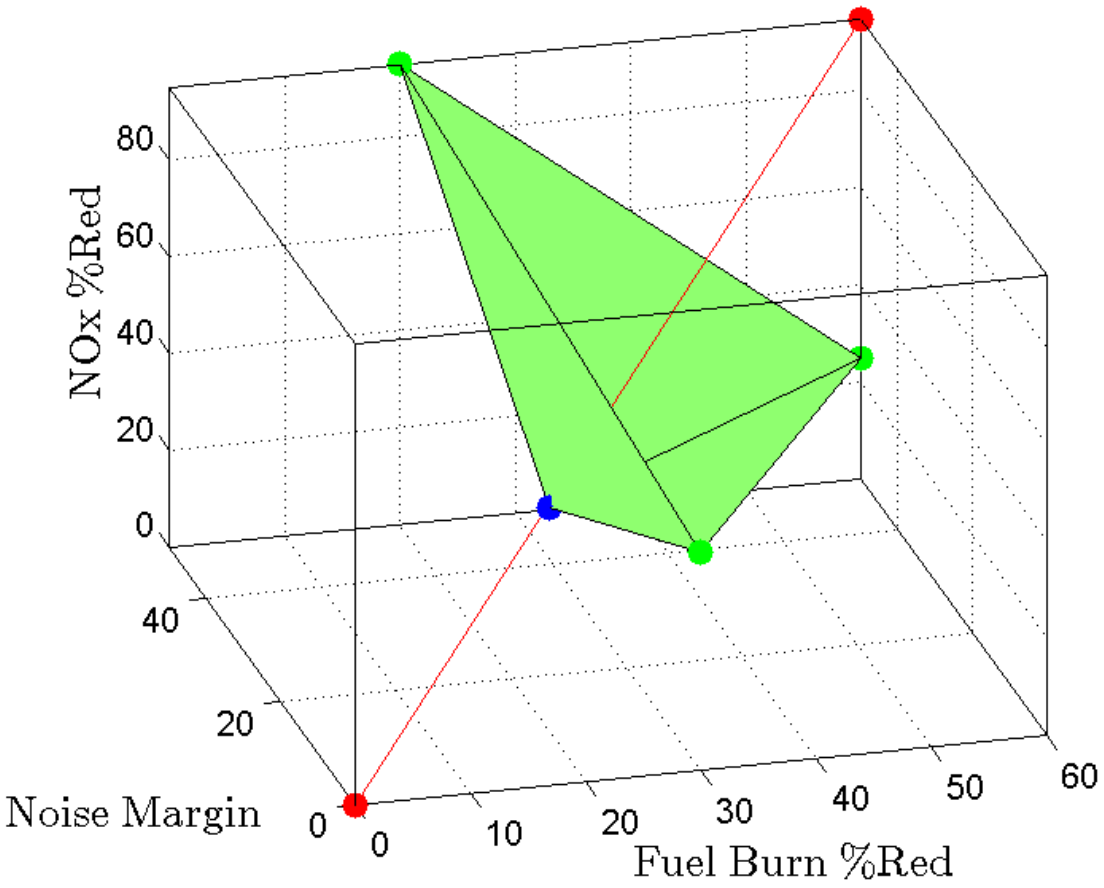

Figure 84: $u(\%FB, NM, \%NOx) = 0.5$ iso-utility surface of underlying multiattribute utility function

The $u(\%FB, NM, \%NOx) = 0.5$ iso-utility surface is created by eliciting a center point and three edge/face points from the decision maker. As Table 27 shows, there are now six known utility points in the three attribute objective space. Currently two corner points, three edge/face points, and a center point are known in the three attribute objective space. Without additional utility points, the response surface fit would be poor.

When assessing single attribute utility functions, the general procedure is to set a minimum and a maximum utility point at utility equals 0 and 1 respectively, identify three different certainty equivalent (using Eqns 42-44.) points along the utility

function, and finally fit a known utility functional form to those points. Eqns. 43-44 help to identify two extra utility values along the single attribute outcomes. This concept is extended to multiple attributes to identify additional utility data points in the three attribute objective space. Eqns. 59-60 can be used to identify two more certainty equivalent points along the red diagonal line that represents the backbone of the underlying multiattribute utility function.

$$u(x_{0.25}, y_{0.25}, z_{0.25}) = 0.5 * u(x_{0.5}, y_{0.5}, z_{0.5}) + 0.5 * u(x^0, y^0, z^0) \tag{59}$$

$$u(x_{0.75}, y_{0.75}, z_{0.75}) = 0.5 * u(x^*, y^*, z^*) + 0.5 * u(x_{0.5}, y_{0.5}, z_{0.5}) \tag{60}$$

Querying the decision maker and using the $CE_{0.5}$ certainty equivalent as an intermediate minimum/maximum as shown in Eqns. 59-60 identifies the $CE_{0.25}$ and $CE_{0.75}$ certainty equivalent points. These points are depicted in Fig. 85 and reported in Table 28.

The blue points in Fig. 85 are the $CE_{0.5}$, $CE_{0.25}$, and $CE_{0.75}$ certainty equivalent points. The three indifference points $\%FB_{u=0.5}$, $NM_{u=0.5}$, and $\%NOx_{u=0.5}$ were elicited using the procedure described earlier to identify points of indifference relative to the $CE_{0.5}$ certainty equivalent point. The same procedure can be repeated for the $CE_{0.25}$, and $CE_{0.75}$ certainty equivalent points to identify the the three indifference points $\%FB_{u=0.25}$, $NM_{u=0.25}$, and $\%NOx_{u=0.25}$ associated with the $CE_{0.25}$ certainty equivalent and the three indifference points $\%FB_{u=0.75}$, $NM_{u=0.75}$, and $\%NOx_{u=0.75}$ associated with the $CE_{0.75}$ certainty equivalent. The decision maker's responses for these interview questions are given in Table 28.

The decision maker's $CE_{0.25}$ certainty equivalent and three indifference points ($\%FB_{u=0.25}$, $NM_{u=0.25}$, and $\%NOx_{u=0.25}$) can be used to approximate a $u(\%FB, NM, \%NOx) = 0.25$ iso-utility surface by joining the points with simplices. The same can be done with the $CE_{0.75}$ certainty equivalent its associated three indifference points ($\%FB_{u=0.75}$,

Table 28: Interview results of decision maker's 14 elicited data points

Description	%FB attribute coordinate	NM attribute coordinate	%NOx attribute coordinate	Utility value
Minimum utility point (origin)	0	0	0	0
Maximum utility point	1	1	1	1
$CE_{0.5}$ center point	22.5	17.5	37.5	0.5
$\%FB_{u=0.5}$ indifference point	20	50	95	0.5
$NM_{u=0.5}$ indifference point	30	0	45	0.5
$\%NOx_{u=0.5}$ indifference point	60	50	25	0.5
$CE_{0.25}$ center point	6	5	10	0.25
$\%FB_{u=0.25}$ indifference point	2	17.5	37.5	0.25
$NM_{u=0.25}$ indifference point	22.5	2	37.5	0.25
$\%NOx_{u=0.25}$ indifference point	20	15	0	0.25
$CE_{0.75}$ center point	35	30	55	0.75
$\%FB_{u=0.75}$ indifference point	30	50	95	0.75
$NM_{u=0.75}$ indifference point	60	17.5	60	0.75
$\%NOx_{u=0.75}$ indifference point	60	50	40	0.75

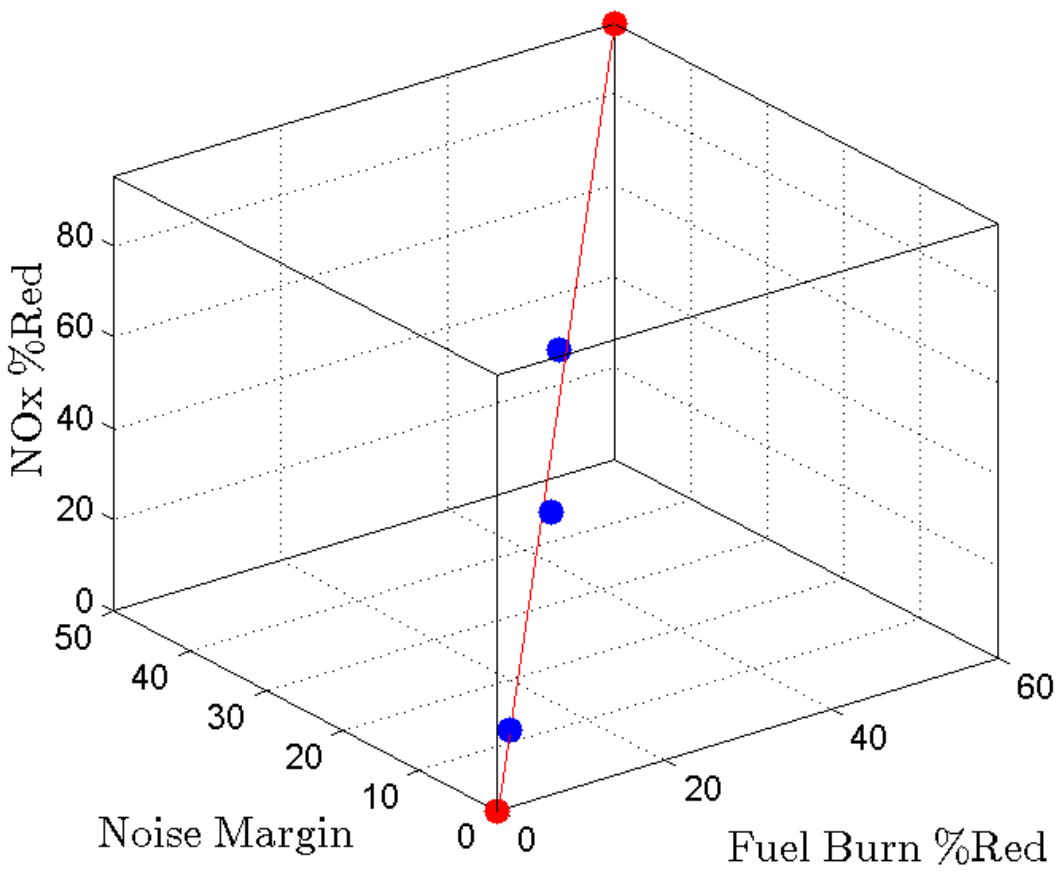

Figure 85: The $CE_{0.5}$, $CE_{0.25}$, and $CE_{0.75}$ certainty equivalent points

$NM_{u=0.75}$, and $\%NOx_{u=0.75}$) to approximate the $u(\%FB, NM, \%NOx) = 0.75$ iso-utility surface. The two surfaces are shown in Fig. 86.

The utility points in Fig. 86 and reported in Table 28 represent 14 distinct data points in the 3 attribute objective space. These points are used to fit a response surface that approximates the decision maker's multiattribute utility function. A first order response surface equation was used to fit the data. After obtaining the multiattribute utility function, consistency checks were performed with the decision maker to verify the elicited points and the fitted utility function. The multiattribute utility function was found to match the decision maker's preferences and is used to calculate the expected utility of the three technology packages under consideration.

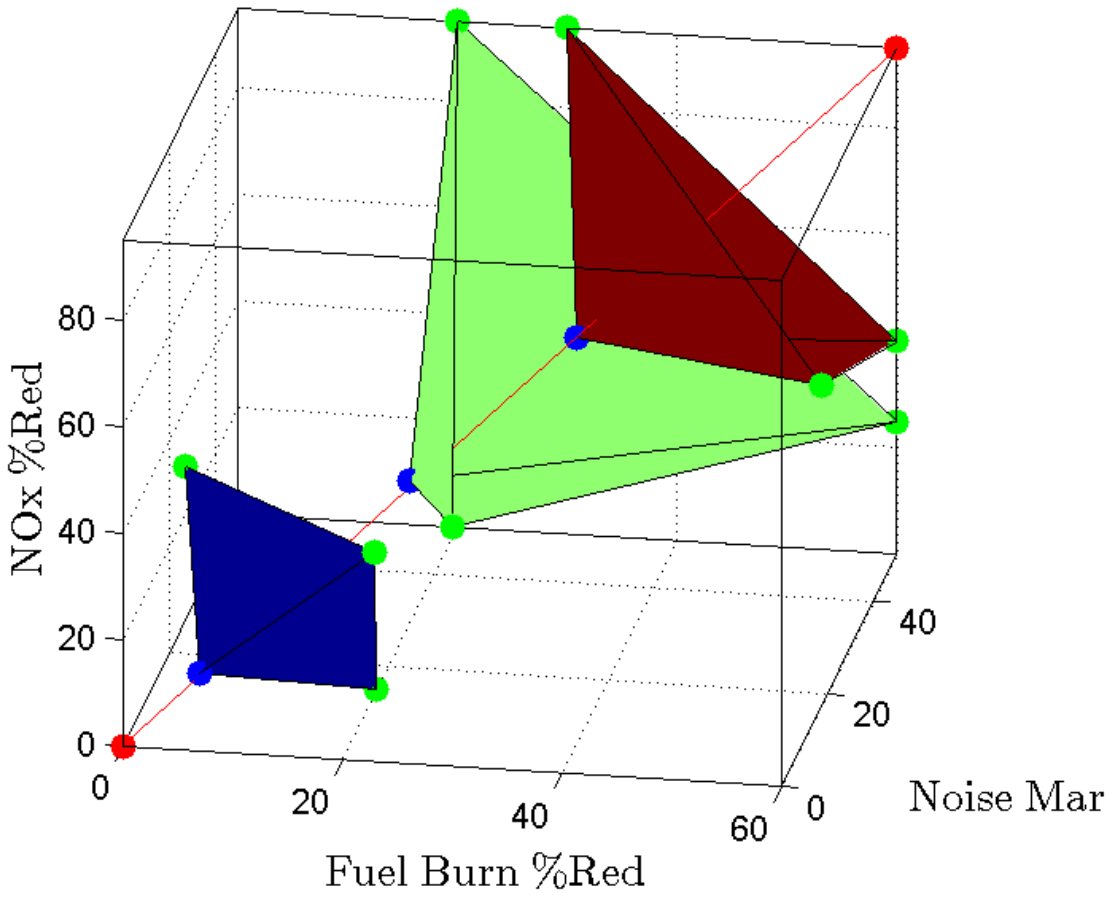

Figure 86: The $u(\%FB, NM, \%NOx) = 0.5$, $u(\%FB, NM, \%NOx) = 0.25$, $u(\%FB, NM, \%NOx) = 0.75$ iso-utility surfaces of underlying multiattribute utility function

5.6.3 Multiattribute ENcoding of Utility (MENU) Method in Three Attributes

The process detailed in the previous section to elicit a decision maker's three attribute utility function is summarized and captured in flowchart depicted in Fig. 87.

This method makes no assumptions about the independence conditions between the attributes and provides a structured and strategic method to elicit utility data from the decision maker. The MENU method does not limit the risk profile of the decision maker. Their risk attitudes arise organically through the elicitation of the certainty equivalents and indifference points. This procedure maintains the axiomatic

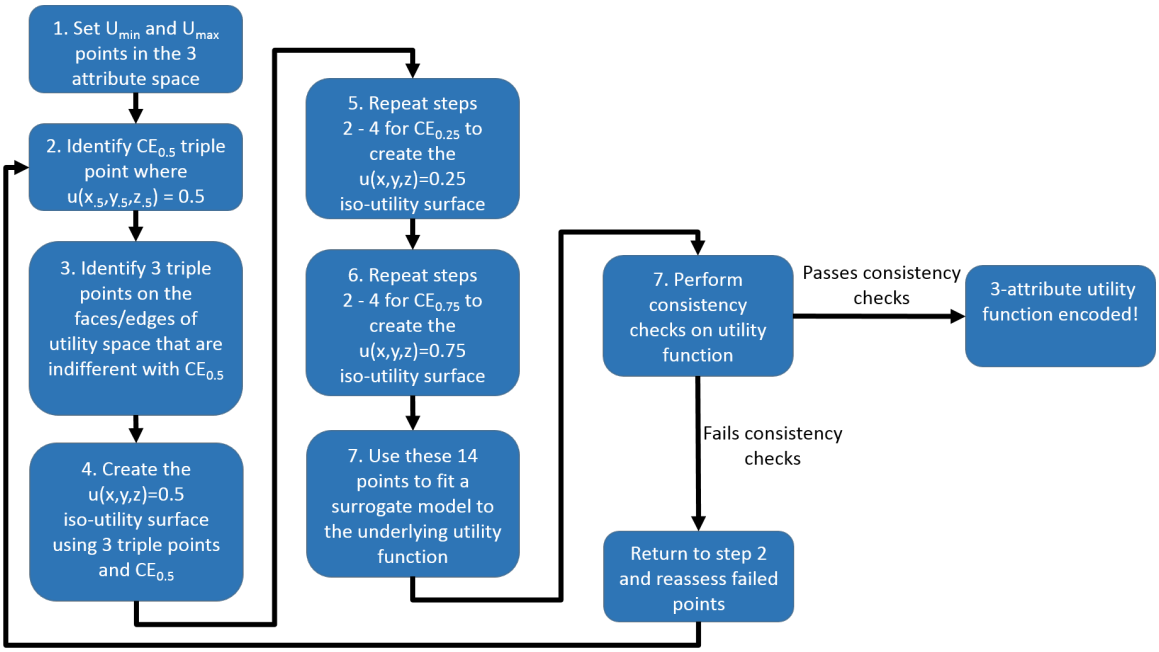

Figure 87: Multiattribute ENcoding of Utility (MENU) Method

principles of utility theory and does not rely on the presumed forms of MAUT which are not always applicable. This answers the last Research Question 4 which asked how the multiattribute utility function for a decision maker could be assessed without assuming the attribute independence conditions of MAUT. The MENU method demonstrates this by eliciting utility values directly from the decision maker in the three attribute objective space and using a response surface equation to represent the underlying multiattribute utility function.

The elicitation process does require a time commitment from the decision maker, but once it is obtained, the same multiattribute utility function can be used to evaluate every technology package in the design space for that decision maker. To those who claim that the investment of effort and time to elicit the multiattribute utility function in this manner is too great, Thurston (Ref. [236]) argues that you get what you pay for. "For most applications in which the subject has collaborated with the decision analyst in defining the design problem and conflicting attribute set, this author's experience has been that the utility assessment procedure takes approximately

1 hour, +/-30 minutes, depending on the number of attributes. The payoff is the ability to accurately quantify, for that particular design, the desirability of alternative tradeoffs and the effect of uncertainty." In the aircraft technology selection problem it is clear that capturing uncertainty to make tradeoffs is a basic requirement and the multiattribute expected utility formulation provides a rational and axiomatic way of doing so.

The multiattribute utility function obtained from the MENU method enables the assessment of expected utility for the outcomes in the three technology package lotteries. Using the probability distributions over the outcomes of each technology package and the decision maker's assessed multiattribute utility function, the expected utility of each lottery can be found by Eqn. 61.

$$E(U(FB, NM, NOx)) = \sum_{i=1}^{n} p(FB_i, NM_i, NOx_i)u(FB_i, NM_i, NOx_i) \qquad (61)$$

The exact value of the expected utility is equal to the triple integral over the continuous probability distributions times their utilities, but in this numerical simulation a summation will be calculated over many small interval cubes to approximate this integral. The intervals are the same ones used to approximate the probability distributions and are chosen such that the error in calculating the expected utility of the technology package lottery is less than 1%.

5.6.4 Three Attribute Utility Results

The results for the expected utility assessment for all three technology packages are summarized in Table 29.

Table 29 shows that the three technology packages under consideration can be rank ordered by their expected utilities. This ranking is consistent with the probability distributions in Figs. 76 and 77 for technology packages 1, 2, and 3 respectively. The multiattribute utility function gives more importance to higher values of %FB

Table 29: Three Attribute Expected Utility Results

Technology Package	Package Description	Expected Utility	Ranking
Tech Package 1	Low %FB reduction, high Noise Margin, and med %NOx reduction	0.37	3
Tech Package 2	High %FB reduction, low Noise Margin, and high %NOx reduction	0.77	1
Tech Package 3	Med %FB reduction, med Noise Margin, and low %NOx reduction	0.59	2

reduction, Noise Margin, and %NOx reduction. Figs. 76 and 77 show that technology package 2 is closest to the ideal corner of the objective space where probability outcomes receive the highest utility and that is why its distribution has the greatest expected utility. This procedure demonstrates how technology packages can be rank ordered in a logical, repeatable, axiomatic fashion that is not only consistent with the decision maker's preferences, but is also traceable back to the probability distributions over the outcomes of each technology package lottery. This capability can be used to evaluate and axiomatically rank order all three attribute technology solutions on the Pareto frontier that were previously considered to be equal.

Three different approaches to calculating utility functions for decision makers have been demonstrated. These include using standard single attribute forms (Eqns. 45-47), using linear interpolation between fixed points, and fitting a response surface to a set of iso-utility points (MENU method).

5.7 Comparison Study

5.7.1 Comparison Study Formulation

A comparison study is performed to demonstrate the usefulness of the multiattribute expected utility formulation of the aircraft technology selection problem relative to current practices. The ERA Dashboard (Fig. 52 [203]) performs tradeoffs on nearly 7,000 different technology solutions in the three attribute objective space. This task is aided by a multiobjective stochastic optimization technique that identifies superior designs in the large combinatorial space of technology solutions [94]. The optimization technique is a genetic algorithm operating on the deterministic values of the attributes and ignoring the uncertainty information for technology package. Even after the genetic algorithm optimization there are still 1,500 Pareto frontier technology packages for a decision maker to select from and all are non-dominated solutions. Current

methods of multicriteria analysis use techniques that are not based on axiomatic fundamentals which have been critiqued in the literature [77, 78]. One common technique is to rank order alternatives by their euclidean distance to an imaginary ideal solution [253]. By this method, the closer a technology package's deterministic attributes are to the imaginary ideal solution, the shorter its Euclidean distance from that ideal and the higher it is ranked. A subset of points from the entire set of technology solutions is identified and their Euclidean distance from the ideal is recorded. The subset of points is ranked by this metric forming the baseline rankings for comparison in this study. The expected utilities of these technology packages is then calculated. The ranking by expected utility is then compared to the baseline rankings. Any contrast between the two methods is identified and analyzed. Since the comparison study focuses on the change in the rankings between the Euclidean distance technique and the expected utility technique formulated in this thesis, its important to ensure that the baseline rankings are meaningful and not within the margin of error. This will ensure that any change in the rankings using the expected utility formulation is significant.

5.7.2 Comparison Study Implementation

All of the Pareto optimal technology packages are ranked by the Euclidean distance technique, a practice currently found in the literature [203]. The lowest Euclidean distance value to the ideal is 0.3285 and represents the ideal technology solution identified by this method. The highest Euclidean distance value from the ideal point is 0.7304 and represents the lowest ranked Pareto optimal technology solution. The range of Euclidean distance values for Pareto optimal technology solutions is not large but five technology solutions are chosen within this range to give the most significance to each technology solutions rank order value. Alternatively, the top five technology solutions in the space could simply have been chosen but their Euclidean distance values would be bunched together near 0.3285 (distance value of top ranked technology

package). If two technology packages have similar Euclidean distance values, then their rank order could be within the margin of error, making it less meaningful. To avoid this the baseline rankings are selected to be as far apart from one another in Euclidean distance as possible ensuring that higher ranked technology solutions really are significantly better than lower ranked ones for this engineering selection method. The five Pareto optimal technology packages are chosen at an approximate interval of 0.1 Euclidean distance between each package. Five non-Pareto optimal technology packages are also selected for comparison in this study. They are also selected by spacing them out as much as possible to give their ranking significance. The non-Pareto optimal technology packages are contained within the interval between the Pareto optimal technology packages at an approximate increment of 0.05 Euclidean distance from the Pareto optimal technology solutions. This selection process gives the rank order value of the baselines the most significance and ensures that the rankings are meaningful. These technology packages and their rankings are provided in Table 30. The last column in Table 30 is the ranking of the technology packages by Euclidean distance. The smaller the distance, the closer that technology package is to the ideal, and the higher its ranking.

Table 30 gives the baseline rankings for 10 technology packages in the multiobjective space, five from the Pareto optimal set and five that are non-Pareto optimal. It also includes the ranking of the worst technology package which is obviously non-Pareto optimal and the lowest ranked technology package in the space by this method. The Euclidean distance rankings only consider the deterministic performance of the technology package given in columns 3-5 of Table 30. This ranking method does not incorporate the uncertainty associated with each technology package or the decision maker's preferences over the attributes, target values in those attributes, or their risk profile. This sort of ranking reflects irrational decision making because it ignores

Table 30: Technology package rankings by Euclidean distance

Description	Tech Package ID number	%FB red	%NOx red	Noise Margin	Distance to Ideal	Distance to Ideal Rank
Pareto frontier package	1	45.18	89.69	35.87	0.329	1
Pareto frontier package	2	38.61	84.09	38.67	0.429	3
Pareto frontier package	3	50.38	91.23	31.63	0.478	5
Pareto frontier package	4	33.31	90.54	36.68	0.528	7
Pareto frontier package	5	28.62	84.48	40.16	0.629	9
Non-Pareto frontier package	6	50.05	87.25	34.15	0.378	2
Non-Pareto frontier package	7	45.22	86.25	33.60	0.447	4
Non-Pareto frontier package	8	45.33	87.48	32.13	0.498	6
Non-Pareto frontier package	9	47.83	91.29	29.75	0.578	8
Non-Pareto frontier package	10	27.92	84.29	37.02	0.679	10
Worst frontier package	11	14.54	58.13	25.91	1.562	11

fundamental aspects of the problem. These shortcomings are addressed by the multiattribute expected utility formulation developed in this thesis. It is important to note that when including uncertainties and decision maker preferences, even for this small subset of technology packages, the selection process becomes nontrivial. Considering these factors concurrently with the performance of each technology package in the multiobjective space complicates the selection process. The decision maker is aided in the selection process by calculating the expected utility of each technology package, which simultaneously incorporates all of the relevant aspects of the problem into a single criterion, and then re-ranking the technology packages by this criterion. This is the final step of the FAAST methodology. The expected utilities are found using the same technique as the three attribute case to generate the joint probability outcomes for each technology package. The same multiattribute expected utility function obtained through the three attribute MENU method is used to determine the utility over the joint probability outcomes. The joint probability outcomes and their utilities are combined into the expected utility metric through Eqn. 61.

5.7.3 Comparison Study Results

The expected utility values and rank ordering of the technology packages are provided in Table 31. The last column in Table 31 is the ranking of the technology packages by its expected utility. The higher the expected utility value, the more preferred that technology package is to the decision maker, and the higher its ranking.

Table 31 shows that the expected utility ranking is nearly completely different (except for the worst case tech package) than the Euclidean distance ranking. The top ranked technology package by Euclidean distance is ranked eighth by expected utility. Nine of the ten technology packages considered in this study changed rank relative to the baseline rankings. The technology packages in this study were chosen in order to emphasize and give the most significance to their rank order by ensuring that

Table 31: Technology package rankings by Expected Utility

Description	Tech Package ID #	% FB red	% NOx red	Noise Margin	Distance to Ideal	Distance to Ideal Rank	Expected Utility Value	Expected Utility Rank
Pareto frontier package	1	45.18	89.69	35.87	0.329	1	0.72	8
Pareto frontier package	2	38.61	84.09	38.67	0.429	3	0.72	7
Pareto frontier package	3	50.38	91.23	31.63	0.478	5	0.92	1
Pareto frontier package	4	33.31	90.54	36.68	0.528	7	0.73	6
Pareto frontier package	5	28.62	84.48	40.16	0.629	9	0.65	10
Non-Pareto frontier package	6	50.05	87.25	34.15	0.378	2	0.89	2
Non-Pareto frontier package	7	45.22	86.25	33.60	0.447	4	0.82	5
Non-Pareto frontier package	8	45.33	87.48	32.13	0.498	6	0.84	4
Non-Pareto frontier package	9	47.83	91.29	29.75	0.578	8	0.88	3
Non-Pareto frontier package	10	27.92	84.29	37.02	0.679	10	0.66	9
Worst frontier package	11	14.54	58.13	25.91	1.562	11	0.26	11

they were as far apart from one another as possible. The fact that the expected utility rankings altered the baseline rankings in spite of this, is an important development for the aircraft technology selection problem. This change in rankings is driven by utility of the decision maker over the three objectives and how uncertainty factors into that through the joint probabilities over the three attributes. Incorporating these relevant factors of the aircraft technology selection problem through expected utility over multiple attributes supports the decision maker to arrive at a rational, traceable, and optimal decision for their preferences.

It is interesting to note that four of the top five ranked solutions using expected utility are actually non-Pareto frontier technology packages. These are likely packages that are just behind the Pareto frontier, with one or two less technologies in their portfolios, but are still performing well enough to receive high probability outcomes in the three attribute objective space and more desirable utility over those outcomes. That combination leads to these technology packages having the highest expected utilities of all the packages considered in this study. Current multicriteria decision analysis tools that ignore uncertainty and its implications to decision analysis disregard these technology packages, that are not only more preferable to the decision maker but may also be less expensive to obtain in terms of technology cost.

The change in expected utility between technology packages in Table 31 is very small or even zero in some cases. This is to be expected since the entire range of utility is from zero to one and there can be many different solutions taking on expected utility values over that finite range. Additionally, the difference in expected utility between the best ranked solution and worst ranked solution (as identified by Euclidean distance) in this subset of technology packages is 0.5, so the actual range of values is half of the possible range for utility. While more significant figures could be used for delineation, the approximation of the triple integral in the three attribute expected utility formulation only ensures accuracy to 0.01 utility. Any resolution of significant

figures beyond 0.01 utility are within the error of the formulation. In some cases technology packages with the same expected utilities indicate they are very similar in uncertainty and location over the three attribute objective space. This occurs when technology packages have essentially the same core set of technologies but have one or two technologies that vary between them, producing similar deterministic and probabilistic performance in the three attribute objective space. This can be seen in Fig. 88 which depicts three technology packages that have the same expected utilities.

These technology packages are right on top of one another in the three attribute objective space and are likely very similar in terms of their technology portfolios. A decision maker will not have much preference difference between them but the expected utility formulation can be used to bring visibility to these similar packages in order to identify the technologies they all have in common. This core set of technologies would be very relevant to a decision maker analyzing the aircraft technology selection problem.

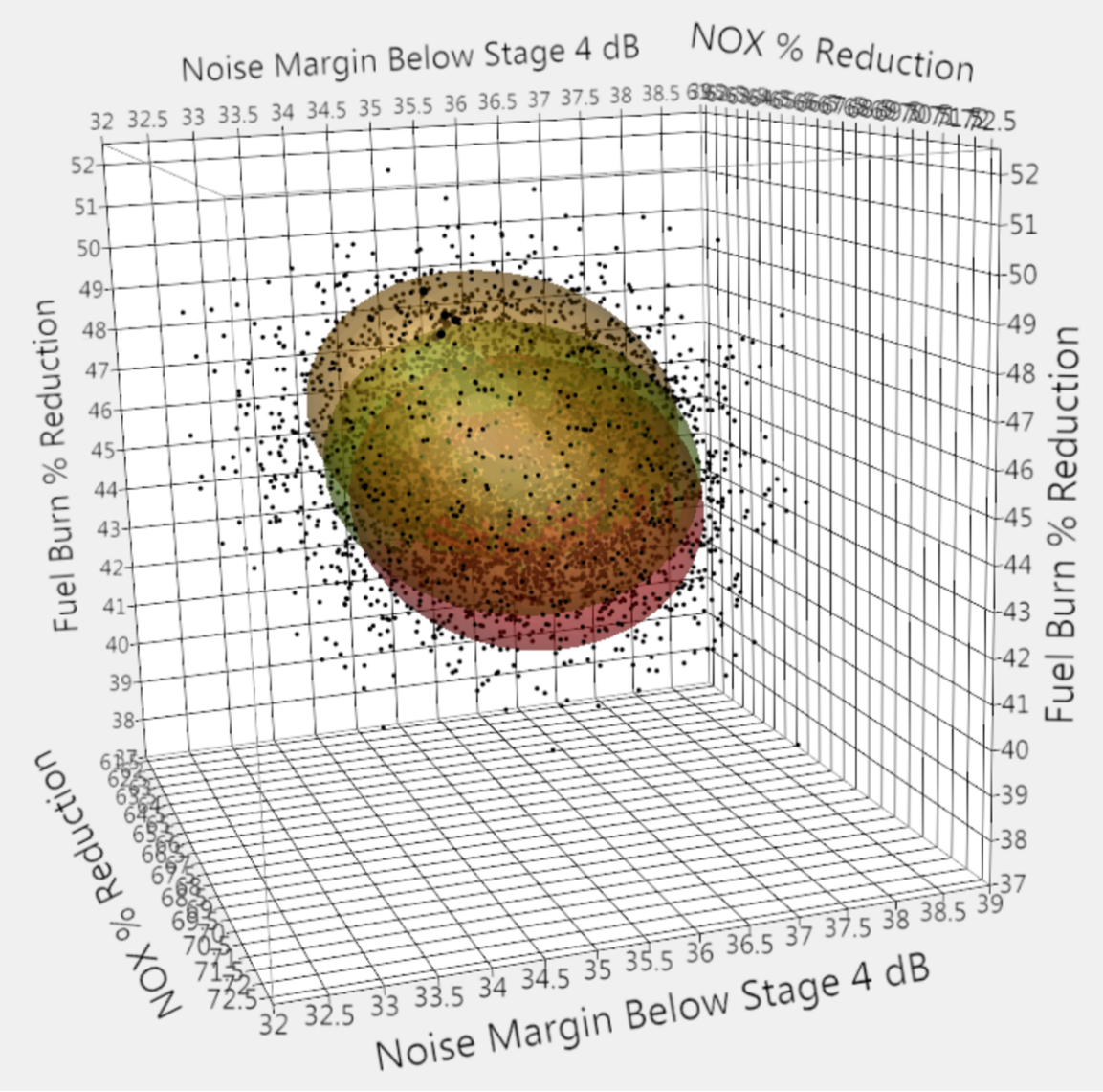

Figure 88: Normal contour ellipsoids for technology packages with the same expected utility

CHAPTER VI

CONCLUSIONS

6.1 Archimedean Copula Selection

The first research question was based on the need to create a method for selecting copulas. A selection tree was created to aid the systems analyst but it was done so subjectively. Research Question 1 was posed to verify and validate the tree objectively.

Can the proposed copula selection tree be shown to be consistent with objective statistics? Given an input vector of copula samples X, and a set of objective statistics S, can the groupings in tree T be reproduced?

The experiments conducted to answer these research questions were intended to show that the resulting copula selection tree is consistent with objective metrics. The hope is that by proving its validity, the community at large will carry it forward as an integral tool for converting qualitative knowledge into quantitative dependence structures in dependence modeling of random variables.

6.2 Impact of Copulas in Aerospace Design

The second research focused on quantifying the effect of using copulas in probabilistic assessments for dependence modeling of complex systems like future technologies in aircraft. It was also intended to demonstrate several different applications of copulas to showcase their usefulness to the aerospace community.

What is the quantified effect of using copulas in aircraft technology assessment? What types of applications are they suited for and how does that affect their impact?

Three different experimental applications utilizing copulas were demonstrated and they proved to successfully reduce the standard deviation of the system response metric. Various applications were shown to display the many ways copulas can be used to better represent existing qualitative knowledge about dependencies input to probabilistic assessments by the aerospace community.

6.3 Aircraft Technology Evaluation with Utility Theory

The third research question was posed to determine how the rational and axiomatic principles of decision analysis can be applied to the aircraft technology selection problem. Decision analysis theory suggests that utility is the most appropriate measure for making engineering design decisions under uncertainty. This research question was posed to demonstrate how that conceptual idea could be applied to make simple single attribute decisions in the aircraft technology selection problem.

How can the concept of expected utility be applied to evaluate and make comparisons between technology packages?

Answering the third research question by recognizing that the uncertainty distribution on a technology package directly allowed for its representation as a lottery that could be evaluated as a set of outcomes in the von Neumann-Morgenstern utility formulation, was a fundamental building block. Demonstrating this notion on single attribute technology packages brought focus to the aircraft technology selection problem through the lens of utility theory. Proving this capability made it possible to pose the final research question.

6.4 Multiattribute Utility Formulation for Aircraft Technology Selection

The fourth research question was a natural continuation from Research Question 3 which focused on the single attribute utility formulation of the aircraft technology

selection problem. However, at its core the technology selection problem is a multi-objective decision making task under uncertainty. This necessitated the extension of the single attribute formulation to multiple attributes.

How can the multiattribute utility function for a decision maker be assessed in the aircraft technology selection problem without assuming the restrictive conditions of attribute preference independence in MAUT?

The difficulty for the aircraft technology selection problem is that it can not subscribe to the independence conditions for preferences between the attributes that are necessary to apply the standard form equations of MAUT. This meant that a new procedure was required to create the multiattribute utility function for the decision maker addressing the aircraft technology selection problem. The answer to this research question culminated in the creation of the Multiattribute ENcoding of Utility (MENU) method for eliciting multiattribute utility functions without restricting the form of the utility function or the risk profile of the decision maker. The MENU method fills a key capability gap for the expected utility formulation of the aircraft technology selection problem.

6.5 Key Contributions

The key contributions of this thesis arise from answering the various research questions that bridged capability gaps in probabilistic assessments. The first contribution is an objectively verified and validated copulas selection tree enabling practitioners to rapidly translate their qualitative knowledge of dependencies into copula families that can probabilistically model that dependence. The second key contribution is the demonstration of three copula applications highlighting representative dependence conditions for random variables that can be captured by copulas in aerospace probabilistic assessments. The third contribution is a rational, axiomatic formulation based

on expected utility for ranking and ultimately choosing a future aircraft technology package best suited for a given decision maker in agreement with their preferences and risk attitudes. The fourth contribution is a strategic elicitation procedure for a multiattribute utility function that is highly applicable by avoiding assumptions about risk attitudes of the decision maker and independence conditions on preferences between the attributes. Both of these concepts are permitted to arise organically and captured through the multiattribute elicitation process. The final contribution is the encapsulating Future Aircraft Assessment and Selection of Technologies (FAAST) methodology for performing probabilistic assessments in an axiomatic fashion that lends itself to rational decision making and selection.

6.6 Concluding Remarks

The research presented in this document is intended to identify gaps in the application of probabilistic methods for assessing and selecting future aircraft technologies, bridging those gaps with a focused research plan, and implementing the resulting Future Aircraft Assessment and Selection of Technologies (FAAST) methodology to demonstrate how it answers the research questions of this thesis. The FAAST methodology provides a structured process for conducting modern probabilistic assessments of complex systems with functional dependencies on random input variables and large amounts of resulting data that is efficiently leveraged to arrive at a rational and axiomatic selection. The use of copula theory demonstrated that including functional dependencies via CAST (CopulA Selection Tree) in probabilistic assessments can have a significant impact on the variance of the system level response metrics. Ignoring these relationships can misrepresent the uncertainty associated with future technologies and lead to poor selection decisions due to misinformation. The implementation of utility theory combined a technology portfolio's performance and uncertainties with decision maker preferences over those probabilities and aggregated that information

over multiple attributes into a single criterion for axiomatically selecting technology packages. Making these decisions without the demonstrated expected utility framework means disregarding critical aspects of the aircraft technology selection problem leading to irrational decision making. Additionally, the comparison study revealed that rankings for Pareto-optimal technology packages using utility theory can be very disparate from conventional ranking methods that are based solely on deterministic performance. Future aircraft technology selections based on deterministic rankings are an inaccurate representation of a decision maker's preferences and can lead to errors in technology selection decisions. The expected utility rankings provide the decision maker with a much more complete picture of their preferences over the technology packages, a capability previously unavailable for the aircraft technology selection problem. The experiments and capability demonstrations utilizing these two theories successively answer each research question to build a complete methodology that supports a decision maker in the assessment and selection of future aircraft technologies.

Aircraft technology assessment and selection is a critical decision making problem for leaders of the aviation industry. Technology development programs are long duration and costly undertakings with significant consequences to manufacturers, operators, and the nation at large. The fruits of investments are not harvested for many years after the investment decision has been made. Errors in early stage investment direction could lead to sub-optimal technologies and system architectures, with no opportunity to recover from such a huge blunder. The implications of this problem are too great to be decided on by the unaided human decision maker. The only remedy is to ensure decision makers are well supported with the right tools and information to achieve the most optimal selection possible. The goal of the FAAST methodology and the contributions of this research like CAST and MENU are intended to give the decision maker the framework and tools for the assessment and rational selection of

future aircraft technologies. This will benefit all stakeholders and help to ensure an environmentally sustainable and bright future for the aviation industry.

6.7 Future Work

Opportunities for future work exist in both the dependence modeling and the decision analysis parts of this thesis. It would be interesting to evaluate the effects of modeling dependence on a large scale project that measures uncertainty with probabilistic assessments. Capturing dependence between input random variables could reduce the number of independent random variables by half, significantly affecting the uncertainty on the system response metrics. This application of copulas on a more holistic level would help to fully understand the implications of using copula theory in design.

It would also be a worthwhile endeavor to apply the MENU formulation to multiple decision makers and assess how utility functions need to adapt in order to make extreme selections. A full scale implementation of the multiattribute expected utility formulation on all 7,000 technology solutions in the ERA objective space and across all ERA advanced architectures would be a very interesting use case of this method. Many insights regarding the valuation of technology packages would be gleaned and important investment decision could be supported through a rational, traceable, axiomatic framework. Expected utility can be used to make direct comparisons between different architectures and is not restricted to comparisons within a particular vehicle architecture. Another interesting application would be to rework the multiobjective genetic algorithm which identifies Pareto optimal technology solutions by operating on deterministic performance parameters [94]. It could be redesigned to operate on a single objective which would be the multiattribute expected utility function which could be used to evaluate the entire objective space while incorporating decision maker preferences and uncertainty of the future technologies.

CHAPTER VII

APPENDICES

7.1 Appendix A: Copula Simulation

7.1.1 Introduction

This is a summary of algorithms used to generate correlated data representing dependent random variables which are described in the text by Nelsen. [154]. It provides a brief background of copulas, discusses how Archimedean Copulas are generated, and presents detailed explanations, procedures, and advice to guide the practitioner in the simulation of copulas functions. We will present this information from a general perspective and without any particular software package in mind. This summary assumes the reader is capable of generating random distributions and performing vector operations on those distributions within their chosen software package.

7.1.2 Background

Copulas are functions that join multiple, single variable marginal distributions by defining the joint distribution between the one dimensional functions. In this way they can be used to describe the dependencies between random variables. Copulas operate on the unit square space so each one dimensional function must be defined between 0 and 1. Copulas also assume that the marginal distributions of the single variable functions are uniform between 0 and 1. An interesting and important property of copulas functions is that while the joint distribution structure it defines can take on any shape, the marginal distribution of the individual single variable marginal distributions will remain uniformly distributed. This will be demonstrated through the simulations below.

There are many different families of copulas functions defined in the literature,[154] and each family has unique properties making them suitable for different applications. An important subset of copulas functions is the Archimedean class which are found to be used in the majority of practical applications. Their frequency of use is due to several reasons[154] including the ease with which they are constructed, the great variety of families that exist within this class, and the desirable properties possessed by these families.

One of the most important and attractive aspects of Archimedean copulas is how they are constructed. They are formed using $generator functions, \phi$ in a simple summation. They all prescribe to the following basic property,

$$C(u, v) = \phi^{(-1)}(\phi(u) + \phi(v)) \tag{62}$$

where C is the copulas function itself, u and v are random variables whose joint distribution is defined by the copulas, and ϕ is the generator functions of the copulas. There are many different types of generator functions which produce different families of copulas within the Archimedean class. As equation (62) shows, the selection of the function to generate the copulas has an important and defining role in the copula's structure and the resulting joint distribution. Table 32 provides a listing of the generator functions provided by Nelsen[154] and also includes the bounds of θ for each generator function.

Table 32: Copulas Generator Functions and Theta Values

Copulas	Generator Function $\phi(t)$	Theta Range
N1 Clayton	$\frac{1}{\theta}(t^{-\theta}-1)$	[-1,∞), excluding 0
N2	$(1-t)^{\theta}$	[1,∞)
N3 AMH	$\ln\left(\frac{1-\theta(1-t)}{t}\right)$	[-1,1)
N4 Gumbel	$(-\ln(t))^{\theta}$	[1,∞)
N5 Frank	$-\ln\frac{e^{-t\theta}-1}{e^{-\theta}-1}$	($-\infty$,∞), excluding 0
N6	$-\ln\left[1-(1-t)^{\theta}\right]$	[1,∞)
N7	$-\ln\left[\theta t+(1-\theta)\right]$	(0,1]
N8	$\frac{1-t}{1+t(\theta-1)}$	[1,∞)
N9	$\ln(1-\theta\ln t)$	(0,1]
N10	$\ln(2t^{-\theta}-1)$	(0,1]
N11	$\ln(2-t^{\theta})$	(0,1/2]
N12	$\left(\frac{1}{t}-1\right)^{\theta}$	[1,∞)
N13	$(1-\ln t)^{\theta}-1$	(0,∞)
N14	$(t^{-1/\theta}-1)^{\theta}$	[1,∞)
N15	$\left(1-t^{1/\theta}\right)^{\theta}$	[1,∞)
N16	$\left(\frac{\theta}{t}+1\right)(1-t)$	[0,∞)
N17	$\ln\left(\frac{(1+t)^{-\theta}-1}{2^{-\theta}-1}\right)$	($-\infty$,∞), excluding 0
N18	$e^{\theta/(t-1)}$	[2,∞)
N19	$e^{\theta/t}-e^{\theta}$	(0,∞)
N20	$e^{t^{-\theta}}-e$	(0,∞)
N21	$1-\left[1-(1-t)^{\theta}\right]^{1/\theta}$	[1,∞)
N22	$\arcsin\left(1-t^{\theta}\right)$	(0,1]

7.1.3 Modeling and Simulation of Copulas

The first algorithm Nelsen [154] discusses for simulating correlated data related by a copula function is known as the Conditional Distribution Method, described in chapter 2 of his text. This method is straightforward in theory but presents a number of of challenges in implementation, which prompt us to consider two other practical algorithms he presents in Chapter 4 which specifically apply to Archimedean copulas. The latter two algorithms are outlined in Exercises 4.13 and 4.14 of his text and will be the focus of this summary.

7.1.3.1 Closed-Form Copula Simulations

When analytical methods can be used to denote the copula in closed form using Eq. 62, copula simulations are easily and vividly conducted in the continuous space. In these cases, the simplest way to visualize the copulas is to plot the functions defined in Table 1 on an evenly spaced grid between two standard uniform variables. This table contains the copula cumulative distribution functions (CDFs) for each family. According to Sklar's Theorem, Eqn. (5), copulas are defined between the CDFs of two random variables. The CDFs can be plotted in 3D where the copula is shown as a surface in the third dimension above the unit square formed by two random variables. This is plotted in Figs. 89-91 for three different Archimedean copula families (Clayton, Gumbel, and Frank) which are commonly found in the literature, at different values of correlation parameter θ.

These 3D CDF surfaces show how all the copula joint distributions converge to 1 but it can be difficult to identify the unique properties of each family from these CDF plots. The copula joint CDF can also be plotted in 2D with the two random variables and the bivariate space shown on a single plane between them. The copula properties can be better visualized by adding contours and ensuring the grid is continuous. The

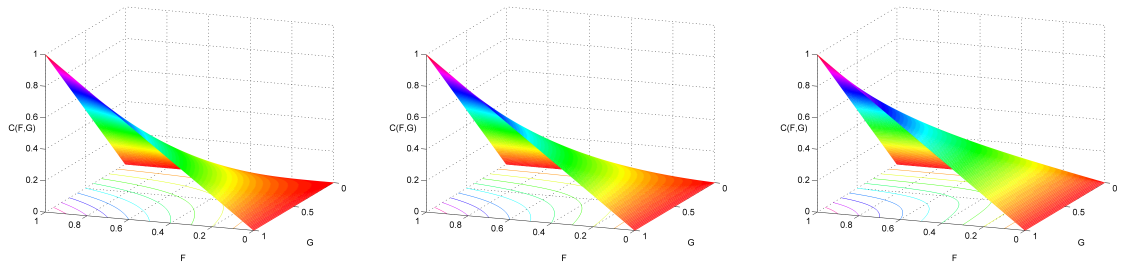

(a) $\theta = 0.2$ (b) $\theta = 0.6$ (c) $\theta = 2.0$

Figure 89: Clayton copula joint distribution 3D CDF surfaces at various values of θ

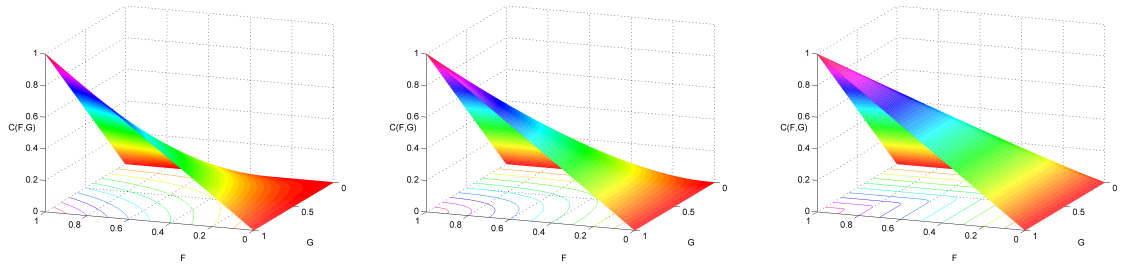

(a) $\theta = 1.05$ (b) $\theta = 2.0$ (c) $\theta = 15.0$

Figure 90: Gumbel copula joint distribution 3D CDF surfaces at various values of θ

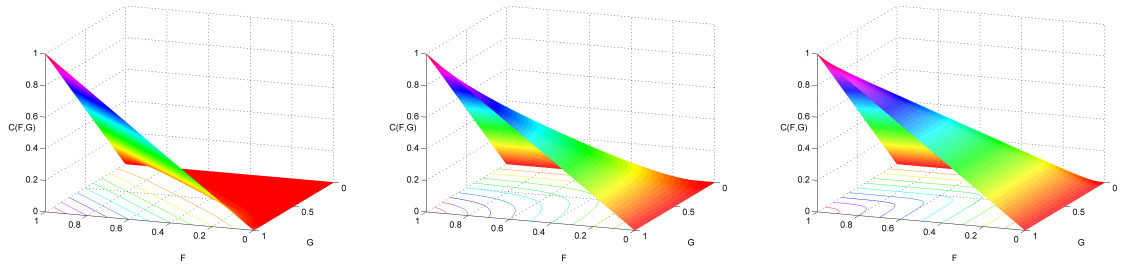

(a) $\theta = -10.0$ (b) $\theta = 5.0$ (c) $\theta = 20.0$

Figure 91: Frank copula joint distribution 3D CDF surfaces at various values of θ

2D CDF contours more clearly show the different ways each family's CDF converges to 1. These contours are shown in Figs. 92-94 at the same values of θ to correspond with the 3D plots in Figs. 89-91.

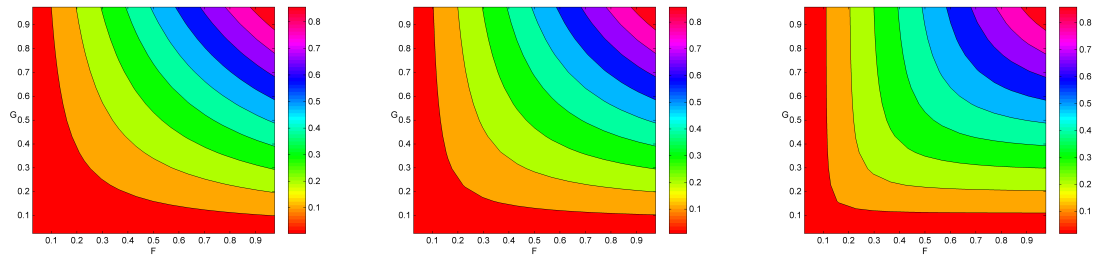

(a) $\theta = 0.2$ (b) $\theta = 0.6$ (c) $\theta = 2.0$

Figure 92: Clayton copula joint distribution 2D CDF contours at various values of θ

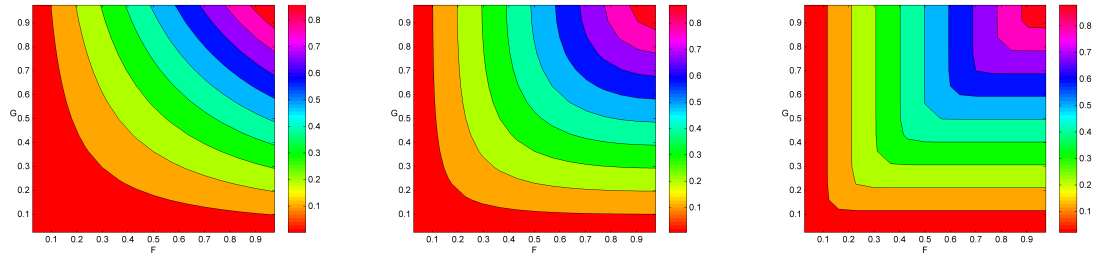

(a) $\theta = 1.05$ (b) $\theta = 2.0$ (c) $\theta = 15.0$

Figure 93: Gumbel copula joint distribution 2D CDF contours at various values of θ

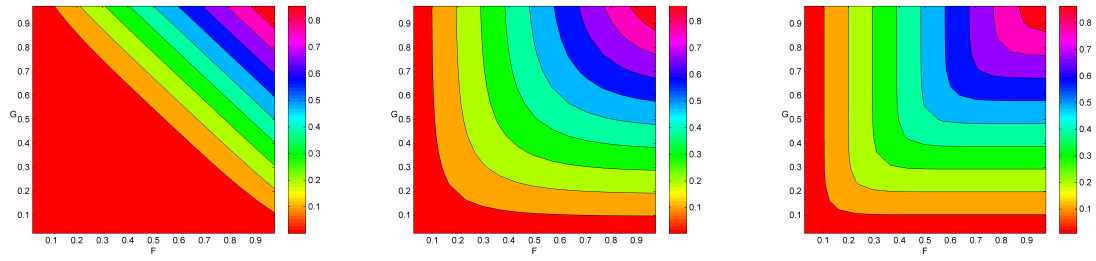

(a) $\theta = -10.0$ (b) $\theta = 5.0$ (c) $\theta = 20.0$

Figure 94: Frank copula joint distribution 2D CDF contours at various values of θ

While the CDF contours better indicate the differences between copulas than their corresponding 3D surfaces, in general this technique is not as revealing as plotting the marginal probability density functions (pdfs). The copula pdfs are often more telling of the correlation structure in the joint distribution because they show the behavior of the copula at each point in the bivariate space rather than an integrated sum. They are related to the copula CDFs through a mixed partial derivative expressed as:

$$c(u,v) = \frac{\partial^2 C(u,v)}{\partial u \partial v} \tag{63}$$

By analytically deriving the form of each family's pdf, the joint pdf can be plotted. This can be done in 3D similar to the copula CDFs, where the copula surface is shown in the third dimension above the unit square formed by two standard uniform random variables. This is demonstrated in Figs. 95-97 for the same Archimedean families and θ values to correspond with the CDF plots above.

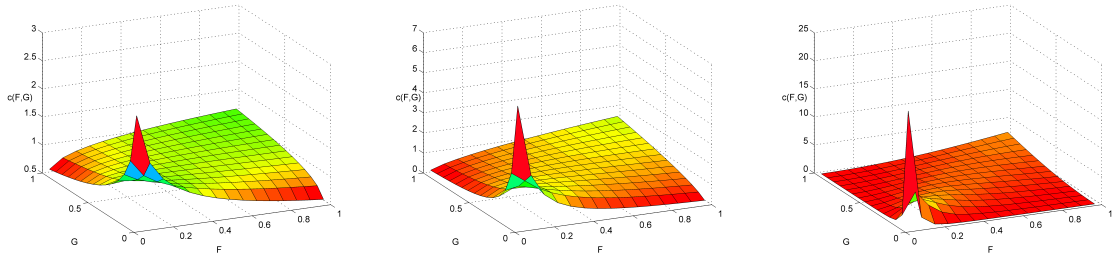

(a) $\theta = 0.2$ (b) $\theta = 0.6$ (c) $\theta = 2.0$

Figure 95: Clayton copula joint distribution 3D pdf surfaces at various values of θ

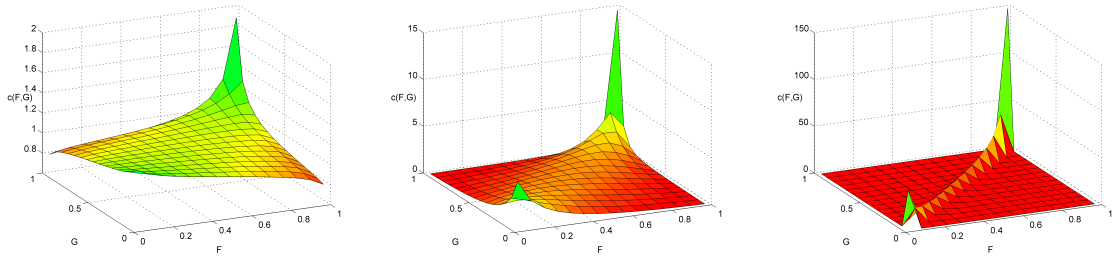

(a) $\theta = 1.05$ (b) $\theta = 2.0$ (c) $\theta = 15.0$

Figure 96: Gumbel copula joint distribution 3D pdf surfaces at various values of θ

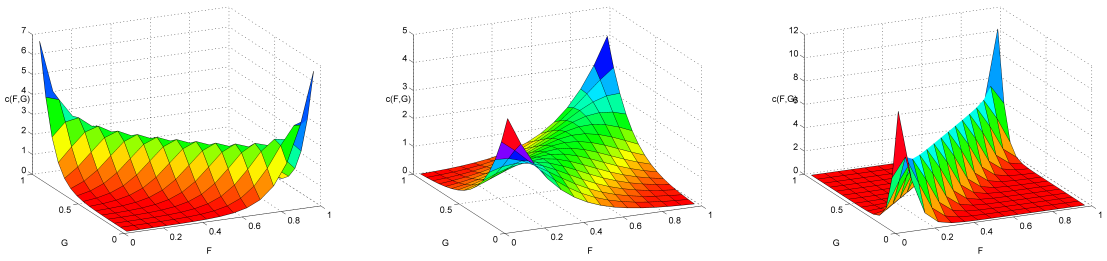

(a) θ = -10.0 (b) θ = 5.0 (c) θ = 20.0

Figure 97: Frank copula joint distribution 3D pdf surfaces at various values of θ

The 3D copula pdf surfaces are very indicative of the dependence structure defined by each copula and its correlation parameter θ. The 2D copula pdf contours corresponding to these 3D surfaces are shown in Figs. 98-100. These contours are important as they reflect the distinguishing features of copulas in a single 2D plane, which is the format most commonly found in the literature. These are used not only to identify copula families but also to select copulas most suitable for a given application. The 3D spikes seen in Figs. 95-97 represent higher concentrations of data points in the joint distribution. In these cases since they all occur at extreme values of the joint distributions, they indicate some form of tail dependence created by the copula. This tail dependence can also be see in the 2D contours of Figs. 98-100. These contours show where the majority of points will be distributed for the given copula simulation. These pdf charts are far more descriptive of the copula dependence structure than their corresponding CDF charts.

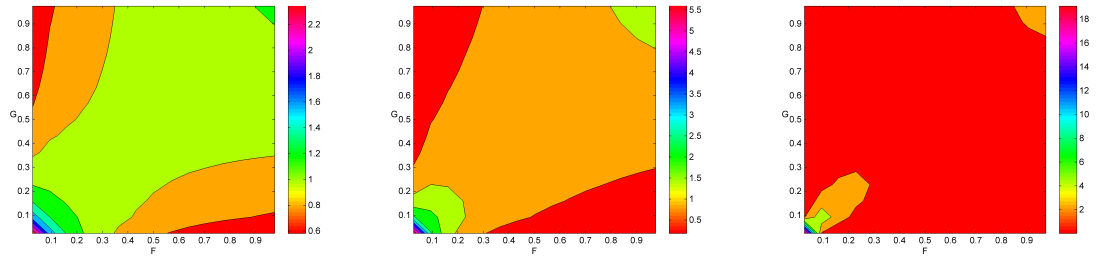

(a) θ = 0.2 (b) θ = 0.6 (c) θ = 2.0

Figure 98: Clayton copula joint distribution 2D pdf contours at various values of θ

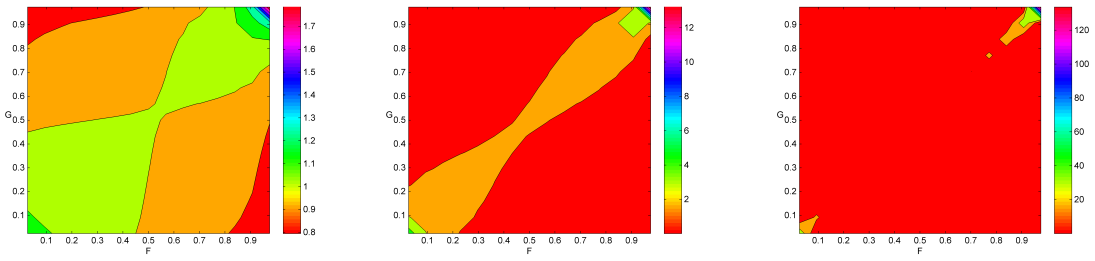

(a) $\theta = 1.05$ (b) $\theta = 2.0$ (c) $\theta = 15.0$

Figure 99: Gumbel copula joint distribution 2D pdf contours at various values of θ

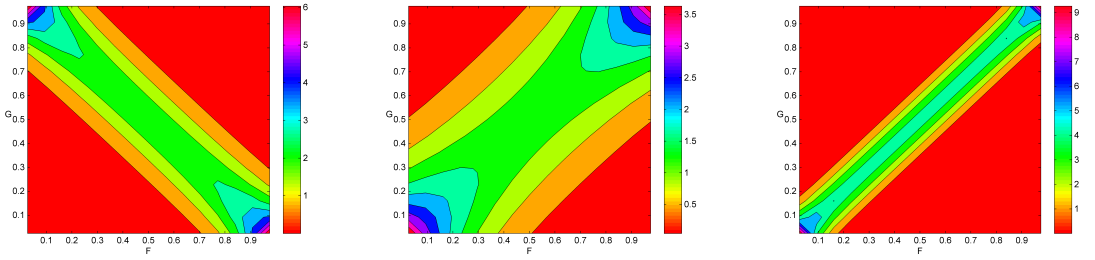

(a) θ = -10.0 (b) $\theta = 5.0$ (c) $\theta = 20.0$

Figure 100: Frank copula joint distribution 2D pdf contours at various values of θ

The figures shown above visualize simulations of three copula families from the Archimedean class, including their pdf and CDF distributions with 3D surfaces and 2D contour plots. These simulations are provided to give the reader an idea of the flexibility and capabilities enabled by copulas. However this is not an exhaustive list of copula families in this class or of other copula classes which exist in the literature. For further reference, Armstrong [8] and Nelsen [155] have cataloged more complete listings of many different copulas.

7.1.3.2 Numerical Simulations

The analytical methods which define copula pdfs and CDFs are helpful to visualize copula structure, but they are limited to when the copula and its associated functions (inverses, derivatives, etc) exist in closed form. When closed forms do not exist numerical simulations are necessary to visualize copulas. Visualizing copulas is useful

for selection purposes, but once a particular copula structure is decided upon; random variables pursuant to that joint distribution structure are needed for practical applications. The literature provides random number generation techniques employing a defined copula structure in the bivariate space. Typically these methods involve the copula cumulative distribution function, its inverse, its derivative, and the inverse of the derivative. Numerical approaches are necessary because the analytical solution for said functions is not trivial or does not exist. The degree of difficulty varies between each method and heavily depends upon the copula selected to correlate the random variables. Three common methods from the literature will be explored in subsequent sections. The first is the Conditional Distribution Method which can be applied analytically for only very simple copula functions. The next two methods are algorithms described by Nelsen [154] in two exercises from his text, exercises 4.13 and 4.14.

7.1.3.3 Conditional Distribution Method (Algorithm 1)

The Conditional Distribution Method is used to generate data for copula correlated random variables and is formally described by Johnson [98]. It leverages the copula partial derivative and its inverse to create a pair of numbers which have a joint distribution defined by the copula. The method is reviewed briefly by Nelsen [154, section 2.9] and is also applied in detail by Chen [33]. While the process itself is simple in theory, the analytical solution can be complex depending on the form of the copula. This is evident from Nelsen's [154] demonstration of the method which uses a simplification to the Ali-Mikhail-Haq copula which is already relatively straightforward. Chen [33] applies the method without simplification in complete analytical form which is considerably more detailed. In general terms the procedure is as follows for n-number of random variables, $X_1, X_2, X_3, ..., X_n$:

1. Generate a sample $X_1 = x_1$, from the marginal distribution of X_1

2. Generate a sample $X_2 = x_2$, from the conditional distribution of X_2 given that $X_1 = x_1$

3. Generate a sample $X_3 = x_3$, from the conditional distribution of X_3 given that$X_1 = x_1$ and $X_2 = x_2$

4. Continue generating samples in this manner for all X_n

In the case of two standard uniform ($U(0,1)$) random variables U and V, with a copula joint distribution $C(u,v)$; first sample u from the marginal distribution U and then sample v from the conditional distribution V, given $U = u$. From a practical perspective the conditional distribution can be found by taking a partial derivative with respect to the conditional variable. This is formulated by Nelsen [154] as:

$$c_u(v) = \Pr\left[V \leq v | U \leq u\right] = \frac{\partial}{\partial u} C(u,v) \tag{64}$$

For an analytical demonstration of the method take the simple copula form,

$$C(u,v) = \frac{uv}{1-(1-u)(1-v)} \tag{65}$$

and find its conditional distribution with respect to u,

$$c_u(v) = \frac{\partial}{\partial u} C(u,v) = \left(\frac{v}{u+v-uv}\right)^2 \tag{66}$$

and then calculate its inverse to find v.

$$v = c_u^{-1}(t) = \frac{u\sqrt{t}}{1-(1-u)\sqrt{t}} \tag{67}$$

The paired desired following the prescribed copula distribution is (u,v). Now it is clear that the difficulty in analytical methods lies in taking the selected copula's derivative and then even more so in taking the inverse of that derivative. When the complexity of the copula form makes analytical methods prohibitive, numerical methods are needed. When employing numerical methods the algorithm for this method is as follows:

1. Generate standard uniformly distributed random variables u and t between 0 and 1
2. Calculate the the conditional distribution of the desired copula, $c_u(v) = \frac{\partial}{\partial u} C(u, v)$
3. Calculate the quasi-inverse of the conditional distribution and set that equal to v, $v = c_u^{(-1)}(t)$
4. The pair (u, v) is the desired sample

Numerical methods allow us to easily generate the required distributions and act upon them to calculate the required function derivatives and inverses. The reason for the presence of the uniform variable t is not always obvious, however after considering that both u and v are random variables it becomes clear that setting a value for u with the conditional distribution $c_u(v)$, does not immediately provide a fixed choice for the value of v. Sampling a particular value of u from U yields a slice of the joint distribution upon which v must lie. The uniform variable t specifies where along that distribution v is located. The Conditional Distribution Method makes no limitations on the types of copulas it can simulate. Two other numerical algorithms which are specifically for Archimedean copulas are discussed in the next sections.

7.1.3.4 Simulation Algorithm 2

This algorithm is intended for Archimedean copulas created by generator functions, $\phi_\theta(t)$, via Eq 62. It is based upon work presented by Genest and Rivest [65] and is summarized in Exercise 4.13 of Nelsen's [154] text as follows:

1. Generate two independent uniform distributions s and t, between 0 and 1;
2. Set $w = K_C^{(-1)}(t)$ where K_C is,

$$K_C(t) = t - \frac{\phi(t)}{\phi'(t^+)} \tag{68}$$

3. Set $u = \phi^{[-1]}(s\phi(w))$;

4. Set $v = \phi^{[-1]}((1-s)\phi(w))$;

5. The desired pair is (u, v)

The algorithm itself is simple enough to comprehend but in practical implementation several challenges arise which are both general to the method and specific to the software package chosen. These will be commented on to aid the practitioner in conducting simulations. The first step is to generate two uniform distributions between 0 and 1 representing the independent random variables s and t. Then calculate K_C for the random variable t as given by equation (68). In order to calculate this, evaluate the value of the chosen generator function, ϕ, for each point in t, i.e. $\phi(t)$. Then compute the derivative of the generator function, $\phi'(t)$. This can be done using a native derivative function or by employing the basic definition of a derivative,

$$f'(a) = \lim_{h \to 0} \frac{f(a+h) - f(a)}{h} \tag{69}$$

If it is not already an internal function, it is useful to to store the preferred method of calculating the derivative as a function which can intake any data vector as an argument. Then compute $K_C(t)$ which actually represents the x-intercept of the tangent line to the curve produced by the generator function $\phi(t)$, as depicted by Nelsen [154, section 4.3].

A practical note is that most software packages find vector manipulation much more efficient than computing serially in loops, so it is recommended that the practitioner maintain distribution data and subsequent calculations in vector form for computational efficiency, particularly for high density simulations.

Next the inverse of $K_C(t)$ is calculated for every point in t. Graphically speaking the inverse is simple to understand; it is the reflection of the function in the line y = x. However numerically, it may be hard to implement this when a closed form

solution is difficult to obtain or does not exist. The inverse can be computed by a native inverse function or it can also be found using a simple interpolation function which uses $K_C(t)$ as its input along with a linearly space vector to calculate the y coordinates that correspond to the given x points. If the inverse function must be created, then it is advisable to store it in a manner where it can be executed by passing any data vector as an argument. This will be useful in the following steps.

Once $K_C^{(-1)}(t)$ is found and set to the intermediate variable w, the random variable u can be computed. To begin finding u first evaluate the generator function ϕ, for each point in w, i.e. $\phi(w)$. Then multiply each element in the independent uniform distribution s by $\phi(w)$, yielding a vector given by $(s\phi(w))$. Next calculate ϕ of this data vector. Then take the inverse of the resulting vector, $\phi(s\phi(w))$. This vector is $\phi^{[-1]}(s\phi(w))$ and should be set equal to u.

The random variable v is similarly computed, with a slight difference in that $\phi(w)$ is multiplied by $1-s$, such that $((1-s)\phi(w))$. Then take the inverse of the resulting vector, $((1-s)\phi(w))$. This vector is $\phi^{[-1]}((1-s)\phi(w))$ and should be set equal to the dependent random variable v. The desired pair of the simulation is (u, v) and follows the joint distribution of the copula formed by the generator ϕ_θ.

The points contained in the correlated data vectors u and v should be plotted in a scatter plot along with their marginal distributions (similar to Figs. 10-13). Since u and v are dependent random variables their joint scatter plots will exhibit interesting and correlated behavior based on the specific copula chosen and its dependence structure. However the marginal distributions of u and v should still be uniform between 0 and 1. This is a basic test that the algorithm was executed correctly, so it is important to examine the marginals of u and v for uniformity.

7.1.3.5 Simulation Algorithm 3

This algorithm is also only for Archimedean copulas constructed from generator functions, $\phi_\theta(t)$, using Eq 62. It is based upon work from Genest and MacKay [64] and is summarized in Exercise 4.14 of Nelsen's [154] text as follows:

1. Generate two independent uniform distributions u and t, between 0 and 1;
2. Set $w = \phi'^{[-1]}(\phi(u)/t)$;
3. Set $v = \phi^{[-1]}(\phi(w) - \phi(u))$;
4. The desired pair is (u, v)

The first step is to generate two uniform distributions between 0 and 1 representing the independent random variables u and t. While maintaining all variables in vector form for computational efficiency, use the chosen copula generator function ϕ, to evaluate $\phi(u)$. Then divide the resulting vector by the independent uniform distribution t. Since $(\phi(u)/t)$ is a ratio whose denominator is a random variable that can take on small values, the practitioner is advised to be cautious of this quotient generating infinity or non-numeric data points which can lead to errors in latter steps of the algorithm, particularly when the inverse is calculated.

Once $(\phi(u)/t)$ has been screened for unwanted data entries, its derivative is calculated using a native function or the derivative function constructed earlier following Eq. (69). Next the inverse of the derivative is found which yields the vector $\phi'^{[-1]}(phi(u)/t)$. This is set equal to an intermediate variable w, which will be used to determine v. In order to do this evaluate $\phi(w)$ and $\phi(u)$ separately. Then take their difference, $(\phi(w) - \phi(u))$, and calculate ϕ of that difference, i.e. $\phi((\phi(w) - \phi(u)))$. Finally using the inverse function determine the inverse of this vector which is $\phi^{[-1]}(\phi(w) - \phi(u))$ and set it to the dependent random variable v. The desired pair of the simulation is (u, v).

The points contained in the correlated data vectors u and v should then be plotted in a scatter plot displaying their joint distributions (similar to Figs. 10-13) along with their marginal distributions. An important check that the algorithm was executed correctly is to examine the marginal distributions for uniformity.

There are many different types of simulations that can be run with different generator functions from Table 32, using varying values of θ and number of points in each simulation. Depending on the choice of the practitioner the resulting copulas simulation can take many different forms.

It has been demonstrated how copulas functions can be simulated utilizing two algorithms discussed in literature [154, 65, 64] and have provided the reader with practical tools and guidance to conduct their own simulations.

7.2 Appendix B: Discriminant Analysis Reports

7.2.1 Introduction

Discriminant analysis is a machine learning algorithm used to predict membership in subgroups based on a given set of covariates. These covariate factors are used to analyze the incoming copulas and assess which subgroup they belong to as they pass through a CAST (CopulA Selection Tree) decision gate. The discriminant analysis reports for all of the tested combinations of covariates at Decision Gate 1 are presented in this in main body of this work. This section of the appendix contains the discriminant analysis reports for the remaining nine decision gates.

7.2.2 Decision Gate 2

Decision Gate 2 receives all copulas predicted as linear by Decision Gate 1 and tries to determine if they are positively or negatively correlated. The objective metrics available to the discriminant analysis algorithm at Decision Gate 2 are Pearson's ρ, Kendall's τ, Spearman's ρ, and Covariance (cov). Several experiments are conducted to determine which covariate is the best discriminator to objectively determine the subgroups leaving this decision gate. First each objective metric is tested individually, beginning with Pearson's ρ whose results are shown in Fig. 101.

This experiment gives 0 mislabeled copulas so Pearson's ρ is a good discriminating metric for this decision gate. For completeness the remaining objective metrics at this decision gate are also tested. The results of Kendall's τ are shown in Fig. 102.

This experiment gives 0 mislabeled copulas indicating that Kendall's τ is also a good discriminant for Decision Gate 2. Spearman's ρ is tested next and its results are shown in Fig. 103.

This experiment gives 0 mislabeled copulas indicating that Spearman's ρ is also a good discriminant for Decision Gate 2. Covariance (cov) is the final covariate to be tested and its results are shown in Fig. 104.

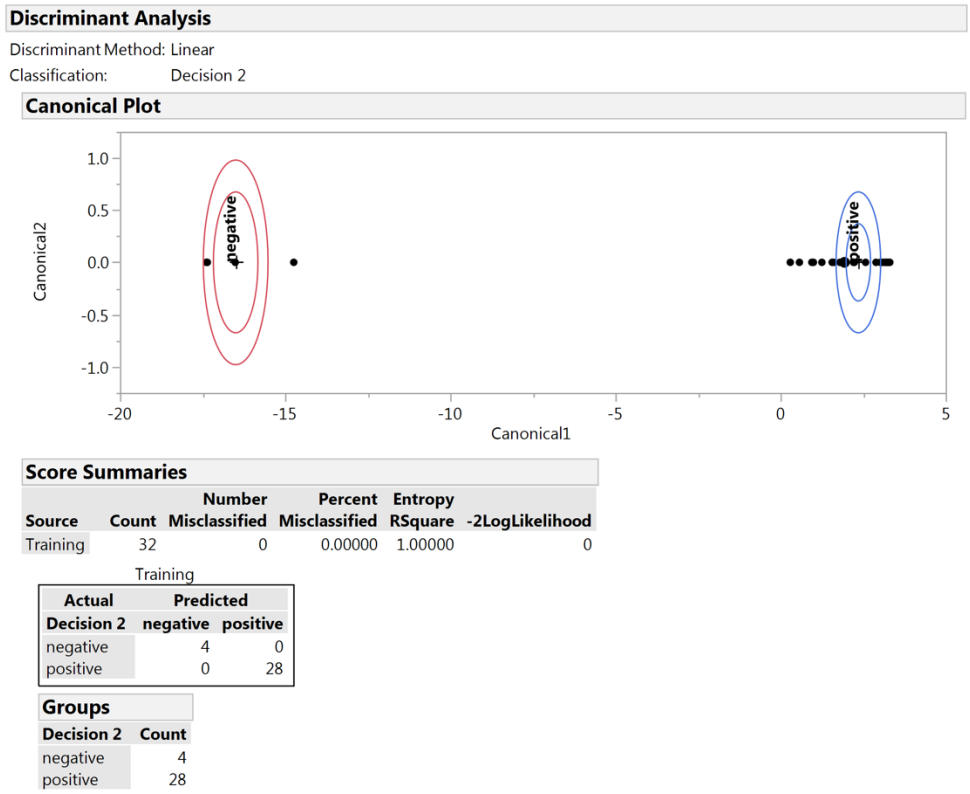

Figure 101: Discriminant analysis at Decision Gate 2 with Pearson's ρ

This experiment gives 0 mislabeled copulas indicating that Covariance (cov) is also a good discriminant for Decision Gate 2. All of the tested covariates are excellent discriminators at this decision gate but only one is needed in the objective tree. Kendall's τ had the narrowest range on its canonical plot indicating greater sensitivity in its metric values to predicting the proper subgroup for copulas leaving Decision Gate 2. The threshold value is recorded and used to label copulas leaving Decision Gate 2 as positive or negative and passed on to Decision Gate 6 and Decision Gate 7.

7.2.3 Decision Gate 3

Decision Gate 3 receives all copulas predicted as nonlinear by Decision Gate 1 and tries to determine whether they have a linear Pareto frontier, a curved Pareto frontier, or an evenly scattered joint distribution. The objective metrics available to the discriminant

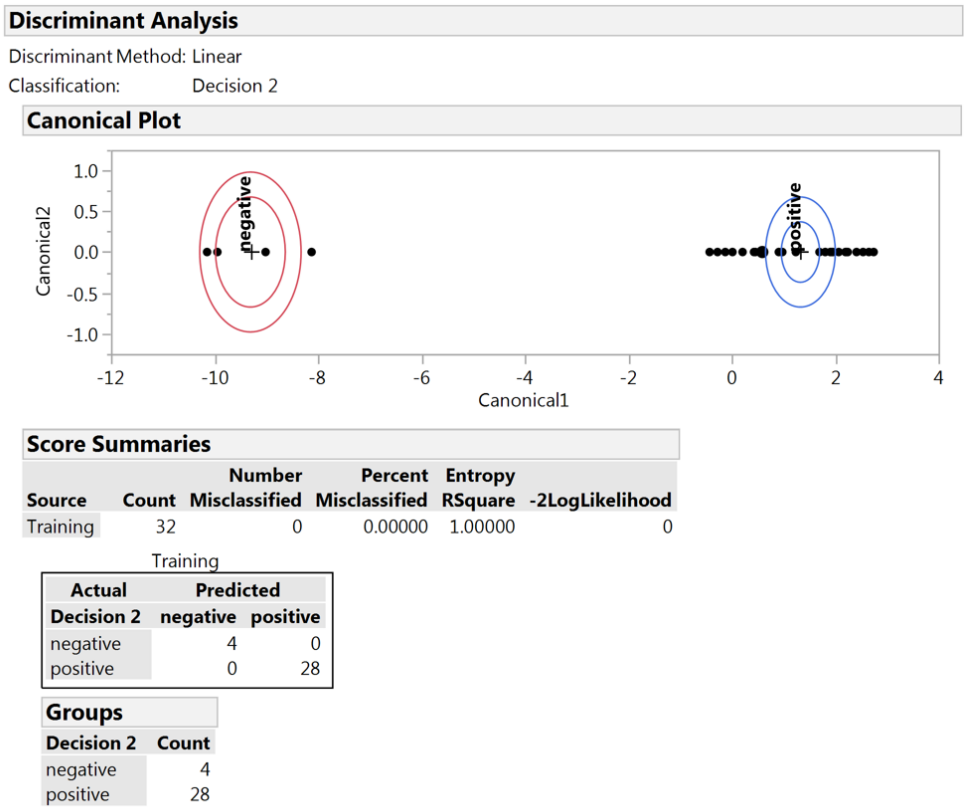

Figure 102: Discriminant analysis at Decision Gate 2 with Kendall's τ

analysis algorithm at Decision Gate 3 are Avg Pareto Inverse Distance ($\bar{d}_{\phi}^{-1}$), Pareto Frontier Point Density (ϕ), Avg Inverse Distance ($\bar{d}^{-1}$). Each of these is tested with single covariate discriminant analysis experiments to determine which is the best discriminator for this decision gate. Avg Pareto Inverse Distance ($\bar{d}_{\phi}^{-1}$) is tested first and the results are shown in Fig. 105.

This experiment gives 1 mislabeled copula indicating that Avg Pareto Inverse Distance ($\bar{d}_{\phi}^{-1}$) is a good discriminator at this decision gate. Next Pareto Frontier Point Density (ϕ) is tested and its discriminant analysis results are shown in Fig. 106.

This experiment gives 3 mislabeled copulas suggesting that Pareto Frontier Point Density (ϕ) is not as good a discriminant as Avg Pareto Inverse Distance ($\bar{d}_{\phi}^{-1}$) for Decision Gate 3. Avg Inverse Distance ($\bar{d}^{-1}$) is the last single covariate to be tested

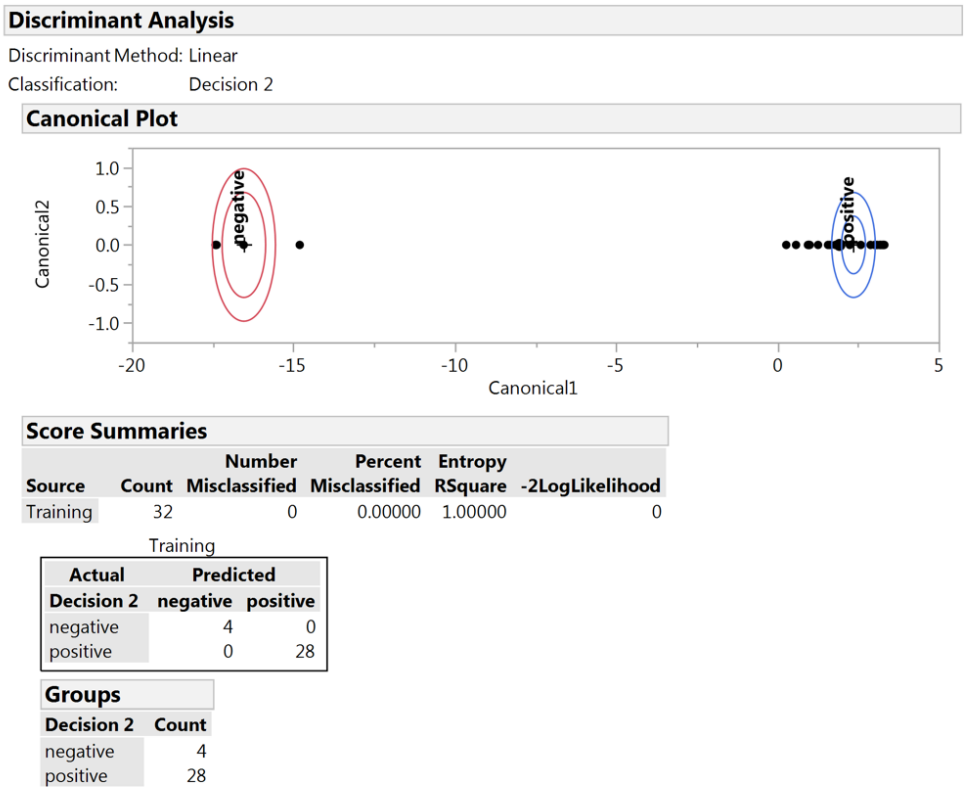

Figure 103: Discriminant analysis at Decision Gate 2 with Spearman's ρ

for this decision gate and its results are given in Fig. 107.

This experiment gives 10 mislabeled copulas indicating that Avg Inverse Distance ($\bar{d}^{-1}$) is not a good discriminant on its own for Decision Gate 3. Next combinations of covariates are tested to see if they can perform better than the single covariates. The first combination tested is Avg Pareto Inverse Distance ($\bar{d}_{\phi}^{-1}$) and Pareto Frontier Point Density (ϕ). The results of this combined discriminant analysis run are shown in Fig. 108.

This experiment gives 5 mislabeled copulas indicating that this combination is not the best discriminator for Decision Gate 3. The next combination is Pareto Frontier Point Density (ϕ) and Avg Inverse Distance ($\bar{d}^{-1}$). The results of this experiment are given in Fig 109.

This experiment gives 5 mislabeled copulas indicating that Pareto Frontier Point

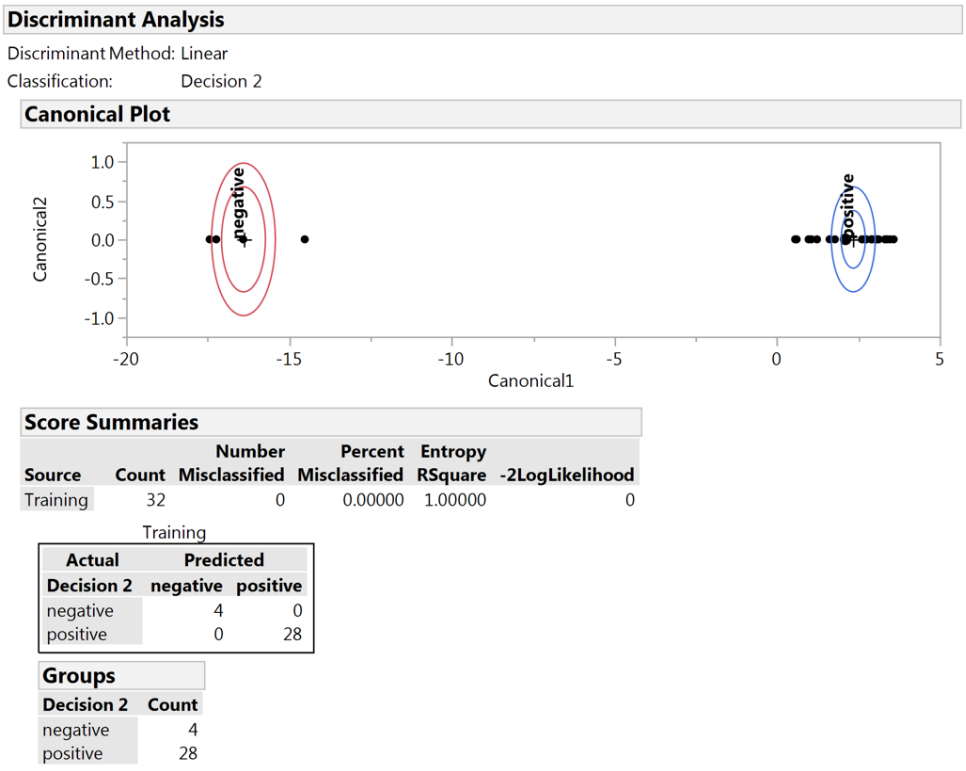

Figure 104: Discriminant analysis at Decision Gate 2 with Covariance (cov)

Density (ϕ) and Avg Inverse Distance ($\bar{d}^{-1}$) are not a better combination than the previous one. The last combination to be tested is Avg Inverse Distance ($\bar{d}^{-1}$) and Avg Pareto Inverse Distance ($\bar{d}_{\phi}^{-1}$). The results of this experiment are shown in Fig 110.

This experiment gives 4 mislabeled copulas suggesting that the Avg Inverse Distance ($\bar{d}^{-1}$) and Avg Pareto Inverse Distance ($\bar{d}_{\phi}^{-1}$) combinations is better than the other tested combinations, but not better than the single covariate Avg Pareto Inverse Distance ($\bar{d}_{\phi}^{-1}$). This will be saved and its threshold values recorded to be used as the main discriminant in Decision Gate 3. Copulas leaving Decision Gate 3 are passed to Decision Gate 4 and Decision Gate 5, or labeled as Leaf E if they are predicted as being evenly scattered.

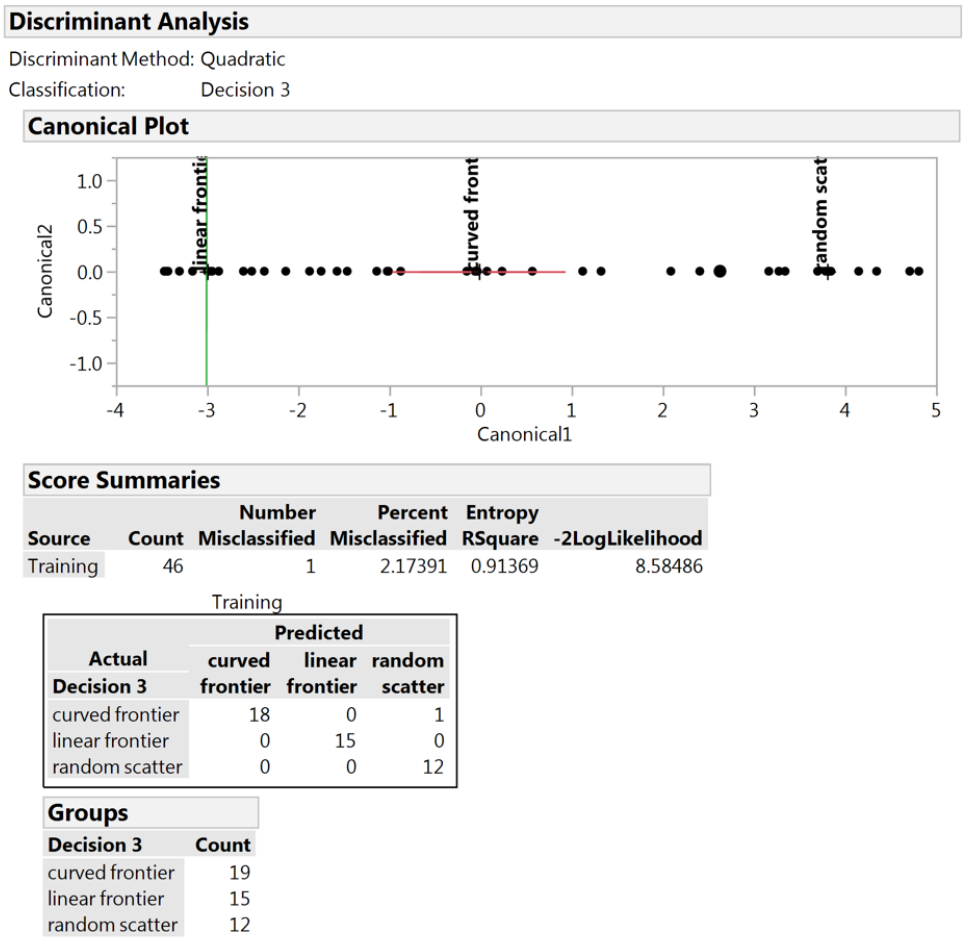

Figure 105: Discriminant analysis at Decision Gate 3 with Avg Pareto Inverse Distance ($\bar{d}_{\phi}^{-1}$)

7.2.4 Decision Gate 4

Decision Gate 4 receives all copulas predicted as having a linear frontier by Decision Gate 3 and tries to determine whether they have sparse or dense corner sampling behind the Pareto frontier. The objective metrics available to the discriminant analysis algorithm at Decision Gate 4 are Upper Density (σ_{Upp}), Pareto Corner Density (σ_{ϕ}), and Pareto Frontier Point Density (ϕ). Each of these is tested with single covariate discriminant analysis experiments to determine which is the best discriminator for this decision gate. Upper Density (σ_{Upp}) is tested first and the results are shown in Fig. 111.

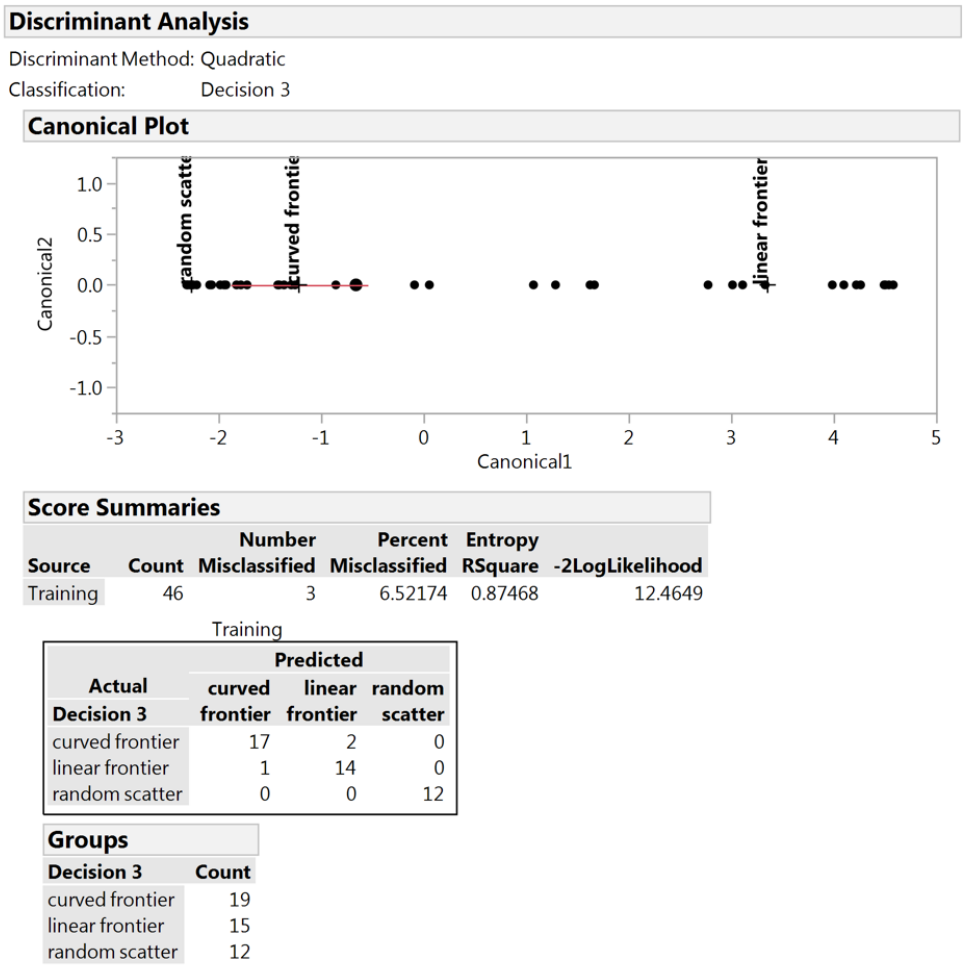

Figure 106: Discriminant analysis at Decision Gate 3 with Pareto Frontier Point Density (ϕ)

This experiment gives 7 mislabeled copulas indicating that Upper Density (σ_{Upp}) is not a good discriminant for this decision gate. The next covariate is Pareto Corner Density (σ_ϕ) and discriminant analysis results are shown in Fig. 112.

This experiment gives 0 mislabeled copulas indicating that Pareto Corner Density (σ_ϕ) is an excellent discriminator for Decision Gate 4. For completeness, Pareto Frontier Point Density (ϕ) is also tested as a single covariate and its results are shown in Fig. 113.

This experiment gives 1 mislabeled copula suggesting that Pareto Frontier Point Density (ϕ) is a good discriminator for Decision Gate 4, but not as good as Pareto

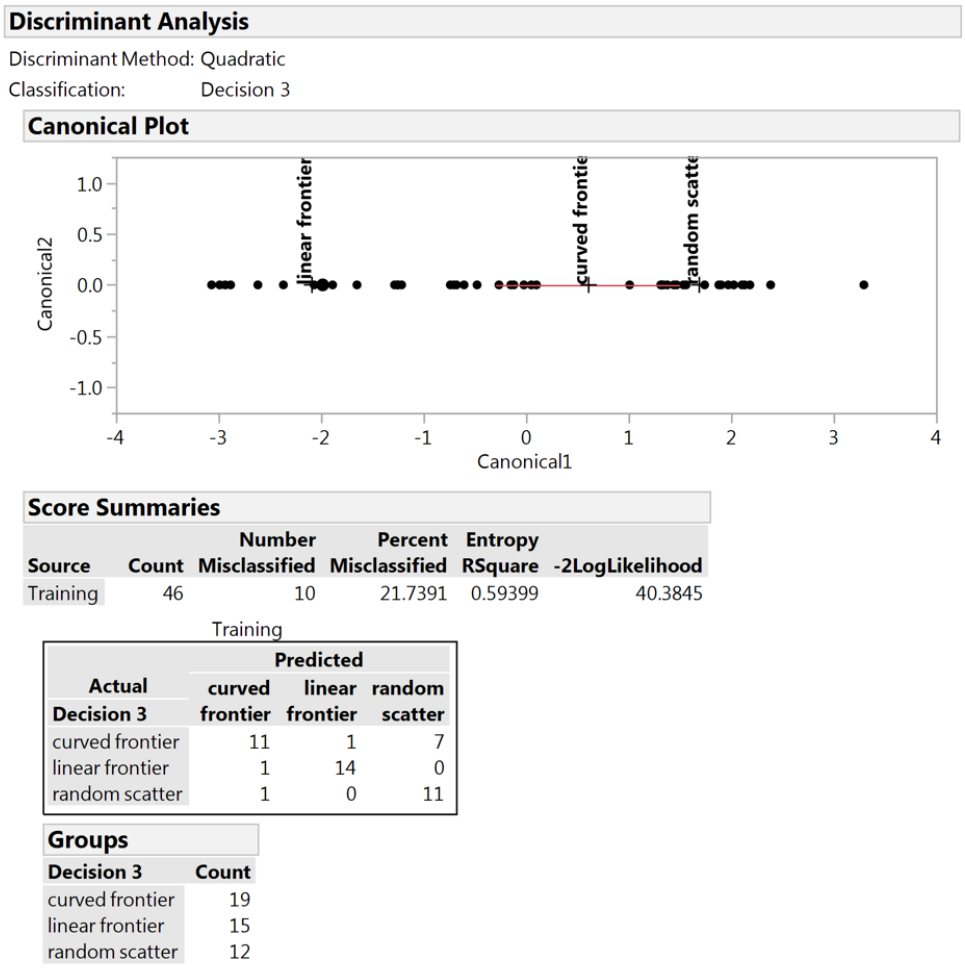

Figure 107: Discriminant analysis at Decision Gate 3 with Avg Inverse Distance ($\bar{d}^{-1}$)

Corner Density (σ_ϕ). The threshold value of Pareto Corner Density (σ_ϕ) is recorded and used to label copulas leaving Decision Gate 4 as having sparse or dense Pareto corner sampling. Sparse copulas are labeled as leaf C and dense copulas are labeled as leaf D.

7.2.5 Decision Gate 5

Decision Gate 5 receives all copulas predicted as having a curved frontier by Decision Gate 3 and tries to determine whether they have sparse or dense corner sampling behind the Pareto frontier. The objective metrics available to the discriminant analysis algorithm at Decision Gate 5 are Upper Density (σ_{Upp}), Pareto Corner Density (σ_ϕ),

Discriminant Analysis

Discriminant Method: Linear

Classification: Decision 3

Canonical Plot

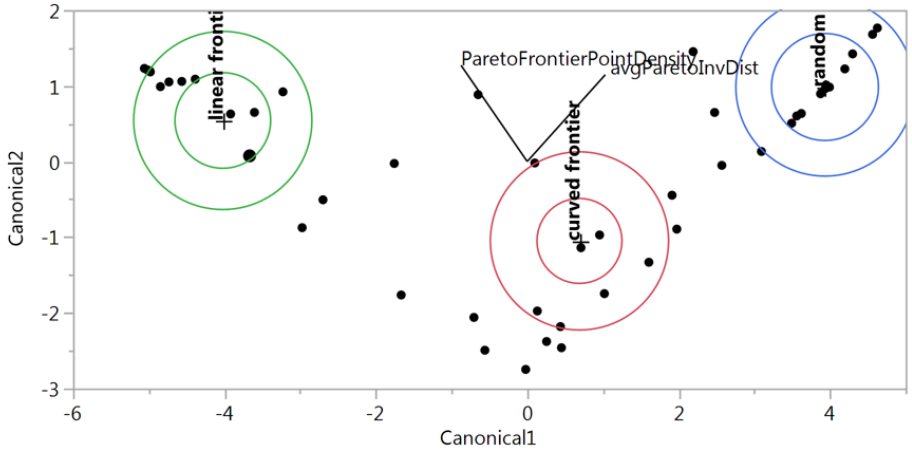

Score Summaries

Source	Count	Number Misclassified	Percent Misclassified	Entropy RSquare	-2LogLikelihood
Training	46	5	10.8696	0.80087	19.8073

Training

Actual Decision 3	Predicted curved frontier	linear frontier	random scatter
curved frontier	15	1	3
linear frontier	1	14	0
random scatter	0	0	12

Groups

Decision 3	Count
curved frontier	19
linear frontier	15
random scatter	12

Figure 108: Discriminant analysis at Decision Gate 3 with Avg Pareto Inverse Distance ($\bar{d}_{\phi}^{-1}$) and Pareto Frontier Point Density (ϕ)

and Pareto Frontier Point Density (ϕ). Each of these is tested with single covariate discriminant analysis experiments to determine which is the best discriminator for this decision gate. Upper Density (σ_{Upp}) is tested first and the results are shown in Fig. 114.

This experiment gives 7 mislabeled copulas indicating that Upper Density (σ_{Upp}) is not a good discriminant for this decision gate. The next covariate is Pareto Corner Density (σ_{ϕ}) and discriminant analysis results are shown in Fig. 115.

Discriminant Analysis

Discriminant Method: Linear

Classification: Decision 3

Canonical Plot

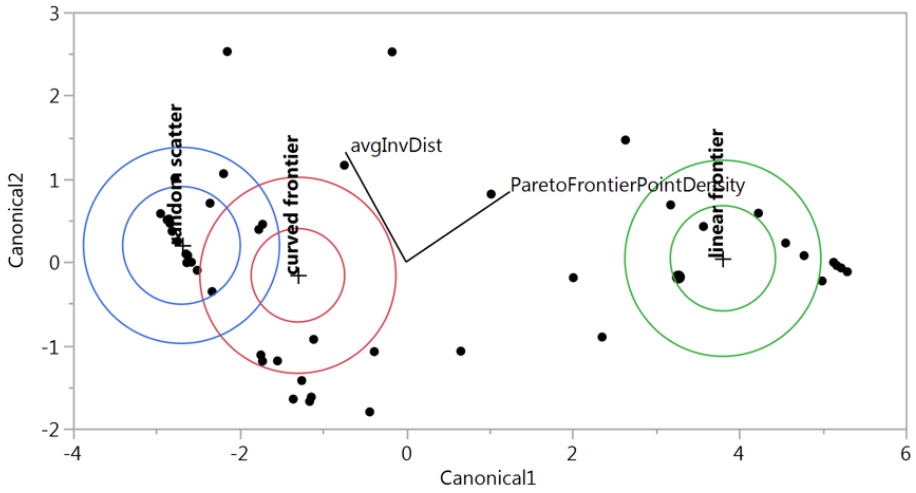

Score Summaries

Source	Count	Number Misclassified	Percent Misclassified	Entropy RSquare	-2LogLikelihood
Training	46	5	10.8696	0.67210	32.6153

Training

Actual Decision 3	Predicted curved frontier	linear frontier	random scatter
curved frontier	15	0	4
linear frontier	1	14	0
random scatter	0	0	12

Groups

Decision 3	Count
curved frontier	19
linear frontier	15
random scatter	12

Figure 109: Discriminant analysis at Decision Gate 3 with Pareto Frontier Point Density (ϕ) and Avg Inverse Distance ($\bar{d}^{-1}$)

This experiment gives 0 mislabeled copulas indicating that Pareto Corner Density (σ_ϕ) is an excellent discriminator for Decision Gate 5. For completeness, Pareto Frontier Point Density (ϕ) is also tested as a single covariate and its results are shown in Fig. 116.

This experiment gives 7 mislabeled copulas suggesting that Pareto Frontier Point Density (ϕ) is not a good discriminator for Decision Gate 5. Pareto Corner Density

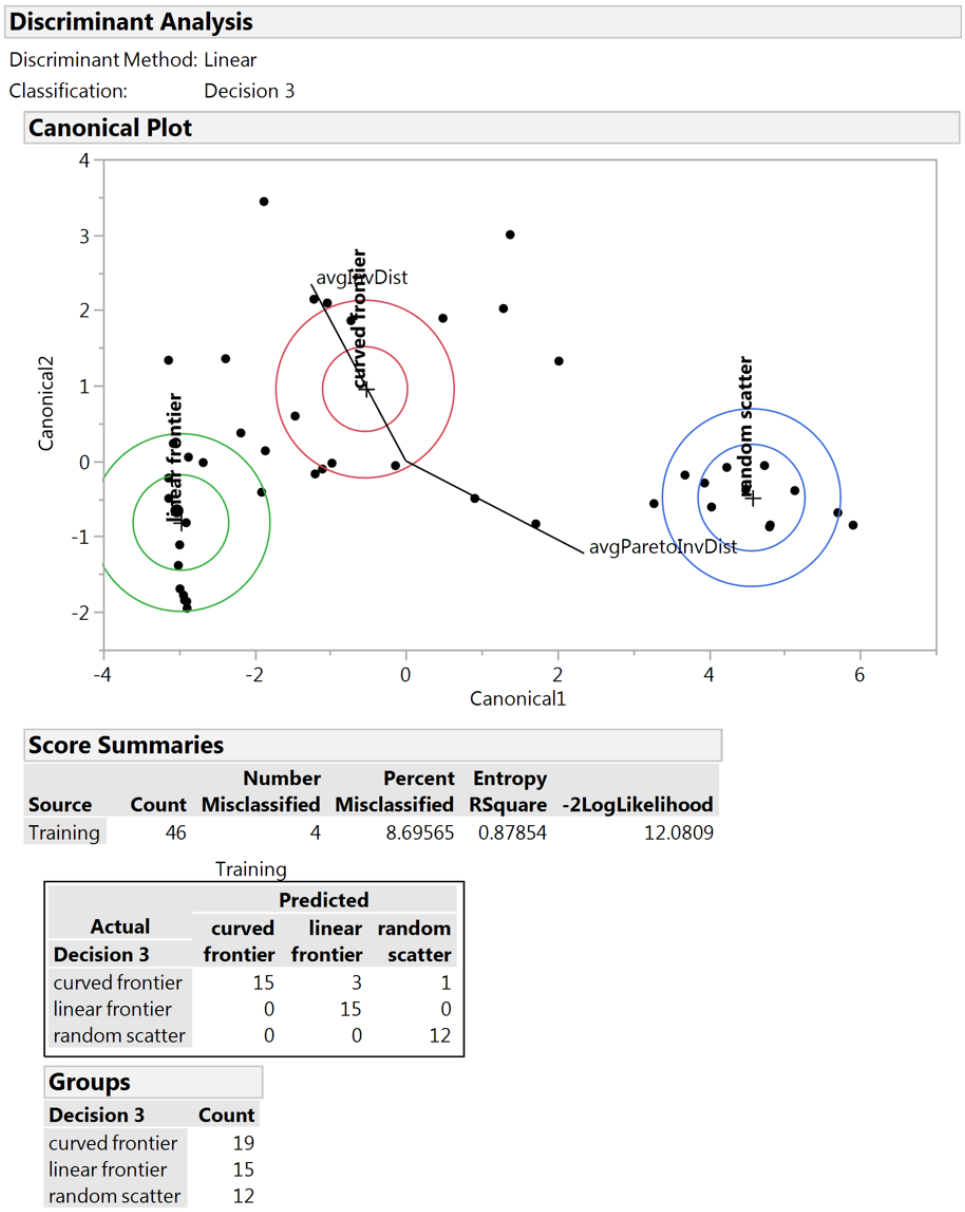

Figure 110: Discriminant analysis at Decision Gate 3 with Avg Inverse Distance ($\bar{d}^{-1}$) and Avg Pareto Inverse Distance ($\bar{d}_{\phi}^{-1}$)

(σ_{ϕ}) is the best performing covariate in the experiments for this deicison gate. Its threshold value is recorded and used to label copulas leaving Decision Gate 5 as having sparse or dense Pareto corner sampling. Sparse copulas are labeled as leaf B and dense copulas are labeled as leaf A.

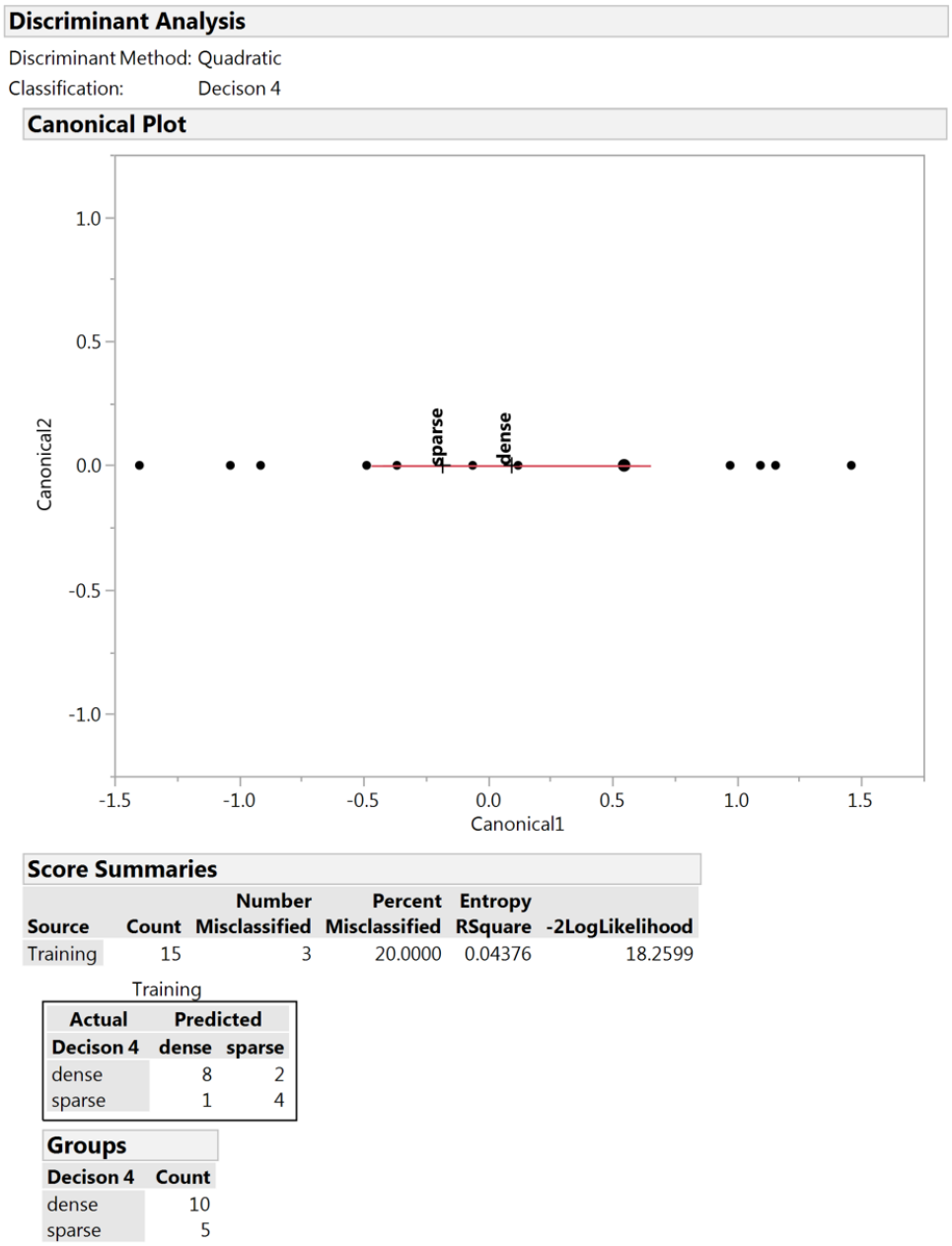

Figure 111: Discriminant analysis at Decision Gate 4 with Upper Density (σ_{Upp})

7.2.6 Decision Gate 6

Decision Gate 6 receives all copulas predicted as negatively correlated by Decision Gate 2 and tries to determine if their dependence structure is tail dependent or evenly distributed. The objective metrics available to the discriminant analysis algorithm

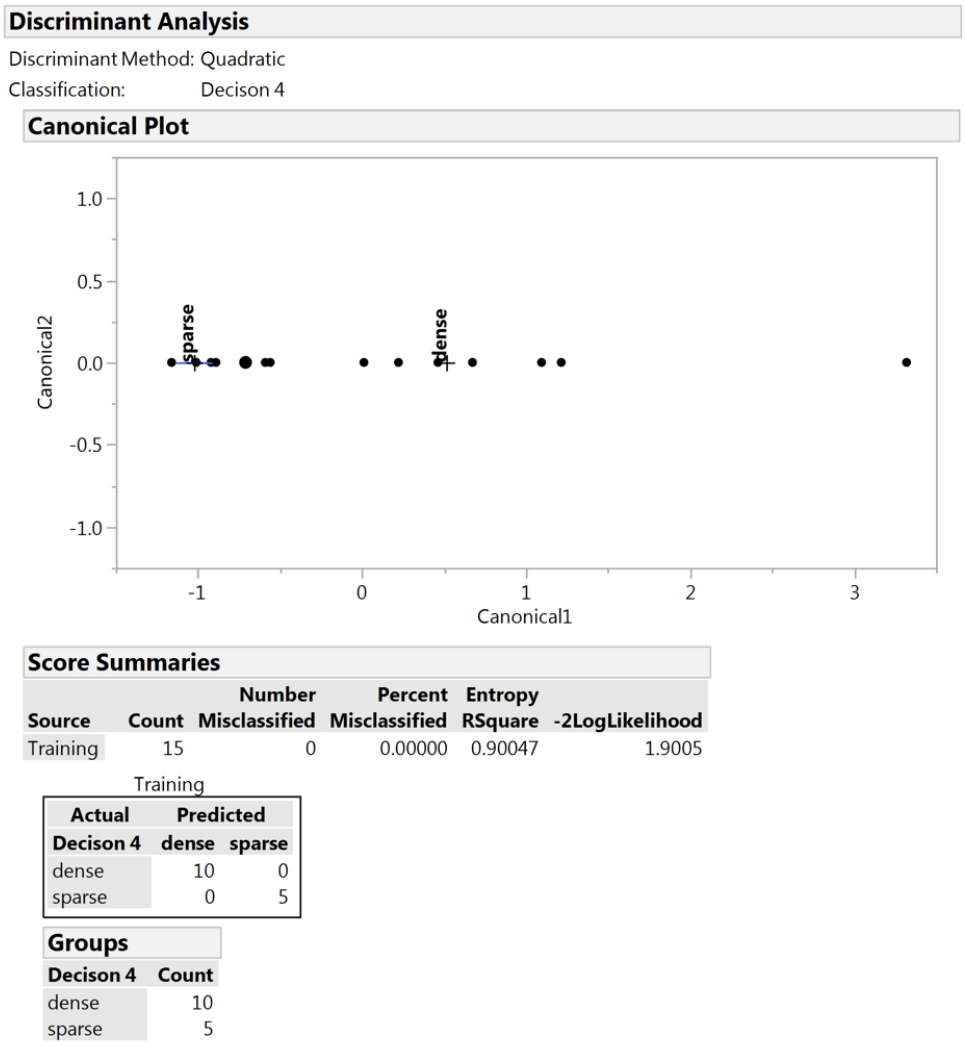

Figure 112: Discriminant analysis at Decision Gate 4 with Pareto Corner Density (σ_ϕ)

at Decision Gate 6 are Avg Inverse Lower Distance ($\bar{d}^{-1}_{Low}$), Avg Inverse Middle Distance ($\bar{d}^{-1}_{Mid}$), and Avg Inverse Upper Distance ($\bar{d}^{-1}_{Upp}$). Single covariate discriminant analysis experiments are conducted to determine which is the best discriminator for this decision gate, beginning with Avg Inverse Lower Distance ($\bar{d}^{-1}_{Low}$). The results are given in Fig. 117.

This experiment gives 0 mislabeled copulas indicating that Avg Inverse Lower Distance ($\bar{d}^{-1}_{Low}$) is a good discriminator for this decision gate. Avg Inverse Middle Distance ($\bar{d}^{-1}_{Mid}$) is tested next and its results are given in Fig. 118.

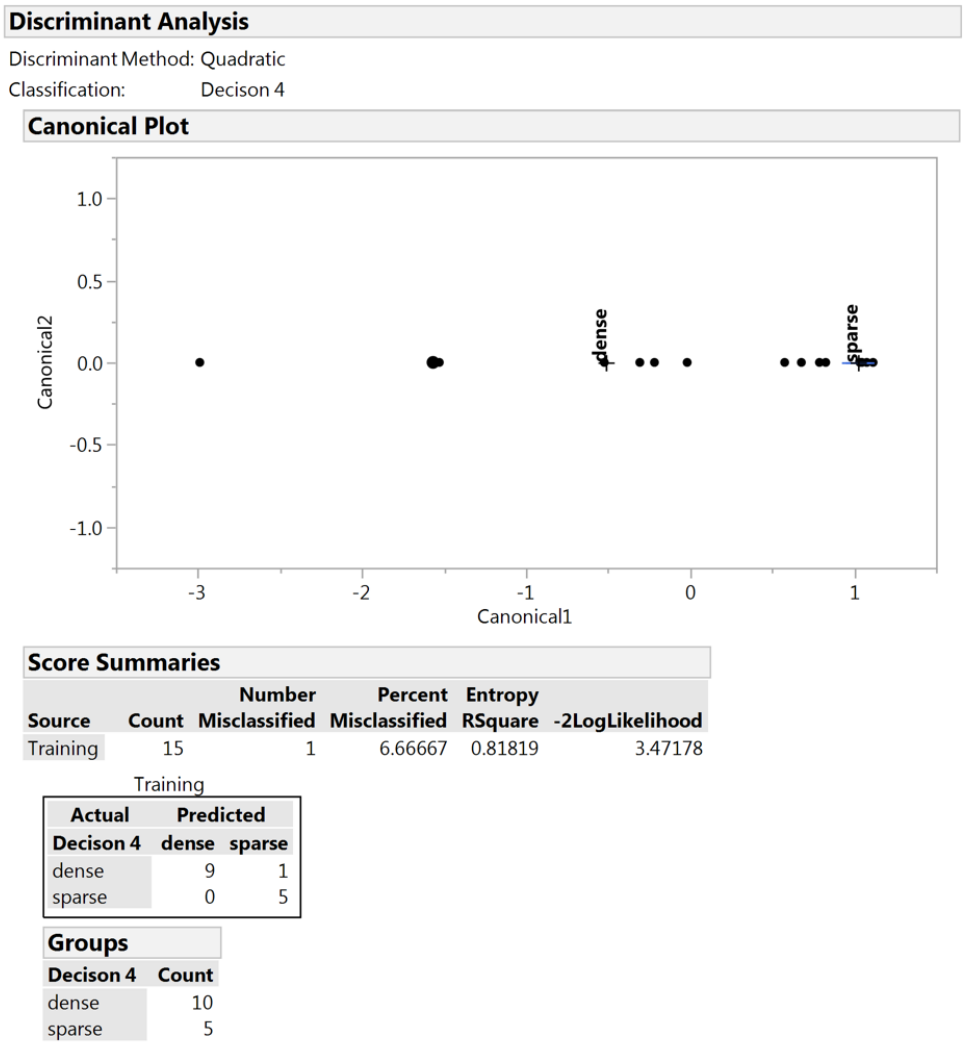

Figure 113: Discriminant analysis at Decision Gate 4 with Pareto Frontier Point Density (ϕ)

This experiment gives 0 mislabeled copulas indicating that Avg Inverse Middle Distance ($\bar{d}^{-1}_{Mid}$) is a good discriminator for this decision gate. Avg Inverse Upper Distance ($\bar{d}^{-1}_{Upp}$) is tested next and its results are given in Fig. 119.

This experiment gives 0 mislabeled copulas indicating that Avg Inverse Upper Distance ($\bar{d}^{-1}_{Upp}$) is also a good discriminator for Decision Gate 6. Since all of these covariates performed well on the relatively small input sample of copulas from Decision Gate 2, the best performing one will be selected. Avg Inverse Middle Distance ($\bar{d}^{-1}_{Mid}$) had the greatest R-squared value and highest probability of prediction amongst all

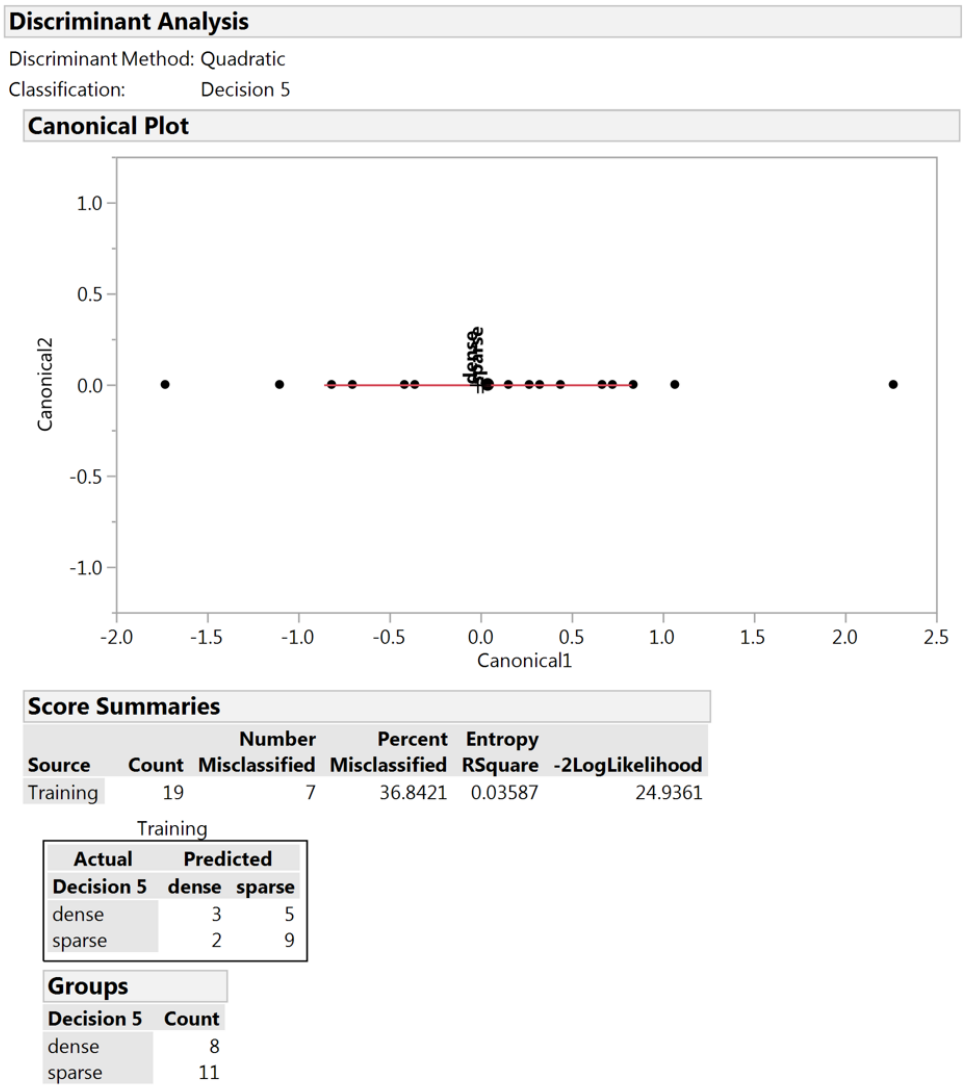

Figure 114: Discriminant analysis at Decision Gate 5 with Upper Density (σ_{Upp})

the covariates. Its threshold value is recorded and used to label copulas leaving Decision Gate 6 as having tail dependent or evenly distributed joint distributions. Tail dependent copulas are labeled as leaf G and evenly distributed copulas are labeled as leaf F.

7.2.7 Decision Gate 7

Decision Gate 7 receives all copulas predicted as positively correlated by Decision Gate 2 and tries to determine if their dependence structure is tail dependent or evenly

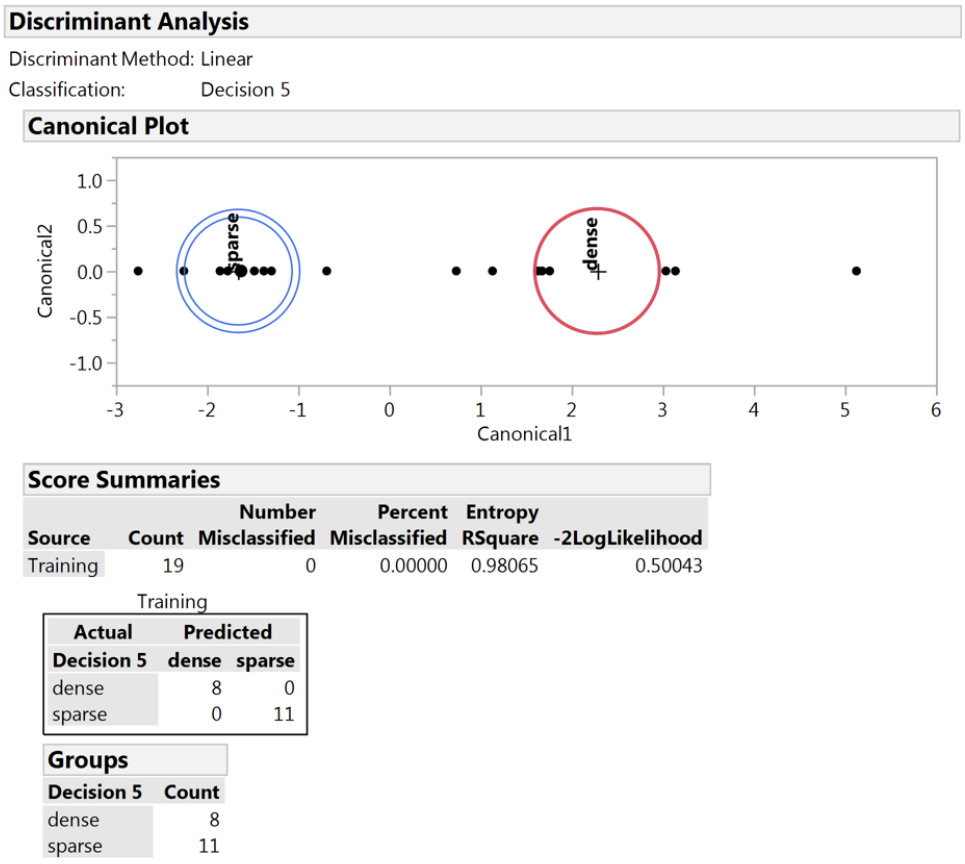

Figure 115: Discriminant analysis at Decision Gate 5 with Pareto Corner Density (σ_ϕ)

distributed. The objective metrics available to the discriminant analysis algorithm at Decision Gate 7 are Avg Distance ($\bar{d}$), Avg Lower Distance ($\bar{d}_{Low}$), Avg Middle Distance ($\bar{d}_{Mid}$), Avg Upper Distance ($\bar{d}_{Upp}$), and Evenness Distribution (ε). Single covariate discriminant analysis experiments are conducted to determine which is the best discriminator for this decision gate, beginning with Avg Distance ($\bar{d}$). These results are given in Fig. 120.

This experiment gives 10 mislabeled copulas indicating that Avg Distance ($\bar{d}$) is not a good discriminator for this decision gate. Avg Lower Distance ($\bar{d_{Low}}$) is tested next and these results are given in Fig. 121.

This experiment gives 12 mislabeled copulas indicating that Avg Lower Distance

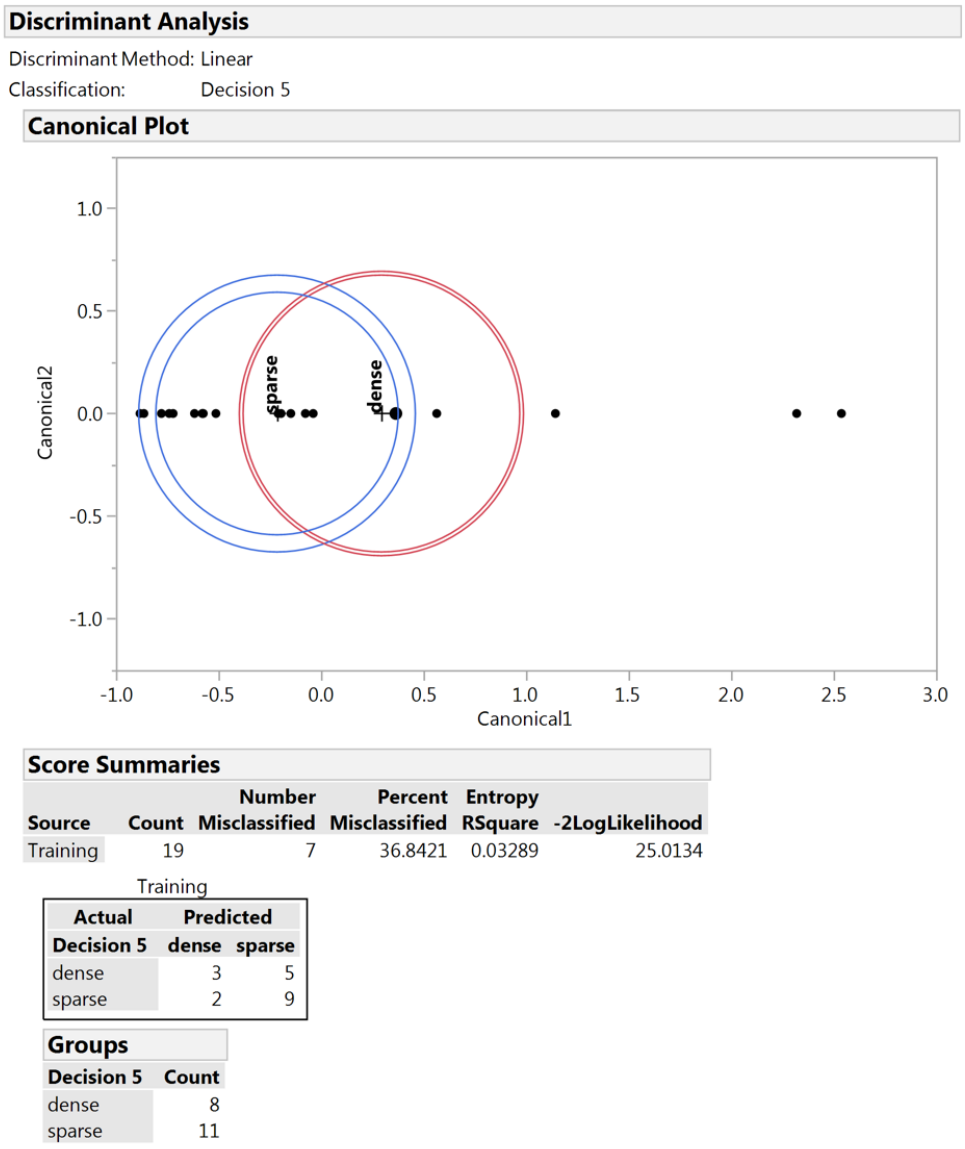

Figure 116: Discriminant analysis at Decision Gate 5 with Pareto Frontier Point Density (ϕ)

($\bar{d}_{Low}$) is not a good discriminator for Decision Gate 7. Avg Middle Distance ($\bar{d}_{Mid}$) is tested next and its results are given in Fig. 122.

This experiment gives 6 mislabeled copulas indicating that Avg Middle Distance ($\bar{d}_{Mid}$) is not a good discriminator for this decision gate. Avg Upper Distance ($\bar{d}_{Upp}$) is tested next and its results are given in Fig. 123.

This experiment gives 11 mislabeled copulas indicating that Avg Upper Distance

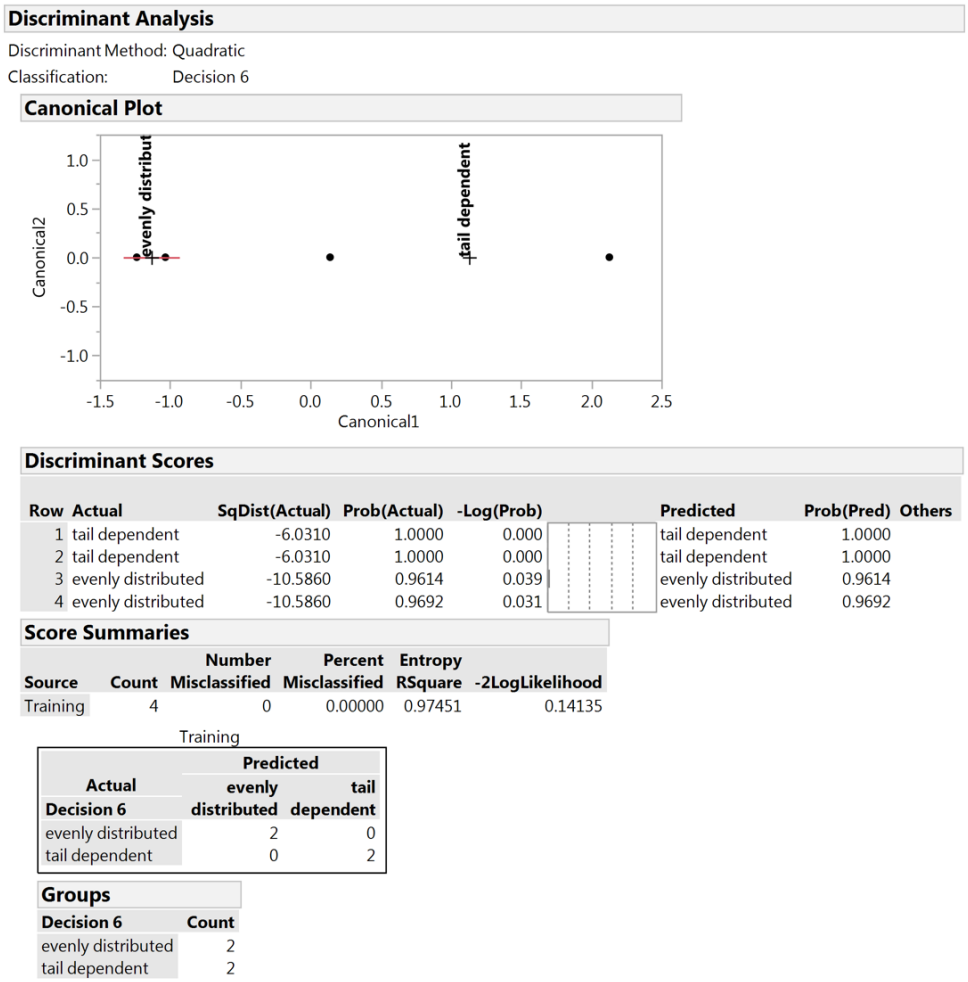

Figure 117: Discriminant analysis at Decision Gate 6 with Avg Inverse Lower Distance ($\bar{d}_{Low}^{-1}$)

($\bar{d}_{Upp}$) is a poor discriminator for this decision gate. Evenness Distribution (ε) is tested next and its results are given in Fig. 124.

This experiment gives 0 mislabeled copulas indicating that Evenness Distribution (ε) is a good discriminator for Decision Gate 7 and far superior to all the other covariates tested for this decision gate. The threshold value of Evenness Distribution (ε) is recorded and used to label copulas leaving Decision Gate 7 as having tail dependent or evenly distributed joint distributions. Tail dependent copulas are passed to Decision Gate 8 and evenly distributed copulas are labeled as leaf H.

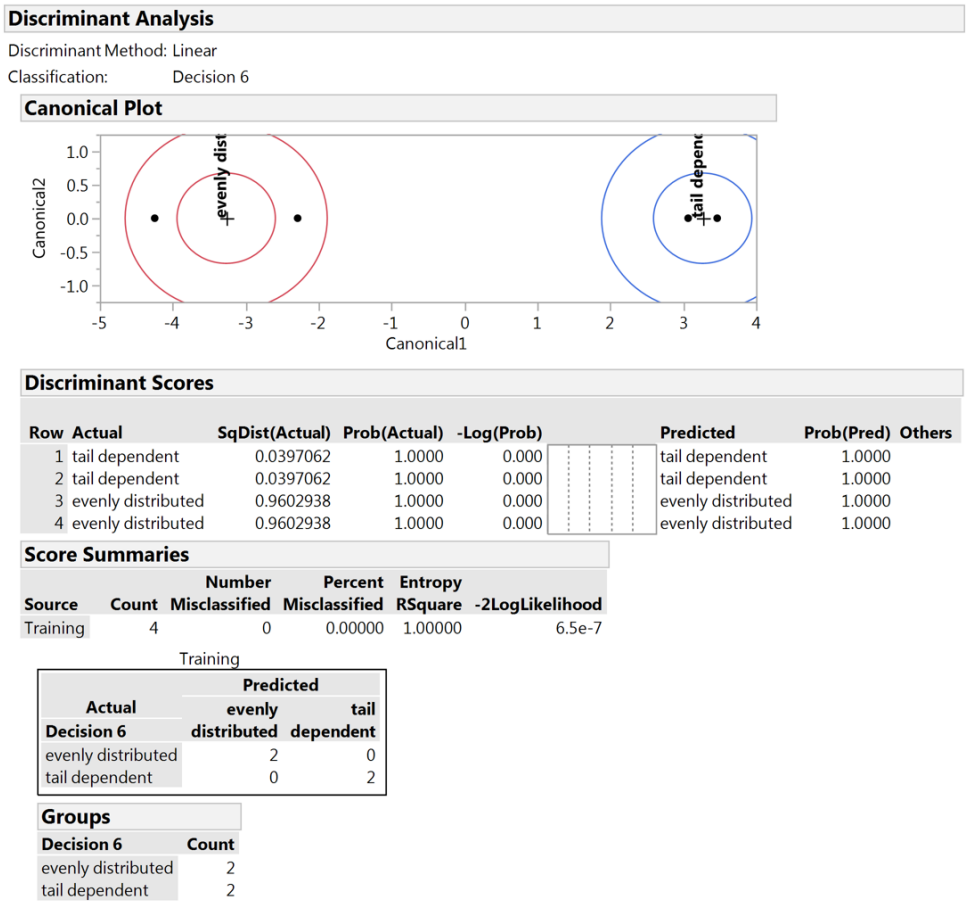

Figure 118: Discriminant analysis at Decision Gate 6 with Avg Inverse Middle Distance ($\bar{d}^{-1}_{Mid}$)

7.2.8 Decision Gate 8

Decision Gate 8 receives all copulas predicted as tail dependent by Decision Gate 7 and tries to determine if their dependence structure exhibits narrow or wide tails. The objective metrics available to the discriminant analysis algorithm at Decision Gate 8 are Avg Lower Distance ($\bar{d}_{Low}$), Avg Middle Distance ($\bar{d}_{Mid}$), and Avg Upper Distance ($\bar{d}_{Upp}$. Single covariate discriminant analysis experiments are conducted first to determine which is the best discriminator for this decision gate, beginning with Avg Lower Distance ($\bar{d}_{Low}$). The results are given in Fig. 125.

This experiment gives 5 mislabeled copulas indicating that Avg Lower Distance ($\bar{d}_{Low}$) is not a good discriminator for this decision gate by itself. Avg Middle Distance

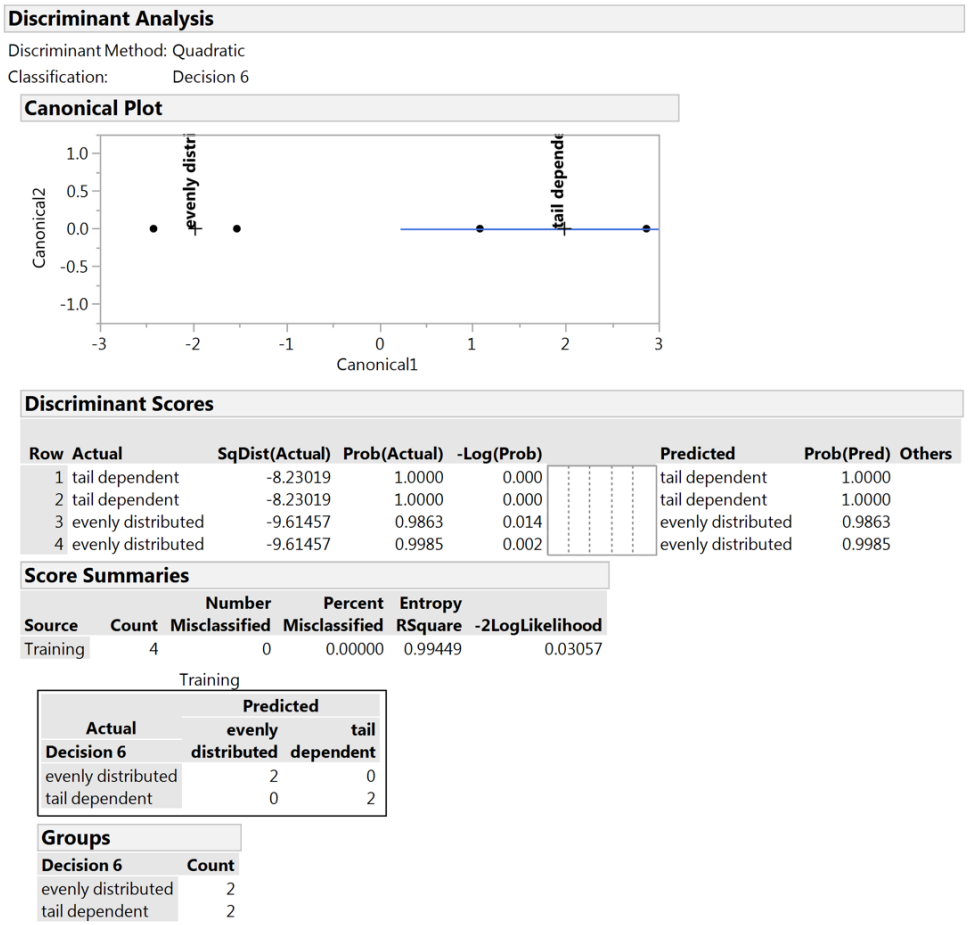

Row	Actual	SqDist(Actual)	Prob(Actual)	-Log(Prob)	Predicted	Prob(Pred)	Others
1	tail dependent	-8.23019	1.0000	0.000	tail dependent	1.0000	
2	tail dependent	-8.23019	1.0000	0.000	tail dependent	1.0000	
3	evenly distributed	-9.61457	0.9863	0.014	evenly distributed	0.9863	
4	evenly distributed	-9.61457	0.9985	0.002	evenly distributed	0.9985	

Source	Count	Number Misclassified	Percent Misclassified	Entropy RSquare	-2LogLikelihood
Training	4	0	0.00000	0.99449	0.03057

Figure 119: Discriminant analysis at Decision Gate 6 with Avg Inverse Upper Distance ($\bar{d}_{Upp}^{-1}$)

($\bar{d}_{Mid}$) is tested next and its results are given in Fig. 126.

This experiment gives 5 mislabeled copulas suggesting that Avg Middle Distance ($\bar{d}_{Mid}$) is not a good discriminator for this decision gate by itself. Avg Upper Distance ($\bar{d}_{Upp}$) is tested next and its results are given in Fig. 127.

This experiment gives 1 mislabeled copula indicating that Avg Upper Distance ($\bar{d}_{Upp}$) is a good single covariate discriminator for this decision gate. Combinations of these covariates are tested next to see if they can perform better than Avg Upper Distance ($\bar{d}_{Upp}$) by itself. The first combination tested is Avg Lower Distance ($\bar{d}_{Low}$) and Avg Middle Distance ($\bar{d}_{Mid}$). The results are given in Fig. 128.

This experiment gives 5 mislabeled copulas indicating that Avg Lower Distance

Discriminant Analysis

Discriminant Method: Linear

Classification: Decision 7

Canonical Plot

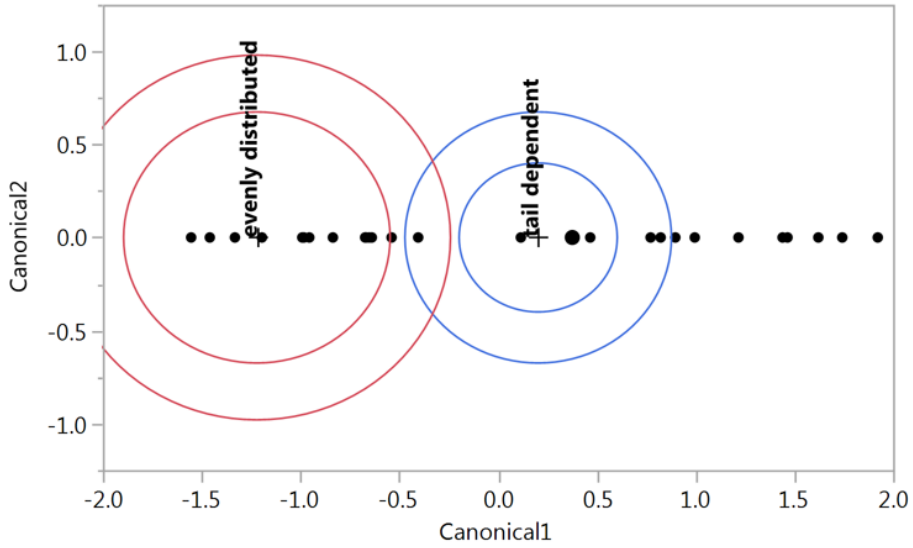

Score Summaries

Source	Count	Number Misclassified	Percent Misclassified	Entropy RSquare	-2LogLikelihood
Training	28	10	35.7143	-0.1718	26.9127

Training

Actual Decision 7	Predicted evenly distributed	Predicted tail dependent
evenly distributed	4	0
tail dependent	10	14

Groups

Decision 7	Count
evenly distributed	4
tail dependent	24

Figure 120: Discriminant analysis at Decision Gate 7 with Avg Distance ($\bar{d}$)

($\bar{d}_{Low}$) and Avg Middle Distance ($\bar{d}_{Mid}$) are not a good combination of covariates to predict membership at Decision Gate 8. The next combination is Avg Middle Distance ($\bar{d}_{Mid}$) and Avg Upper Distance ($\bar{d}_{Upp}$). The results are given in Fig. 129.

This experiment gives 2 mislabeled copula indicating that Avg Middle Distance ($\bar{d}_{Mid}$) and Avg Upper Distance ($\bar{d}_{Upp}$) are not a good combination of covariates to

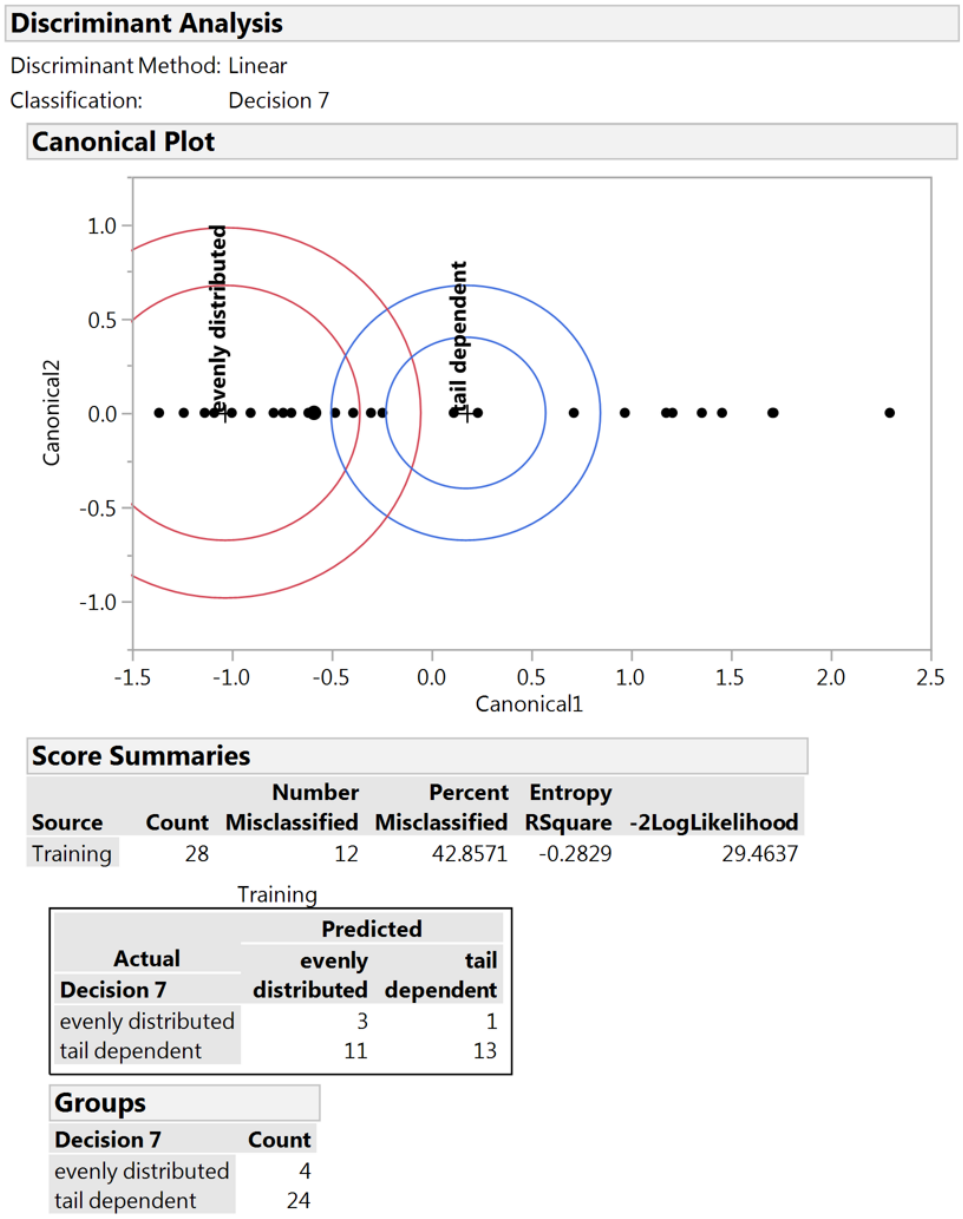

Figure 121: Discriminant analysis at Decision Gate 7 with Avg Lower Distance ($\bar{d}_{Low}$)

predict membership at Decision Gate 8. The next combination is Avg Lower Distance ($\bar{d}_{Low}$) and Avg Upper Distance ($\bar{d}_{Upp}$). The results are given in Fig. 130.

This experiment gives 1 mislabeled copula indicating that Avg Lower Distance ($\bar{d}_{Low}$) and Avg Upper Distance ($\bar{d}_{Upp}$) are a good combination of covariates to predict membership at Decision Gate 8. Comparing with Avg Upper Distance ($\bar{d}_{Upp}$) as

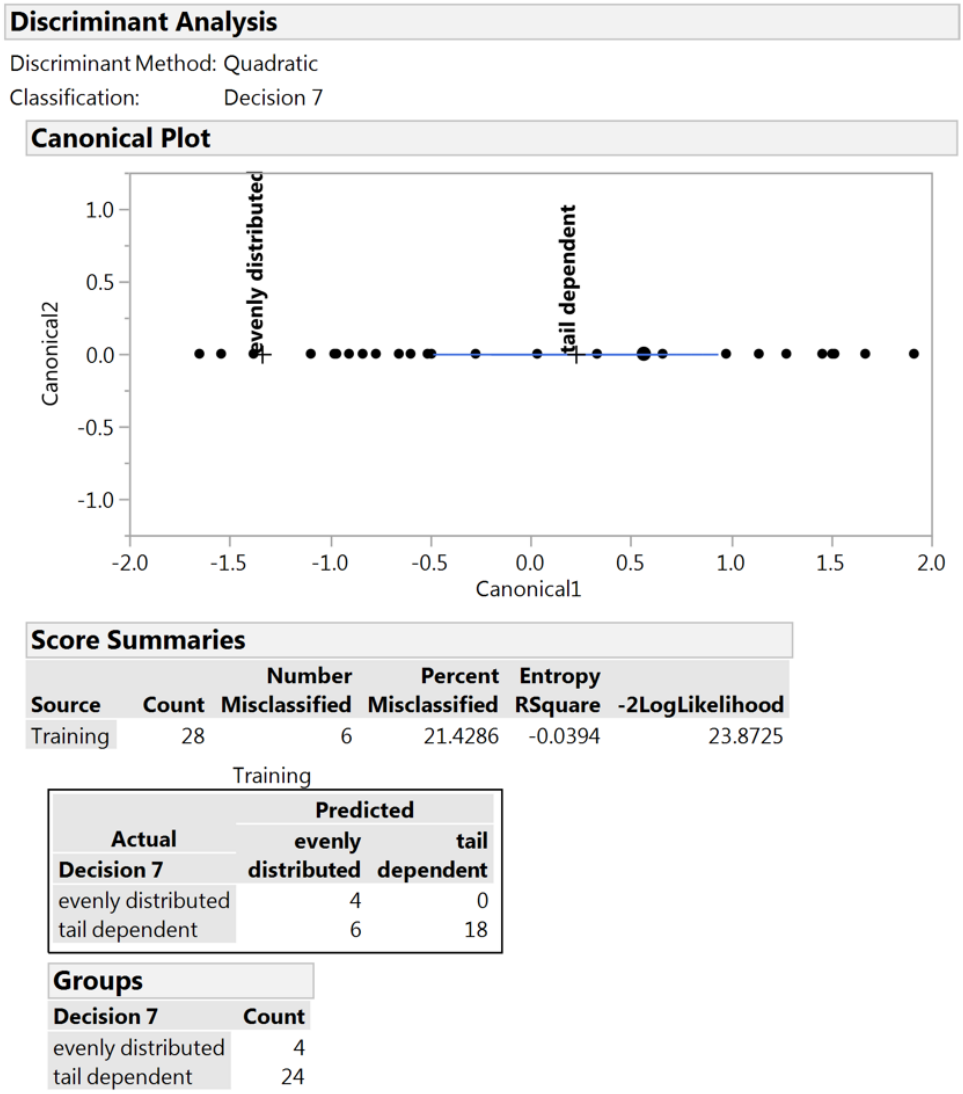

Figure 122: Discriminant analysis at Decision Gate 7 with Avg Middle Distance ($\bar{d}_{Mid}$)

a single covariate, the combination of Avg Lower Distance ($\bar{d}_{Low}$) and Avg Upper Distance ($\bar{d}_{Upp}$) has a higher R-squared value and a better probability of prediction so it will be chosen as the best discriminator for Decision Gate 8. The threshold values of Avg Lower Distance ($\bar{d}_{Low}$) and Avg Upper Distance ($\bar{d}_{Upp}$) are recorded and used to label copulas leaving Decision Gate 8 as having narrow or wide tail dependence. Wide tail dependent copulas are passed to Decision Gate 9 and narrow tail dependent copulas are passed to Decision Gate 10.

Discriminant Analysis

Discriminant Method: Linear

Classification: Decision 7

Canonical Plot

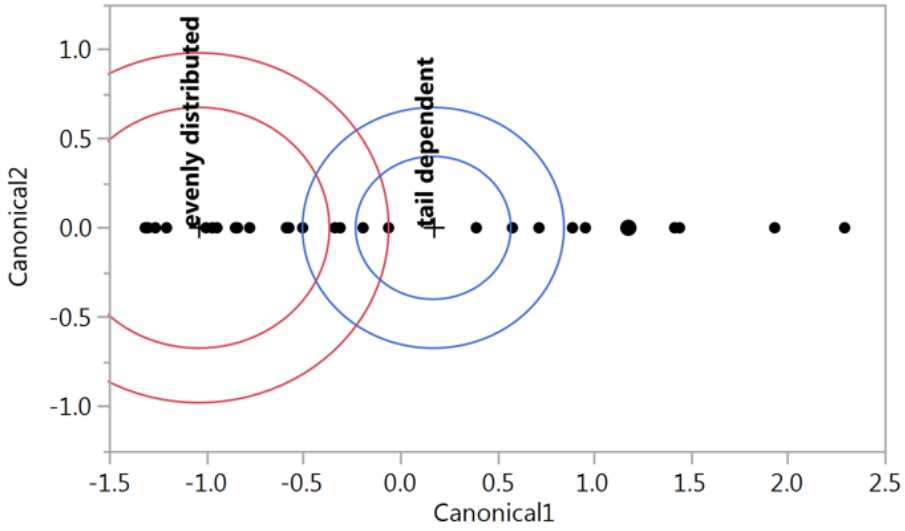

Score Summaries

Source	Count	Number Misclassified	Percent Misclassified	Entropy RSquare	-2LogLikelihood
Training	28	11	39.2857	-0.2848	29.5079

Training

Actual Decision 7	Predicted evenly distributed	Predicted tail dependent
evenly distributed	3	1
tail dependent	10	14

Groups

Decision 7	Count
evenly distributed	4
tail dependent	24

Figure 123: Discriminant analysis at Decision Gate 7 with Avg Upper Distance ($\bar{d}_{Upp}$)

7.2.9 Decision Gate 9

Decision Gate 9 receives all copulas predicted as having narrow tail dependence by Decision Gate 8 and tries to determine if their dependence structure exhibits left, right, or both tail dependence. The objective metrics available to the discriminant

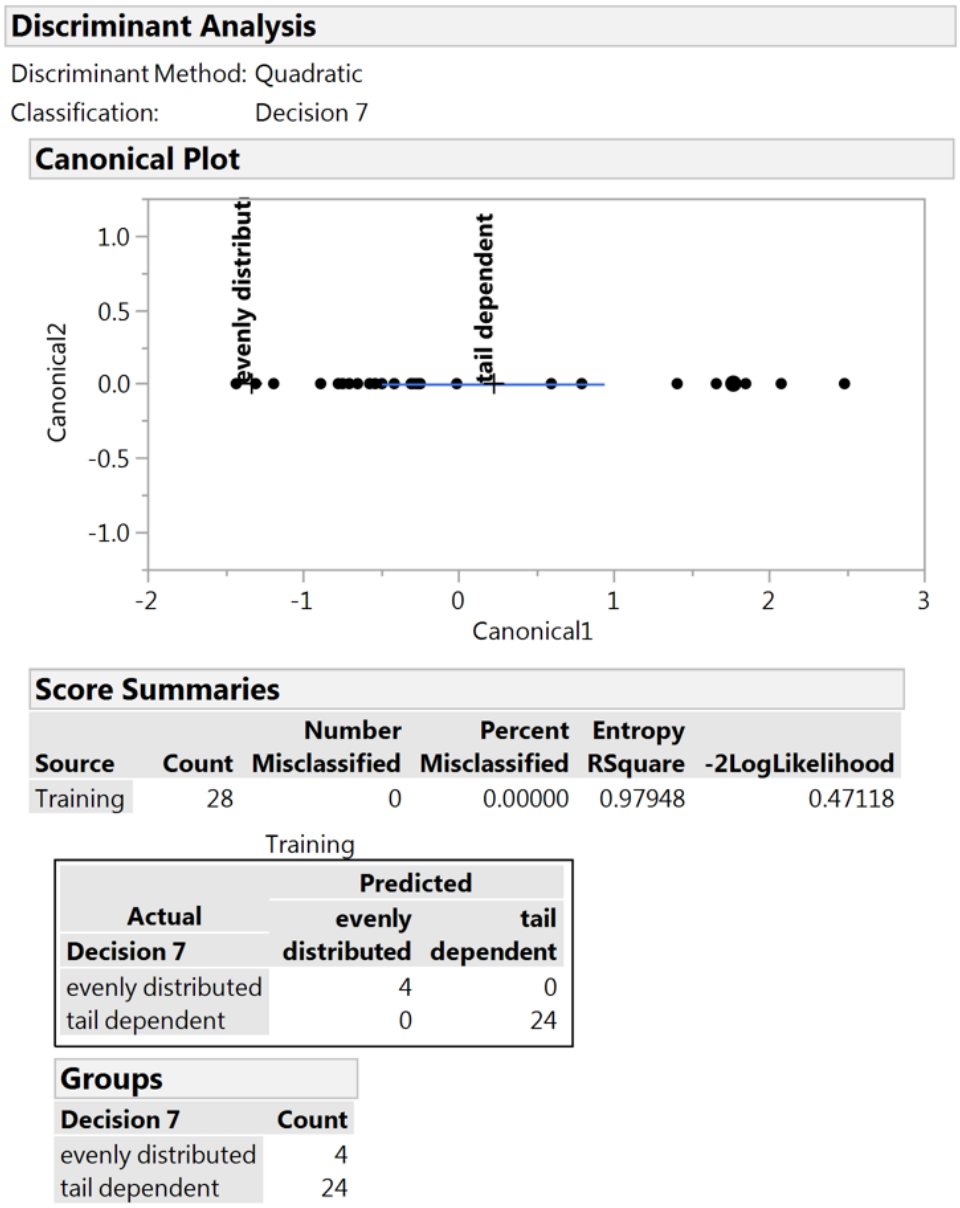

Figure 124: Discriminant analysis at Decision Gate 7 with Evenness Distribution (ε)

analysis algorithm at Decision Gate 9 are Avg Distance ($\bar{d}$), Avg Lower Distance ($\bar{d}_{Low}$), Avg Middle Distance ($\bar{d}_{Mid}$), Avg Upper Distance ($\bar{d}_{Upp}$), and Upper to Lower Ratio (υ). Single covariate discriminant analysis experiments are conducted first to determine which is the best discriminator for this decision gate, beginning with Avg Distance ($\bar{d}$). The results are given in Fig. 131.

Discriminant Analysis

Discriminant Method: Linear

Classification: Decision 8

Canonical Plot

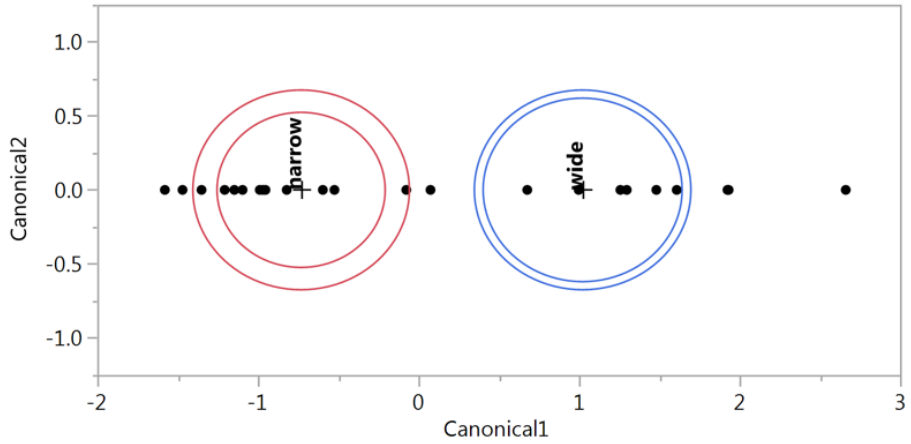

Score Summaries

Source	Count	Number Misclassified	Percent Misclassified	Entropy RSquare	-2LogLikelihood
Training	24	5	20.8333	0.35928	20.8882

Training

Actual Decision 8	Predicted narrow	wide
narrow	12	2
wide	3	7

Groups

Decision 8	Count
narrow	14
wide	10

Figure 125: Discriminant analysis at Decision Gate 8 with Avg Lower Distance ($\bar{d}_{Low}$)

This experiment gives 5 mislabeled copulas indicating that Avg Distance ($\bar{d}$) is not a good discriminator for this decision gate by itself. Avg Lower Distance ($\bar{d}_{Low}$) is tested next and its results are given in Fig. 132.

This experiment gives 4 mislabeled copulas suggesting that Avg Lower Distance ($\bar{d}_{Low}$) is not a good discriminator for this decision gate by itself. Avg Middle Distance ($\bar{d}_{Mid}$) is tested next and its results are given in Fig. 133.

This experiment gives 7 mislabeled copulas suggesting that Avg Middle Distance ($\bar{d}_{Mid}$) is not a good discriminator for this decision gate by itself. Avg Upper Distance

Discriminant Analysis

Discriminant Method: Linear

Classification: Decision 8

Canonical Plot

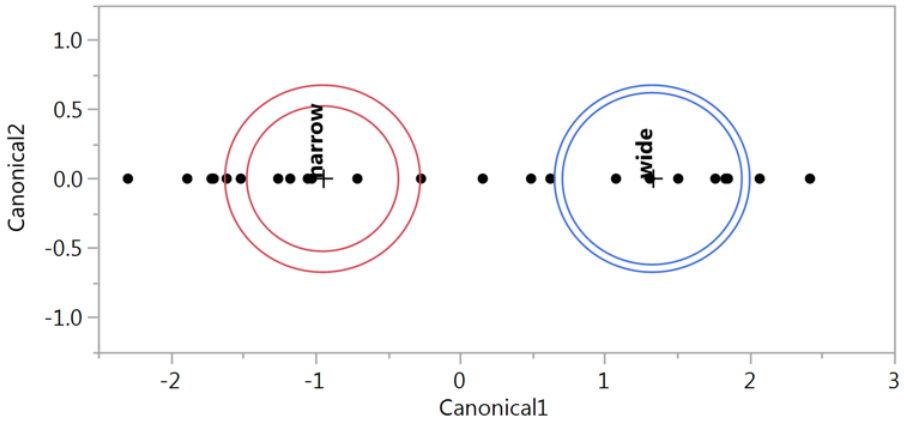

Score Summaries

Source	Count	Number Misclassified	Percent Misclassified	Entropy RSquare	-2LogLikelihood
Training	24	5	20.8333	0.48544	16.7752

Training

Actual Decision 8	Predicted narrow	Predicted wide
narrow	11	3
wide	2	8

Groups

Decision 8	Count
narrow	14
wide	10

Figure 126: Discriminant analysis at Decision Gate 8 with Avg Middle Distance ($\bar{d}_{Mid}$)

($\bar{d}_{Upp}$) is tested next and its results are given in Fig. 134.

This experiment gives 5 mislabeled copulas indicating that Avg Upper Distance ($\bar{d}_{Upp}$) is not a good single covariate discriminator for this decision gate by itself. Upper to Lower Ratio (υ) is tested next and its results are given in Fig. 135.

This experiment gives 0 mislabeled copulas indicating that Upper to Lower Ratio (υ) is a good single covariate discriminator for this decision gate. It is far superior to all the other covariates tested and is selected as the best discriminator for Decision

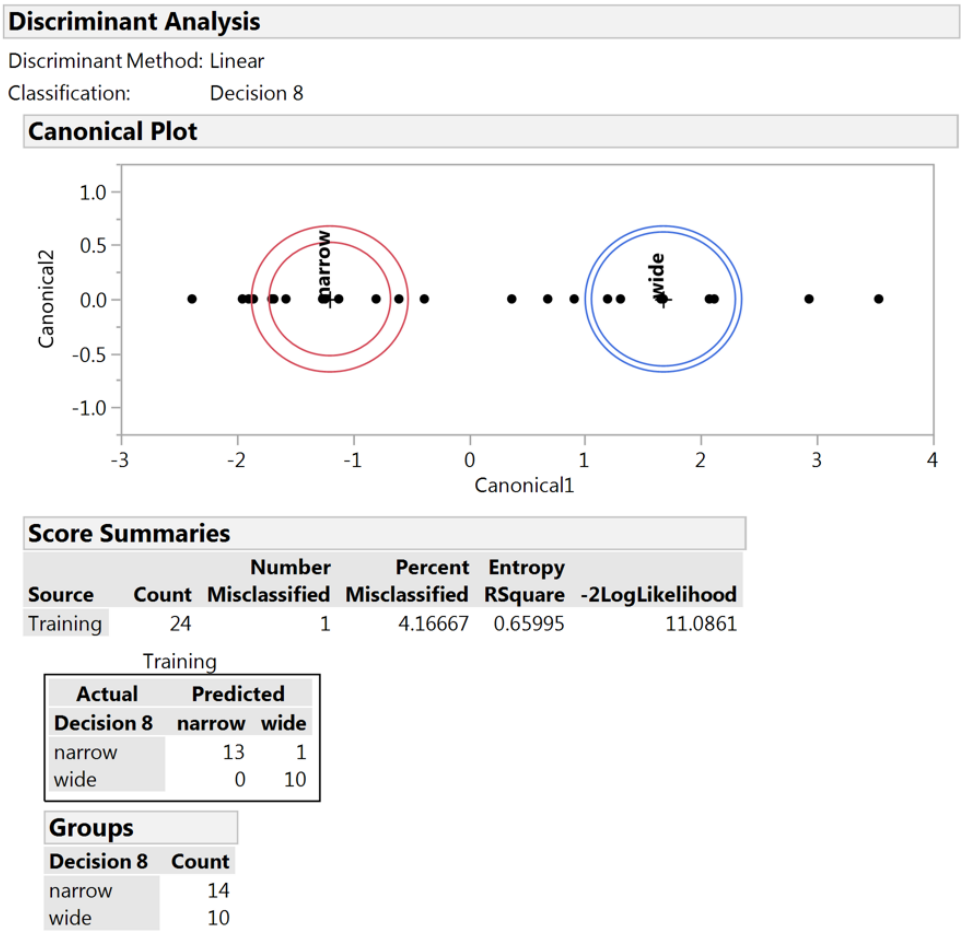

Figure 127: Discriminant analysis at Decision Gate 8 with Avg Upper Distance ($\bar{d}_{Upp}$)

Gate 9. The threshold values of Upper to Lower Ratio (υ) are recorded to delineate the three subgroups leaving Decision Gate 9 as having left, right, or both tail dependence. Left tail dependent copulas are labeled as Leaf I, right tail dependent copulas are labeled as Leaf J, and both tail dependent copulas are labeled as Leaf K.

7.2.10 Decision Gate 10

Decision Gate 10 receives all copulas predicted as having wide tail dependence by Decision Gate 8 and tries to determine if their dependence structure exhibits left, right, or both tail dependence. The objective metrics available to the discriminant analysis algorithm at Decision Gate 10 are Avg Distance ($\bar{d}$), Avg Lower Distance

Discriminant Analysis

Discriminant Method: Linear

Classification: Decision 8

Canonical Plot

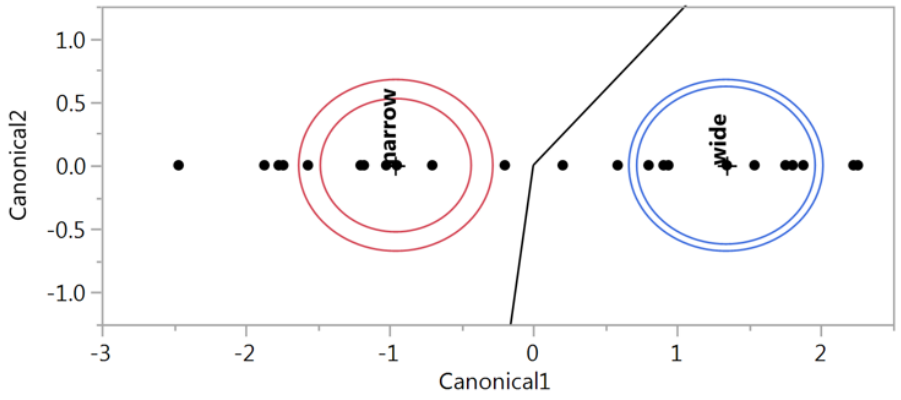

Score Summaries

Source	Count	Number Misclassified	Percent Misclassified	Entropy RSquare	-2LogLikelihood
Training	24	4	16.6667	0.49846	16.3508

Training

Actual Decision 8	Predicted narrow	Predicted wide
narrow	11	3
wide	1	9

Groups

Decision 8	Count
narrow	14
wide	10

Figure 128: Discriminant analysis at Decision Gate 8 with Avg Lower Distance ($\bar{d}_{Low}$) and Avg Middle Distance ($\bar{d}_{Mid}$)

($\bar{d}_{Low}$), Avg Middle Distance ($\bar{d}_{Mid}$), Avg Upper Distance ($\bar{d}_{Upp}$), and Upper to Lower Ratio (υ). Single covariate discriminant analysis experiments are conducted first to determine which is the best discriminator for this decision gate, beginning with Avg Distance ($\bar{d}$). The results are given in Fig. 136.

This experiment gives 5 mislabeled copulas indicating that Avg Distance ($\bar{d}$) is not a good discriminator for this decision gate by itself. Avg Lower Distance ($\bar{d}_{Low}$) is tested next and its results are given in Fig. 137.

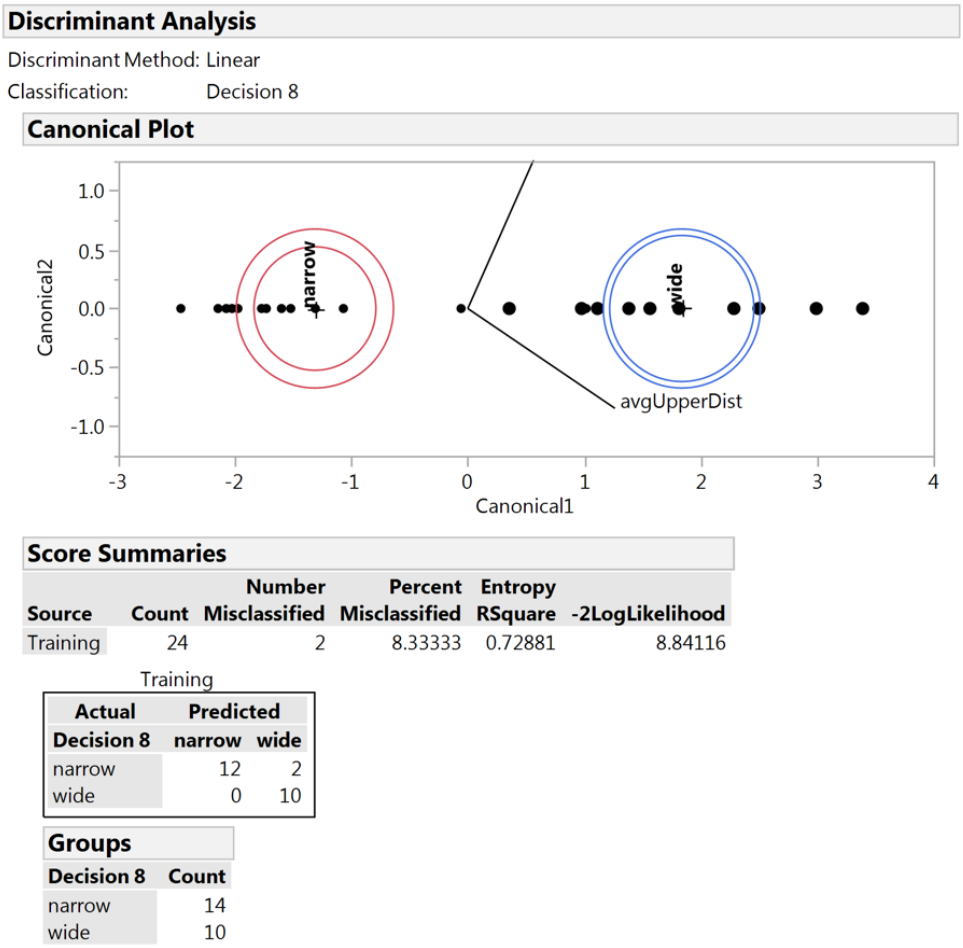

Figure 129: Discriminant analysis at Decision Gate 8 with Avg Middle Distance ($\bar{d}_{Mid}$) and Avg Upper Distance ($\bar{d}_{Upp}$)

This experiment gives 1 mislabeled copula suggesting that Avg Lower Distance ($\bar{d}_{Low}$) is a good discriminator for this decision gate. Avg Middle Distance ($\bar{d}_{Mid}$) is tested next and its results are given in Fig. 138.

This experiment gives 6 mislabeled copulas suggesting that Avg Middle Distance ($\bar{d}_{Mid}$) is not a good discriminator for this decision gate by itself. Avg Upper Distance ($\bar{d}_{Upp}$) is tested next and its results are given in Fig. 139.

This experiment gives 6 mislabeled copulas indicating that Avg Upper Distance ($\bar{d}_{Upp}$) is not a good single covariate discriminator for this decision gate by itself. Upper to Lower Ratio (υ) is tested next and its results are given in Fig. 140.

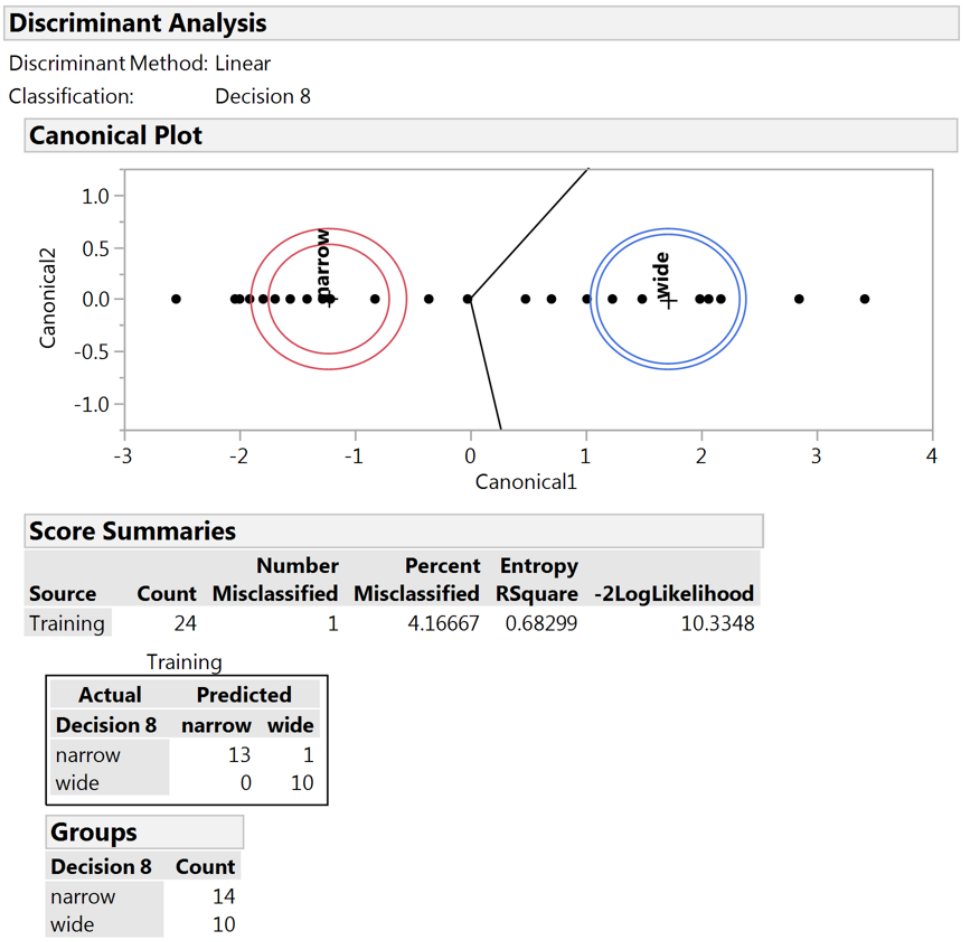

Figure 130: Discriminant analysis at Decision Gate 8 with Avg Lower Distance ($\bar{d}_{Low}$) and Avg Upper Distance ($\bar{d}_{Upp}$)

This experiment gives 0 mislabeled copulas indicating that Upper to Lower Ratio (υ) is a good single covariate discriminator for this decision gate. It is far superior to all the other covariates tested and is selected as the best discriminator for Decision Gate 10. The threshold values of Upper to Lower Ratio (υ) are recorded to delineate the three subgroups leaving Decision Gate 10 as having left, right, or both tail dependence. Left tail dependent copulas are labeled as Leaf L, right tail dependent copulas are labeled as Leaf M, and both tail dependent copulas are labeled as Leaf N.

Discriminant Analysis

Discriminant Method: Linear

Classification: Decision 9

Canonical Plot

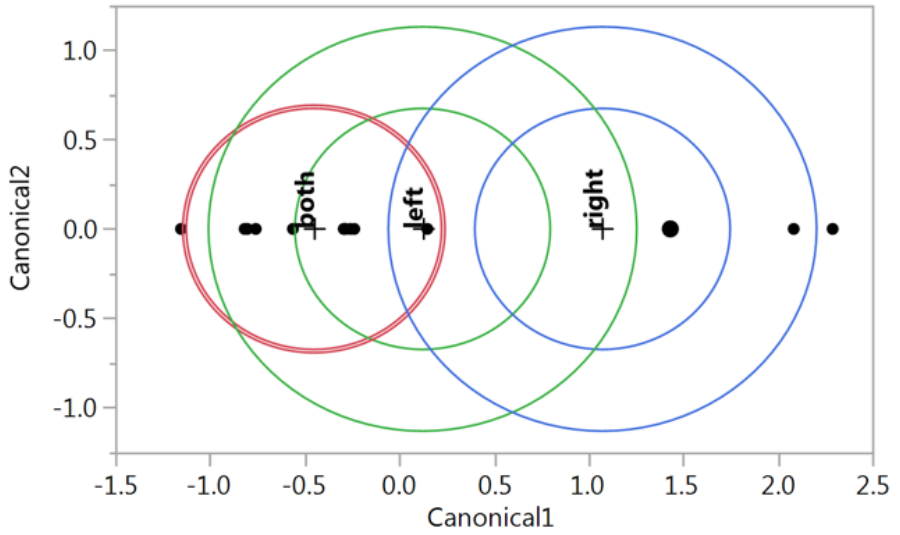

Score Summaries

Source	Count	Number Misclassified	Percent Misclassified	Entropy RSquare	-2LogLikelihood
Training	14	5	35.7143	0.07347	25.4234

Training

Actual Decision 9	Predicted both	left	right
both	7	1	0
left	2	0	1
right	1	0	2

Groups

Decision 9	Count
both	8
left	3
right	3

Figure 131: Discriminant analysis at Decision Gate 9 with Avg Distance ($\bar{d}$)

Discriminant Analysis

Discriminant Method: Linear

Classification: Decision 9

Canonical Plot

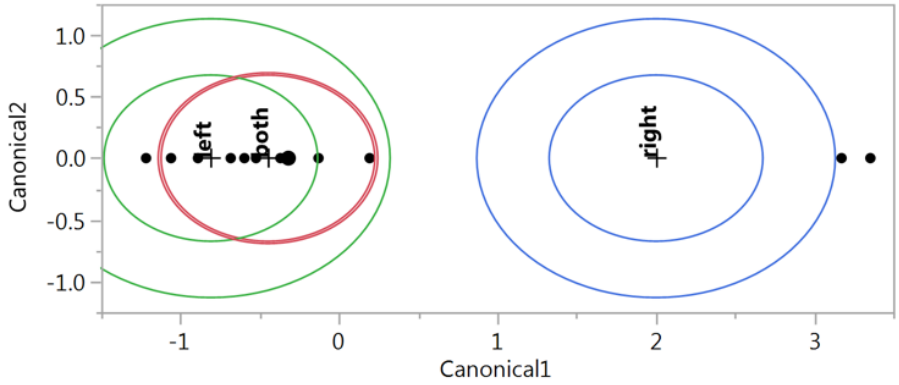

Score Summaries

Source	Count	Number Misclassified	Percent Misclassified	Entropy RSquare	-2LogLikelihood
Training	14	4	28.5714	0.15938	23.0658

Training

Actual Decision 9	Predicted both	left	right
both	6	2	0
left	1	2	0
right	1	0	2

Groups

Decision 9	Count
both	8
left	3
right	3

Figure 132: Discriminant analysis at Decision Gate 9 with Avg Lower Distance ($\bar{d}_{Low}$)

7.3 Appendix C: Utility Theory

7.3.1 Utility Function Properties

Utility is a relative concept to each decision maker, not an absolute one. Based on the possible consequences in their problem, a decision maker can create their utility scale and unit of measure by choosing a minimum and maximum point relative to two of the consequences in their set. Then they can assess the remaining consequences relative to these two defined utilities. Keeney and Raiffa [105] explain that if $x_1, x_2, ..., x_n$

Discriminant Analysis

Discriminant Method: Linear

Classification: Decision 9

Canonical Plot

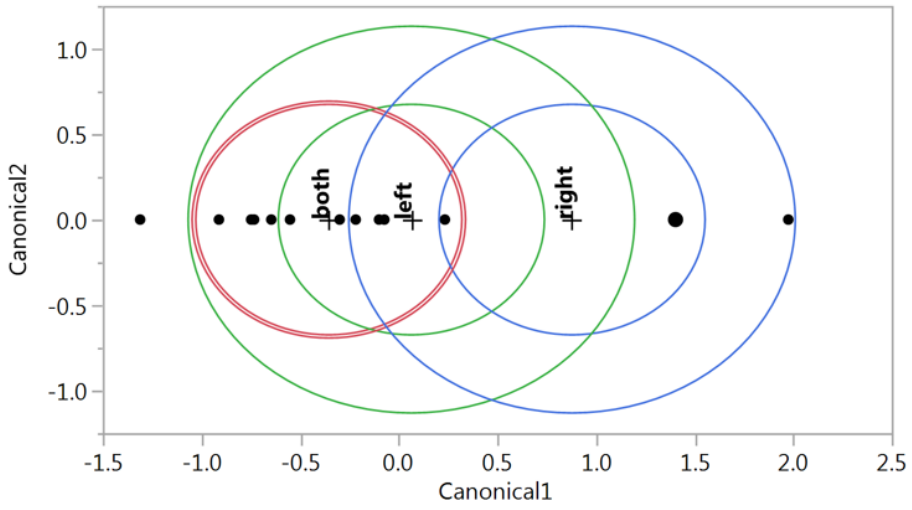

Score Summaries

Source	Count	Number Misclassified	Percent Misclassified	Entropy RSquare	-2LogLikelihood
Training	14	7	50.0000	0.01669	26.9813

Training

Actual Decision 9	Predicted both	left	right
both	5	3	0
left	2	0	1
right	1	0	2

Groups

Decision 9	Count
both	8
left	3
right	3

Figure 133: Discriminant analysis at Decision Gate 9 with Avg Middle Distance ($\bar{d}_{Mid}$)

are possible consequences, x^* is the most desribale consequence, and x^0 is the least desirable consequence, then the a common utility scale to use is $u(x^*) = 1$ and $u(x^0) = 0$. Then the decision maker should assess all the other possible consequences, x, in their set relative to these points by determining the probability π such that the

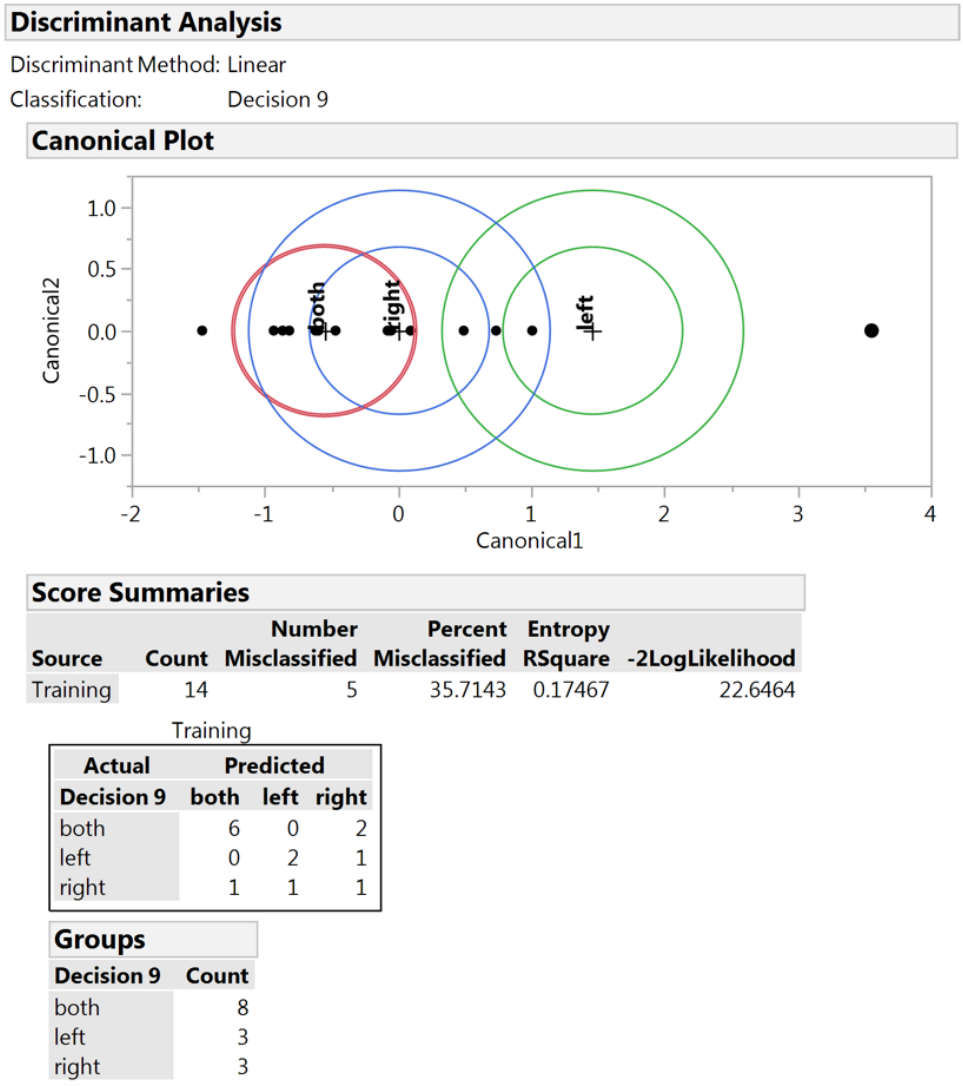

Figure 134: Discriminant analysis at Decision Gate 9 with Avg Upper Distance ($\bar{d}_{Upp}$)

decision maker is indifferent between x and the lottery,

$$u(x) = \pi u(x^*) + (1 - \pi)u(x^0) = \pi \tag{70}$$

which gives π chance at x^* and a $1 - \pi$ chance at x^0. In addition the utility of x must equal the expected utility of the lottery, so Eq. 70 can be set equal to the assessed probability π of each of the consequences. This direct assessment technique can be difficult to complete in cases where there are many possible consequences. In

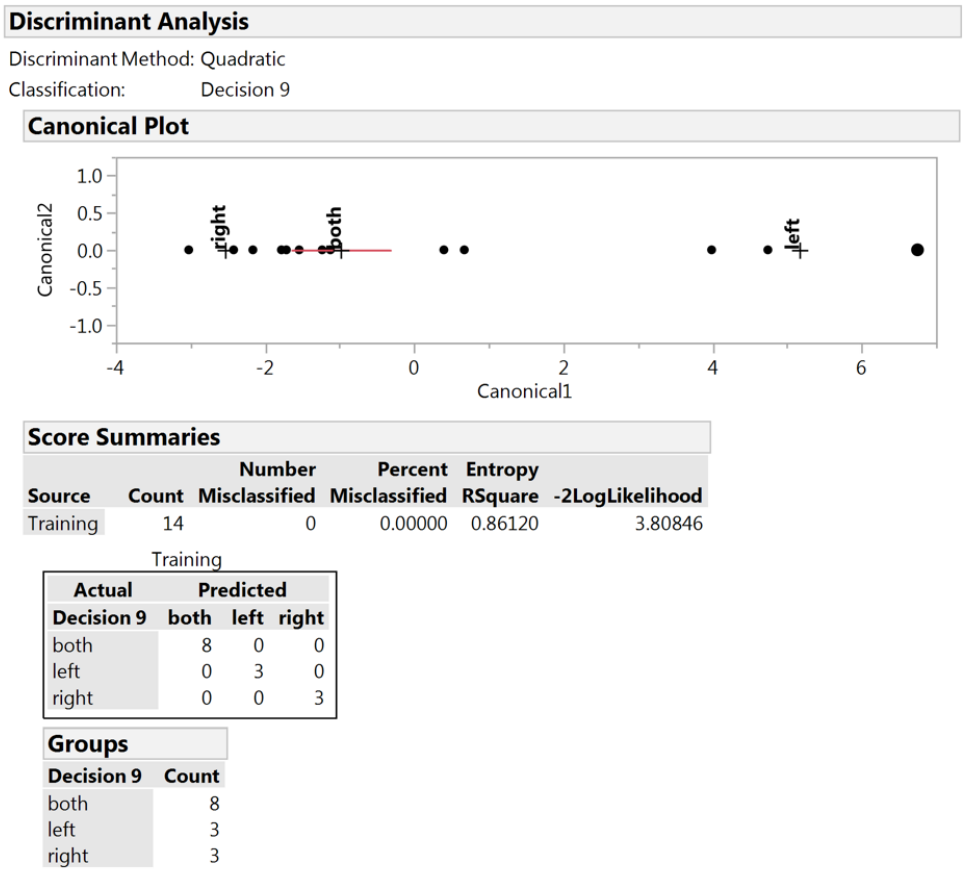

Figure 135: Discriminant analysis at Decision Gate 9 with Upper to Lower Ratio (υ)

those cases it is recommended to assess the utilities of a few different points directly, and then fit a generic utility function curve to these assessed points. The shape and functional form of the curve is based in large part on the decision maker's attitude towards risk.

7.3.1.1 Monotonicity

Monotonicity is often a reasonable characteristic of many attributes and hence a useful property of utility functions. For example when judging monetary assets, most decision makers prefer a larger amount to a smaller amount and this is reflected by monotonically increasing utility functions. If X is a set of monetary assets and u is their utility function, we expect to see the consistency given by,

Discriminant Analysis

Discriminant Method: Linear

Classification: Decision 10

Canonical Plot

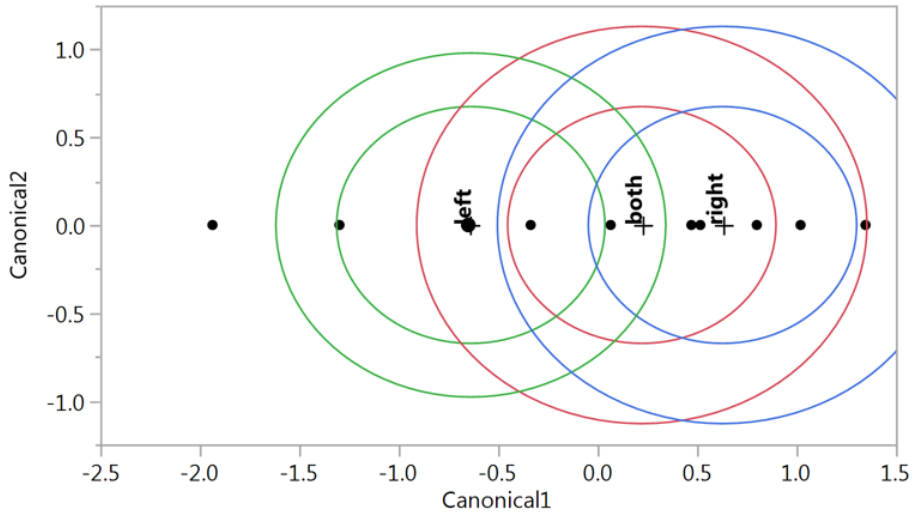

Score Summaries

Source	Count	Number Misclassified	Percent Misclassified	Entropy RSquare	-2LogLikelihood
Training	10	5	50.0000	0.13717	18.7907

Training

Actual Decision 10	Predicted both	left	right
both	0	1	2
left	0	3	1
right	1	0	2

Groups

Decision 10	Count
both	3
left	4
right	3

Figure 136: Discriminant analysis at Decision Gate 10 with Avg Distance ($\bar{d}$)

$$[x_1 > x_2] \Leftrightarrow [u(x_1) > u(x_2)] \tag{71}$$

Utility functions can also be monotonically decreasing by transforming the attribute scale. This can be done by taking a difference relative to some baseline value and using the resulting scale to assess decreasing utility. Utility functions do not have

Figure 137: Discriminant analysis at Decision Gate 10 with Avg Lower Distance ($\bar{d}_{Low}$)

to be monotonic, but as a result they can not prescribe to some basic properties of general utility functions. These include not having a unique certainty equivalent, no risk premium, and the first derivative will be zero for at least one value of x. Keeney and Raiffa [105] recommended a method of dealing with nonmonotonic utility functions by decomposing the range of the given attribute into intervals such that each interval is monotonic, and treat each interval individually. Further information on nonmonotonic utility functions can be found in chapter 4 of their text.

Discriminant Analysis

Discriminant Method: Linear

Classification: Decision 10

Canonical Plot

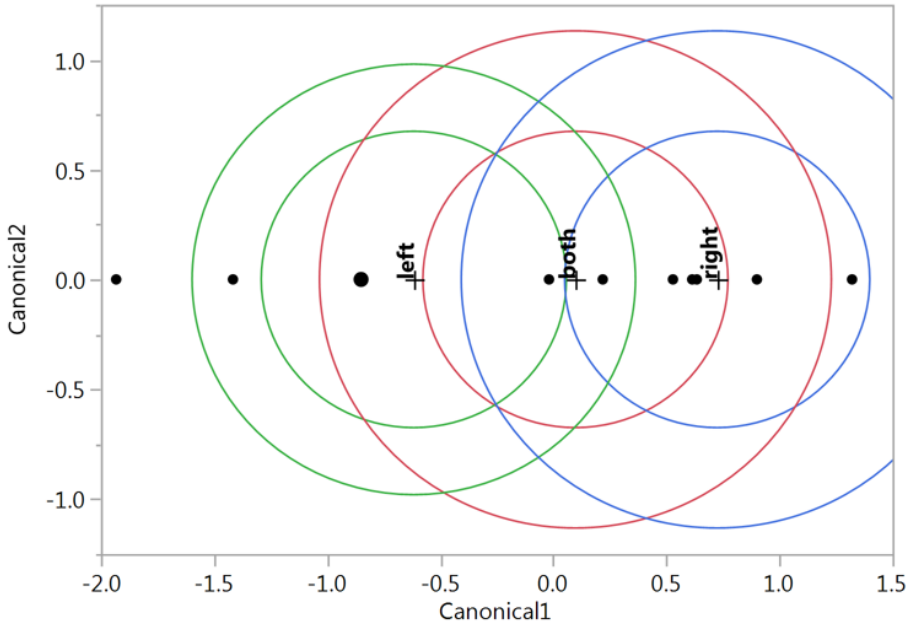

Score Summaries

Source	Count	Number Misclassified	Percent Misclassified	Entropy RSquare	-2LogLikelihood
Training	10	6	60.0000	0.14742	18.5675

Training

Actual Decision 10	Predicted both	left	right
both	0	1	2
left	1	2	1
right	1	0	2

Groups

Decision 10	Count
both	3
left	4
right	3

Figure 138: Discriminant analysis at Decision Gate 10 with Avg Middle Distance ($\bar{d}_{Mid}$)

Discriminant Analysis

Discriminant Method: Linear

Classification: Decision 10

Canonical Plot

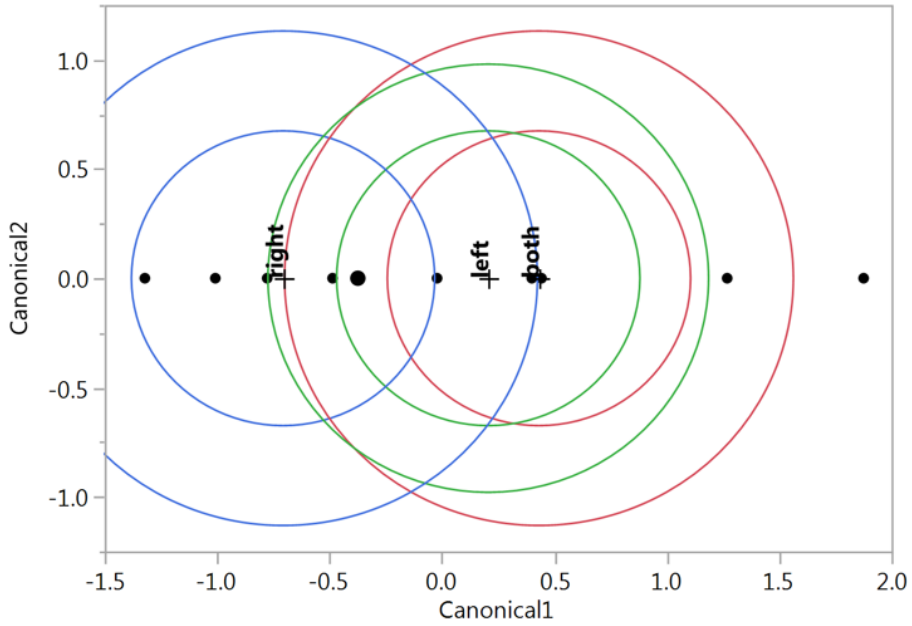

Score Summaries

Source	Count	Number Misclassified	Percent Misclassified	Entropy RSquare	-2LogLikelihood
Training	10	6	60.0000	0.11435	19.2876

Training

Actual Decision 10	Predicted both	left	right
both	2	0	1
left	2	0	2
right	0	1	2

Groups

Decision 10	Count
both	3
left	4
right	3

Figure 139: Discriminant analysis at Decision Gate 10 with Avg Upper Distance ($\bar{d}_{Upp}$)

7.3.1.2 Certainty Equivalent

A fundamental concept of utility theory is that of the certainty equivalent, which is explained in detail by Keeney and Raiffa (1976) in their informative text, Decisions

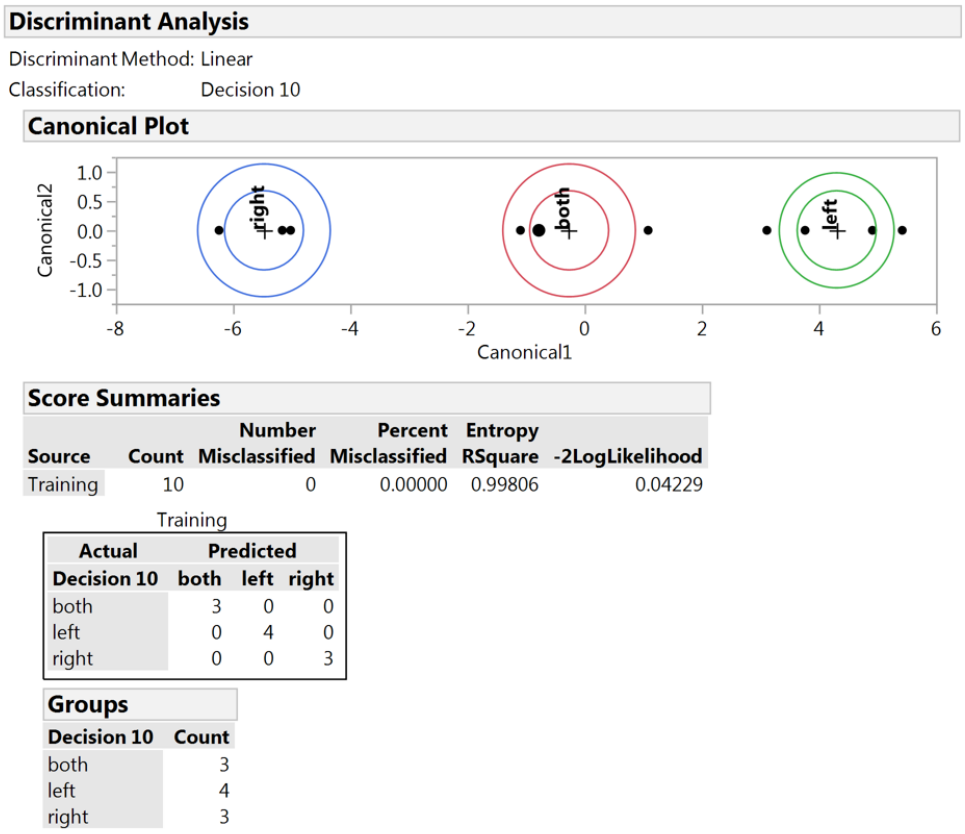

Figure 140: Discriminant analysis at Decision Gate 10 with Upper to Lower Ratio (υ)

with Multiple Objectives. A certainty equivalent of a lottery is an amount x, such that the decision maker is indifferent between the lottery outcome and the amount x for certain. Certainty equivalent is a unique value for monotonic utility functions. 2 lotteries are strategically equivalent if they have the same certainty equivalent. For linear utility functions, the certainty equivalent is equal to the expected consequence of the lottery. An important property of the exponential utility function is that if all the consequences of a lottery are increased by a fixed amount, the certainty equivalent is also increased by that same amount. This idea is useful for evaluating certainty equivalents of similar lotteries, as explained in Theorem 4.2 of their text.

The certainty equivalent is a fundamental concept in utility theory and has many uses including the assessment of utility functions. Fortunately it is also a simple

notion to understand, as explained by Keeney and Raiffa [105]. Given a lottery that has multiple consequences $x_1, x_2, ..., x_n$, with probabilities $p_1, p_2, ..., p_n$, respectively, the uncertain consequence (i.e., a random variable) of the lottery is denoted $\widetilde{x}$, and the expected consequence of the lottery is $\bar{x}$. The expected value of the lottery is written as

$$\bar{x} \equiv E(\widetilde{x}) = \sum_{i=1}^{n} p_i x_i \tag{72}$$

and the expected utility of the lottery is

$$E[u(\widetilde{x})] = \sum_{i=1}^{n} p_i u(x_i) \tag{73}$$

Using these concepts, the certainty equivalent of this lottery is an amount $\hat{x}$ which makes the decision maker indifferent between choosing the lottery and the amount $\hat{x}$ for certain. Mathematically the utility of $\hat{x}$ is written

$$u(\hat{x}) = E[u(\widetilde{x})] \tag{74}$$

and the certainty equivalent $\hat{x}$ is given by

$$\hat{x} = u^{-1}(Eu(\widetilde{x})) \tag{75}$$

There are a couple of important points to note regarding the certainty equivalent. First is that certainty equivalent will take on a single unique value for monotonic utility functions. Secondly the certainty equivalent can be written in integral form when the consequences of a lottery are expressed by a probability density function f, rather than by individual consequences. In that case the expected consequence of the lottery, $\bar{x}$ is written as

$$\bar{x} = E(\widetilde{x}) = \int x f(x) dx \tag{76}$$

and the utility of the certainty equivalent is given by

$$u(\hat{x}) = E[u(\widetilde{x})] = \int u(x)f(x)dx. \tag{77}$$

Two lotteries are strategically equivalent if they have the same certainty equivalent. For linear utility functions, the certainty equivalent is equal to the expected consequence of the lottery. An important property of the exponential utility function is that if all the consequences of a lottery are increased by a fixed amount, the certainty equivalent is also increased by that same amount. This idea is useful for evaluating certainty equivalents of similar lotteries, as explained in Theorem 4.2 of their text [105].

7.3.1.3 Utility and Risk

In utility theory, risk attitudes are reflected in the shape of utility functions. A decision maker's feelings towards taking chances (e.g., entering a lottery) will determine how their utility function looks. To understand this it is necessary to discuss lotteries and expectations. Consider a lottery with only two consequences, x_1 and x_2 with equal probability. The expected consequence of the lottery, $\bar{x}$, is given by $(x_1 + x_2)/2$. If a decision maker was asked to choose between receiving the expected consequence $\bar{x}$ for sure or enter the lottery and assume its inherent risk, and they chose $\bar{x}$ instead of the lottery, they would be risk averse. This is because they prefer the certain consequence $\bar{x}$ over assuming the risk involved in the lottery. Keeney and Raiffa [105] define a decision maker as risk averse if they always prefer the expected consequence of any nondegenrate lottery (a lottery where no single consequence has a probability 1 of occurring) to that lottery itself.

Another way to understand this concept is to examine the lottery in terms of utility. It was mentioned earlier that expected utility of a lottery can also be written as $E[u(\widetilde{x})]$. Since a risk averse decision maker always prefers the expected consequence

of a lottery $E(\widetilde{x}$ over the lottery itself, it means that their utility of the expected consequence, is always greater than the utility of the lottery:

$$u[E(\widetilde{x})] > E[u(\widetilde{x})] \tag{78}$$

The lack of willingness to take the risk of the lottery implies that this decision maker's utility function is concave. Keeney and Raiffa [105] provide a proof of this statement, but it suffices here to understand that concave utility functions (e.g., $u(x) = ln(2x)$) indicate that the decision maker is risk averse.

The opposite of a risk averse decision maker is a risk prone decision maker. This is a decision maker who always prefer a non-degenerate lottery to the expected consequence of that lottery. Their utility of the expected consequence, $u[E(\widetilde{x})]$, is always less than the utility of the lottery:

$$u[E(\widetilde{x})] < E[u(\widetilde{x})] \tag{79}$$

The willingness of this decision maker to always enter the lottery implies that their utility function is convex. A proof for this statement is also provided by Keeney and Raiffa [105], but here it is sufficient to understand that convex utility functions (e.g., $u(x) = 2x^2)$) belong to risk prone decision makers.

A risk neutral decision maker is the remaining type of decision maker. These decision makers are indifferent towards choosing between the expected consequence for sure and entering the lottery. For them, the utility of the expected consequence, $u[E(\widetilde{x})]$, is equal to the utility of the lottery:

$$u[E(\widetilde{x})] = E[u(\widetilde{x})] \tag{80}$$

These decision makers have linear utility functions, e.g., $u(x) = 2x$.

7.3.1.4 Risk Premium

Another concept related to risk in lotteries is that of the risk premium. For increasing utility functions, the risk premium, RP, of a lottery, $\widetilde{x}$ is defined as the expected value of the lottery, $\bar{x}$, minus its certainty equivalent, $\hat{x}$. With the definitions mentioned previously, this can be found by

$$RP(\widetilde{x}) = \bar{x} - \hat{x} = E(\widetilde{x}) - u^{-1}(Eu(\widetilde{x}) \tag{81}$$

For increasing utility functions, A decision maker is risk averse if their risk premium is positive for all nondegenerate lotteries. The risk premium can also be thought of as the amount of the particular attribute in question, that the decision maker is willing to forgo from the average (expected consequence, $\bar{x}$) to avoid the risks associated with the lottery.

7.3.1.5 Measure of Risk Aversion

It is important to distinguish utility functions and be able to tell when one decision maker is more or less prone to risk. One might think that the degree of concavity is a good measure of risk aversion, however this is not true. This can be seen by examining some simple but different exponential utility functions which can have the using different second derivatives, yet their risk premium is the same. This is because utility functions that are positive linear transformations of one another are strategically equivalent, and their second derivatives do not reveal further information about their risk aversion. However the sign of the second derivative will tell us if the utility function is concave (negative for all x) or convex (positive for all x). As mentioned earlier this can tell us if the decision maker is risk averse (concave utility function) or risk prone (convex utility function). Using this idea Keeney and Raiffa [105] provide a risk aversion function which is a proper measure of how risk averse a decision maker is for increasing utility functions. They give the local risk aversion,

$r(x)$, at x, as

$$r(x) \equiv -\frac{u''(x)}{u'(x)} \tag{82}$$

They state the risk aversion function maintains only the relevant information about the utility function in terms of its risk properties. Additionally they state that a decision maker is constantly risk averse if r is a positive constant for all x, risk neutral if r is zero, and risk constantly risk prone if r is a negative constant for all x.

7.4 Appendix D: Ranking and selection method for uncertain populations

7.4.1 Two Stage Ranking and Selection

The Two Stage Ranking and selection procedure was originally developed by Dudewicz and Dalal (1975) and was expounded upon by Rinott (1978). This a technique for comparing the means of normally distributed populations. The inherent randomness in the random variables and probability distributions produces results, which if we select from amongst, we can never be absolutely sure we chosen the best one. This procedure enables us to specify the probability with which we can select the right system (Correct Selection) that is close enough to the actual best system but within a specified indifference value. In the first stage make a fixed number of replications of all systems. Then we use the resulting variance estimates to determine how many more replications from each system are necessary in a second stage to make a decision with the specified constraints (probability of correct selection and indifference value from best system). Must be assumed that the random variables representing the systems are normally distributed. If number of micro replications (individual system replications) is large enough, about 20, then central limit theorem yields approximate normality (Goldsman et. al. 1991, sec 3.2). This procedure does not need to know the system variances and the variances dont have to be the same. The smaller (tighter) the indifference zone, the greater the amount of sampling required from each alternative (Goldsman et. al. 1991). The larger the variance of a system in the first stage, the more replications are necessary in the second stage to ensure a proper selection.

REFERENCES

[1] Abbas, A. E., Budescu, D. V., Yu, H.-T., and Haggerty, R., "A comparison of two probability encoding methods: Fixed probability vs. fixed variable values," *Decision Analysis*, vol. 5, p. 190202, Dec 2008.

[2] Adelman, H. M. and Haftka, R. T., "Sensitivity analysis of discrete structural systems," *AIAA Journal*, vol. 24, pp. 823–832, May 1986.

[3] Airbus, "Global market forecast 2013-2032," tech. rep., Airbus, 2013.

[4] Akram, F., Prior, M., and Mavris, D., "An improved methodology for gas turbine technology portfolio planning, including technology synergy matrices and real options analysis," in *49th AIAA Aerospace Sciences Meeting including the New Horizons Forum and Aerospace Exposition*, AIAA 2011-578, 2011.

[5] Albert, J., "What is a probability?." Bowling Green State University http://www-math.bgsu.edu/ albert/m115/probability/outline.html, 1996.

[6] Anderson, J., *Aircraft Performance and Design*. WCB/McGraw-Hill, 1999.

[7] Anderson, T. W., "On the distribution of the two-sample cramer-von mises criterion," *The Annals of Mathematical Statistics 33*, vol. 3, pp. 1148–1159, 1962.

[8] Armstrong, M., "Copula catalogue part 1 : Bivariate archimedean copulas," *CERNA*, pp. 1–20, 2003.

[9] Arrow, K., *Social Choice and Individual Values*. Yale University Press, 1963.

[10] Aust, C., Bell, S., Harrison, E., Heard, R., Heath, A., and Mellor, J., "Passenger aircraft development trends," tech. rep., 2007.

[11] Batson, R. G., "Cost risk analysis methodology: A state-of-the-art review," *National Estimator*, pp. 21–49, 1989.

[12] Batson, R. G. and Love, R. M., "Risk analysis approach to transport aircraft technology assessment," *Journal of Aircraft*, vol. 25, no. 2, pp. 99–105, 1988.

[13] Becker, G., DeGroot, M., and Marschak, J., "Measuring utility by a single-response sequential method," *Behavioral Science*, vol. 9, pp. 226–232, 1964.

[14] Bedford, T. and Cooke, R., "A new generic model for applying maut," *European Journal of Operations Research*, vol. 118, pp. 589–604, 1999.

[15] Bedford, T. and Cooke, R., *Probabilistic Risk Analysis: Foundations and Methods*. Cambridge University Press, 2001.

[16] Benzia, K., Bounceur, A., Mir, S., and Euler, R., "Parametric test metrics estimation," in *17th International Mixed-Signals, Sensors and Systems Test Workshop (IMS3TW)*, IEEE, May 2011.

[17] Bernardo, J. E., Besson, C., Pfaender, H., Schutte, J., and Mavris, D. N., "A multi-stage surrogate modeling approach to examine vehicle-level technology impacts at the airport-level," in *53rd AIAA Aerospace Sciences Meeting*, no. AIAA 2015-0743, 2015.

[18] Bernoulli, D., "Exposition of a new theory on the measurement of risk," *Commentaries of the Imperial Academy of Science of Saint Petersburg*, 1738.

[19] Bernoulli, J., *Ars conjectandi, The Art of Conjecturing*. 1713. posthumous work, published by his nephew, Niklaus Bernoulli.

[20] Bernoulli, N., "Essay d'analyse sur les jeux de hazard (essays on the analysis of games of chance)." Correspondence of Nicolas Bernoulli with Pierre Remond de Montmort concerning the St. Petersburg Game, 1713.

[21] Bird, G. A., *Molecular Gas Dynamics and the Direct Simulation of Gas Flows*, vol. 1. Clarendon Press, 1994.

[22] Boeing, "737 max airport compatibility brocuhure," tech. rep., Boeing Company, 2014.

[23] Boeing, "787 airplane characteristics for airport planning," Tech. Rep. D6-58333, Boeing Company, 2014.

[24] Boeing, "Current market outlook, 2014-2033," tech. rep., Boeing Company, http://www.boeing.com/boeing/commercial/cmo/, 2014.

[25] Box, G. E. P. and Draper, N. R., *Empirical model-building and response surfaces*. Wiley, 1987.

[26] Boyce, L., "Probabilistic structural analysis methods for improving space shuttle engine reliability," *Journal of Propulsion and Power*, vol. 5, pp. 426–430, July-Aug. 1989.

[27] Brooks, D. G. and OLeary, T. J., "A comparison of encoding techniques," *OMEGA The International Journal of Management Science*, vol. 11, no. 1, pp. 49–55, 1983.

[28] Brown, A., DeHaye, M., and DeLessio, S., "Application of probabilistic methods to assess risk due to resonance in the design of j-2x rocket engine turbine blades," in *52nd AIAA/ASME/ASCE/AHS/ASC Structures, Structural Dynamics and Materials Conference*, AIAA 2011-1939, 2011.

[29] Brown, A., DeHaye, M., and DeLessio, S., "Probabilistic methods to determine resonance risk and damping for rocket turbine blades," *Journal of Propulsion and Power*, vol. 29, pp. 1367–1373, 2013.

[30] Cafarella, J. R., "Cross validation of selection of variables in multiple regression," Tech. Rep. AFIT/GOR/MA/79D-2, Air Force Inst Of Technology, Wright-Patterson AFB, OH School Of Engineering, 1979.

[31] Cascetta, E., *Transportation Systems Analysis*, vol. 29. Springer Optimization and Its Applications, 2009.

[32] Chedrik, V. V., Ishmuratov, F. Z., Kuzmina, S. I., and Zichenkov, M. C., "Strength/aeroelasticity research at multidisciplinary structural design of high aspect ratio wing," in *27th International Congress Of The Aeronautical Sciences*, ICAS 2010, Central Aerohydrodynamic Institute (TsAGI), Zhukovsky, Russia, 2010.

[33] Chen, X. T., "Modelling with parameter-mixture copulas," Master's thesis, The University Of Sydney, October 2006.

[34] Cheung, R. C. C., Lee, D.-U., Luk, W., and Villasenor, J. D., "Hardware generation of arbitrary random number distributions from uniform distributions via the inversion method," *IEEE Transactions On Very Large Scale Integration (VLSI) Systems*, vol. 15, pp. 952–962, 2007.

[35] Collier, F., "Overview of nasas environmentally responsible aviation (era) project," tech. rep., NASA Environmentally Responsible Aviation Project Pre-Proposal Meeting, Washington DC, February 2010.

[36] Collier, F., "Nasa aeronautics environmentally responsible aviation project," tech. rep., NASA, http://www.aeronautics.nasa.gov/isrp/era/, 2012.

[37] Committee, S. E., "Sesar master plan d5," tech. rep., SESAR Consortium and Eurocontrol, April 2008.

[38] Conrow, E., *Effective Risk Management: Some Keys to Success*. American Institute of Aeronautics and Astronautics, 2nd ed., 2003.

[39] Conrow, E., "Evaluation of subjective probability statements," in *AIAA SPACE 2010 Conference & Exposition*, AIAA 2010-8739, 2010.

[40] Conrow, E., "Space program schedule change probability distributions," in *AIAA SPACE 2010 Conference & Exposition*, AIAA 2010-8834, 2010.

[41] Conrow, E. H., "Technology readiness levels and space program schedule change," *Journal of Spacecraft and Rockets*, vol. 48, no. 6, 2011.

[42] Converse, G. and Giffin, R., "Extended parametric representation of compressors fans and turbines, vol. i - cmpgen users manual," Contractor Report NASA CR-174645, March 1984.

[43] Cooke, R., *Stakeholder Preference Elicitation*. Springer, 2007. Appearing in I. Linkov et al. (eds.), Environmental Security in Harbors and Coastal Areas, pg 149-160.

[44] Council, N. S. T., "National aeronautics researchand development plan," tech. rep., Executive Office of the President, 2010.

[45] Cramer, H., "On the composition of elementary errors," *Scandinavian Actuarial Journal*, 1928.

[46] Cukier, R. I., Levine, H. B., and Shuler, K. E., "Nonlinear sensitivity analysis of multiparameter model systems," *Journal of Computational Physics*, vol. 26, no. 1, pp. 1–42, 1978.

[47] Cunningham, E., "Probability of crashing from monte carlo simulation," *Journal of Spacecraft and Rockets*, vol. 16, pp. 348–350, 1979.

[48] Daskilewicz, M. J., *Methods for Parameterizing And Exploring Pareto Frontiers Using Barycentric Coordinates*. PhD thesis, Georgia Institute of Technology, 2013.

[49] Davidson, D., Suppes, P., and Siegel, S., *Decision Making: An Experimental Approach*. Stanford University Press, 1957.

[50] DeLaurentis, D. and Mavris, D., "Uncertainty modeling and management in multidisciplinary analysis and synthesis," in *38th Aerospace Sciences Meeting and Exhibit*, AIAA 2000-422, 2000.

[51] DellElce, L. and Kerschen, G., "Probabilistic assessment of lifetime of low-earth-orbit spacecraft: Uncertainty propagation and sensitivity analysis," *Journal Of Guidance, Control, And Dynamics*, pp. 1–14, 2014.

[52] Devroye, L., *Non- Uni form Random Variate Generation*. Springer-Verlag, 1986.

[53] Du, X., "Probabilistic engineering design," chapter 7, University of Missouri-Rolla, September 2005.

[54] Dubos, G. F., Saleh, J. H., and Braun, R., "Technology readiness level, schedule risk, and slippage in spacecraft design," *Journal of Spacecraft and Rockets*, vol. 45, no. 4, 2008.

[55] Durrleman, V., Nikeghbali, A., and Roncalli, T., "A simple transformation of copulas," in *Groupe de Recherche Operationnelle, Bercy-Expo*, 2000.

[56] EIA, "Short-term energy and winter fuels outlook (steo)," tech. rep., US Energy Information Agency, October 2015.

[57] Elseifi, M., Khalessi, M., and Lin, H. Z., "A convex set based optimization algorithm for structural reliability analysis," in *19th AIAA Applied Aerodynamics Conference*, AIAA 2001-1520, 2001.

[58] Eppinger, S., Whitney, D., Smith, R., and Gebala, D., "A model-based method for organizing tasks in product development," *Research in Engineering Design*, vol. 6, p. 113, 1994.

[59] FAA, "Faa long-range aerospace forecasts fiscal years 2020, 2025, and 2030," tech. rep., Federal Aviation Administration, September 2007.

[60] FAA, "Faa aerospace forecast fiscal years 2013-2033," tech. rep., Federal Aviation Administration, 2013.

[61] Gelfand, A. E. and Smith, A. F. M., "Sampling-based approaches to calculating marginal densities," *Journal of the American Statistical Association*, vol. 85, no. 410, pp. 398–409, 1990.

[62] Geman, S. and Geman, D., "Stochastic relaxation, gibbs distributions, and the bayesian restoration of images," *IEEE Transactions on Pattern Analysis and Machine Intelligence PAMI-6*, p. 721741, 1984.

[63] Genest, C. and MacKay, J., "The joy of copulas: Bivariate distributions with uniform marginals," *The American Statistician*, vol. 40, no. 4, pp. 280–283, 1986.

[64] Genest, C. and MacKay, R. J., "Copules archimdiennes et familles de lois bidimensionnelles dont les marges sont donnes," *The Canadian Journal of Statistics*, vol. 14, pp. 145–159, June 1986.

[65] Genest, C. and Rivest, L.-P., "Statistical inference procedures for bivariate archimedean copulas," *Journal of the American Statistical Association*, vol. 88, pp. 1034–1043, September 1993.

[66] Giere, R. N., *Understanding Scientific Reasoning*. Holt, Rinehart and Winston, 2nd ed., 1984.

[67] Gigerenzer, G., Swijtink, Z., Porter, T., Daston, L., Beatty, J., and Kruger, L., *The empire of chance: How probability changed science and everyday life*. Cambridge University Press, 1989.

[68] Glassman, A., "Design geometry and design/off-design performance computer codes for compressors and turbines," Tech. Rep. NASA CR 198433, NASA, 1995.

[69] Green, J. E., "Laminar flow control back to the future?," 38th Fluid Dynamics Conference and Exhibit, June 2008. AIAA 2008-3738.

[70] Green, L., Lin, H.-Z., and Khalessi, M., "Probabilistic methods for uncertainty propagation applied to aircraft design," in *20th AIAA Applied Aerodynamics Conference*, AIAA 2002-3140, 2002.

[71] Guynn, M. D., Berton, J. J., Tong, M. T., and Haller, W. J., "Advanced single-aisle transport propulsion design options revisited," in *Aviation Technology, Integration, and Operations Conference*, 2013.

[72] Hart and Iliff, "Comfort line: Falling oil prices," tech. rep., Hart and Iliff Fuel and Energy Systems, 2015.

[73] Haukaas, T., "Expected utility theory," tech. rep., University of British Columbia,, 2014. white paper.

[74] Haukaas, T., "Probability theory," tech. rep., University of British Columbia,, 2014. white paper.

[75] Haukaas, T., "Uncertainty and risk," tech. rep., University of British Columbia,, 2014. white paper.

[76] Hazelrigg, G. A., *Systems Engineering: An Approach to Information-Based Design*. Prentice Hall, 1996.

[77] Hazelrigg, G. A., "A framework for decision-based engineering design," *ASME Journal of Mechanical Design*, vol. 120, pp. 653–658, Dec 1998.

[78] Hazelrigg, G. A., "Validation of engineering design alternative selection methods," *Taylor & Francis Engineering Optimization*, vol. 35, no. 2, pp. 103–120, 2003.

[79] Hendricks, E., Jimenez, H., and Mavris, D., "A systems engineering enabled capability for commercial aviation strategic planning," in *47th AIAA Aerospace Sciences Meeting*, AIAA 2009-1199, 2009.

[80] Hering, C. and Stadtmuller, U., "Estimating archimedean copulas in high dimensions," *Scandinavian Journal of Statistics*, vol. 39, no. 3, pp. 461–479, 2012.

[81] Hill, P. and Peterson, C., *Mechanics and Thermodynamics of Propulsion*. Addison-Wesley, second ed., 1992.

[82] Holland, J. H., *Adaptation in Natural and Artificial Systems*. University of Michigan Press, 1975.

[83] Hormann, W. and Leydold, J., "Continuous random variate generation by fast numerical inversion," *ACM Transactions on Modeling and Computer Simulation*, vol. 13, pp. 347–362, October 2003.

[84] Huang, M., Wang, Q., Li, Y., and Ao, L., "An approach for improvement of avionics reliability assessment based on copula theory," *IEEE*, 2011.

[85] Hutchings, C. and Stump, E., "Adaptive cost models for rapidly evolving technologies," in *AIAA SPACE 2008 Conference & Exposition*, AIAA 2008-7702, 2008.

[86] Huyse, L., Bonivtch, A., Pleming, J., Riha, D., Waldhart, C., and Thacker, B., "Verification of stochastic solutions using polynomial chaos expansions," in *47th AIAA/ASME/ASCE/AHS/ASC Structures, Structural Dynamics, and Materials Conference*, 2006.

[87] IATA, "Iata airline industry forecast 2013-2017," tech. rep., International Air Transport Association, 2013.

[88] IATA, "Iata technology roadmap," Tech. Rep. 4, International Air Transport Association, June 2013.

[89] Igarashi, S., "Analysis of gas film lubrication using the monte carlo direct simulation method," *Rarefied Gas Dynamics: Theory and Simulations*, pp. 303–310, 1994.

[90] IIWG, "Commercial aircraft design characteristics -trends and growth projections," tech. rep., International Industry Working Group, January 2007.

[91] Ingram, C., Jimenez, H., Schutte, J., and Mavris, D. N., "Comparison of advanced vehicle concepts through pareto-optimal technology sets," in *53rd AIAA Aerospace Sciences Meeting*, no. AIAA 2015-0515, 2015.

[92] Jackson, J. E., *A User's Guide to Principal Components*. Wiley Series in Probability and Statistics, 1991.

[93] Jefferies, R., "Continuous lower energy, emissions and noise program overview," tech. rep., FAA CLEEN, 2010.

[94] Jimenez, H., Acuff, C., and Mavris, D. N., "Study of resource constraints and environmental performance objectives in pareto-optimal aircraft technology portfolios," in *Aviation Technology, Integration, and Operations Conference*, AIAA 2013-4319, 2013.

[95] Jimenez, H., Burdette, G., Schutte, J., and Mavris, D., "Probabilistic technology assessment for nasa environmentally responsible aviation (era) vehicle concepts," in *11th AIAA Aviation Technology, Integration, and Operations (ATIO) Conference*, AIAA 2011-6967, 2011.

[96] Jobe, C. E., "Prediction of aerodynamic drag," Tech. Rep. AFWAL-TM-84-203, Air Force Wright Aeronautical Laboratories, 1984.

[97] Johnson, D., "The triangular distribution as a proxy for the beta distribution in risk analysis," *The Statistician*, vol. 46, no. 2, pp. 387–398, 1997.

[98] Johnson, M. E., *Multivariate Statistical Simulation*. Wiley: New York, 1987.

[99] Jolliffe, I. T., *Principal Component Analysis*. Springer Series in Statistics, 2002.

[100] Joslin, R. D., "Aircraft laminar flow control," *Annual Review of Fluid Mechanics*, vol. 30, pp. 1–29, 1998.

[101] Joslin, R. D., "Overview of laminar flow control," Tech. Rep. 1998-208705, NASA, 1998. Pg 81-87.

[102] JPDO, "Next generation air transportation system in brief," tech. rep., Joint Planning and Development Office, Washington, DC, 2006.

[103] Kahneman, D., Slovic, P., and Tversky, A., *Judgment Under Uncertainty: Heuristics and Biases*. Cambridge University Press, 1982.

[104] Keefer, D. K. and Bodily, S. E., "Three-point approximations for continuous random variables," *Management Science*, vol. 29, no. 5, pp. 595–609, 1983.

[105] Keeney, R. and Raiffa, H., *Decisions with Multiple Objectives*. Cambridge University Press, 1993. First published in 1976 by John Wiley and Sons Inc.

[106] Kendall, M., "A new measure of rank correlation," *Biometrika*, vol. 30, no. 1, pp. 81–93, 1938.

[107] Kennedy, G. J., Kenway, G. W., and Martins, J. R. R. A., "High aspect ratiowing design: Optimal aerostructural tradeoffs for the next generation of materials," in *52nd Aerospace Sciences Meeting*, AIAA 2014-0596, 2014.

[108] Kestner, B. K., Schutte, J. S., Gladin, J. C., and Mavris, D. N., "Ultra high bypass ratio engine sizing and cycle selection study for a subsonic commercial aircraft in the n+2 timeframe," in *Proceedings of ASME Turbo Expo 2011*, no. GT2011-45370, 2011.

[109] Kestner, B. K., Schutte, J. S., Tai, J. C., Perullo, C. A., and Mavris, D. N., "Surrogate modeling for simultaneous engine cycle and technology optimization for next generation subsonic aircraft," in *Proceedings of ASME Turbo Expo 2012*, no. GT2012-68724, 2012.

[110] Kestner, B. K., Schutte, J. S., Tai, J. C., Perullo, C. A., and Mavris, D. N., "Surrogate modeling for simultaneous engine cycle and technology optimization for next generation subsonic aircraft," in *Proceedings of ASME Turbo Expo 2012*, no. GT2012-68724, (Copenhagen, Denmark), Aerospace Systems Design Laboratory (ASDL), June 2012.

[111] Khalessi, M. and Lin, H., "Most-probable-point-locus structural reliability method," in *34th Structures, Structural Dynamics and Materials Conference*, AIAA 1993-1439, 1993.

[112] Khuri, A. I., *Response Surface Methodology and Related Topics*. World Scientific, 2006.

[113] Kirby, M. and Mavris, D., "A method for technology selection based on benefit, available schedule and budget resources," in *2000 World Aviation Conference*, AIAA 2000-5563, 2000.

[114] Kirby, M. and Mavris, D., "The environmental design space," in *26th International Congress of the Aeronautical Sciences*, vol. 26th International Congress of the Aeronautical Sciences, Georgia Institute of Technology, 2008.

[115] Kirby, M. R. and Mavris, D. N., "Forecasting technology uncertainty in preliminary aircraft design," in *1999 World Aviation Conference*, SAE Paper 1999-01-5631, (San Francisco, CA), Georgia Institute of Technology, October 1999.

[116] Kirby, M. R., *A Methodology for Technology Identification, Evaluation, and Selection in Conceptual and Preliminary Aircraft Design*. PhD thesis, Georgia Institute of Technology, 2001.

[117] Kirkpatrick, S., Gelatt, C. D., and Vecchi, M. P., "Optimization by simulated annealing," *Science*, vol. 220, no. 4598, 1983.

[118] Kiureghian, A. D. and Ditlevsen, O., "Aleatory or epistemic? does it matter?," *Structural Safety*, vol. 31, no. 2, pp. 105–112, 2009.

[119] Kiwiel, K. C., "Convergence and efficiency of subgradient methods for quasiconvex minimization," *Mathematical Programming*, vol. 90, no. 1, pp. 1–25, 2001.

[120] Kolmogorov, A., "Sulla determinazione empirica di una legge di distribuzione (on the empirical determination of a distribution law)," *Giornale dell Istituto Italiano degli Attuari*, vol. 4, no. 1, pp. 83–91, 1933.

[121] Kroese, D. P., Brereton, T., Taimre, T., and Botev, Z. I., "Why the monte carlo method is so important today," *Wiley Interdisciplinary Reviews: Computational Statistics*, vol. 6, no. 6, pp. 386–392, 2014.

[122] Kumar, P., "Probability distributions and estimation of ali-mikhail-haq copula," *Applied Mathematical Sciences*, vol. 4, no. 14, pp. 657–666, 2010.

[123] Landry, S. J. and Archer, J., "Modeling the effect of uncertainty and nextgen concepts and technologies on the national airspace system," in *14th AIAA Aviation Technology, Integration, and Operations Conference*, AIAA 2014-2422, 2014.

[124] Largent, M. C., *A Probabilistic Risk Management Based Process for Planning and Management of Technology Development*. PhD thesis, Georgia Institute of Technology, March 2003.

[125] Le-Maitre and Knio, *Spectral Methods for Uncertainty Quantification*. Springer, 2010.

[126] Lee, K., Nam, T., Perullo, C., and Mavris, D., "Reduced-order modeling of a high-fidelity propulsion system simulation via probabilistic principal component analysis and neural networks," in *13th AIAA/ISSMO Multidisciplinary Analysis Optimization Conference*, no. AIAA 2010-9193, 2010.

[127] Lee, T.-S. and Thomas, L. D., "Cost growth models for nasas programs," *Journal of Probability and Statistical Science*, vol. 1, no. 2, pp. 265–279, 2003.

[128] Lin, H., "Calculation of failure probability by using x-space most-probable-point," in *34th Structures, Structural Dynamics and Materials Conference*, AIAA 1993-1624, 1993.

[129] Lin, H.-Z., Khalessi, M., Lin, M., Fox, E., and Elseifi, M., "Development of unipass - a unified probabilistic assessment software system," in *19th AIAA Applied Aerodynamics Conference*, AIAA 2001-1644, 2001.

[130] Lin, L., "A concordance correlation coefficient to evaluate reproducibility," *Biometrics (International Biometric Society)*, vol. 45, pp. 255–268, March 1989.

[131] Lyle, K., Padula, S., and Stockwell, A., "Application of probabilistic analysis to aircraft impact dynamics," in *44th AIAA/ASME/ASCE/AHS/ASC Structures, Structural Dynamics, and Materials Conference*, AIAA 2003-1482, 2003.

[132] Lytle, J., "The numerical propulsion system simulation: A multidisciplinary design for aerospace vehicles," Technical Memorandum NASA TM-1999-209194, NASA Glenn Research Center, Cleveland, Ohio, September 1999.

[133] Lytle, J., "The numerical propulsion system simulation: An overview," Technical Memorandum NASA TM-2000-209915, NASA Glenn Research Center, Cleveland, Ohio, June 2000.

[134] Mahalanobis, P. C., "On tests and measures of group divergence," *Journal of the Asiatic Society of Bengal*, vol. 26, pp. 541–588, 1930.

[135] Mankins, J. C., "Technology readiness levels," tech. rep., NASA Office of Space Access and Technology - Advanced Concepts Office, 1995.

[136] Manski, C. F., "The structure of random utility models," *Springer Theory and Decision*, vol. 8, no. 3, pp. 229–254, 1977.

[137] Mavris, D. and Bandte, O., "Comparison of two probabilistic techniques for the assessment of economic uncertainty," in *19th Annual Aonference of the International Society of Parametric Analysts*, 1997.

[138] Mavris, D., Bandte, O., and Brewer, J. T., "A method for the identification and assessment of critical technologies needed for an economically viable hsct," in *Proceedings of the 1st AIAA Aircraft Engineering, Technology, and Operations Congress*, (Los Angeles, CA), 1995.

[139] Mavris, D., Mantis, G., , and Kirby, M., "Demonstration of a probabilistic technique for the determination of aircraft economic viability," AIAA-1997-5585-706.

[140] Mavris, D. and Bandte, O., "Economic uncertainty assessment using a combined design of experiments / monte carlo simulation approach with application to an hsct," in *17th Annual Conference of the International Society of Parametric Analysts*, 1995.

[141] Mavris, D. and Bandte, O., "A probabilistic approach to multivariate constrained robust design simulation," in *1997 World Aviation Congress*, AIAA 1997-5508, 1997.

[142] Mavris, D. and Garcia, E., "Framework for the assessment of capacity and throughput technologies," in *2000 World Aviation Conference*, AIAA 2000-5612, 2000.

[143] McCormick, D. J. and Olds, J. R., "Approximation of probabilistic distributions using selected discrete simulations," in *2000 8th AIAA/USAF/NASA/ISSMO Symposium on Multidisciplinary Analysis and Optimization*, AIAA 2000-4863, September 2000.

[144] McCulloch, W. and Pitts, W., "A logical calculus of ideas immanent in nervous activity," *Bulletin of Mathematical Biophysics*, vol. 5, no. 4, pp. 115–133, 1943.

[145] McNeil, A. J., Frey, R., and Embrechts, P., *Quantitative Risk Management: Concepts, Techniques and Tools*. Princeton University Press, 2015.

[146] Mehmani, A., Zhang, J., Chowdhury, S., and Messac, A., "Surrogate-based design optimization with adaptive sequential sampling," in *53rd AIAA/ASME/ASCE/AHS/ASC Structures, Structural Dynamics and Materials Conference*, AIAA 2012-1527, 2012.

[147] Mercer, C., Haller, W., and Tong, M., "Adaptive engine technologies for aviation co2 emissions reduction," in *42nd AIAA/ASME/SAE/ASEE Joint Propulsion Conference & Exhibit*, AIAA 2006-5105, July 2006.

[148] Metropolis, N., Rosenbluth, A. W., Rosenbluth, M. N., Teller, A. H., and Teller, E., "Equation of state calculations by fast computing machines," *Journal of Chemical Physics*, vol. 21, 1953.

[149] Missoum, S., Dribusch, C., and Beran, P., "A multifidelity approach for the construction of explicit decision boundaries: Application to aeroelasticity," in *50th AIAA/ASME/ASCE/AHS/ASC Structures, Structural Dynamics, and Materials Conference*, AIAA 2009-2193, May 2009.

[150] Morgan, M. G. and Henrion, M., *Uncertainty: A Guide to Dealing with Uncertainty in Quantitative Risk and Policy Analysis*. Cambridge University Press, 1990.

[151] Moss, J. N. and Bird, G. A., "Direct simulation monte carlo simulations of hypersonic flows with shock interactions," *AIAA Journal*, vol. 43, pp. 2565–2573, Dec 2005.

[152] Mosteller, F. and Nogee, P., "An experimental measurement of utility," *Journal of Political Economy*, vol. 59, pp. 371–404, 1951.

[153] Myers, R. H. and Montgomery, D. C., *Response Surface Methodology*. J. Wiley & Sons, 2nd ed., 2002.

[154] Nelsen, R. B., *An Introduction to Copulas*. Springer, 1st ed., 1999.

[155] Nelsen, R. B., *An Introduction to Copulas*. Springer, 2nd ed., 2006.

[156] Neufville, R. D., *Applied Systems Analysis: Engineering Planning and Technology Management*. McGraw-Hill, Inc, 1990.

[157] Noh, Y., Choi, K. K., and Du, L., "Reliability-based design optimization of problems with correlated input variables using a gaussian copula," *Structural and Multidisciplinary Optimization,*, vol. 38, pp. 1–16, 2009.

[158] Norman, P. D., Lister, D. H., Lecht, M., Madden, P., Park, K., Penanhoat, O., Plaisance, C., and Renger, K., "Development of the technical basis for a new emission parameter covering the whole aircraft operation (nepair)," Final Technical Report G4RD-CT-2000-00182, European Commission, September 2003.

[159] NRA, A. R. M. D., "Advanced concept studies awardees," tech. rep., NASA, 2008.

[160] on Climate Change, I. P., "Summary for policymakers: Aviation and the global atmosphere," tech. rep., WMO and UNEP, 1999.

[161] Onat, E. and Klees, G., "A method to estimate weight and dimensions of large and small gas turbine engines," Contractor Report NASA-CR-159481, Boeing Aerospace Company, January 1979.

[162] Onwubolu, G. C. and Babu, B. V., *New Optimization Techniques in Engineering*. 2004.

[163] Opricovica, S. and Tzeng, G.-H., "Compromise solution by mcdm methods: A comparative analysis of vikor and topsis," *European Journal of Operational Research*, vol. 156, no. 2, p. 445455, 2004.

[164] Organization, W. H., "The environmental health criteria document on community noise," tech. rep., WHO, 1993.

[165] Park, S. K. and Miller, K. W., "Random number generators: Good ones are hard to find," *Communications of the ACM*, vol. 31, p. 1192 1201, 1988.

[166] Pascal and de Fermat, "Fermat and pascal on probability," *Euvres de Fermat*, vol. 2, pp. 288–314, 1654. ed. Tannery and Henry, letters published in Paris 1894.

[167] Paul-Dubois-Taine, A. and Nadarajah, S., "Sensitivity-based sequential sampling of cokriging response surfaces for aerodynamic data," in *31st AIAA Applied Aerodynamics Conference*, AIAA 2013-2652, 2013.

[168] Pearson, K., "Mathematical contributions to the theory of evolution on a form of spurious correlation which may arise when indices are used in the measurement of organs," *Proceedings of the Royal Society of London*, vol. 60, pp. 489–498, January 1896.

[169] Penner, J. E., Lister, D. H., Griggs, D. J., Dokken, D. J., and McFarland, M., "Aviation and the global atmosphere," Tech. Rep. ISBN: 92-9169-, Intergovernmental Panel on Climate Change, 1999.

[170] Penzo, P. A. and Skidmore, L. J., "Monte carlo simulation of the midcourse guidance for lunar flights," *AIAA Journal*, vol. 1, Apr 1963.

[171] Pettit, C. and Beran, P., "Polynomial chaos expansion applied to airfoil limit cycle oscillations," in *45th AIAA/ASME/ASCE/AHS/ASC Structures, Structural Dynamics & Materials Conference*, 2004.

[172] Phadke, M. S., *Quality Engineering Using Robust Design*. Prentice Hall, 1st ed., 1995.

[173] Pitman, J., *Probability*. Springer Science & Business Media, 2012.

[174] Policonomics, "Risk and uncertainty ii: Risk aversion," tech. rep., 2012.

[175] Porter, A. L., *Forecasting and Management of Technology*. New York: John Wiley & Sons, 1991.

[176] Porter, A. L., Rossini, F. A., and Carpenter, S. R., *A Guidebook for Technology Assessment and Impact Analysis*. North Holland Series in System Science and Engineering, 1980.

[177] Prandini, M., Lygeros, J., Nilim, A., and Sastry, S., "A probabilistic framework for aircraft conflict detection," in *Guidance, Navigation, and Control Conference and Exhibit*, AIAA 1999-4144, 1999.

[178] Raczynski, C., Kirby, M., and Mavris, D., "A dynamic process for strategic roadmapping and technology portfolio management," in *6th AIAA Aviation Technology, Integration and Operations Conference (ATIO)*, AIAA 2006-7789, 2006.

[179] Ramsey, F. P., "Truth and probability," *The Foundations of Mathematics and other Logical Essays*, 1926. adapted and posthumously published.

[180] Rao, S. S., *Engineering Optimization: Theory and Practice*. 2009.

[181] Richey, M., "The evolution of markov chain monte carlo methods," *The American Mathematical Monthly*, vol. 117, no. 5, pp. 383–413, 2010.

[182] Robbins, H. and Monro, S., "A stochastic approximation method," *The Annals of Mathematical Statistics*, vol. 22, no. 3, pp. 400–407, 1951.

[183] Roberts, B., Lind, R., and Kumar, M., "Polynomial chaos analysis of mav's in turbulence," in *AIAA Atmospheric Flight Mechanics Conference*, 2011.

[184] Ronse, A. and Mooij, E., "Statistical impact prediction of decaying objects," *Journal of Spacecraft and Rockets*, vol. 51, pp. 1797–1810, Nov 2014.

[185] Rooney, B. and Hartong, A., "A discrete-event simulation of turnaround time and manpower of military rlvs," in *Space 2004 Conference and Exhibit*, AIAA 2004-6111, 2004.

[186] Rosario, R. D., Follen, G., Wahls, R., and Madavan, N., "Subsonic fixed wing project overview of technical challenges for energy efficient, environmentally compatible subsonic transport aircraft," tech. rep., NASA, 2012.

[187] Rosic, B. V. and Diekmann, J. H., "Methods for the uncertainty quantification of aircraft simulation models," *Journal of Aircraft*, pp. 1–9, 2014.

[188] Roskam, J., *Airplane Design Part V: Component Weight Estimation*. DAR Corporation, 2003.

[189] Rubin, D. B., "Comment on "the calculation of posterior distributions by data augmentation," by m. a. tanner and w. h. wong," *Journal of the American Statistical Association*, pp. 543–546, 1987.

[190] Rui, C. and Pu, G., "Convertible bond pricing model based on copula approach," International Conference on Management Science & Engineering (18th), September 2011.

[191] Rumelhart, D. E. and McClelland, J., *Parallel Distributed Processing: Explorations in the Microstructure of Cognition*. Cambridge: MIT Press, 1986.

[192] Rumpfkeil, M., Yamazaki, W., and Dimitri, M., "A dynamic sampling method for kriging and cokriging surrogate models," in *49th AIAA Aerospace Sciences Meeting including the New Horizons Forum and Aerospace Exposition*, AIAA 2011-883, Jan 2011.

[193] Ruppert, D., *Statistics and Data Analysis for Financial Engineering*. Springer Texts in Statistics, 2011.

[194] Ryan, R. and Townsend, J., "Application of probabilistic analysis/design methods in space programs - the approaches, the status, and the needs," in *34th Structures, Structural Dynamics and Materials Conference*, AIAA 1993-1381, April 1993.

[195] Saaty, T. and Alexander, J., *Conflict Resolution: The Analytic Hierarchy Process*. Praeger New York, 1989.

[196] Sage, A. P., *Methodology for Large-Scale Systems*. McGraw-Hill Book Company, 1977.

[197] Sambridge, M. and Mosegaard, K., "Monte carlo methods in geophysical inverse problems," *Reviews of Geophysics*, vol. 40, Sep 2002.

[198] Savage, L., *The Foundations of Statistics*. John Wiley and Sons Inc, 1954.

[199] Schlaifer, R., *Analysis of Decisions Under Uncertainty*. McGraw-Hill Book Company, 1969.

[200] Schrage, D. P., "Application of georgia tech generic ippd methodology to support implementation of the nasa/industry phase iia propulsion plan high speed research program," tech. rep., Georgia Institute of Technology, 1999.

[201] Schrauf, G. H. and Horstmann, K. H., "Simplified hybrid laminar flow control," *European Congress on Computational Methods in Applied Sciences and Engineering*, July 2004.

[202] Schutte, J., *Simultaneous Multi-Design Point Approach to Gas Turbine On-Design Cycle Analysis for Aircraft Engines*. Doctoral Thesis, Georgia Institute of Technology, Atlanta, Georgia, May 2009.

[203] Schutte, J., Jimenez, H., and Mavris, D., "Technology assessment of nasa environmentally responsible aviation advanced vehicle concepts," in *49th AIAA Aerospace Sciences Meeting including the New Horizons Forum and Aerospace Exposition*, no. AIAA 2011-0006, 2011.

[204] Schutte, J. and Mavris, D. N., "Evaluation of n+2 technologies and advanced vehicle concepts," in *53rd AIAA Aerospace Sciences Meeting*, no. AIAA 2015-0514, 2015.

[205] Schutte, J., Kestner, B., Tai, J., and Mavris, D., "Updates and modeling enhancements to the assessment of nasa environmentally responsible aviation technologies and vehicle concepts," in *50th AIAA Aerospace Science Meeting*, AIAA 2012-0336.

[206] Schwartz, B., *The Paradox of Choice - Why More is Less*. Harper Perennial, 2004.

[207] Science, N. and Council, T., "Biennial update: National aeronautics research and development plan," tech. rep., Executive Office Of The President Of The United States, February 2010.

[208] Sedlmeier, P. and Gigerenzer, G., "Intuitions about sample size: The empirical law of large numbers," *Journal of Behavioral Decision Making*, vol. 10, no. 1, p. 3351, 1997.

[209] Shah, A. and Chamis, C., "Probabilistic assessment of large structures under pressure," in *39th AIAA/ASME/ASCE/AHS/ASC Structures, Structural Dynamics, and Materials Conference and Exhibit*, AIAA 1998-1824, 1998.

[210] Shi, P. and Mahadevan, S., "Aircraft structures reliability under corrosion fatigue," in *19th AIAA Applied Aerodynamics Conference*, AIAA 2001-1377, 2001.

[211] Sklar, A., "Fonctions de rpartition n dimensions et leurs marges," *Publ Inst Statist Univ Paris*, pp. 8:229–231, 1959.

[212] Sky, S. E. and Research, A. T. M., "The roadmap for sustainable air traffic management: European atm master plan," tech. rep., SESAR, 2012.

[213] Slade, R., Sharp, P., Jones, R., and Toropov, V., "Analysis, optimization and probabilistic assessment of an airbag landing system for the exomars space mission," in *11th AIAA/ISSMO Multidisciplinary Analysis and Optimization Conference*, AIAA 2006-7001, Sep 2006.

[214] Slantchev, B. L., "Game theory: Preferences and expected utility," April 2012. Department of Political Science, University of California.

[215] Smart, W., *An Introduction to the Theory of Value on the Lines of Menger, Wieser, and Bohm-Bawerk*. University of Glasgow, 1891.

[216] Smirnov, N. V., "Table for estimating the goodness of fit of empirical distributions," *The Annals of Mathematical Statistics 19*, vol. 2, pp. 279–281, 1948.

[217] Soban, D. S. and Mavris, D. N., "Assessing the impact of technology on aircraft systems using technology impact forecasting," *Journal of Aircraft*, vol. 50, pp. 1380–1393, 2013.

[218] Sobol, I., "Uniformly distributed sequences with an additional uniform property," *USSR Computational Mathematics and Mathematical Physics*, vol. 16, no. 5, p. 236242, 1976.

[219] Soufiani, H. A., Parkes, D. C., and Xia, L., "Random utility theory for social choice," *Conell University Library*, 2012.

[220] Southwest Research Institute, San Antonio, TX, *FPI User's and Theoretical Manual*, 1995.

[221] Spearman, C., "The proof and measurement of association between two things," *The American Journal of Psychology*, vol. 15, pp. 72–101, January 1904.

[222] Spetzler, C. S. and Holstein, C.-A. S. V., "Probability encoding in decision analysis," *Management Science*, vol. 22, November 1975.

[223] Stadlober, E., "Binomial random variate generation: A method based on ratio of uniforms," in *The First International Conference on Statistical Computing*, 1991.

[224] Stein, W. E. and Keblis, M. F., "A new method to simulate the triangular distribution," *Elsevier Mathematical and Computer Modelling*, vol. 49, pp. 1143–1147, 2009.

[225] Sues, R., Oakley, D., Rhodes, G., and Hopkins, D., "Reliability-based optimization for design of aeropropulsion components," in *37th Structure, Structural Dynamics and Materials Conference*, AIAA 1996-1609, 1996.

[226] Suh, E. S., Furst, M. R., Mihalyov, K. J., and de Weck, O., "Technology infusion for complex systems: A framework and case study," *Wiley InterScience, Systems Engineering*, vol. 13, no. 2, 2010.

[227] Suh, N., *The Principals of Design*. Oxford University Press, 1988.

[228] Sun, Q., Fan, J., and Boyd, I. D., "Improved sampling techniques for the direct simulation monte carlo method," *Computers & Fluids*, vol. 38, no. 2, p. 475479, 2009.

[229] Sundaram, S., Viswanath, P. R., and Subaschandar, N., "Viscous drag reduction using riblets on a swept wing," *AIAA JOURNAL*, vol. 37, pp. 851–856, July 1999.

[230] Szekely, G. and Rizzo, M., "Brownian distance covariance," *The Annals of Applied Statistics*, vol. 3, pp. 1236–1265, 2009.

[231] Szekely, G., Rizzo, M., and Bakirov, N., "Measuring and testing dependence by correlation of distances," *The Annals of Stastistics*, vol. 35, pp. 2769–2794, 2007.

[232] Taguchi, G., *Introduction to Quality Engineering: Designing Quality into Products and Processes*. 1986.

[233] Taguchi, G., *System of Experimental Design*. White Plains, New York: Unipub/Kraus International Publications, 1987.

[234] Taylor, B., "Methodus incrementorum directa et inversa (direct and reverse methods of incrementation)," *Pearsonianis: prostant apud Gul. Innys*, pp. 21–23 (Proposition VII, Theorem 3, Corollary 2), 1715. London.

[235] Taylor, J. and Curran, F., "Integrated technology assessment center (itac) update," in *38th AIAA/ASME/SAE/ASEE Joint Propulsion Conference & Exhibit, July 2002*, AIAA 2002-3550, 2002.

[236] Thurston, D. L., "Real and misconceived limitations to decision based design with utility analysis," *ASME Journal of Mechanical Design*, vol. 123, 2001.

[237] Timson, F. S., "Measurement of technical performance in weapon system development programs: A subjective probability approach," tech. rep., The Rand Corporation, 1968.

[238] Tong, M., Halliwell, I., and Ghosn, L., "A computer code for gas turbine engine weight and disk life estimation," in *ASME Turbo Expo*, no. GT-2002-30500, 2002.

[239] Tribus, M., *Rational Descriptions, Decisions and Designs*. Pergamon Press Inc, Maxwell House, 1969.

[240] Twiss, B. C., *Forecasting for Technologists and Engineers: A Practical Guide for Better Decisions*. Peter Peregrinus Ltd, 1992.

[241] Vanderplaats, G. N., *Numerical Optimization Techniques for Engineering Design*. Colorado Springs CO: Vanderplaats Research and Development, 3rd ed., 2001.

[242] Viswanath, P., "Aircraft viscous drag reduction using riblets," *Progress in Aerospace Sciences, Elsevier Science Ltd.*, vol. 38, pp. 571–600, 2002.

[243] von Mises, R., *Wahrscheinlichkeit, Statistik und Wahrheit*. Springer, 2nd ed., 1936.

[244] von Neumann, J. and Morgenstern, O., *Theory of Games and Economic Behavior*. Princeton University Press, 1944.

[245] von Winterfeldt, D. and Edwards, W., *Decision Analysis and Behavioral Research*. Cambridge University Press, 1986.

[246] Walsh, M. J., "Turbulent boundary layer drag reduction using riblets," in *AlAA 20th Aerospace Sciences Meeting*, AIAA-82-0169, 1982.

[247] Walsh, M. J., III, W. L. S., and McGinleyt, C. B., "Riblet drag reduction at flight conditions," in *6th Applied Aerodynamics Conference*, no. AIAA 1988-2554, January 1988.

[248] Weisbin, C. R., Rodriguez, G., Elfes, A., and Smith, J. H., "Toward a systematic approach for selection ofnasa technology portfolios," *Wiley Periodicals, Inc, Systems Engineering*, vol. 7, no. 4, 2004.

[249] Whitelegg, J., "Aviation: The social, economic and environmental impact of flying," tech. rep., Stockholm Environment Institute, University of York, Lancaster, Ashden Trust, London, 2000.

[250] Wiener, N., "The homogeneous chaos," *American Journal of Mathematics*, vol. 60, p. 897936, October 1938.

[251] Williams, T. M., "Practical use of distribution in network analysis," *Journal of the Operational Research Society*, vol. 43, pp. 265–270, March 1992.

[252] Xiu, D., *Numerical Methods for Stochastic Computations: A Spectral Method Approach*. Princeton University Press, 2010.

[253] Yoon, K. P. and Hwang, C. L., *Multiple Attribute Decision Making: An Introduction*. SAGE Publications, 1992.

[254] Zaidi, T., Jimenez, H., and Mavris, D. N., "Copulas theory for probabilistic assessment - an overview with application to airplane performance analysis," *AIAA Journal of Aircraft*, vol. 52, no. 6, pp. 1802–1820, 2015.

[255] Zhang, J., Messac, A., Zhang, J., and Chowdhury, S., "Improving the accuracy of surrogate models using inverse transform sampling," in *53rd AIAA/ASME/ASCE/AHS/ASC Structures, Structural Dynamics and Materials Conference*, AIAA 2012-1429, 2012.

[256] Zhigljavsky, A. A., *Theory of Global Random Search*. Springer Netherlands, 1991.

[257] Zio, E. and Pedroni, N., "Literature review of methods for representing uncertainty," tech. rep., Foundation for an Industrial Safety Culture, 2013.

[258] Zorumski, W., "Aircraft noise prediction program theoretical manual, part 1," Technical Memorandum NASA TM-83199-Pt-1, NASA Langley Research Center, Hampton, Virginia, February 1982.

[259] Zorumski, W., "Aircraft noise prediction program theoretical manual, part 2," Technical Memorandum NASA TM-83199-Pt-2, NASA Langley Research Center, Hampton, Virginia, February 1982.

VITA

Turab Zaidi hails from New York City, NY and graduated from Aviation High School in NY. He enrolled in the undergraduate program of the Daniel Guggenheim School of Aerospace Engineering at the Georgia Institute of Technology in 2004 and received his Bachelor of Science degree in Aerospace Engineering in May 2008. He then transferred to the Aerospace Systems Design Lab (ASDL) at the School of Aerospace Engineering to pursue his graduate studies. He obtained his Master of Science degree in December 2009 and began his Ph.D. candidacy in August 2010. He earned his Doctor of Philosophy (Ph.D.) degree in July 2016. During the course of his graduate studies at Georgia Tech, he authored/co-authored peer-reviewed articles (AIAA Journal of Aircraft) and conference proceedings (AIAA Aviation Conference). He has also prepared three journal paper manuscripts for submission based on his thesis work that will be published after review. He holds a Federal Aviation Administration (FAA) Airman's Airframe and Powerplant Maintenance Certification. He is a member of the American Institute of Aeronautics and Astronautics (AIAA). His other interest include playing team sports, traveling abroad, and spending time with his family and close friends.